Epigenome and chromosome dynamics in the fungal pathogen *Zymoseptoria tritici*

Dissertation

in fulfilment of the requirements for the degree “Dr. rer. nat.” of the Faculty of Mathematics and Natural Sciences at the Christian Albrechts University of Kiel

submitted by
Mareike Möller
Kiel, May 2018

First referee: **Prof. Dr. Eva Holtgrewe Stukenbrock**

Second referee: **Prof. Dr. Martijn Rep**

Date of the oral examination: **06.07.2018**

Contents

Summary

Fungal genomes exhibit extraordinary intra- and interspecies diversity. Although advances in population genetic studies highlight genome variability, little is known about the underlying mechanisms driving this diversification. The main focus of this thesis is to elucidate dynamics and mechanisms of genome stability and chromosome loss in the fungal plant pathogen *Zymoseptoria tritici*.

In **Chapter I**, we discuss recent advancements in the field of fungal plant pathogen genome evolution. We conclude that modern agriculture has a large impact on pathogen populations and their genetic diversity. Important drivers of genome evolution are transposable elements that facilitate high diversity and rapid adaptation.

Genome diversity is also a key observation made for populations of the wheat pathogen *Z. tritici.* Besides structural variation of chromosomes, there are particular chromosomes, termed accessory chromosomes that show presence/absence polymorphisms between different isolates. While loss and gain of these chromosomes was so far associated with meiosis, we show in **Chapter II** that accessory chromosomes are highly instable during mitotic growth resulting in high rates of chromosome losses. High temperature furthermore increases the loss rates and promotes instability and rearrangements of core and accessory chromosomes. We demonstrate that accessory chromosome losses affect fitness *in planta*, indicating an adaptive role of chromosome dynamics in *Z. tritici*.

Besides structural differences in terms of transposable element and gene abundance, accessory chromosomes have been shown to be highly heterochromatic since they are highly enriched with H3K27me3, a facultative heterochromatin-associated histone mark. Transposable elements, also found to be enriched on accessory chromosomes, are silenced by H3K9me3. In **Chapter III** we investigate the consequences of loss of these heterochromatin-associated histone marks on the stability of core and accessory chromosomes. We find that loss of H3K27me3 increases the stability of accessory chromosomes by significantly reducing the rate of chromosome losses. However, absence of H3K9me3 led to severe genome instability resulting in chromosome rearrangements, breakages, large segmental duplications affecting core as well as accessory chromosomes. Furthermore, transposable element transcription is enhanced when H3K9me3 is absent. We conclude that H3K9me3 and transposable element silencing are crucial for genome stability, while H3K27me3 has a specific role for transmission of accessory chromosomes.

Besides histone modifications, DNA methylation plays an important role in genome regulation. In *Z. tritici*, DNA methylation has been shown to be absent due to the inactivation of a DNA methyltransferase gene, *Ztdim2*. In **Chapter IV**, we provide evidence that DNA methylation is present in *Z. tritici*. We find that some isolates contain a functional *Ztdim2* gene, possibly obtained by introgression from closely related species, and consequently exhibit high amounts of DNA methylation. In addition, we demonstrate small, but detectable amounts of DNA methylation even in strains that do not contain a functional *Ztdim2*. This can be explained by the presence of a second, maintenance methyltransferase that is encoded by a highly diverse gene.

Taken together, we demonstrate that epigenetic regulation is a crucial component of genome stability in *Z. tritici* that likely contributes to the high genomic diversity in natural populations.

Zusammenfassung

Die Genome von Pilzen weisen eine außergewöhnliche Vielfalt innerhalb und zwischen Arten auf. Obwohl Fortschritte in populationsgenetischen Studien die Variabilität von Genomen hervorheben, ist wenig über die zugrunde liegenden Mechanismen bekannt, welche die Diversifikation vorantreiben. Der Schwerpunkt dieser Arbeit ist die Untersuchung der Dynamiken und Mechanismen der Genom- und Chromosomenstabilität des pathogenen Pilzes *Zymoseptoria tritici*.

In **Kapitel I** besprechen wir die jüngsten Fortschritte im Forschungsgebiet der Genomevolution von Pflanzenpathogenen. Wir kommen zu dem Schluss, dass die moderne Landwirtschaft einen großen Einfluss auf die Struktur und die genetische Vielfalt von Pathogen Populationen hat. Wichtige Faktoren der Genomevolution sind mobile genetische Elemente, die eine hohe Diversität und schnelle Anpassung ermöglichen.

Auch in Populationen des Weizenpathogens *Z. tritici* wurde eine große genetische Diversität dokumentiert. Neben struktureller Variation von Chromosomen gibt es spezielle Chromosomen, die als akzessorische Chromosomen bezeichnet werden und deren An- und Abwesenheit in verschiedenen Isolaten variiert. Während Vorhandensein oder Fehlen dieser Chromosomen bisher mit Meiose in Verbindung gebracht wurde, zeigen wir in **Kapitel II**, dass akzessorische Chromosomen auch während vegetativem Wachstums sehr instabil sind, was zu hohen Chromosomenverlusten führt. Erhöhte Temperaturen steigern die Verlustraten zusätzlich und fördern Instabilität und Umstrukturierung von Chromosomen. Wir zeigen, dass der Verlust von akzessorischen Chromosomen die Fähigkeit des Pilzes zur Infektion der Pflanze beeinflusst, was auf eine adaptive Rolle der Chromosomendynamik in *Z. tritici* hinweist.

Neben strukturellen Unterschieden, besonders mobile genetische Elemente und Häufigkeit von Genen betreffend, sind akzessorische Chromosomen geprägt von Heterochromatin. Die Histonmodifikation H3K27me3, ein Marker für fakultatives Heterochromatin, ist besonders häufig auf den akzessorischen Chromosomen zu finden. Mobile genetische Elemente, die auf akzessorischen Chromosomen besonders häufig vorkommen, werden durch H3K9me3 inaktiviert. In **Kapitel III** untersuchen wir die Folgen des Verlustes dieser Heterochromatin-assoziierten Histonmodifikationen für die Stabilität von Chromosomen. Wir stellen fest, dass der Verlust von H3K27me3 die Stabilität der akzessorischen Chromosomen erhöht, wodurch die Rate der

Chromosomenverluste signifikant reduziert wird. Das Fehlen von H3K9me3 führte jedoch zu dramatischer Instabilität des gesamten Genoms, was sich in Form von Chromosomenumstrukturierungen, dem Abbruch von Chromosomenenden und großen Bereichen von duplizierten Sequenzen äußert. Außerdem ist die Transkription von mobilen genetischen Elemente erhöht, wenn H3K9me3 nicht vorhanden ist. Wir kommen zu dem Schluss, dass H3K9me3 und die Inaktivierung von mobilen genetischen Elementen essentiell für die Aufrechterhaltung der Genomstabilität sind, während H3K27me3 eine spezifische Rolle bei der Weitergabe von akzessorischen Chromosomen spielt.

Neben Histonmodifikationen spielt die DNA-Methylierung eine wichtige Rolle bei der Regulation des Genoms. Frühere Studien kamen zu dem Schluss, dass aufgrund der Inaktivierung des DNA-Methyltransferase-Gens *Ztdim2*, DNA-Methylierung in *Z. tritici*, nicht vorhanden sei. In **Kapitel IV** zeigen wir, dass DNA-Methylierung in *Z. tritici* existiert. Wir stellen fest, dass einige Isolate ein funktionierendes *Ztdim2* Gen enthalten, welches wahrscheinlich durch Introgression aus eng-verwandten Arten erhalten wurde, und die dadurch DNA-Methylierung aufweisen. Darüber hinaus demonstrieren wir geringe, aber nachweisbare Mengen an DNA-Methylierung auch in den Isolaten, die kein funktionelles *Ztdim2* Gen enthalten. Dies lässt sich durch das Vorhandensein eines zweiten, sehr diversen Gens erklären, das mutmaßlich für eine weitere DNA-Methyltransferase kodiert, die wichtig ist für die Erhaltung von DNA-Methylierung.

Mit dieser Arbeit zeigen wir, dass epigenetische Regulation eine entscheidende Komponente der Genomstabilität in *Z. tritici* ist, die wahrscheinlich zur hohen genetischen Vielfalt in den natürlich vorkommenden Populationen beiträgt.

General Introduction

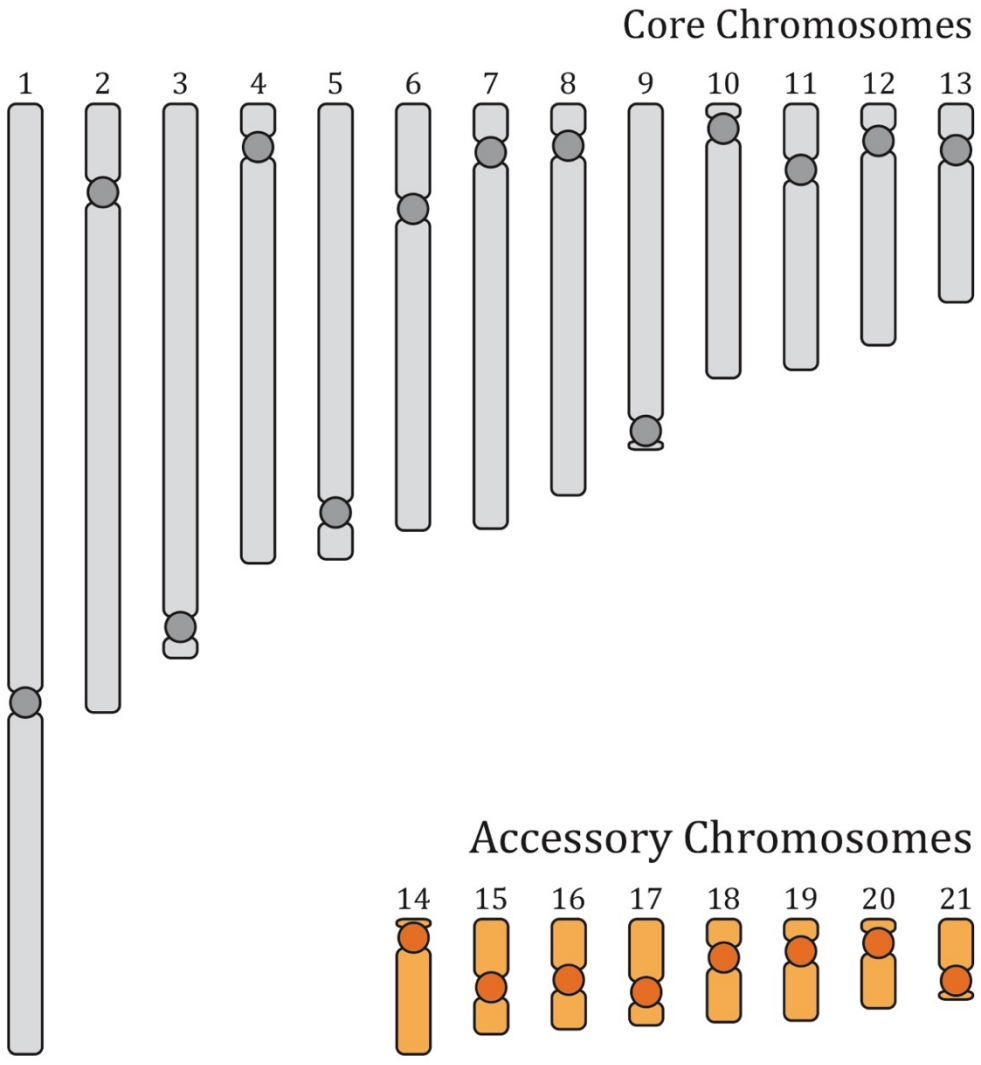

General Introduction

The ability to evolve and adapt to changing environments is essential for every organism to survive. The molecular basis of evolution and adaptation are changes at the genetic level. Genetic variability can be found throughout all forms of life and resembles the consequences of evolution. Variability on a genomic level appears in distinct ways and ranges from single nucleotide polymorphisms to large structural rearrangements, genome size variation and ploidy differences. Although more and more of these variabilities are detected based on large-scale population genetic studies, little is known about the mechanisms that enable genome diversification.

Comparative genomics and population genomic analyses have demonstrated that the genomes of fungal pant pathogens display high variability and can evolve very rapidly (Raffaele & Kamoun, 2012). Due to reoccurring strong selection pressures pathogens have to rapidly adapt to changing environmental conditions (McDonald & Stukenbrock, 2016). Recent studies suggest that transposable elements (TEs) are important drivers of rapid adaptation (Grandaubert *et al.*, 2014; Faino *et al.*, 2016). They can contribute to genetic diversity either directly by mutation of sequences (e.g. integration) or indirectly by recruitment of genome defense mechanisms resulting in silencing and inactivation (Hollister & Gaut, 2009). Furthermore, multiple copies of similar TEs in the genome can serve as targets for recombination and thereby promote genome rearrangements (Kazazian, 2004).

In many fungal genomes, specific regions that are enriched with transposable elements have been identified (Raffaele & Kamoun, 2012; Möller & Stukenbrock, 2017). While some comprise distinct compartments located on core chromosomes, entire chromosomes deviate in structure and TE content from core chromosomes in some species. Often, these compartments or chromosomes are important for pathogenicity and contain virulence factors. For example, lineage-specific chromosomes in *Fusarium* species confer host specificity (Ma *et al.*, 2010; Vlaardingerbroek *et al.*, 2016), while lineage-specific regions in *Verticillium dahliae* (De Jonge *et al.*, 2013) and AT-rich regions in *Leptosphaeria maculans* (Rouxel *et al.*, 2011) harbor virulence genes. However, the function of these compartments can vary and is not always associated with a fitness benefit. E.g., some accessory chromosomes of the wheat pathogen *Zymoseptoria tritici* were shown to confer reduced fitness during plant infection (Habig *et al.*, 2017). Besides divergence in genetic composition, the chromatin structure of these regions has been shown to be mainly

heterochromatic (Galazka & Freitag, 2014; Soyer *et al.*, 2014; Schotanus *et al.*, 2015). Chromatin immunoprecipitation (ChIP) sequencing discovered enrichment with heterochromatin-associated histone marks, namely H3K9me3 and H3K27me3 methylation. While H3K9me3 is strongly associated to repeated sequences and reflects enrichment of transposable elements, H3K27me3 is considered as a hallmark of accessory chromosomes in fungi (Figure 1) (Galazka & Freitag, 2014; Schotanus *et al.*, 2015).

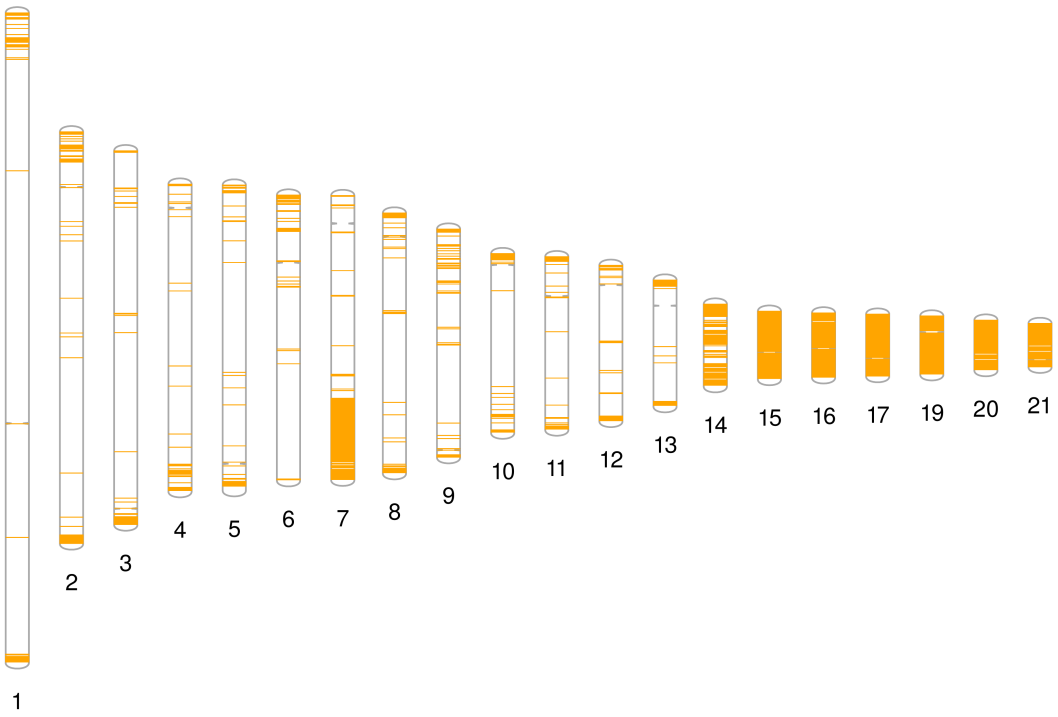

Figure 1. Enrichment of H3K27me3 (orange) on core and accessory chromosomes of *Zymoseptoria tritici* isolate Zt09. H3K27me3 enrichment on core chromosomes (1 – 13) is predominantly located in the subtelomeric regions, except for the right arm of chromosome 7. Here, an accessory chromosome possibly fused to a core chromosome. In contrast to the core chromosomes, the entire length of accessory chromosomes (14 – 21) is enriched with the facultative heterochromatin mark H3K27me3. Chromosome 18 is not present in the isolate Zt09 (Schotanus *et al.*, 2015). Chromosomes and enrichment were visualized using PhenoGram (Wolfe *et al.*, 2013).

The wheat pathogen *Zymoseptoria tritici* provides an excellent model system to study genome and chromosome dynamics. *Z. tritici* is a hemibiotrophic pathogen specialized to infect wheat and responsible for extensive annual yield loss in Europe and North America (Ponomarenko *et al.*, 2011; Fones & Gurr, 2015; Torriani *et al.*, 2015). The divergence of this pathogen from wild grass infecting sister species co-occurred with the domestication of wheat in the Fertile Crescent (Stukenbrock *et al.*, 2007, 2011). Infection takes place in the leaves, where the fungus colonizes the mesophyll after entering through stomata

(Rudd *et al.*, 2015; Haueisen *et al.*, 2017). Reproduction occurs both asexually, with the formation of pycnidia, or sexually involving the formation of pseudothecia. The genetic diversity between *Z. tritici* isolates is very high. Population genetic studies estimated the diversity found in one field to be as high as the diversity detected on a global scale (McDonald & Martinez, 1991; Linde *et al.*, 2002). The genome of the reference isolate IPO323 comprises 21 chromosomes that are completely assembled from telomere to telomere (Goodwin *et al.*, 2011). Out of these 21 chromosomes, thirteen are considered as core chromosomes and eight as accessory chromosomes. Accessory chromosomes show presence/absence polymorphisms between different isolates and display structural rearrangements (Figure 2).

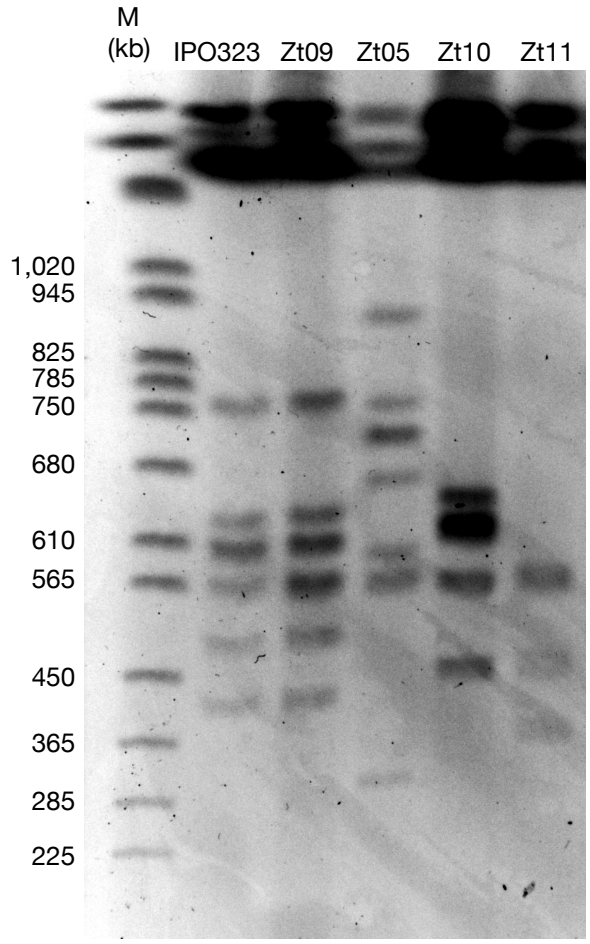

Figure 2. Pulsed-field gel electrophoresis separating accessory chromosomes of different *Zymoseptoria tritici* isolates. Structure and number of accessory chromosomes are highly variable between isolates. Shown here are the reference isolate IPO323, Zt09 (a derivate of IPO323 that lost chromosome 18 during sub-culturing in the laboratory), Zt05 (collected in Denmark), Zt10 and Zt11 (both originating from Iran). The loss of chromosome 18 in Zt09 cannot be detected because of its similar size to chromosomes 16 and 17 that form one band at ~ 610 kb. Chromosome size marker (M): *Saccharomyces cerevisiae*.

They furthermore contain a higher TE content and lower gene density compared to core chromosomes and display very little transcriptional activity (Goodwin *et al.*, 2011; Kellner *et al.*, 2014; Grandaubert *et al.*, 2015). Moreover, they have been shown to be unstable during meiosis (Wittenberg *et al.*, 2009). However, telomeres and centromeres, important structural components of chromosome stability, do not differ between core and accessory chromosomes (Schotanus *et al.*, 2015). As observed in other fungi, all accessory chromosomes of *Z. tritici* are highly enriched with the facultative heterochromatin mark H3K27me3. Interestingly, the right chromosome arm of core chromosome 7 resembles an accessory chromosome with a similar H3K27me3 enrichment suggesting potential rearrangements between core and accessory chromosomes (Figure 1) (Schotanus *et al.*, 2015). The high variability in chromosome structure and the particular histone methylation pattern on accessory chromosomes make *Z. tritici* an excellent model to study the effect of epigenetics on chromosome dynamics.

Scope of the Thesis

Chapter I

"Evolution and genome architecture in fungal plant pathogens"

Fungal genomes display high variability. Especially fungal plant pathogens have been shown to rapidly adapt to changing environments and selection pressures, likely mediated by modern agriculture. In this review, we outline recent studies on genome evolution in fungal plant pathogens and discuss possible mechanisms and population dynamics that drive the extraordinary genome flexibility.

- What is the role of modern agriculture in evolution of fungal plant pathogens?
- How does the population size affect genome evolution?
- To what extent do transposable elements and epigenetic regulation contribute to genetic variation?

Chapter II

"Extraordinary genome instability and widespread chromosome rearrangements during vegetative growth"

Accessory chromosomes in *Zymoseptoria tritici* are unstable during meiosis, however, little is known about the stability during asexual growth.
Based on previous observations, we hypothesize that chromosome loss is not unique to meiosis but readily occurs during mitotic growth. The main objectives of this study are:

- At what rate do chromosome losses occur during mitosis *in vitro* and *in planta*?
- Are specific accessory chromosomes lost at a higher rate than others?
- Does temperature stress affect chromosome stability?
- Is the observed chromosome loss specific to *Z. tritici* or a conserved phenomenon shared with sister species?
- What are the phenotypic consequences of chromosome losses *in planta* and *in vitro*?

Chapter III

"The role of heterochromatin in genome and chromosome stability in a fungal plant pathogen"

In Chapter II we demonstrated that accessory chromosomes are lost at a high rate during mitotic growth. Previous studies showed that accessory chromosomes of *Z. tritici* differ from core chromosomes in terms of transcription and transposable element content and display a particular heterochromatic pattern. These findings and similar observations of specific enrichment of facultative heterochromatin on accessory chromosomes in other fungi led to the hypothesis that histone modifications are involved in the stability and transcriptional regulation of accessory chromosomes. In this chapter, we study the effect of absence of the heterochromatin histone marks H3K9me3 and H3K27me3 on chromosome loss and genome stability in *Z. tritici*. The research questions addressed in this study are:

- How does absence of a heterochromatic histone mark influence the distribution of other histone marks?
- Does loss of H3K9me3 and H3K27me3 result in transcriptional activation of otherwise silenced genes?
- What are the consequences of the methyltransferase deletions on genome and chromosome stability over extended periods of mitotic growth?

Chapter IV

"DNA methylation varies in *Zymoseptoria* species"

DNA methylation is considered to be absent in *Zymoseptoria tritici* due to inactivation of a DNA methyltransferase gene, *Ztdim2*. Based on genome analyses of multiple *Z. tritici* genomes, we hypothesize that a number of *Z. tritici* isolates contain a functional *Ztdim2* gene. Furthermore, we identified a second putative DNA methyltransferase encoding gene in the genomes of all examined isolates. Hence, we hypothesize that DNA methylation is not completely absent in *Z. tritici*. To further investigate the presence of DNA methylation we focused on the following objectives:

- How many isolates contain a putatively functional *Ztdim2* gene?
- Is DNA methylation detectable in the strains that contain an intact *Ztdim2*?
- Does the second putative DNA methyltransferase catalyze DNA methylation, even in strains containing an inactive *Ztdim2*?

Chapter I

Evolution and genome architecture in fungal plant pathogens

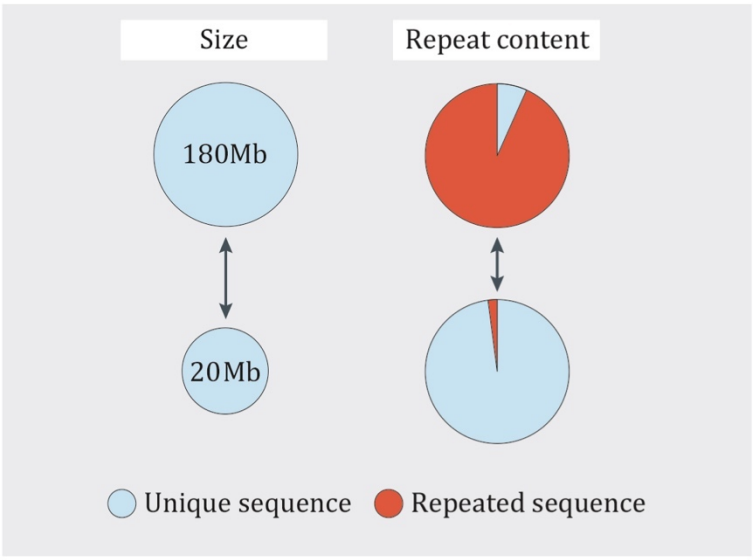

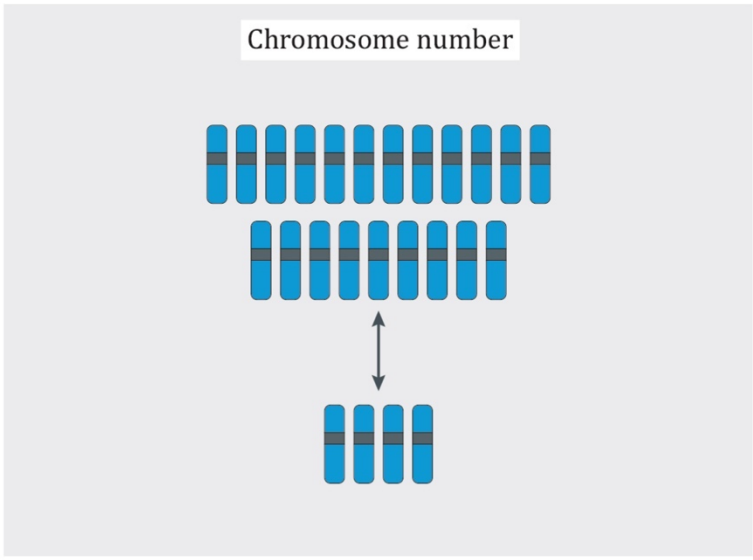

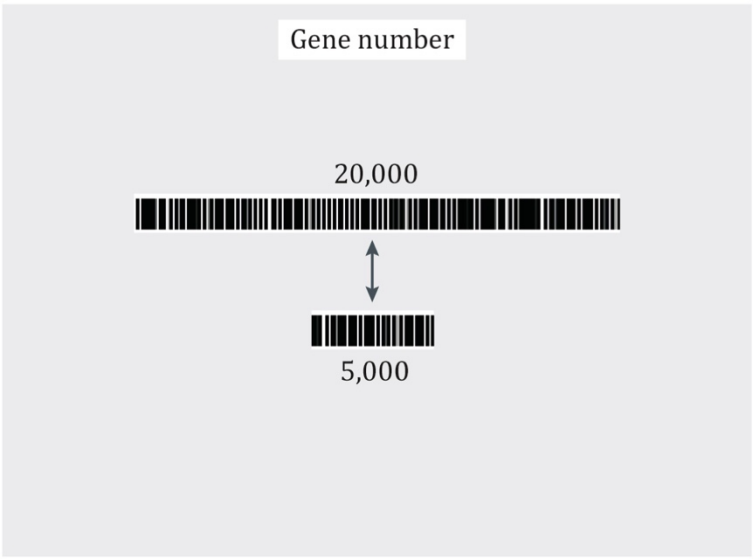

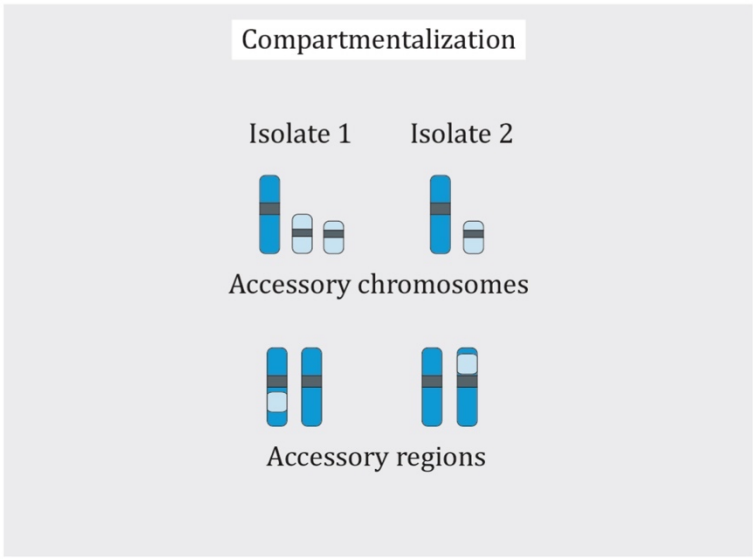

Title picture is modified from
Möller & Stukenbrock 2017,
“Evolution and genome architecture in fungal plant pathogens”
Nature Reviews Microbiology

Chapter I

Evolution and genome architecture in fungal plant pathogens

Mareike Möller & Eva H. Stukenbrock

Environmental Genomics, Christian-Albrechts University of Kiel, Am Botanischen Garten 1–9, 24118 Kiel, Germany.

Max Planck Institute of Evolutionary Biology, August-Thienemann-Straße 2, 24306 Plön, Germany.

This review has been published in *Nature Reviews Microbiology*, Volume 15, pages 756–771 (2017), doi:10.1038/nrmicro.2017.76

Abstract

The fungal kingdom comprises some of the most devastating plant pathogens. Sequencing the genomes of fungal pathogens has shown a remarkable variability in genome size and architecture. Population genomic data enable us to understand the mechanisms and the history of changes in genome size and adaptive evolution in plant pathogens. Although transposable elements predominantly have negative effects on their host, fungal pathogens provide prominent examples of advantageous associations between rapidly evolving transposable elements and virulence genes that cause variation in virulence phenotypes. By providing homogeneous environments at large regional scales, managed ecosystems, such as modern agriculture, can be conducive for the rapid evolution and dispersal of pathogens. In this Review, we summarize key examples from fungal plant pathogen genomics and discuss evolutionary processes in pathogenic fungi in the context of molecular evolution, population genomics and agriculture.

Key points

- During crop production, fungal plant pathogens cause severe yield losses. Uniform agricultural ecosystems are conducive for the rapid evolution and dissemination of pathogens.

- The genomes of fungal plant pathogens can vary in size and composition, even between closely related species. Differences in the content of transposable elements cause variation in genome architecture.

- Variation in genome architecture results from differences in population genetic factors, including effective population size and the strength of genetic drift.

- During periods of low effective population size, non-adaptive mutations, such as transposable elements, can invade genomes and shape their architecture.

- Transposable elements contribute to the establishment and maintenance of rapidly evolving genome compartments that can comprise virulence genes. High mutation rates in these compartments support the evolution of new virulence phenotypes.

Main

Infectious diseases have an enormous economic impact on crop production worldwide. Among the most devastating plant pathogens are fungi that use plant tissues for their reproduction and dispersal[1]. Fungal plant pathogens exhibit remarkable genomic and reproductive plasticity, and are represented in different phyla throughout the fungal tree of life (Fig. 1). This widespread distribution suggests that there have been numerous transitions from non-pathogenic to pathogenic lifestyles and vice versa[2]. Fungi can infect and colonize all plant tissues and have evolved different strategies to feed on plant-derived substrates. Broadly speaking, plant pathogens are defined as biotrophs[3], necrotrophs[4,5] and hemibiotrophs (Table 1).

Plant pathogens colonize their host by escaping host defences (induced and non-induced), which include physical and chemical barriers, and specific resistance proteins that target pathogen-produced molecules[6,7]. To avoid recognition by the host immune system and to suppress host defences, fungi secrete 'effectors' that act in the apoplastic space or the symplastic space[3]. Some effectors are translocated to cellular compartments (for example, chloroplasts or nuclei), where they manipulate host transcription to favour pathogen invasion[8,9]. Other effectors manipulate host defences by interfering with plant metabolism[10]. To counteract pathogen invasion, plants produce resistance proteins; these proteins are activated by effector-mediated signals and are responsible for signal-transduction events that activate plant defences and block pathogen growth[7]. Ultimately, the outcome of infection is determined by the ability of the pathogen to overcome the immune system of the host and the ability of the plant to block pathogen invasion[7].

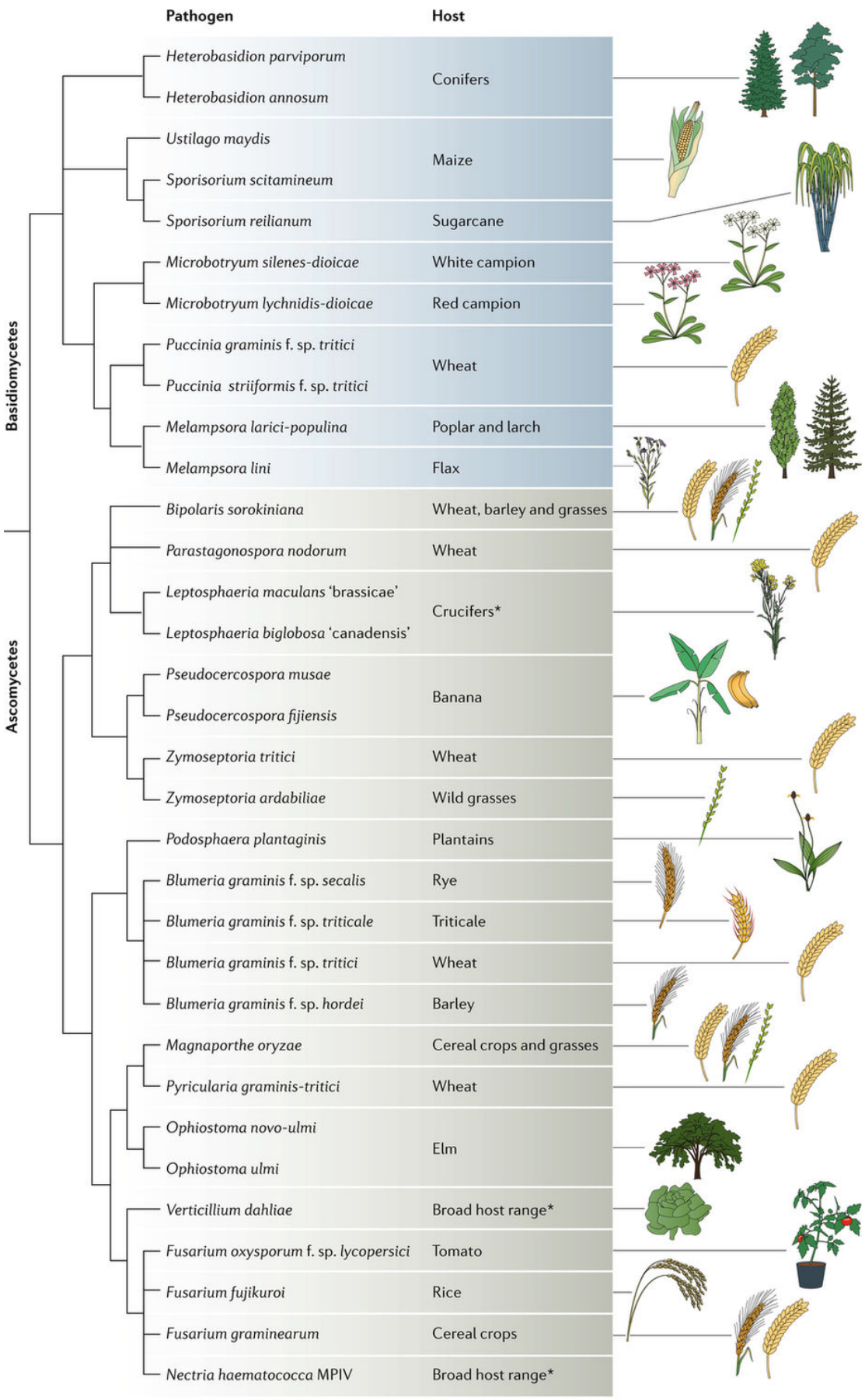

Nature Reviews | Microbiology

Figure 1. Fungal plant pathogens with diverse lifestyles and hosts. This figure shows the phylogenetic relationships between the major groups of fungal plant pathogens that belong to the two fungal phyla Ascomycetes and Basidiomycetes, and their respective host plants (right hand side). *In the case of a broad host range, the host plant of a reference isolate that was used for genome sequencing is depicted. The phylogenetic tree was generated using phyloT, based on NCBI taxonomy and visualized using interactive Tree of Life (iTOL)[137]. f. sp., *formae speciales*.

Table 1. Genome and lifestyle characteristics of different fungal plant pathogens.

Species (isolate)	Isolate-specific host	Species-specific host	Lifestyle	Reproduction	Genome size (Mb)*	% Repetitive sequence*	Genome features linked to pathogenicity‡	Refs
Sporisorium scitamineum (Sscl8)	Sugar cane	Sugar cane	Biotroph	Sexual	20	6.7	Repeat-rich gene clusters that encode effector candidates	48
Ustilago maydis (521)	Maize	Maize	Biotroph	Sexual	20	6.7	Repeat-rich gene clusters that encode effector candidates	48, 66
Microbotryum lychnidis-dioicae (p1A1 Lamole)	Red campion	Red campion	Biotroph	Sexual	33	14	Repeat-rich gene clusters that encode effector candidates	103, 104
Melampsora larici-populina (98AG31)	Poplar and larch	Poplar and larch	Biotroph	Sexual and asexual	101	45	ND#	73
Puccinia graminis f. sp. *tritici* (CDL75-36–700-3, race SCCL)	Wheat	Wheat and barley	Biotroph	Sexual and asexual	89	45	Highly polymorphic effector candidates	73
Zymoseptoria tritici (IPO323)	Wheat	Wheat	Hemi-biotroph	Sexual and asexual	40	• 18.6 (genome mean) • 16.6 (core) • 33.6 (accessory)	• Orphan regions are enriched in *in planta*-expressed genes • Possible function of accessory chromosomes in virulence	45, 57, 58
Leptosphaeria biglobosa 'canadensis' (J154)	Mustard	Crucifers	Necrotroph	Sexual and asexual	32	3.9	ND#	71
Leptosphaeria maculans 'brassicae' (v23.1.3)	Oilseed rape	Crucifers	Hemi-biotroph	Sexual and asexual	45	35.5 (99.8% of all repeats located in AT-isochores)	• Enrichment of effector candidates and chromatin-mediated effector candidate regulation in AT isochores • Conditionally dispensable chromosome contains avirulence-encoding gene	29, 60
Blumeria graminis f. sp. *tritici* (96224)	Wheat	Various	Biotroph	Sexual and asexual	180	90	Presence and/or absence of polymorphisms of candidate effectors	140, 141
Blumeria graminis f. sp. *hordei* (DH14)	Barley	Various	Biotroph	Sexual and asexual	120	64	Repeat-rich accessory regions that encode infection-specific transcribed genes	142
Magnaporthe oryzae (70–15)	Rice	Various crops and wild grasses	Hemi-biotroph	Sexual and asexual	41	10	Highly polymorphic effector candidates and translocations of effector genes	22, 143
Ophiostoma novo-ulmi (H327)	Elm	Elm	Necrotroph	Sexual and asexual	32	3.4	ND#	144
Verticillium dahliae (VdLs17)	Lettuce	Various	Necrotroph	Asexual	37	12	Enrichment of *in planta*-expressed effector candidates in LS# regions	16, 44
Fusarium solani/*Nectria haematococca* MPVI (77-13-4)	Pea	Various	Hemi-biotroph	Sexual and asexual	54	• < 5 (core) • >10–25 (supernumerary)	LS chromosomes confer host specificity and virulence	46
Fusarium graminearum (PH-1)	Wheat	Wheat and barley	Hemi-biotroph	Sexual and asexual	36	<3	Enrichment of *in planta*-expressed and species-specific genes in regions of high SNP# density	145
Fusarium oxysporum f. sp. *lycopersici* (4287)	Tomato	Various	Hemi-biotroph	Asexual	60	28 (~74% of TEs# located on LS# chromosomes)	LS chromosomes confer host specificity and virulence	43

LS, lineage-specific; ND, no data; TEs, transposable elements. *Genome size and repeat content refer to the respective reference isolate. Isolate-specific hosts refer to the host plant from which the reference isolate was collected. In some cases, other isolates of the same species infect other hosts. ‡Genome characteristics have been inferred from comparative genomics analyses.

In natural ecosystems, the antagonistic interaction between plants and their pathogens drives a co-evolutionary dynamic in which plants evolve to recognize pathogens, and pathogens evolve to avoid plant defence systems[11,12,13,14]. These co-evolutionary processes shape genetic variation at the genomic and population levels in both plants and pathogens. However, in managed ecosystems, crops evolve through artificial (rather than natural) selection, in which agriculturally desired traits are favoured. Therefore, pathogens may be confronted with the replacement of host resistance factors in each new growing season. Moreover, instant changes in the genetic make-up of host populations can occur over regional and continental scales, at which new crop cultivars are distributed. The complete replacement of host genotypes and resistance factors over large geographical areas selects for the recurrent replacement of virulence phenotypes, the fast and efficient spread of virulent pathogens (Fig. 2).

We still lack systematic comparisons of pathogens on wild and cultivated plants that assess whether agriculture selects for rapid evolution in fungal pathogens. However, comparative genomic analyses of plant and animal pathogens have revealed that fungi have the capacity to rapidly evolve and adapt to new environmental conditions[15,16,17,18,19]. In fungal plant pathogens, transposable elements and genome plasticity have been described as important drivers of rapid evolution[20,21,22], which challenges the development of sustainable management strategies for plant production and protection.

In this Review, we summarize key examples from fungal plant pathogen genomics and discuss evolutionary processes in pathogenic fungi in the light of molecular evolution, population genetics and agriculture. In addition, we consider how the field can move forward, considering the roles of genome plasticity and population genetics parameters in pathogen evolution.

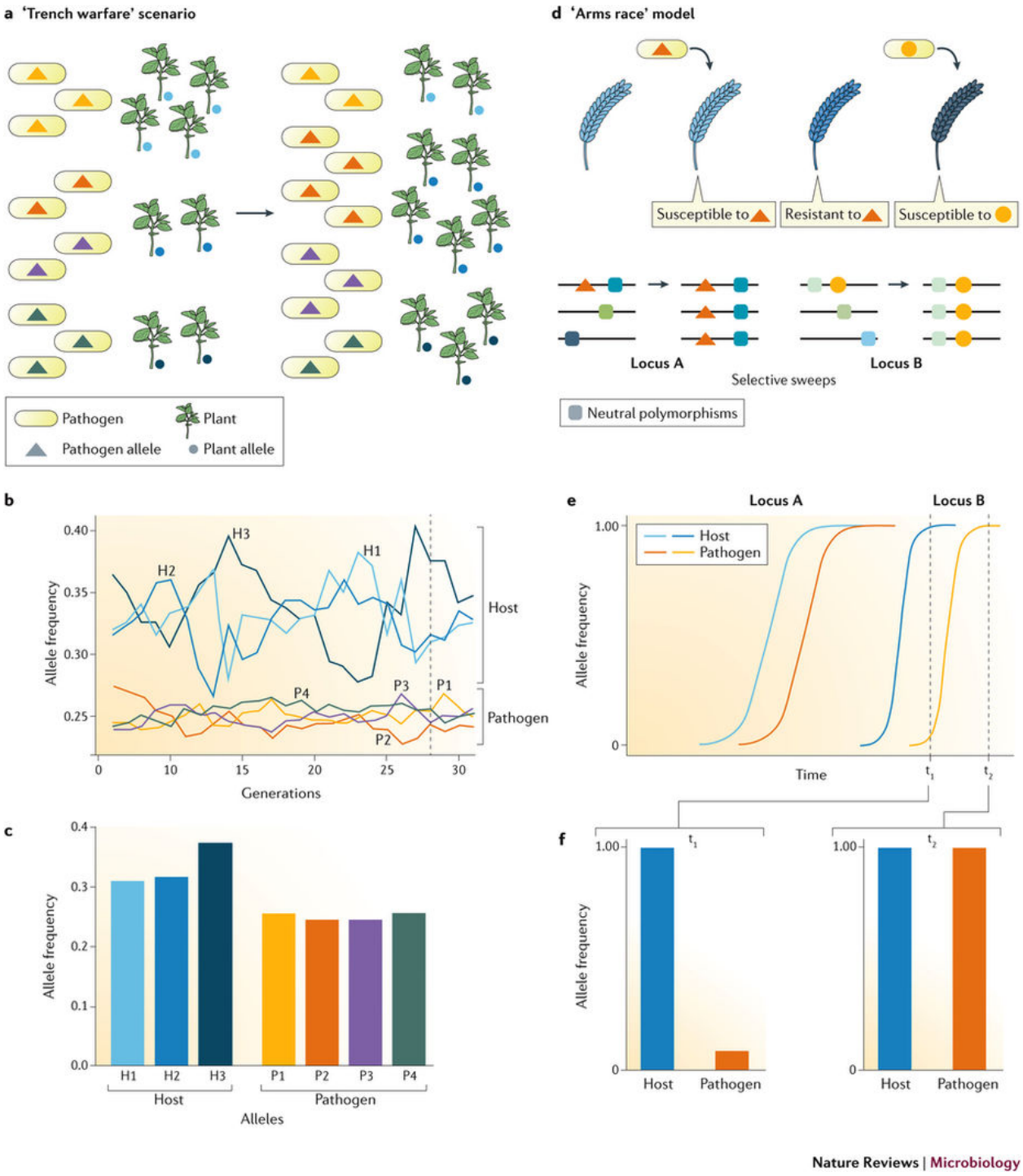

Figure 2. Models of host–pathogen co-evolution. a–c | The 'trench warfare' scenario. **a** | The trench warfare scenario can occur in heterogeneous environments, such as those present in natural ecosystems, in which local adaptation leads to a diversity of effector and resistance alleles in the host–pathogen populations that are maintained over evolutionary time. **b** | Positive diversifying selection (balancing selection) maintains multiple alleles in the host (H1, H2 and H3) and the pathogen (P1, P2, P3 and P4) populations over evolutionary time. The vertical line shows a random time point. **c** | Inference of allele frequencies at a given generation shows an excess of alleles at intermediate frequencies in the host and pathogen populations. **d–f** | 'Arms race' model. **d** | The arms race model describes the recurrent fixation of alleles at co-evolving loci in a

host–pathogen system and reflects the dynamics in agricultural ecosystems. The interactions between effectors and resistance gene products determine the outcome of pathogen infection; pathogens that have effector alleles that enable successful invasion select for new resistance alleles in the host. A new resistance allele confers a fitness advantage and is selected for by positive directional selection. The allele will reach fixation when all individuals in the host population have the respective resistance allele. A new virulence allele that confers susceptibility in the host population is strongly selected for and is fixed in the pathogen population. This cycle continues ad infinitum. Positive selection of a highly advantageous allele can result in a selective sweep (local depletion of genomic variation), as the allele is fixed in the population. **e** | In agricultural ecosystems, new alleles in the host population can be introduced very rapidly (blue lines), which drives the recurrent fixation of alleles in pathogen populations (orange and yellow lines) by positive directional selection. The vertical lines show a random time point. **f** | At the start of a new season (t_1), a crop that has a new resistance allele (blue) is introduced. In the beginning, the frequency of the respective virulence allele (orange) in the pathogen population is low, but rapidly increases until it reaches fixation (t_2).

Pathogen evolution and agriculture

Managed and natural ecosystems represent different environments for the propagation and evolution of pathogens. The host population in an agricultural field consists of densely, but uniformly (both in space and time), distributed genetically identical individuals. Moreover, cultivars of agricultural crops are genetically highly similar and mainly differ at a few loci that have been targets for selective crop breeding. By contrast, the host population in a natural ecosystem consists of genetically diverse individuals that are heterogeneously distributed in space and time.

Arabidopsis thaliana has been a valuable model for studying the co-evolutionary dynamics of plants and pathogens in natural ecosystems. Resistance genes in *A. thaliana* represent some of the most variable genes in the genome, which suggests that pathogens select for genetic variation at interacting loci[23,24]. The effect of ecological variation in wild host–pathogen systems has furthermore been extensively studied in two model pathosystems: flax–rust *Linum marginale–Melampsora lini* and *Plantago*–mildew *Plantago lanceolata–Podosphaera plantaginis*[12,25,26]. These studies have shown that both biotic (biological) and abiotic (environmental) factors contribute to the metapopulation dynamics of pathogens on wild plants. However, in both pathosystems, a main determinant of genetic variation and disease prevalence is antagonistic host–pathogen co-evolution. Consequently, metapopulation dynamics of both pathogens in a natural ecosystem are characterized by

recurrent population extinction and re-colonization events, which lead to population bottlenecks and the severe loss of genetic variation at local scales[25,26].

How do these dynamics compare with the dynamics in managed ecosystems that have uniform host distributions and in which a complete change in the genetic make-up of the host population can occur from one year to the next? The introduction of new host resistance genes in managed ecosystems can also trigger the local extinction of pathogen populations and give rise to the rapid emergence of new populations that are genetically distinct from the ancestral populations. Population genetics analyses (on the basis of temporal and spatial sampling) of the poplar rust fungus *Melampsora larici-populina* revealed substantial changes in the structure of the pathogen population, which coincided with the breakdown of a major poplar resistance gene[27]. A few virulent *M. larici-populina* isolates gave rise to this new population, which rapidly expanded and replaced the ancestral rust population on poplar trees in France within 20 years[27].

Existing pathogen populations may also rapidly evolve to overcome new host resistances. A study of the pathogen *Leptosphaeria maculans* 'brassicae', which causes blackleg disease in oilseed rape, showed how fast a new plant resistance gene can be overcome by positive selection of a mechanism that increases local genetic diversity[28]. Changes in the frequency of effector alleles in this pathogen were monitored in response to a new oilseed rape resistance gene, *RLM7*. The product of this gene, RLM7, recognizes the effector gene product AvrLm7, which is a virulence factor expressed by *L. maculans* 'brassicae' during infection. The introduction of RLM7 caused a rapid allelic diversification of *AVRLM7*, which included mutations that prevent recognition by RLM7. Over four years, the frequency of virulent *AVRLM7 L. maculans* 'brassicae' isolates increased by 40%[28]. *AVRLM7* is found in a repeat-rich genomic compartment that is characterized by an increased mutation rate; this promoted the rapid escape of host resistances[29]. Repeat-rich genome compartments are found in numerous other fungal pathogen genomes and will be described in detail below.

The rapid evolution of crop pathogens is also promoted by agricultural trade that distributes genetically identical crops between continents[30]. Not only are agricultural products moved around but also pathogens are introduced to new continents, and species that would otherwise be separated by continents come into contact with each other. The consequences of agricultural trade are recently exemplified by the emergence of the

wheat blast pathogen *Magnaporthe oryzae* (also known as *Pyricularia oryzae*) in Bangladesh[31,32]. Population genomics and phylogenetic analyses have shown that the *M. oryzae* lineage that caused the outbreak in Bangladesh originated from South America and was probably introduced through infected wheat material imported from Brazil[31]. The global movement of pathogens with crop or forestry products can also promote the emergence of new hybrid pathogens by mixing native and introduced pathogen species (for example, the emergence of Dutch elm disease). The mixing of geographically separated lineages of *Ophiostoma novo-ulmi* and *Ophiostoma ulmi* through trade gave rise to new virulent pathogens, which greatly affected the European population of elm trees[33,34].

In short, agricultural ecosystems, including managed forest systems, represent environments that are highly conducive for the rapid evolution and dispersal of fungal plant pathogens[35]. Managed ecosystems can promote large and stable populations of pathogens that can respond to rapid changes in host resistance factors by evolving new virulence traits[35]. Understanding the evolution mechanisms of plant pathogens in managed and natural ecosystems should help researchers to develop more diverse selection environments, which could slow down rates of evolution in crop pathogens[35].

Host–pathogen co-evolution

The host is the strongest driver of evolution in a pathogen, as successful infection is required for reproduction and dispersal. Therefore, infection-related genes are under strong selection pressure in pathogen genomes. Some of these genes encode conserved proteins that are important for *in planta* signalling, invasive growth and the formation of specific infection structures. Others are rapidly evolving virulence-related genes, the products of which include effectors that directly interact with plant defence proteins.

Genomic signatures of selection can be used to identify traits that are involved in host–pathogen interactions. This is because genes or loci that are subjected to strong positive or negative selection pressure can be identified by the distribution of polymorphisms (variable sites in species) and substitutions (variable sites between species), and the proportions of non-synonymous mutations and synonymous mutations in coding sequences[36]. The co-evolution of effectors and resistance genes can result in two different scenarios that are distinguished as 'trench warfare' or 'arms race' evolution[37] (Fig. 2). Both types of selection favour genetic variation, but the genomic signatures are markedly different. Several different statistical tests have been applied to search genomes for signatures of selection in plant–pathogen systems. Statistical test parameters such as Tajimas D explore the site frequency spectra of polymorphisms[38], whereas other methods contrast the patterns of intraspecific polymorphisms and interspecific divergence patterns. For example, the McDonald–Kreitmann test detects signals of selection by comparing non-synonymous and synonymous divergence to non-synonymous and synonymous polymorphisms[15].

Under the trench-warfare scenario, a diverse set of alleles are maintained at the co-evolving locus, a phenomenon that is referred to as balancing selection[39] (Fig. 2a). This may occur in heterogeneous environments (such as natural ecosystems), in which natural selection favours different alleles in distinct metapopulations (populations of the same species, which are spatially separated) that have specialized to distinct local ecological conditions. The genomic signature of balancing selection is an excess of polymorphisms at intermediate (balanced) frequencies in the population (Fig. 2b,c). Genetic variation of resistance genes in natural plant populations is, to a large extent, maintained by balancing selection[40]. An experimentally validated example is the disease resistance gene *RPP13* in *A. thaliana*. RPP13 interacts with an avirulence protein produced by the oomycete pathogen *Hyaloperonospora parasitica*. Allelic

variation in *RPP13* is maintained by balancing selection imposed by polymorphic avirulence alleles in the pathogen population[23].

Arms race evolution drives the continuous replacement of alleles (selective sweep) in the pathogen population in response to the continuous emergence of new resistance alleles in the host[39] (Fig. 2d). The genomic signature of a selective sweep is a local depletion of genetic variation in the genomic region that surrounds the locus under selection (Fig. 2e,f). During a selective sweep, neighbouring polymorphisms will also become fixed, which results in strong linkage disequilibrium across the regions. Genetic variation at the locus is re-introduced over time through recombination and by new mutations; however, the selected locus can be identified by having a different pattern of genetic variation compared with neutrally evolving loci. In particular, the selected locus will contain an excess of low-frequency alleles that can distinguish the locus from neighbouring regions. Genome-wide maps of selective sweeps were generated for the two anther smut species, *Microbotryum lychnidis-dioicae* and *Microbotryum silenes-dioicae*, using estimates of nucleotide variation, frequency-spectra of polymorphisms and statistical genetics[41]. The analyses revealed recent signatures of selective sweeps in putative pathogenicity related genes that are probably important in the host specialization of pathogenic *Microbotryum* spp.

Antagonistic host–pathogen co-evolution requires the maintenance and generation of genetic variation in both partners. The dynamic of resistance genes and virulence genes involves a combination of trench-warfare and arms race evolution. In managed ecosystems, the dynamic of arms races occurs at a much faster pace than in natural ecosystems, selecting specifically for rapid evolution in crop pathogens. Furthermore, trench-warfare evolution is probably less important in pathogens of crop plants, owing to the uniform composition and distribution in time and space of host individuals. Through the comparative analyses of genome structures and compositions, we have gained detailed insight into the genomics of adaptive evolution in several fungal pathogens and the role that genome plasticity has in evolutionary changes. Below, we summarize particular characteristics of fungal plant pathogen genomes and discuss these in the light of adaptation.

Genomic variation in fungal pathogens

Genes that are located in genomic environments with high mutation and/or recombination rates can evolve faster through the increased generation of novel mutations that selection can act on[39]. Effector genes that are located in transposable element-rich regions (which have higher mutations rates) will accumulate more mutations, some of which may be beneficial non-synonymous changes that confer a fitness advantage. Natural selection can thereby indirectly select for an association of effector genes with rapidly evolving transposable element-rich regions. Genome-based studies of plant pathogenic fungi have indeed shown that virulence-related genes are typically located in transposable element-rich genomic compartments or on specific chromosomes that have higher rates of sequence evolution[29,42,43,44] (Fig. 3; Table 1). These regions include accessory or lineage-specific chromosomes[43,45,46,47], AT-rich isochores[29], transposon-rich 'islands' (Ref. 44), and clusters of tandem duplicated genes[48]. The increased rates of evolution in particular regions of pathogen genomes have given rise to the term 'two-speed genomes' (Ref. 49). Distinct regions in pathogen genomes evolve at different rates, and the rapidly evolving compartments of plant pathogen genomes (Fig. 3) can also be seen as regions in one extreme of a continuum of evolutionary rates. Below, we describe particular characteristics of rapidly evolving pathogen genomes.

Accessory chromosomes. Accessory chromosomes show non-Mendelian inheritance and are present in some, but not all, individuals in a population (Figs 3,4). In the field of fungal genetics and phytopathology, accessory chromosomes have drawn a lot of attention as they can encode specific virulence determinants. Accessory chromosomes are typically enriched with repetitive DNA and have a lower gene density than the core genome. Moreover, accessory chromosomes encode genes that have higher incidences of non-synonymous substitutions, which indicates a lower efficacy of selection in removing non-adaptive mutations in coding sequences on these chromosomes[50]. They are found in different eukaryotic taxa, including plants, animals and fungi, and are referred to by different names, such as B-chromosomes, supernumerary chromosomes or lineage-specific chromosomes[51]. In this Review, we will use the terms accessory and lineage-specific chromosomes.

The first characterization of virulence traits encoded by an accessory chromosome was in the pathogen *Nectria haematococca* (anamorph *F. solani)*[52].
N. haematococca isolates that infect peas have an accessory chromosome that encodes cluster of pea pathogenicity (PEP) genes that are necessary for virulence in pea plants[53]. Isolates that do not have the chromosome are avirulent on peas but can infect other hosts. This indicates that the accessory chromosomes have a role in defining the host range of *N. haematococca* isolates. A related species, *F. oxysporum*, has similar accessory chromosomes, which are termed lineage-specific chromosomes, as they distinguish the specific host of the pathogen[43]. These lineage-specific chromosomes also encode effectors and effector-inducing transcription factors that are important for pathogenicity[54]. Notably, there is evidence that lineage-specific chromosomes can move horizontally and mediate the exchange of host specificities between *F. oxysporum* lineages. This is a potential mechanism that has evolved to compensate for the lack of sexual reproduction in this pathogen[43].

The genome of the reference isolate IPO323 of the wheat pathogen *Zymoseptoria tritici* has eight accessory chromosomes, which are up to 1 Mb in size and can be lost and generated *de novo* during meiosis and mitosis[45,55,56] (Fig. 4). Accessory chromosomes are found in several species in the *Zymoseptoria* genus, which suggests that they represent an ancestral dynamic trait that predates existing species diversification[15]. The accessory chromosomes of *Z. tritici* are not enriched in effector genes; however, quantitative trait locus mapping and detailed phenotyping of progeny with and without different accessory chromosomes have revealed that accessory chromosomes have a role during *in planta* disease development[57]. Strains that lacked particular chromosomes showed statistically significant increases in several virulence traits. Interestingly, preliminary data suggest that the effect of the accessory chromosomes in *Z. tritici* is dependent on host genotype, which indicates an effect of balancing selection on the maintenance of these chromosomes over long evolutionary times[15] (M. Habig and E.H.S., unpublished observations).

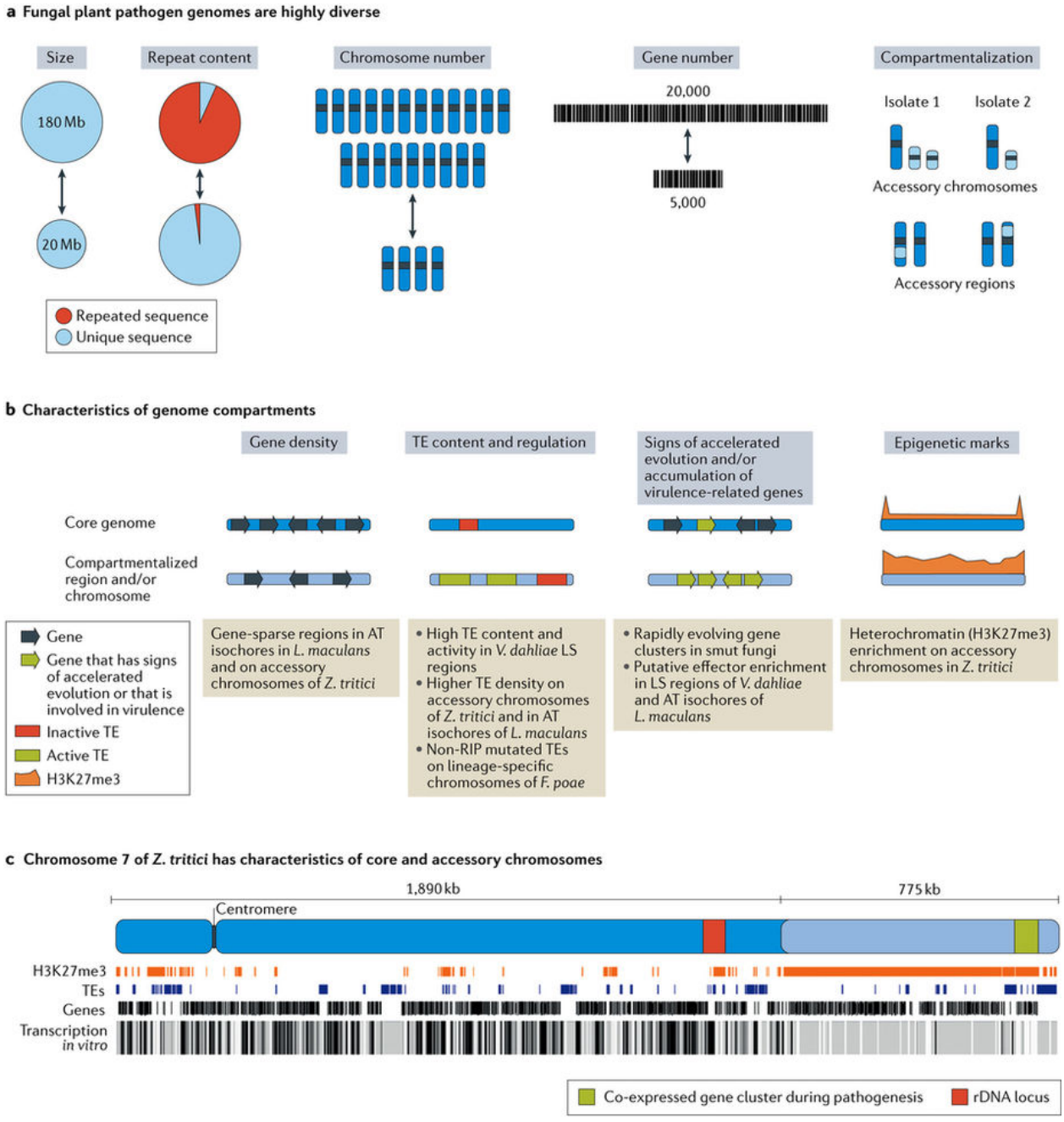

Figure 3. Characteristics of fungal plant pathogen genomes. a | The genome architecture of fungal plant pathogens is highly diverse. Genomes vary in total size, repeat content and gene number. The genome organization can vary from few chromosomes to many, and can include accessory chromosomes and particular genome compartments. **b |** Specific characteristics that distinguish genome compartments from the core genome include lower gene density, higher transposable element content, higher rates of evolution and distinct epigenetic marks[16,44,138,139]. **c |** Chromosome 7 of *Zymoseptoria tritici* has characteristics of both core and accessory chromosomes[61]. The right arm is enriched with the heterochromatin-associated histone mark H3K27me3 and is poorly transcribed[61]. A ribosomal DNA (rDNA) locus close to the start of the accessory region may be involved in the fusion of an accessory chromosome to a core chromosome. A gene cluster that is potentially involved in virulence and the

production of secondary metabolites is transcribed at the right arm of the chromosome in the accessory-like region[62]. Active transcription of the accessory chromosome region must be mediated by chromatin remodelling during infection. *F. poae*, *Fusarium poae*; *L. maculans*, *Leptosphaeria maculans*; LS, lineage-specific; RIP, repeat-induced point; TE, transposable element; *V. dahliae*, *Verticillium dahliae*. Figure adapted from Ref. 61.

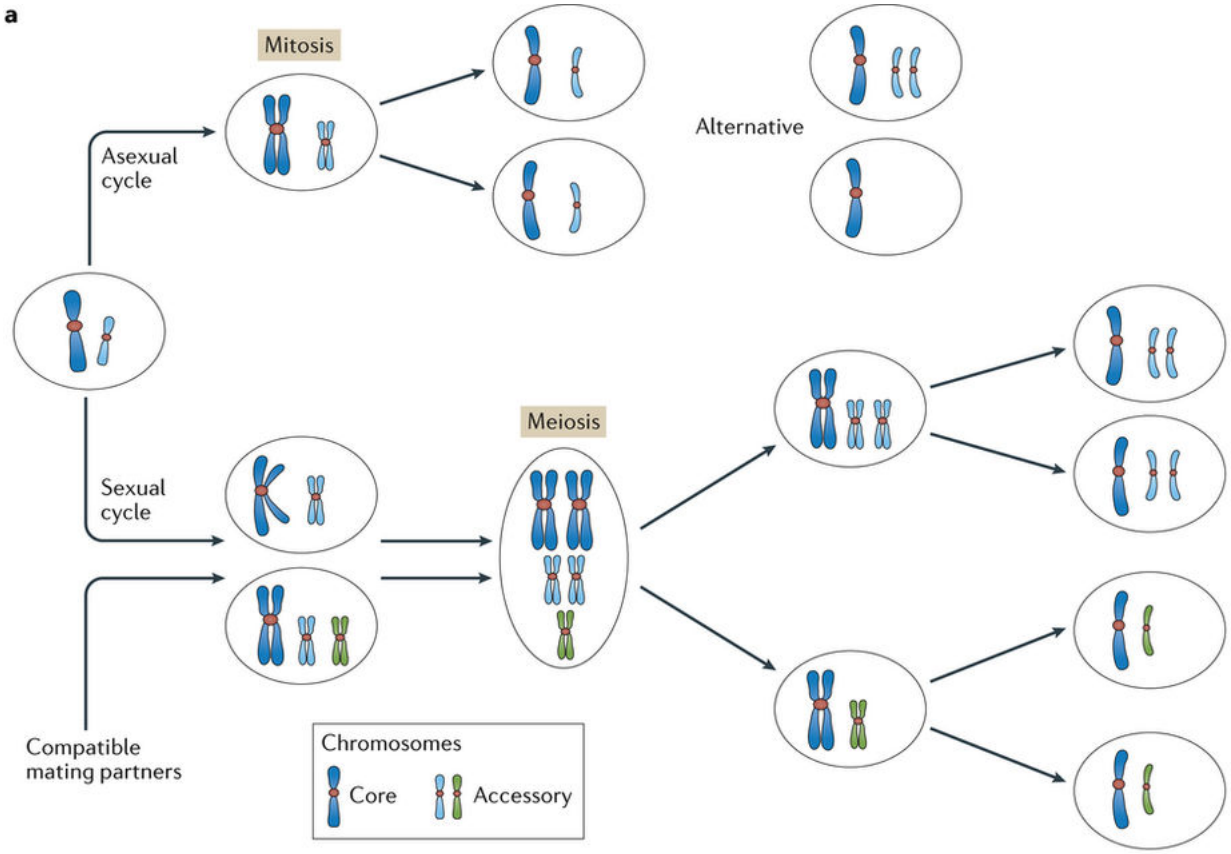

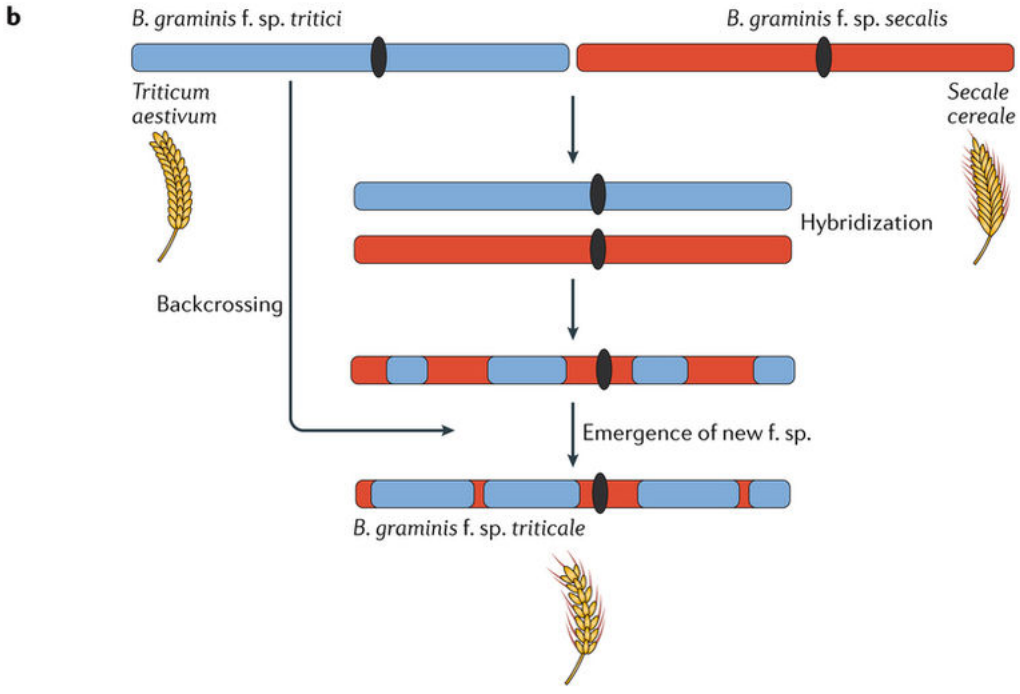

Nature Reviews | Microbiology

Figure 4. Accessory chromosome dynamics and hybridization in pathogenic fungi. **a |** The reproductive mode of fungal pathogens ranges from strictly clonal to obligate out-crossing. Many species have mixed reproductive systems and their life cycles include both asexual and sexual stages. Accessory chromosomes, which are found in several pathogenic fungal species, were shown to be lost during both mitosis and meiosis, resulting in aneuploid progeny strains[55]. The underlying mechanisms that are responsible for chromosome instability are unknown. A possible cause for chromosome loss during mitosis could be errors during the segregation of sister chromatids (alternative scenario during mitosis). **b |** Hybridization of two *Blumeria graminis* formae speciales (f. sp.), *B. graminis* f. sp. *tritici* (blue) and *B. graminis* f. sp. *secalis* (red), led to the emergence of a new pathogen, *B. graminis* f. sp. *triticale*, which infects the hybrid crop triticale; a hybrid of wheat and rye[17]. After the initial hybridization, the triticale-infecting hybrid backcrossed with *B. graminis* f. sp. *tritici*. This example illustrates an extraordinarily fast adaptation to a new host that is mediated by a combination of parental virulence factors necessary for host infection.

Transposable element-rich genome compartments. The genomes of several pathogenic fungi (pathogens of wild and cultivated hosts), include genome compartments that exist as accessory 'islands' on core chromosomes (Fig. 3). These regions can span several hundred kilobases and can encode virulence determinants[16,43,44,58,59]. Accessory compartments often resemble accessory chromosomes, as they are gene-sparse, enriched in transposable elements, and are highly variable in sequence composition and structure. In *L. maculans* 'brassicae' and *Z. tritici*, transposable element-rich genome compartments are also characterized by epigenetic modifications that further associate with distinct patterns of transcription and accumulation of mutations[60,61,62] (Box 1; Fig. 3). The source of distinct epigenetic modifications may derive from the ability of repetitive DNA to induce particular epigenetic changes[63,64] (Box 1).

Transposable element-rich genome compartments may be generated by structural rearrangements or they may evolve in regions with suppressed recombination[65]. Single-molecule real-time (SMRT) sequencing data have enabled more detailed analyses of transposable element-rich genome compartments in pathogenic fungi. In the wilt pathogen *Verticillium dahliae* and in *Z. tritici*, accessory genome compartments originate from structural rearrangements and unfaithful DNA repair across repeated sequences[44,58]. The discovery of active transposable elements in accessory compartments in *V. dahliae* further supports a role for transposable elements in shaping these genomic regions[44,58]. In *Z. tritici*, a transposable element-rich

compartment on chromosome 7 has similar sequence composition (gene density, gene annotation and GC content) and histone modifications as the accessory chromosomes of the pathogen, and may be an ancestral accessory chromosome that has fused with a core chromosome (Fig. 3c).

Pathogen genomes that have low transposable element content can also contain rapidly evolving genomic regions that favour effector evolution. The genomes of the three smut fungi *Ustilago maydis*, *Sporisorium scitamineum* and *Sporisorium reilianum*[48,66,67] have a low transposable element content (7%); however, the few transposable elements that are present are associated with virulence gene clusters[66] (Table 1). These gene clusters show signatures of accelerated evolution and gene diversification that are driven by a high rate of tandem gene duplications, which are facilitated by the repetitive DNA[48].

A local accumulation of transposable elements may occur in regions in which recombination is suppressed; for example, in non-recombining mating-type loci of heterothallic fungi[65]. Thus far, few studies have addressed recombination rates across genome compartments of pathogenic fungi, and the correlation between recombination and transposable element content has been poorly addressed. However, recombination seems to be significantly reduced in the accessory chromosomes of *Z. tritici*, which supports a role for recombination in shaping the genome architecture of fungal pathogens, including the initial emergence and maintenance of transposable element-rich compartments[68].

Box 1: Silencing of transposable elements in compartmentalized regions

In sexually reproducing populations, transposable elements can be transmitted during meiosis. Asexual lineages have a lower probability of acquiring new transposable elements; however, once invaded, they are more susceptible to their expansion and deleterious effects[126]. Different mechanisms to prevent and control the spread of transposable elements in fungal genomes have been described, which include DNA methylation, the production of small RNAs that are involved in quelling and meiotic silencing[127], and repeat-induced point (RIP) mutation[93] (see the figure). RIP mutation is a process that mutates duplicated DNA sequences in the genome through homology recognition[128,129]. Signatures of RIP mutation are C to T and G to A mutations, which have been described in several genomes of fungal plant pathogens, including both

ascomycete and basidiomycete species[29,130,131]. Experimental evidence for active RIP mutation has been shown in *Leptosphaeria maculans*[132] but is still lacking in other fungal pathogen species. Interestingly, studies of histone and DNA methylation and RIP mutation in fungal plant pathogens have revealed a correlated non-random distribution of heterochromatin, DNA methylation and RIP mutations[61,133,134].

Highly expressed effector genes have, in many cases, been shown to associate with transposable element-rich compartments. Mechanisms that enable gene transcription in the vicinity of transposable elements are therefore crucial in many plant pathogen genomes. Epigenetic modifications have been shown to have an important role in the maintenance of genome compartments and effector expression. In the genus *Zymoseptoria*, lineage-specific or accessory chromosomes show enrichment for the 'facultative' heterochromatic histone methylation mark H3K27me3 (Refs 61,135,136). Furthermore, in *Fusarium graminearum* and *Fusarium fujikuroi*, H3K27me3 has a crucial role in the regulation of genes that are related to pathogenicity[135,136]. In *Z. tritici*, H3K27me3 is significantly enriched on the accessory chromosomes but is only observed in the subtelomeric regions (the DNA immediately neighbouring the telomeres) of the core chromosomes[61]. Thus, genes on the accessory chromosomes may be regulated by chromatin modifications, similarly to genes related to pathogenicity in *Fusarium* spp. In *in vitro* experiments on *Leptosphaeria maculans* 'brassicae', another histone mark (H3K9me3) contributed to the regulation of effector genes embedded in repeat-rich DNA[60]. Marked upregulation of effector genes during plant infection suggests that dynamic chromatin modifications are associated with the pathogenic lifestyle of *L. maculans* 'brassicae'. Furthermore, in *L. maculans* 'brassicae', RIP mutation can have an important role in silencing transposable elements and in effector evolution[29].

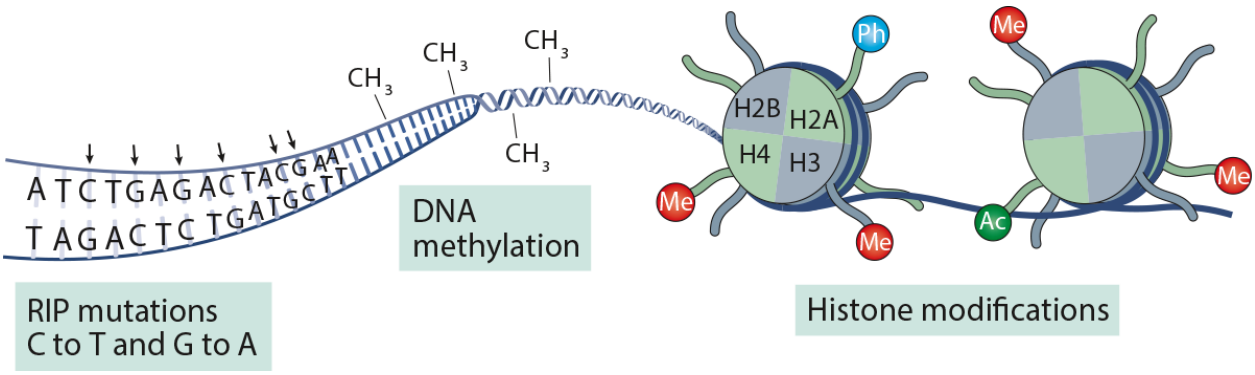

Genome architecture and plasticity. The genomes of several hundred fungal plant pathogens have been sequenced, which has provided a key resource for the analysis of genome architecture. An important discovery was that the genome architecture, notably the genome size and transposable element content, can vary greatly between closely related species. A detailed comparison of 18 genomes of species in the class Dothideomycetes (including the genomes of several prominent plant pathogens, including *Alternaria brassicicola*, *Pyrenophora tritici-repentis*, *Z. tritici* and *Cladosporium fulvum*) revealed a particular phenomenon described as mesosynteny[69]. Mesosynteny refers to the conservation of gene content in chromosomes, but variation in gene order and orientation[70]. Thus, species with mesosynteny have an excess of intra-chromosomal rearrangements. The underlying mechanisms that are responsible for this phenomenon are poorly understood, but they may relate to the specific transposition mechanisms of genomic elements that are abundant in species in the Dothideomycetes.

Another remarkable discovery among species in the Dothideomycetes is the large variation in genome sizes. Species in the *L. maculans–Leptosphaeria biglobosa* species complex are pathogens of cruciferous plants. *L. maculans* 'brassicae' is the only member that has a high transposable element content (35%)[71]. By contrast, the genomes of four other members of the *L. maculans– L. biglobosa* species complex contain less than 4% repeat sequences, which indicates a recent invasion of transposable elements in *L. maculans* 'brassicae' (Refs 29,71). Similar examples of lineage-specific expansions of transposable element families in related fungal plant pathogens include *Pseudocercospora* spp. in the Sigatoka disease complex of the banana plant[72]. Genome size variation and the distribution of different transposable element families between the three species *Pseudocercospora musae* (83 Mb), *Pseudocercospora eumusae* (54 Mb) and *Pseudocercospora fijiensis* (74 Mb), suggest that lineage-specific transposable element expansions have an important role during species divergence.

Transposable element invasions in fungal genomes can result in the expansion of certain gene families and also substantial changes in genome architecture, which includes chromosome numbers[43,73]. For example, differences in genome organization are present among plant pathogens in the genus *Fusarium*[43,74]. *Fusarium graminearum* and *F. oxysporum* represent two closely related virulent pathogens that have distinct lifestyles and markedly different genome architectures. The genome of *F.*

oxysporum (60 Mb) comprises 20% repetitive DNA and 15 chromosomes, and includes lineage-specific chromosomes[43]. By contrast, the genome of *F. graminearum* comprises only 3% repetitive DNA and a total of four chromosomes.

In summary, pathogenic fungi exhibit high levels of genome plasticity and variable genome architectures. The variation that is observed between related species is mainly due to differences in transposable element containment. Although transposable elements predominantly have negative effects on their host genome, fungal pathogens provide remarkable examples of the advantageous association between transposable elements and rapidly evolving virulence determinants. Below, we consider mechanisms that can cause the observed differences in genome architecture and transposable element content among related species.

Population genetics and evolution

The evolution of gene variants in a population is governed by a set of evolutionary forces. Essentially, genetic variation is the product of mutations and recombination that contribute to variation in the genome (Box 2). The fate of any given mutation or allele in the genome is determined by natural selection and genetic drift (stochastic events), and the relative contribution of these processes is determined by the effective population size (N_e) of the species. In terms of evolution, the N_e is more relevant than the actual number of individuals in a population. N_e expresses the degree to which gene frequencies are transmitted across generations. Thus, a large population can behave genetically similar to a small population if only a minor fraction contributes to the next generation[75]. Notably, asexual species generally have a lower N_e than sexually reproducing species, as offspring are essentially copies of their parents. In populations that have a large N_e, the effect of genetic drift is relatively small compared with populations that have a small N_e. Two important points to consider here are that the N_e of an organism can vary over time and, consequently, the importance of genetic drift in genome evolution can also vary over time.

Box 2: Determinants of genome evolution: genetic drift and selection

Genetic diversity results from mutation (including point mutations, deletions, insertions and duplications) and recombination (including chromosome crossover and heterozygote gene conversion during meiosis), which contribute to allelic variation within and among chromosomes. The fitness effect of a mutation can be classified into three categories: first, mutations can be selectively neutral, thus there is no fitness effect for individuals that have the particular mutation; second, mutations can be deleterious and reduce the fertility or survival of an individual; and, third, mutations can be advantageous and increase the fitness of an individual. The three categories comprise a continuum of fitness effects that range from completely deleterious (individuals that have the mutations either die or are infertile) to highly adaptive (individuals that have the mutations are among the only individuals that can reproduce in the population).

The fate of neutral mutations is determined purely by chance; a population genetics process termed 'genetic drift'. As biological populations have finite sizes, a mutation that evolves by genetic drift will, over time, either be lost or become spread and

ultimately fixed in the population. This process is determined by the demography of the population, its size and its variation in time (for example, population growth or bottleneck) and space (also known as population structure)[99].

Conversely, the fate of non-neutral mutations depends on their fitness, which is their relative selective advantage or disadvantage (selection coefficient '*s*'). Positively and negatively selected mutations are also affected by genetic drift, which can counteract the effect of selection. Mutations that have negative effects can therefore spread in the population by chance, whereas positively selected mutations might be lost. The relative importance of these two forces is determined by the effective population size (N_e) and the selection coefficient of mutations. In particular, genetic drift will dominate when $s < 1/4\ N_e$ (Ref. 75).

Evolution with and without sexual reproduction. The reproductive modes of fungi range from predominantly clonal to obligate out-crossing (Fig. 4; Table 1). The advantages of clonal reproduction are that co-adapted allele combinations are maintained in the population and that fit genotypes can be rapidly propagated[76]. By contrast, sexual reproduction can enable a rapid response to environmental changes by increasing the efficacy by which natural selection can fix and combine advantageous mutations[77]. In some species, sexual mating is directly linked to pathogenicity and therefore constitutes an important step in life cycles. For example, the dikaryotic filamentous structures that are required for the invasive growth of smut fungi, such as *U. maydis*, are only formed through sexual mating; therefore, cells that are unable to mate are avirulent[78]. In addition, mating can be important for the production of sexual spores, such as ascospores, basidiospores and zygospores, as dispersal propagules and for long-time survival in the environment. Below, we consider the importance of sex in the context of genome evolution.

A pattern that is shared among most sexually reproducing species is that meiotic recombination events are unevenly distributed along chromosomes. In many species, fine-scale variation in the recombination rate is due to the presence of recombination hotspots, at which crossover events tend to concentrate. In *Z. tritici*, variation in recombination rates has been studied using both experimental mating and population genomic analyses[68,79]. These studies demonstrate exceptionally high rates of recombination (~60 cM per Mb) and a high abundance of intragenic recombination

hotspots that may facilitate the rapid fixation of advantageous mutations. Preliminary data from a comparative study of *Z. tritici* and its sister species *Zymoseptoria ardabiliae* show that in *Z. tritici* the recombination rate varies across and between chromosomes, with smaller core chromosomes having a higher rate of recombination. Fine-scale variation in recombination rate is mainly explained by the distribution of recombination hotspots that frequently colocalize with genes, although these data require validation. The recombination landscapes of *Z. tritici* and its sister species *Z. ardabiliae* show some conservation, whereas recombination hotspot positions are not conserved[79] and even vary between independent crosses of *Z. tritici*[68]. The consequence of such a dynamic recombination landscape is that orthologous genes can be exposed to markedly different rates of recombination and therefore evolve at varying rates in closely related species[41]. High recombination rates and recombination hotspots in, or near, coding sequences are also found in other species, such as *M. oryzae*, *F. graminearum* and *Microbotryum violaceum*[41,80,81], which suggests that high recombination rates may be a more general mechanism to accelerate gene evolution in pathogenic fungi.

Clonal populations are sometimes considered to be 'evolutionarily impaired', because of their inability to recombine advantageous mutations that occur at independent loci in the genome. In addition, non-advantageous and deleterious mutations may accumulate in the genome in an irreversible manner, a phenomenon that is termed 'Muller's ratchet' (Ref. 82). If these are the consequences of clonal propagation, why are asexual species common and successful among fungal plant pathogens?

Studies are required to understand the long-term evolutionary processes in asexual fungal pathogens. However, the association between transposable elements and effector genes suggests that high mutation rates in repetitive genome compartments support effector innovation and adaptation, as shown in clonal populations of the rice blast pathogen *M. oryzae* and the *Fusarium* wilt pathogen *F. oxysporum*[29,42,43]. The complete fitness effects of mutations that are mediated by transposable elements have not been assessed in fungal pathogens. However, transposable elements also cause non-adaptive and deleterious changes that reduce the fitness of the host. Population genomic data of well-assembled fungal genomes and measures of mutational fitness effects are required to address the effects of transposable elements on adaptive evolution.

Another factor to consider is the time span of asexual reproduction[83]. Evidence of rare or cryptic sex has been documented in asexual species, such as *V. dahliae* and *F. oxysporum*, by analyses of multilocus genotypes, mating-type frequencies and the conservation of meiosis-related genes[84,85]. Furthermore, unisexual mating, in which meiotic basidiospores are produced from the fusion of mitotically produced nuclei, has been documented in the otherwise heterothallic human pathogen *Cryptococcus neoformans*[86]. These findings suggest that recombination, even if rare or occurring as unisexual or parasexual reproduction, may counteract the effect of Muller's ratchet and contribute to adaptive evolution in species that are otherwise predominantly clonal.

Interestingly, sexual reproduction has been lost or decreased in several important crop pathogens that have evolved from sexual progenitors on wild hosts[87,88,89]. The loss of sexual reproduction in the rice blast pathogen *M. oryzae* and the rust fungus *Puccinia striiformis* forma specialis (f. sp.) *tritici* coincided with the emergence of clonal linages that successfully achieved global spread on agricultural hosts[87,90]. However, in Asia, the population genetics structure of these species is characterized by sexual recombination and high levels of genetic variation[91,92]. As Asia is the point of origin for both pathogens, the sexual populations probably reflect the ancestral population biology of both species. To what extent the clonality of many crop pathogens is a product of agricultural environments remains unclear and can only be elucidated by further population genetics studies of pathogens of wild plants.

The origin of transposable element invasions and expansions. Transposable elements are mobile genetic elements that replicate by invading the genome of a host cell. Most transposable elements exert negative effects, as they replicate and can be inserted into functionally important DNA, which can be damaging to the host organism. Fungi have evolved a wide range of genome defence mechanisms to silence transposable elements, including DNA methylation, heterochromatin, repeat-induced point (RIP) mutation and small RNAs[93] (Box 1). Interestingly, these mechanisms exhibit variability between closely related species, which suggests another layer of variation in genome evolution and variation in the co-evolution of transposable elements and the host cell[94].

Closely related species can vary considerably in the composition and abundance of transposable element families. The composition of these families can vary from the

lineage-specific dynamics of ancestral transposable elements or from lineage-specific introductions of transposable elements through infection and horizontal transfer (for example, endogenous retroviruses)[95,96]. In addition, expansions of transposable elements may be caused by different conditions. At the mechanistic level, transposable elements may be activated by various environmental stresses[97], or they may expand when genome defences become inactivated or less efficient[94]. In terms of population genetics, transposable element expansions can occur during prolonged asexual reproduction, as deleterious mutations, such as an increase in the copy number of transposable elements, accumulate in the genome in the absence of sexual recombination[98]. An increase in the strength of genetic drift, which can occur in organisms that have low N_e, may also result in the expansion of transposable elements[99].

Correlation analyses of genome sizes and N_e using data from many different taxa have shown that multicellular organisms with large genomes generally have smaller N_e and contain more transposable elements than those with small genomes[75]. A model that was proposed to explain these correlations posits that a new mutation (for example, the insertion or transposition of a transposable element that has a selective disadvantage, with a selection coefficient (s) <0) can be fixed by genetic drift despite being under negative selection pressure if the product $N_e \times s$ is small[99]. This can be explained by the reduced efficacy of selection and the increased effect of genetic drift in organisms that have a small N_e (Box 2). Therefore, the invasion and proliferation of transposable elements in pathogens may have occurred during periods in which the N_e was small. A small N_e can be the product of a population bottleneck or of asexual reproduction; features that are both frequently observed in fungal plant pathogens[87,89,90,100,101].

Across the genome, the strength of genetic drift and selection may vary. This difference primarily results from variation in recombination across the genome. Just as asexual species may accumulate more transposable elements, regions in the genome that recombine less may also accumulate more transposable elements and non-adaptive mutations as a consequence of stronger genetic drift and a lower efficacy of selection. A model to illustrate this phenomenon is provided by dimorphic mating-type chromosomes that carry genes that are responsible for mating compatibility[65,102]. Dimorphic mating chromosomes and mating-type loci are characterized by a

suppression of recombination, which has fundamental consequences for the evolution of these chromosomes. For example, in *Neurospora tetrasperma*, genes that are encoded by the *mat a* and *mat A* chromosomes have an excess of allele-specific non-synonymous codon substitutions; this is consistent with less efficient negative selection and linkage disequilibrium in these non-recombination regions[102]. Furthermore, in the smut fungus *M. lychnidis-dioicae*, mating-type chromosomes are also characterized by an accumulation of non-synonymous substitutions, and an excess of repetitive DNA and structural rearrangements[65,103,104]. These features resemble the evolutionary patterns in transposable element-rich compartments, including accessory chromosomes and repeat islands, and illustrate how the suppression of recombination may support the emergence and maintenance of rapidly evolving genome compartments.

In summary, genome analyses have shown that compartmentalized genomes in many fungal plant pathogens originate from transposable element invasions and expansions. Variation in population genetics parameters (including natural selection and genetic drift) can explain the different quantitative and qualitative distributions of transposable elements in fungal species. In particular, population bottlenecks that result in low N_e and prolonged clonal reproduction may favour the invasion and expansion of transposable elements in pathogen genomes. Last, it has also been proposed that transposable element invasion in the genomes of fungal plant pathogens could involve selection beyond the species level, with species that have higher levels of transposable elements being less likely to become extinct[49]. However, the evolutionary relevance of such 'clade -selection' is debated[105].

Heterokaryons and heterozygosity. The examples above build on the genome analyses of haploid genome sequences. Indeed, the nuclei and hyphae of many fungal pathogens are haploid, except during transient diploid stages that form during sexual life cycles. However, many ascomycete and basidiomycete fungi have heterokaryotic life stages, in which genetically distinct nuclei coexist within the same cell; this provides another layer of genetic variation. Heterokaryons may arise through mating or hyphal fusion of homokaryotic individuals, and represent a more complex association of the two parental genomes relative to diploidy[106]. Interestingly, experimental mating of genetically distinct homokaryons of the pathogenic white rot fungus *Heterobasidion parviporum* showed that nuclear ratios in heterokaryons

frequently deviate from a 1:1 ratio and that the environment can affect the frequencies of nuclei[107]. The underlying nuclear ratio in *H. parviporum* heterokaryons affects gene expression and growth rate, and also potentially affects virulence, as shown in heterokaryons of *Heterobasidion annosum*, which is the causative agent of root and butt rot in conifers[108].

Another interesting example can be found in the life cycle of agriculturally important rust fungi that have complex life cycles that often involve two hosts and the production of several types of spore, including haploid pycniospores (n), dikaryotic aeciospores ($n + n$) and diploid ($2n$) teliospores. The wheat stripe rust fungus *P. striiformis* f. sp. *tritici* infects wheat by dikaryotic aeciospores produced on the alternative host *Berberis vulgaris*. During infection of wheat, the pathogen propagates asexually to produce dikaryotic urediniospores or diploid teliospores that function as inoculum for new infections on wheat and *B. vulgaris*, respectively[88]. Genome sequencing and assembly of the diploid asexual stage identified regions of exceptionally high heterozygosity[109]. How this is advantageous for pathogenicity is unclear; however, the asexual form of *P. striiformis* f. sp. *tritici* may benefit from variation in heterozygous genomic regions. The genetic and functional dissection of the dikaryotic, diploid and haploid stages of rust fungi life cycles are required to understand the importance of nuclear variability in virulence.

Hybridization, introgression and horizontal gene transfer. Hybridization refers to the fusion or mating of non-conspecific individuals[110]. Recurrent backcrossing between hybrids and parental species is referred to as introgression, and both hybridization and introgression are thought to be important for the evolution of fungal plant pathogens. Both can occur when intersterility is incomplete, which enables sexual mating or cellular fusion between non-conspecific lineages. Under the appropriate conditions, the outcome of introgression or hybridization can be successful, which may generate new lineages or new adaptive traits in existing species. Hybridization can involve both sexual and asexual interactions. Homoploid hybrids may emerge from sexual mating, which results in hybrids that have the same chromosome number as the parental species[111]. By contrast, in heteroploid hybrids, both parental genomes are entirely or partially maintained, which results in aneuploid or polyploid hybrids[112,113].

Phylogenetic studies and comparative genome analyses have provided several examples of hybrid fungal plant pathogens that have originated from interspecific mating[110,114]. Hybrids can propagate as new distinct lineages if they are fertile, can compete with coexisting parental species and may have adaptive traits that enable them to colonize a new host. In some cases, hybrids can represent transient stages that backcross with the parental species and function as a 'bridge' for the transfer of genetic material from one species to the other through 'introgressive hybridization' (Refs 110,115) (Fig. 4). This is typically the outcome if the fitness of the hybrid is inferior to the parental species. However, hybrid genetic elements may persist and increase in frequency if they confer a selective advantage.

An interesting example of hybridization is provided by a recent population genomics study of the cereal mildew pathogen *Blumeria graminis*. This revealed an unusual distribution of SNPs in *B. graminis* f. sp. *triticale*[17], a lineage that infects triticale (a hybrid of wheat and rye) (Fig. 4). The genome of *B. graminis* f. sp. *triticale* comprises a mosaic of *B. graminis* f. sp. *tritici* and *B. graminis* f. sp. *secalis* genomic segments with only a small number of private polymorphisms (not present in *B. graminis* f. sp. *tritici* and *B. graminis* f. sp. *secalis*), which is consistent with a recent hybridization event[17]. The results from this study suggested that after initial hybridization (between *B. graminis* f. sp. *tritici* and *B. graminis* f. sp. *secalis*) the triticale-infecting hybrid backcrossed a few times with the parental *B. graminis* f. sp. *tritici*. The recent emergence of *B. graminis* f. sp. *triticale* (within the past 30 years) shows the rapid adaptation of a hybrid fungal plant pathogen to a new hybrid host.

With the availability of genome sequences from many different taxa, there is increasing evidence of multiple gene transfers between species and even between kingdoms[116]. Notably, horizontal gene transfer has been identified between fungal plant pathogens. For example, *Parastagonospora nodorum* and *Pyrenophora tritici-repentis* are wheat pathogens, and both have an almost identical effector gene that is involved in host susceptibility, known as ToxA[117,118,119]. Comparative genome analyses and population genetics analyses of the *TOXA* allele revealed that it was inserted in the *P. tritici-repentis* genome through horizontal gene transfer from *P. nodorum*[117]. In this case, the transfer probably occurred either through hyphal fusion or from a wheat-associated vector, such as a virus or bacterium. Interestingly, *TOXA* was identified in the genome of a third wheat pathogen, *Bipolaris sorokiniana*[120], and thus is an example of a gene

that is readily taken up by different wheat pathogens to induce host susceptibility[119]. Studies have revealed similar signatures of horizontal gene transfer in the genomes of other fungal plant pathogens. The abundance of phylogenetic 'outlier' genes suggests that the acquisition of foreign DNA from other fungi, bacteria or plants can contribute to genome and phenotype evolution[121,122,123]. However, evidence for mechanisms of horizontal gene transfer in fungi is sparse and further studies are necessary to validate the importance of this process in genome evolution[43].

Conclusions and outlook

So far, our research on the genomes of fungal plant pathogens has been descriptive and has focused on the diversity of mechanisms that promote the rapid evolution of pathogenicity related traits. However, the underlying population genetics processes that have been important in shaping genome architecture in pathogens are still poorly understood; understanding them will require improved models for the inference of mutational and recombination processes. These should incorporate the particularities of fungal pathogen genomes, including high and variable mutation and recombination rates, marked variation in transposable element content and genome compartmentalization.

Given the discovery of substantial levels of genome plasticity, fungal plant pathogens currently function as model organisms to address fundamental questions in evolutionary biology beyond plant pathology, such as the importance of sexual reproduction, the evolution of gene organization, and chromosomal stability and integrity[44,48,58]. This understanding may also have relevance to cancer research. Cancer cells are known to accumulate a wide range of somatic mutations, including whole chromosome duplications and losses, and structural rearrangements. Fungal pathogens may, with their highly dynamic genomes, function as new models in the research of cancer cell evolution[124,125].

Finally, agriculture can markedly affect demographic fluctuations of crop-associated pathogens by providing homogeneous environments, which may be conducive for the evolution and dispersal of pathogens. We need to improve our understanding of the effect of environmental conditions on the population genetics structure of plant pathogens. Changes in population genetics parameters over time may have a crucial role in shaping genome architecture, including advantageous associations between transposable elements and rapidly evolving effector genes.

References

1. Fisher, M., Henk, D. & Briggs, C. Emerging fungal threats to animal, plant and ecosystem health. *Nature* **484**, 186–194 (2012).
2. James, T. Y. *et al.* Reconstructing the early evolution of Fungi using a six-gene phylogeny. *Nature* **443**, 818–822 (2006).
3. Lo Presti, L. *et al.* Fungal effectors and plant susceptibility. *Annu. Rev. Plant Biol.* **66**, 513–545 (2015).
4. Wolpert, T. J., Dunkle, L. D. & Ciuffetti, L. M. Host-selective toxins and avirulence determinants: what's in a name? *Annu. Rev. Phytopathol.* **40**, 251–285 (2002).
5. Friesen, T. L., Faris, J. D., Solomon, P. S. & Oliver, R. P. Host-specific toxins: effectors of necrotrophic pathogenicity. *Cell. Microbiol.* **10**, 1421–1428 (2008).
6. Javelle, M., Vernoud, V., Rogowsky, P. M. & Ingram, G. C. Epidermis: the formation and functions of a fundamental plant tissue. *New Phytol.* **189**, 17–39 (2011).
7. Jones, J. D. & Dangl, J. L. The plant immune system. *Nature* **444**, 323–329 (2006).
8. Weiberg, A. *et al.* Fungal small RNAs suppress plant immunity by hijacking host RNA interference pathways. *Science* **342**, 118–123 (2013).
9. Manning, V. A. & Ciuffetti, L. M. Localization of Ptr ToxA produced by *Pyrenophora tritici-repentis* reveals protein import into wheat mesophyll cells. *Plant Cell* **17**, 3203–3212 (2005).
10. Djamei, A. *et al.* Metabolic priming by a secreted fungal effector. *Nature* **478**, 395–398 (2011).
11. Bergelson, J., Kreitman, M., Stahl, E. A. & Tian, D. Evolutionary dynamics of plant *R*-genes. *Science* **292**, 2281–2285 (2001).
12. Barrett, L. G. *et al.* Diversity and evolution of effector loci in natural populations of the plant pathogen *Melampsora lini*. *Mol. Biol. Evol.* **26**, 2499–2513 (2009).
13. Dodds, P. N. *et al.* Direct protein interaction underlies gene-for-gene specificity and coevolution of the flax resistance genes and flax rust avirulence genes. *Proc. Natl Acad. Sci. USA* **103**, 8888–8893 (2006).
14. Kanzaki, H. *et al.* Arms race co-evolution of *Magnaporthe oryzae AVR-Pik* and rice *Pik* genes driven by their physical interactions. *Plant J.* **72**, 894–907 (2012).
15. Stukenbrock, E. H. *et al.* The making of a new pathogen: Insights from comparative population genomics of the domesticated wheat pathogen *Mycosphaerella graminicola* and its wild sister species. *Genome Res.* **21**, 2157–2166 (2011).
16. de Jonge, R. *et al.* Extensive chromosomal reshuffling drives evolution of virulence in an asexual pathogen. *Genome Res.* **23**, 1271–1282 (2013).
17. Menardo, F. *et al.* Hybridization of powdery mildew strains gives rise to pathogens on novel agricultural crop species. *Nat. Genet.* **48**, 201–205 (2016).
This study provides an example of rapid adaptation to new host plants. The hybridization of two *Blumeria graminis* formae speciales resulted in the emergence of a new pathogen that infects a hybrid crop of wheat and rye.
18. Selmecki, A., Forche, A. & Berman, J. Genomic plasticity of the human fungal pathogen *Candida albicans. Eukaryot. Cell* **9**, 991–1008 (2010).
19. Farrer, R. A. *et al.* Multiple emergences of genetically diverse amphibian-infecting chytrids include a globalized hypervirulent recombinant lineage. *Proc. Natl Acad. Sci. USA* **108**, 18732–18736 (2011).
20. Raffaele, S. & Kamoun, S. Genome evolution in filamentous plant pathogens: why bigger can be better. *Nat. Rev. Microbiol.* **10**, 417–430 (2012).
21. Seidl, M. F. & Thomma, B. P. Sex or no sex: evolutionary adaptation occurs regardless. *Bioessays* **36**, 335–345 (2014).

22. Galazka, J. M. & Freitag, M. Variability of chromosome structure in pathogenic fungi — of 'ends and odds'. *Curr. Opin. Microbiol.* **20**, 19–26 (2014).
23. Allen, R. L. *et al.* Host–parasite coevolutionary conflict between *Arabidopsis* and Downy Mildew. *Science* **306**, 1957–1960 (2004).
24. Cao, J. *et al.* Whole-genome sequencing of multiple *Arabidopsis thaliana* populations. *Nat. Genet.* **43**, 956–963 (2011).
25. Thrall, P. H. *et al.* Rapid genetic change underpins antagonistic coevolution in a natural host–pathogen metapopulation. *Ecol. Lett.* **15**, 425–435 (2012).
26. Laine, A.-L., Burdon, J. J., Nemri, A. & Thrall, P. H. Host ecotype generates evolutionary and epidemiological divergence across a pathogen metapopulation. *Proc. R. Soc. B Biol. Sci.* **281**, 20140522 (2014).
27. Persoons, A. *et al.* The escalatory Red Queen: population extinction and replacement following arms-race dynamics in poplar rust. *Mol. Ecol.* **26**, 1902–1918 (2016).
28. Daverdin, G. *et al.* Genome structure and reproductive behaviour influence the evolutionary potential of a fungal phytopathogen. *PLoS Pathog.* **8**, e1003020 (2012).
29. Rouxel, T. *et al.* Effector diversification within compartments of the *Leptosphaeria maculans* genome affected by Repeat-Induced Point mutations. *Nat. Commun.* **2**, 202 (2011).
30. Brown, J. K. & Hovmøller, M. S. Aerial dispersal of pathogens on the global and continental scales and its impact on plant disease. *Science* **297**, 537–541 (2002).
31. Islam, M. T. *et al.* Emergence of wheat blast in Bangladesh was caused by a South American lineage of *Magnaporthe oryzae*. *BMC Biol.* **14**, 84 (2016).
32. Castroagudin, V. L. *et al.* Wheat blast disease caused by *Pyricularia graminis-tritici* sp. nov. Preprint at *bioRxiv* http://dx.doi.org/10.1101/051151 (2016).
33. Brasier, C. M. Rapid evolution of introduced plant pathogens via interspecific hybridization. *Bioscience* **51**, 123 (2001).
34. Brasier, C. M. & Kirk, S. A. Rapid emergence of hybrids between the two subspecies of *Ophiostoma novo-ulmi* with a high level of pathogenic fitness. *Plant Pathol.* **59**, 186–199 (2010).
35. McDonald, B. A. & Stukenbrock, E. H. Rapid emergence of pathogens in agro-ecosystems: global threats to agricultural sustainability and food security. *Phil. Trans. R. Soc. B* **371**, 20160026 (2016).
36. Stukenbrock, E. H. Evolution, selection and isolation: a genomic view of speciation in fungal plant pathogens. *New Phytol.* **199**, 895–907 (2013).
37. Brown, J. K. & Tellier, A. Plant–parasite coevolution: bridging the gap between genetics and ecology. *Annu. Rev. Phytopathol.* **49**, 345–367 (2011).
38. Hörger, A. C. *et al.* Balancing selection at the tomato *RCR3* guardee gene family maintains variation in strength of pathogen defense. *PLoS Genet.* **8**, e1002813 (2012).
39. Tellier, A., Moreno-Gámez, S. & Stephan, W. Speed of adaptation and genomic footprints of host– parasite coevolution under arms race and trench warfare dynamics. *Evolution.* **68**, 2211–2224 (2014).
40. Van der Hoorn, R. A., De Wit, P. J. & Joosten, M. H. Balancing selection favors guarding resistance proteins. *Trends Plant Sci.* **7**, 67–71 (2002).
41. Badouin, H. *et al.* Widespread selective sweeps throughout the genome of model plant pathogenic fungi and identification of effector candidates. *Mol. Ecol.* **26**, 2041–2062 (2016).
42. Chuma, I. *et al.* Multiple translocation of the *AVR-Pita* effector gene among chromosomes of the rice blast fungus *Magnaporthe oryzae* and related species. *PLoS Pathog.* **7**, e1002147 (2011).

43. Ma, L.-J. *et al.* Comparative genomics reveals mobile pathogenicity chromosomes in *Fusarium*. *Nature* **464**, 367–373 (2010).
44. Faino, L. *et al.* Transposons passively and actively contribute to evolution of the two-speed genome of a fungal pathogen. *Genome Res.* **26**, 1091–1100 (2016).
This study describes the importance of transposable elements in the formation of lineage-specific regions and their differential regulation in distinct genome compartments in *V. dahliae.*
45. Goodwin, S. B. *et al.* Finished genome of the fungal wheat pathogen *Mycosphaerella graminicola* reveals dispensome structure, chromosome plasticity, and stealth pathogenesis. *PLoS Genet.* **7**, e1002070 (2011).
46. Coleman, J. J. *et al.* The genome of *Nectria haematococca*: contribution of supernumerary chromosomes to gene expansion. *PLoS Genet.* **5**, e1000618 (2009).
47. Williams, A. H. *et al.* Comparative genomics and prediction of conditionally dispensable sequences in legume-infecting *Fusarium oxysporum formae speciales* facilitates identification of candidate effectors. *BMC Genomics* **17**, 191 (2016).
48. Dutheil, J. Y. *et al.* A tale of genome compartmentalization: the evolution of virulence clusters in smut fungi. *Genome Biol. Evol.* **8**, 681–704 (2016).
This study provides details of the evolution of virulence-associated gene clusters in *S. scitamineum* that are driven by tandem gene duplication and transposable elements.
49. Dong, S., Raffaele, S. & Kamoun, S. The two-speed genomes of filamentous pathogens: waltz with plants. *Curr. Opin. Genet. Dev.* **35**, 57–65 (2015).
50. Stukenbrock, E. H. *et al.* Whole-genome and chromosome evolution associated with host adaptation and speciation of the wheat pathogen *Mycosphaerella graminicola*. *PLoS Genet.* **6**, e1001189 (2010).
51. Houben, A., Banaei-Moghaddam, A. M., Klemme, S. & Timmis, J. N. Evolution and biology of supernumerary B chromosomes. *Cell. Mol. Life Sci.* **71**, 467–478 (2014).
52. Miao, V. P., Covert, S. F. & VanEtten, H. D. A fungal gene for antibiotic resistance on a dispensable ('B') chromosome. *Science* **254**, 1773 (1991).
53. Temporini, E. D. & VanEtten, H. D. Distribution of the pea pathogenicity (*PEP*) genes in the fungus *Nectria haematococca* mating population VI. *Curr. Genet.* **41**, 107–114 (2002).
54. van der Does, H. C. *et al.* Transcription factors encoded on core and accessory chromosomes of *Fusarium oxysporum* induce expression of effector genes. *PLoS Genet.* **12**, e1006401 (2016).
55. Wittenberg, A. H. J. *et al.* Meiosis drives extraordinary genome plasticity in the haploid fungal plant pathogen *Mycosphaerella graminicola*. *PLoS ONE* **4**, e5863 (2009).
56. Croll, D., Zala, M. & McDonald, B. A. Breakage– fusion–bridge cycles and large insertions contribute to the rapid evolution of accessory chromosomes in a fungal pathogen. *PLoS Genet.* **9**, e1003567 (2013).
57. Stewart, E. l. *et al.* Quantitative trait locus mapping reveals complex genetic architecture of quantitative virulence in the wheat pathogen *Zymoseptoria tritici*. *Mol. Plant Pathol.* http://dx.doi.org/10.1111/ mpp.12515 (2017).
58. Plissonneau, C. & Stürchler, A. The evolution of orphan regions in genomes of a fungal pathogen of wheat. *mBio* **7**, e01231-16 (2016).
In this study, comparison of the genome structure of two *Z. tritici* isolates identifies large chromosomal inversions and losses and/or gains of transposable element clusters, which highlights intraspecies genome diversity.

59. Chiara, M. *et al.* Genome sequencing of multiple isolates highlights subtelomeric genomic diversity within *Fusarium fujikuroi*. *Genome Biol. Evol.* **7**, 3062–3069 (2015).
60. Soyer, J. L. *et al.* Epigenetic control of effector gene expression in the plant pathogenic fungus *Leptosphaeria maculans*. *PLoS Genet.* **10**, e1004227 (2014).
Effectors in *L. maculans* are located in AT-rich genome compartments. In this study, their regulation is shown to be mediated by the presence and absence of heterochromatin during infection.
61. Schotanus, K. *et al.* Histone modifications rather than the novel regional centromeres of *Zymoseptoria tritici* distinguish core and accessory chromosomes. *Epigenetics Chromatin* **8**, 1 (2015).
In this study, Genome-wide comparison of histone methylation marks reveals distinct patterns of the facultative heterochromatin mark H3K27me3 on core and accessory chromosomes.
62. Kellner, R. *et al.* Expression profiling of the wheat pathogen *Zymoseptoria tritici* reveals genomic patterns of transcription and host-specific regulatory programs. *Genome Biol. Evol.* **6**, 1353–1365 (2014).
63. Miao, V. P., Freitag, M. & Selker, E. U. Short TpA-rich segments of the ζ-η region induce DNA methylation in *Neurospora crassa. J. Mol. Biol.* **300**, 249–273 (2000).
64. Tamaru, H. & Selker, E. U. Synthesis of signals for *de novo* DNA methylation in *Neurospora crassa. Mol. Cell. Biol.* **23**, 2379–2394 (2003).
65. Fontanillas, E. *et al.* Degeneration of the non-recombining regions in the mating-type chromosomes of the anther-smut fungi. *Mol. Biol. Evol.* **32**, 928–943 (2014).
66. Kämper, J. *et al.* Insights from the genome of the biotrophic fungal plant pathogen *Ustilago maydis*. *Nature* **444**, 97–101 (2006).
67. Schirawski, J. *et al.* Pathogenicity determinants in smut fungi revealed by genome comparison. *Science* **330**, 1546–1548 (2010).
68. Croll, D., Lendenmann, M. H., Stewart, E. & McDonald, B. A. The impact of recombination hotspots on genome evolution of a fungal plant pathogen. *Genetics* **201**, 1213–1228 (2015).
69. Ohm, R. A. *et al.* Diverse lifestyles and strategies of plant pathogenesis encoded in the genomes of eighteen *Dothideomycetes fungi*. *PLoS Pathog.* **8**, e1003037 (2012).
70. Hane, J. K. *et al.* A novel mode of chromosomal evolution peculiar to filamentous *Ascomycete fungi*. *Genome Biol.* **12**, 1 (2011).
71. Grandaubert, J. *et al.* Transposable element-assisted evolution and adaptation to host plant within the *Leptosphaeria maculans–Leptosphaeria biglobosa* species complex of fungal pathogens. *BMC Genomics* **15**, 891 (2014).
This study shows that the expansion of transposable elements in one member of the *L. maculans–L. biglobosa* species complex correlates to the evolution of pathogenicity in this species.
72. Chang, T.-C. *et al.* Comparative genomics of the sigatoka disease complex on banana suggests a link between parallel evolutionary changes in *Pseudocercospora fijiensis* and *Pseudocercospora eumusae* and increased virulence on the banana host. *PLoS Genet.* **12**, e1005904 (2016).
73. Duplessis, S. *et al.* Obligate biotrophy features unraveled by the genomic analysis of rust fungi. *Proc. Natl Acad. Sci. USA* **108**, 9166–9171 (2011).
74. Niehaus, E.-M. *et al.* Comparative 'omics' of the *Fusarium fujikuroi* species complex highlights differences in genetic potential and metabolite synthesis. *Genome Biol. Evol.* **8**, 3574 (2016).
75. Lynch, M. & Walsh, B. *The origins of genome architecture* (Sinauer Associates Sunderland, 2007).

76. McDonald, B. A. & Linde, C. Pathogen population genetics, evolutionary potential, and durable resistance. *Annu. Rev. Phytopathol.* **40**, 349–379 (2002).
77. Marais, G. & Charlesworth, B. Genome evolution: recombination speeds up adaptive evolution. *Curr. Biol.* **13**, R68–R70 (2003).
78. Feldbrügge, M., Kämper, J., Steinberg, G. & Kahmann, R. Regulation of mating and pathogenic development in *Ustilago maydis*. *Curr. Opin. Microbiol.* **7**, 666–672 (2004).
79. Stukenbrock, E. H. & Dutheil, J. Y. Comparison of fine-scale recombination maps in fungal plant pathogens reveals dynamic recombination landscapes and intragenic hotspots. Preprint at *bioRxiv* https://dx.doi.org/10.1101/158907 (2017).
80. Zheng, Y. *et al.* Development of microsatellite markers and construction of genetic map in rice blast pathogen *Magnaporthe grisea*. *Fungal Genet. Biol.* **45**, 1340–1347 (2008).
81. Talas, F. & McDonald, B. A. Genome-wide analysis of *Fusarium graminearum* field populations reveals hotspots of recombination. *BMC Genomics* **16**, 996 (2015).
This study provides details of the genomic structure of *Fusarium graminearum* field populations, which reveals a high degree of sexual recombination and gene flow that enables rapid adaptation to changing environments.
82. Muller, H. J. Some genetic aspects of sex. *Am. Nat.* **66**, 118–138 (1932).
83. Taylor, J. W., Jacobson, D. J. & Fisher, M. C. The evolution of asexual fungi: reproduction, speciation and classification. *Annu. Rev. Phytopathol.* **37**, 197–246 (1999).
84. Milgroom, M. G., del Mar Jiménez-Gasco, M., García, C. O., Drott, M. T. & Jiménez-Díaz, R. M. Recombination between clonal lineages of the asexual fungus *Verticillium dahliae* detected by genotyping by sequencing. *PLoS ONE* **9**, e106740 (2014).
85. Short, D. P. G., Gurung, S., Hu, X., Inderbitzin, P. & Subbarao, K. V. Maintenance of sex-related genes and the co-occurrence of both mating types in *Verticillium dahliae*. *PLoS ONE* **9**, e112145 (2014).
86. Ni, M. *et al.* Unisexual and heterosexual meiotic reproduction generate aneuploidy and phenotypic diversity *de novo* in the yeast *Cryptococcus neoformans. PLoS Biol.* **11**, e1001653 (2013).
87. Couch, B. C. *et al.* Origins of host-specific populations of the blast pathogen *Magnaporthe oryzae* in crop domestication with subsequent expansion of pandemic clones on rice and weeds of rice. *Genetics* **170**, 613–630 (2005).
88. Jin, Y., Szarbo, L. J. & Carson, M. Century-old mystery of *Puccinia striiformis* life history solved with the identification of *Berberis* as an alternate host. *Phytopathology* **100**, 432–435 (2010).
89. Xhaard, C. *et al.* The genetic structure of the plant pathogenic fungus *Melampsora larici-populina* on its wild host is extensively impacted by host domestication. *Mol. Ecol.* **20**, 2739–2755 (2011).
90. Ali, S. *et al.* Origin, migration routes and worldwide population genetic structure of the wheat yellow rust pathogen *Puccinia striiformis* f.sp*. tritici*. *PLoS Pathog.* **10**, e1003903 (2014).
91. Saleh, D. *et al.* Sex at the origin: an Asian population of the rice blast fungus *Magnaporthe oryzae* reproduces sexually. *Mol. Ecol.* **21**, 1330–1344 (2012).
92. Ali, S., Leconte, M., Walker, A. S., Enjalbert, J. & Vallavieille-Pope, C. Reduction in the sex ability of worldwide clonal populations of *Puccinia striiformis* f.sp *tritici*. *Fungal Genet. Biol.* **47**, 828–838 (2010).
93. Smith, K. M. *et al.* Epigenetics of filamentous fungi. *Rev. Cell Biol. Mol. Med.* http://dx.doi.org/ 10.1002/3527600906.mcb.201100035 (2012).
94. Dhillon, B., Cavaletto, J. R., Wood, K. V. & Goodwin, S. B. Accidental amplification and inactivation of a methyltransferase gene eliminates cytosine methylation in *Mycosphaerella graminicola*. *Genetics* **186**, 67–77 (2010).

95. Levin, H. L. & Moran, J. V. Dynamic interactions between transposable elements and their hosts. *Nat. Rev. Genet.* **12**, 615–627 (2011).
96. Daboussi, M.-J. & Capy, P. Transposable elements in filamentous fungi. *Annu. Rev. Microbiol.* **57**, 275–299 (2003).
97. Capy, P., Gasperi, G., Biémont, C. & Bazin, C. Stress and transposable elements: co-evolution or useful parasites? *Heredity (Edinb.)* **85**, 101–106 (2000).
98. Dolgin, E. S. & Charlesworth, B. The fate of transposable elements in asexual populations. *Genetics* **174**, 817–827 (2006).
99. Lynch, M. & Conery, J. S. The origins of genome complexity. *Science* **302**, 1401–1404 (2003).
100. Halkett, F. *et al.* Genetic discontinuities and disequilibria in recently established populations of the plant pathogenic fungus *Mycosphaerella fijiensis*. *Mol. Ecol.* **19**, 3909–3923 (2010).
101. Munkacsi, A. B., Stoxen, S. & May, G. *Ustilago maydis* populations tracked maize through domestication and cultivation in the Americas. *Proc. R. Soc. B Biol. Sci.* **275**, 1037–1046 (2008).
102. Whittle, C. A. & Johannesson, H. Evidence of the accumulation of allele-specific non-synonymous substitutions in the young region of recombination suppression within the mating-type chromosomes of *Neurospora tetrasperma*. *Heredity (Edinb.)* **107**, 305–314 (2011).
103. Badouin, H. *et al.* Chaos of rearrangements in the mating-type chromosomes of the anther-smut fungus *Microbotryum lychnidis-dioicae*. *Genetics* **200**, 1275–1284 (2015).
104. Perlin, M. H. *et al.* Sex and parasites: genomic and transcriptomic analysis of *Microbotryum lychnidis-dioicae*, the biotrophic and plant-castrating anther smut fungus. *BMC Genomics* **16**, 1 (2015).
105. Okasha, S. *Evolution and the Levels of Selection*. (Oxford Univ. Press, 2006).
106. Anderson, J. B. & Kohn, L. M. *in Sex in Fungi: Molecular Determination and Evolutionary Implications.* (eds Heitman J. *et al.*) 333–348 (ASM Press, 2007).
107. James, T. Y., Stenlid, J., Olson, Å. & Johannesson, H. Evolutionary significance of imbalanced nuclear ratios within heterokaryons of the Basidiomycete fungus *Heterobasidion parviporum*. *Evolution.* **62**, 2279–2296 (2008).
108. Olson, A. & Stenlid, J. Plant pathogens: mitochondrial control of fungal hybrid virulence. *Nature* **411**, 438 (2001).
109. Zheng, W. *et al.* High genome heterozygosity and endemic genetic recombination in the wheat stripe rust fungus. *Nat. Commun.* **4**, 2673 (2013).
110. Stukenbrock, E. H. The role of hybridization in the evolution and emergence of new fungal plant pathogens. *Phytopathology* **106**, 104–112 (2016).
111. Stukenbrock, E. H., Christiansen, F. B., Hansen, T. T., Dutheil, J. Y. & Schierup, M. H. Fusion of two divergent fungal individuals led to the recent emergence of a unique widespread pathogen species. *Proc. Natl Acad. Sci. USA* **109**, 10954–10959 (2012).
112. Inderbitzin, P., Davis, R. M., Bostock, R. M. & Subbarao, K. V. The ascomycete *Verticillium longisporum* is a hybrid and a plant pathogen with an expanded host range. *PLoS ONE* **6**, e18260 (2011).
113. Shoji, J.-Y., Charlton, N. D., Yi, M., Young, C. A. & Craven, K. D. Vegetative hyphal fusion and subsequent nuclear behavior in *Epichloë* grass endophytes. *PLoS ONE* **10**, e0121875 (2015).
114. Schardl, C. & Craven, K. Interspecific hybridization in plant-associated fungi and oomycetes: a review. *Mol. Ecol.* **12**, 2861–2873 (2003).
115. Baack, E. J. & Rieseberg, L. H. A genomic view of introgression and hybrid speciation. *Curr. Opin. Genet. Dev.* **17**, 513–518 (2007).

116. Richards, T. A. *et al.* Phylogenomic analysis demonstrates a pattern of rare and ancient horizontal gene transfer between plants and fungi. *Plant Cell* **21**, 1897–1911 (2009).
117. Friesen, T. L. *et al.* Emergence of a new disease as a result of interspecific virulence gene transfer. *Nat. Genet.* **38**, 953–956 (2006).
118. Liu, Z. *et al.* The Tsn1–ToxA interaction in the wheat– *Stagonospora nodorum* pathosystem parallels that of the wheat–tan spot system. *Genome* **49**, 1265–1273 (2006).
119. Faris, J. D. *et al.* A unique wheat disease resistance-like gene governs effector-triggered susceptibility to necrotrophic pathogens. *Proc. Natl Acad. Sci. USA* **107**, 13544–13549 (2010).
120. Mcdonald, M. C., Ahren, D., Simpfendorfer, S., Milgate, A. & Solomon, P. S. The discovery of the virulence gene *ToxA* in the wheat and barley pathogen *Bipolaris sorokiniana*. *Mol. Plant Pathol.* http://dx.doi.org/10.1111/mpp.12535 (2017).
This study shows that horizontal gene transfer of ToxA confers host-specific virulence across pathogens that infect wheat.
121. Nikolaidis, N., Doran, N. & Cosgrove, D. J. Plant expansins in bacteria and fungi: evolution by horizontal gene transfer and independent domain fusion. *Mol. Biol. Evol.* **31**, 376–386 (2014).
122. de Jonge, R. *et al.* Tomato immune receptor Ve1 recognizes effector of multiple fungal pathogens uncovered by genome and RNA sequencing. *Proc. Natl Acad. Sci. USA* **109**, 5110–5115 (2012).
123. Gardiner, D. M. *et al.* Comparative pathogenomics reveals horizontally acquired novel virulence genes in fungi infecting cereal hosts. *PLoS Pathog.* **8**, e1002952 (2012).
124. Burrell, R. A., McGranahan, N., Bartek, J. & Swanton, C. The causes and consequences of genetic heterogeneity in cancer evolution. *Nature* **501**, 338–345 (2013).
125. Garsed, D. W. *et al.* The architecture and evolution of cancer neochromosomes. *Cancer Cell* **26**, 653–667 (2014).
126. Wright, S. & Finnegan, D. Genome evolution: sex and the transposable element. *Curr. Biol.* **11**, R296–R299 (2001).
127. Dang, Y., Yang, Q., Xue, Z. & Liu, Y. RNA interference in fungi: pathways, functions, and applications. *Eukaryot. Cell* **10**, 1148–1155 (2011).
128. Cambareri, E. B., Jensen, B. C., Schabtach, E. & Selker, E. U. Repeat-induced G-C to A-T mutations in *Neurospora. Science* **244**, 1571–1575 (1989).
129. Gladyshev, E. & Kleckner, N. Direct recognition of homology between double helices of DNA in *Neurospora crassa. Nat. Commun.* **5**, 3509 (2014).
130. Laurie, J. D. *et al.* Genome comparison of barley and maize smut fungi reveals targeted loss of RNA silencing components and species-specific presence of transposable elements. *Plant Cell* **24**, 1733–1745 (2012).
This study details a genome comparison of three closely related smut fungi that reveals transposable element expansion in *Ustilago hordei* and the loss of RNAi components in *U. maydis.*
131. Hood, M. E., Katawczik, M. & Giraud, T. Repeat-induced point mutation and the population structure of transposable elements in *Microbotryum violaceum*. *Genetics* **170**, 1081–1089 (2005).
132. Idnurm, A. & Howlett, B. J. Analysis of loss of pathogenicity mutants reveals that repeat-induced point mutations can occur in the Dothideomycete *Leptosphaeria maculans*. *Fungal Genet. Biol.* **39**, 31–37 (2003).
133. Zemach, A., McDaniel, I. E., Silva, P. & Zilberman, D. Genome-wide evolutionary analysis of eukaryotic DNA methylation. *Science* **328**, 916–919 (2010).

134. Galagan, J. E. & Selker, E. U. RIP: The evolutionary cost of genome defense. *Trends Genet.* **20**, 417–423 (2004).
135. Studt, L. *et al.* Knock-down of the methyltransferase Kmt6 relieves H3K27me3 and results in induction of cryptic and otherwise silent secondary metabolite gene clusters in *Fusarium fujikuroi. Environ. Microbiol.* **18**, 4037–4054 (2016).
136. Connolly, L. R., Smith, K. M. & Freitag, M. The *Fusarium graminearum* histone H3 K27 methyltransferase KMT6 regulates development and expression of secondary metabolite gene clusters. *PLoS Genet.* **9**, e1003916 (2013).
137. Letunic, I. & Bork, P. Interactive tree of life (iTOL): an online tool for phylogenetic tree display and annotation. *Bioinformatics* **23**, 127–128 (2007).
138. Grandaubert, J., Bhattacharyya, A. & Stukenbrock, E. H. RNA-seq based gene annotation and comparative genomics of four fungal grass pathogens in the genus *Zymoseptoria* identify novel orphan genes and species-specific invasions of transposable elements. *G3 (Bethesda)* **5**, 1323–1333 (2015).
139. Vanheule, A. *et al.* Living apart together: crosstalk between the core and supernumerary genomes in a fungal plant pathogen. *BMC Genomics* **17**, 670 (2016).
140. Spanu, P. D. *et al.* Genome expansion and gene loss in powdery mildew fungi reveal tradeoffs in extreme parasitism. *Science* **330**, 1543–1546 (2010).
141. Wicker, T. *et al.* The wheat powdery mildew genome shows the unique evolution of an obligate biotroph. *Nat. Genet.* **45**, 1092–1096 (2013).
142. Hacquard, S. *et al.* Mosaic genome structure of the barley powdery mildew pathogen and conservation of transcriptional programs in divergent hosts. *Proc. Natl Acad. Sci. USA* **110**, E2219–E2228 (2013).
143. Dean, R. A. *et al.* The genome sequence of the rice blast fungus *Magnaporthe grisea*. *Nature* **434**, 980–986 (2005).
144. Forgetta, V. *et al.* Sequencing of the Dutch elm disease fungus genome using the Roche/454 GS-FLX Titanium System in a comparison of multiple genomics core facilities. *J. Biomol. Tech.* **24**, 39–49 (2013).
145. Cuomo, C. A. *et al.* The *Fusarium graminearum* genome reveals a link between localized polymorphism and pathogen specialization. *Science* **317**, 1400–1402 (2007).

Acknowledgements

The authors thank B. McDonald, M. Freitag, J. Haueisen and J. Dutheil for helpful discussions and comments in regard to a previous version of this Review. Research carried out in the group of E.H.S. is funded by the Max Planck Society, Germany, and a personal grant from the State of Schleswig-Holstein, Germany, to E.H.S.

Glossary

Biotrophs
Pathogens that manipulate host defences and obtain their nutrients from living plant cells through specialized 'feeding' structures or hyphae formed intracellularly in the host.

Necrotrophs
Pathogens that kill host cells by secreting toxins and enzymes to obtain nutrients for growth and reproduction.

Hemibiotrophs
Pathogens that undergo a longer latent or biotrophic phase followed by a switch to necrotrophic growth.

Effectors
Pathogen-produced molecules that are secreted during infection to manipulate host defences and facilitate pathogen invasion.

Apoplastic space
Space outside of the plant plasma membrane.

Symplastic space
Space on the inner side of the plant plasma membrane.

Cultivars
Varieties of crop plants of the same species that have distinct phenotypes and genotypes. Distinct cultivars are obtained by plant breeding, whereby desired traits are selected and propagated.

Transposable elements
Genetic elements that move from one location in the genome of their host to another. Transposable elements are also known as transposons.

Metapopulation dynamics
Local fluctuations in the (actual as well as effective) population size of spatially separated populations that belong to the same species.

Non-synonymous mutations
Nucleotide changes in coding sequences that alter the amino acid sequence in the translated proteins.

Synonymous mutations
Nucleotide changes in coding sequences that alter the codons, but not the amino acid sequence, in translated proteins.

Trench warfare
A model that predicts constant diversity in a host–pathogen system, due to the maintenance of multiple alleles at a co-evolving locus by positive diversifying selection or balancing selection.

'Arms race' evolution
The co-evolution of host and pathogen alleles, which results in the recurrent fixation of advantageous alleles at a co-evolving locus. The fixation of advantageous alleles is mediated by positive directional selection.

Tajima's D
A statistical test parameter that is used in population genetics and DNA sequence analyses. Tajima's test is used to identify sequences that do not fit the neutral theory model, by which the fate of any mutation is determined by genetic drift.

Divergence patterns
The distribution of substitutions varies along the genome, as different parts of the genome evolve by processes and by different rates. The underlying pattern of divergence can be investigated to unravel the history of mutational events and the effect of selection versus neutral processes on the sequence evolution.

Selective sweep
An increase in the frequency of an advantageous allele (and closely linked chromosomal segments) that is caused by positive selection. Sweeps initially decrease genetic variation and subsequently lead to a local excess of rare alleles (homozygosity excess) as new unique mutations accumulate.

Linkage disequilibrium
The non-random association of alleles at different loci.

Accessory chromosomes
Chromosomes that are not present in all isolates of the same pathogenic species. Such chromosomes often encode determinants of host specificity.

Heterothallic
In heterothallic species, two individuals that have opposite mating types are required for sexual reproduction. By contrast, homothallic organisms have both mating types in one thallus.

Mesosynteny
A term that refers to the conservation of gene content on chromosomes, but a variation in the gene order and orientation. This is a phenomenon that is, thus far, particularly described in dothideomycete fungi.

Effective population size
(N_e). The approximate number of breeding individuals that produce offspring that live to reproductive age. This number influences the rate of loss of genetic variation, the efficiency of natural selection, and the accumulation of beneficial and deleterious mutations. It is frequently much smaller than the number of individuals in a population.

Sexual spores
Spores that originate from sexual crossings that differ morphologically from asexual spores.

Muller's ratchet
The irreversible accumulation of deleterious mutations in organisms that reproduce asexually.

Parasexual
A process whereby genetic material is exchanged between fused hyphae or cells without meiosis. Parasexuality enables the organism to recombine its genome and generate new genotypes in the absence of sexual mating.

Selection coefficient
The average proportional reduction in fitness of one genotype relative to another owing to selection (designated by '*s*').

Heterokaryons
Cells that contain two or more genetically distinct nuclei.

Introgressive hybridization
The transfer of genes from one species to another through hybridization followed by backcrossing with the parental species.

Chapter II

Extraordinary genome instability and widespread chromosome rearrangements during vegetative growth

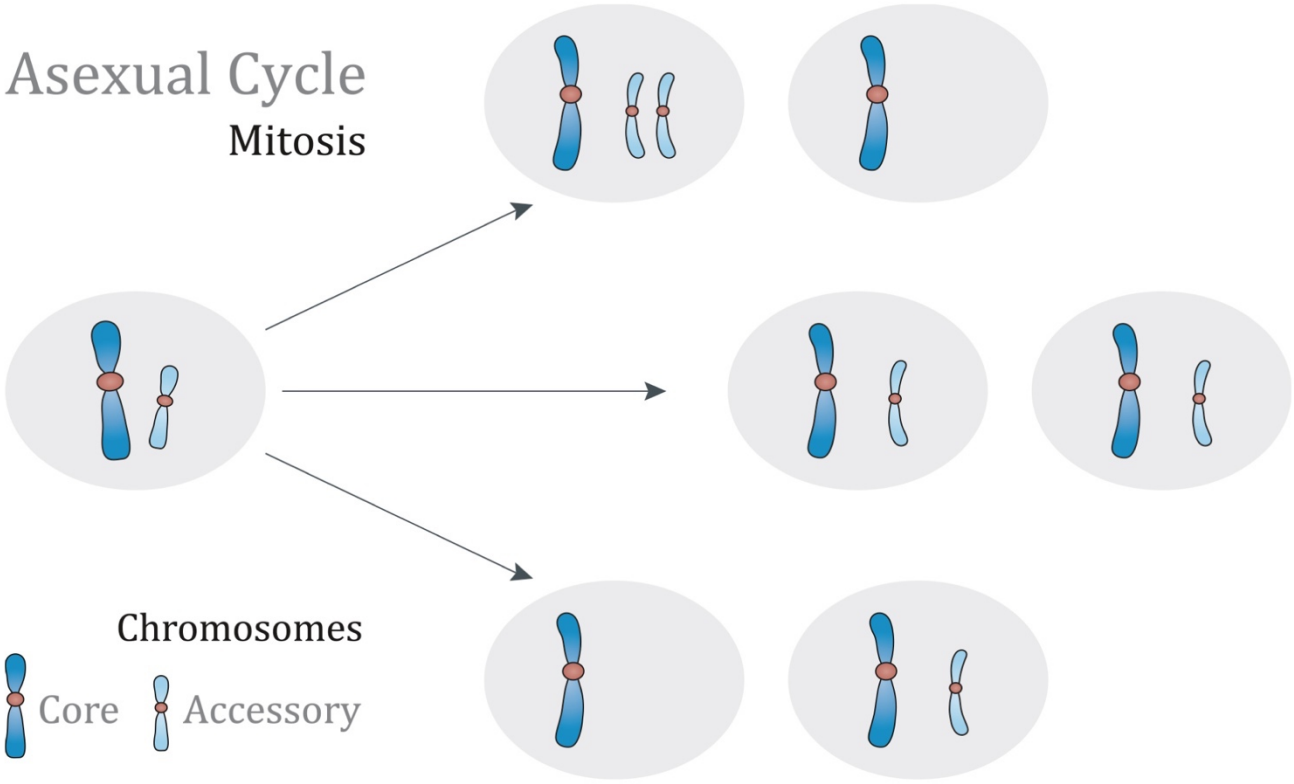

Title picture is modified from
Möller & Stukenbrock 2017,
“Evolution and genome architecture in fungal plant pathogens”
Nature Reviews Microbiology

Chapter II

Extraordinary genome instability and widespread chromosome rearrangements during vegetative growth

Mareike Möller[1,2], Michael Habig[1,2], Michael Freitag[3], and Eva H. Stukenbrock[1,2]

[1]Environmental Genomics, Christian-Albrechts University, Am Botanischen Garten 1-9, D-24118 Kiel, Germany

[2]Max Planck Institute for Evolutionary Biology, August-Thienemann-Str. 2, D-24306 Plön, Germany

[3]Department of Biochemistry and Biophysics, Oregon State University, Corvallis, OR 97331-7305, United States of America

This manuscript is published as a preprint on *bioRxiv* (doi: 10.1101/304915) and currently submitted to a peer-reviewed journal.

Abstract

The haploid genome of the pathogenic fungus *Zymoseptoria tritici* is contained on "core" and "accessory" chromosomes. While 13 core chromosomes are found in all strains, as many as eight accessory chromosomes show presence/absence variation and rearrangements among field isolates. We investigated chromosome stability using experimental evolution, karyotyping and genome sequencing. We report extremely high and variable rates of accessory chromosome loss during mitotic propagation *in vitro* and *in planta*. Spontaneous chromosome loss was observed in 2 to >50 % of cells during four weeks of incubation. Similar rates of chromosome loss in the closely related *Z. ardabiliae* suggest that this extreme chromosome dynamic is a conserved phenomenon in the genus. Elevating the incubation temperature greatly increases instability of accessory and even core chromosomes, causing severe rearrangements involving telomere fusion and chromosome breakage. Chromosome losses do not impact the fitness of *Z. tritici in vitro*, but some lead to increased virulence suggesting an adaptive role of this extraordinary chromosome instability.

Introduction

Pathogenic fungi pose global threats to agriculture, human, and animal health. Pathogens infecting plants and animals have been shown to rapidly adapt to changing environments, including industrial agriculture and medical treatments, usually in response to adaptive pressure caused by the widespread use of fungicides and pharmaceuticals (Selmecki *et al.*, 2010; Bennett *et al.*, 2014). The genomes of many prominent fungal plant pathogens exhibit high levels of structural variation including isolate- or lineage-specific regions often characterized by high repeat contents, and accessory chromosomes varying in frequency among individual isolates (De Jonge *et al.*, 2013; Persoons *et al.*, 2014; Plissonneau & Stürchler, 2016). Structural variation is often associated with meiotic recombination, but highly variable regions are also found in asexually and mostly asexually reproducing species (Wang *et al.*, 2006; Chuma *et al.*, 2011; Faino *et al.*, 2016). In several plant pathogenic fungi, determinants of virulence, so called effector proteins, are located in dynamic regions of the genome (Miao *et al.*, 1991a; Coleman *et al.*, 2009; Ma *et al.*, 2010). Accessory chromosomes often carry genes that encode virulence determinants and are linked to pathogenicity. Therefore, the absence of a particular chromosome in some species results in avirulent phenotypes (Ma *et al.*, 2010; Tsuge *et al.*, 2016; Vlaardingerbroek *et al.*, 2016; van Dam *et al.*, 2018). Little is known about the mechanisms that drive the dynamics of accessory chromosomes and highly variable regions in genomes of eukaryotic pathogens.

The plant pathogenic fungus *Zymoseptoria tritici* causes disease on wheat, especially in Northern Europe and North America, resulting in extensive annual yield loss (Fones & Gurr, 2015; Torriani *et al.*, 2015). The *Z. tritici* reference isolate IPO323 contains eight accessory chromosomes with sizes ranging from 0.4 to 1 Mb, accounting for 12% of the entire genome (Goodwin *et al.*, 2011). Chromosome rearrangements, including complete loss of accessory chromosomes, are a frequent phenomenon in this fungus and have been widely studied as a consequence of meiosis (Wittenberg *et al.*, 2009; Croll *et al.*, 2015; Fouche *et al.*, 2017). Infection experiments with *Z. tritici* strains in which single or multiple accessory chromosomes had been deleted showed that at least some accessory chromosomes encode virulence factors that determine host specificity (Habig *et al.*, 2017). In contrast to the core chromosomes, accessory chromosomes are enriched with transposable elements and have low gene density (Goodwin *et al.*, 2011). Chromatin of accessory chromosomes shows hallmarks of constitutive and facultative heterochromatin, consistent with the observed transcriptional silencing of genes present

on these chromosomes (Kellner *et al.*, 2014; Rudd *et al.*, 2015; Schotanus *et al.*, 2015). The centromeres, subtelomeric regions and telomeric repeats of accessory chromosomes are indistinguishable from those of core chromosomes (Schotanus *et al.*, 2015), suggesting that accessory chromosomes contain all the required regions for proper chromosome segregation. The unusual high number of accessory chromosomes, in combination with the extreme variability in chromosome content among field isolates or progeny from controlled crosses, make *Z. tritici* an excellent eukaryotic model to study accessory chromosomes and their dynamics (Mehrabi *et al.*, 2007; Wittenberg *et al.*, 2009; Stukenbrock *et al.*, 2010; Goodwin *et al.*, 2011). Here, we provide evidence for unexpectedly high rates of chromosome loss and changes during asexual propagation, both *in vitro* and *in planta*. We describe the types of structural rearrangements and overall variation in chromosome stability in this important crop pathogen.

Results

Accessory chromosomes are lost at a very high rate *in vitro*

To assess the stability of accessory chromosomes in *Z. tritici* we conducted an *in vitro* long-term growth experiment. We used the *Z. tritici* isolate IPO323Δchr18, derived from the reference strain IPO323 for which there is a completely assembled genome (Goodwin *et al.*, 2011). IPO323Δchr18 lost chromosome 18 during previous *in vitro* propagation, and is here referred to as Zt09 (Kellner *et al.*, 2014). We propagated fungal cells in liquid culture at 18°C, including eight transfers to fresh medium. After four weeks (representing ~80 cell divisions per cell), 576 single strains originating from three replicate cultures were tested for the presence of the seven accessory chromosomes from the Zt09 progenitor by a PCR assay. The presence of marker regions, located close to the centromere, and the right and left telomere repeats of each accessory chromosome, were tested (Table S1). When the screening by PCR suggested absence of an accessory chromosome, we further validated the result by electrophoretic separation of the fungal chromosomes by pulsed field gel electrophoresis (PFGE) (Figure 1 A and B). Thirty eight of the 576 (~7 %) tested strains lacked one accessory chromosome. We did not find strains that lacked more than one chromosome, but observe a clear trend where accessory chromosomes 14, 15 and 16 were lost more frequently than smaller accessory chromosomes (Table 1). For example, chromosome 14 was absent in eighteen strains, chromosome 15 in eight and 16 in nine strains. The small chromosomes 20 and 21 were

lost only in two and one strain, respectively, whereas chromosomes 17 and 19 were never absent following the *in vitro* propagation (Table 1 and Table S2).

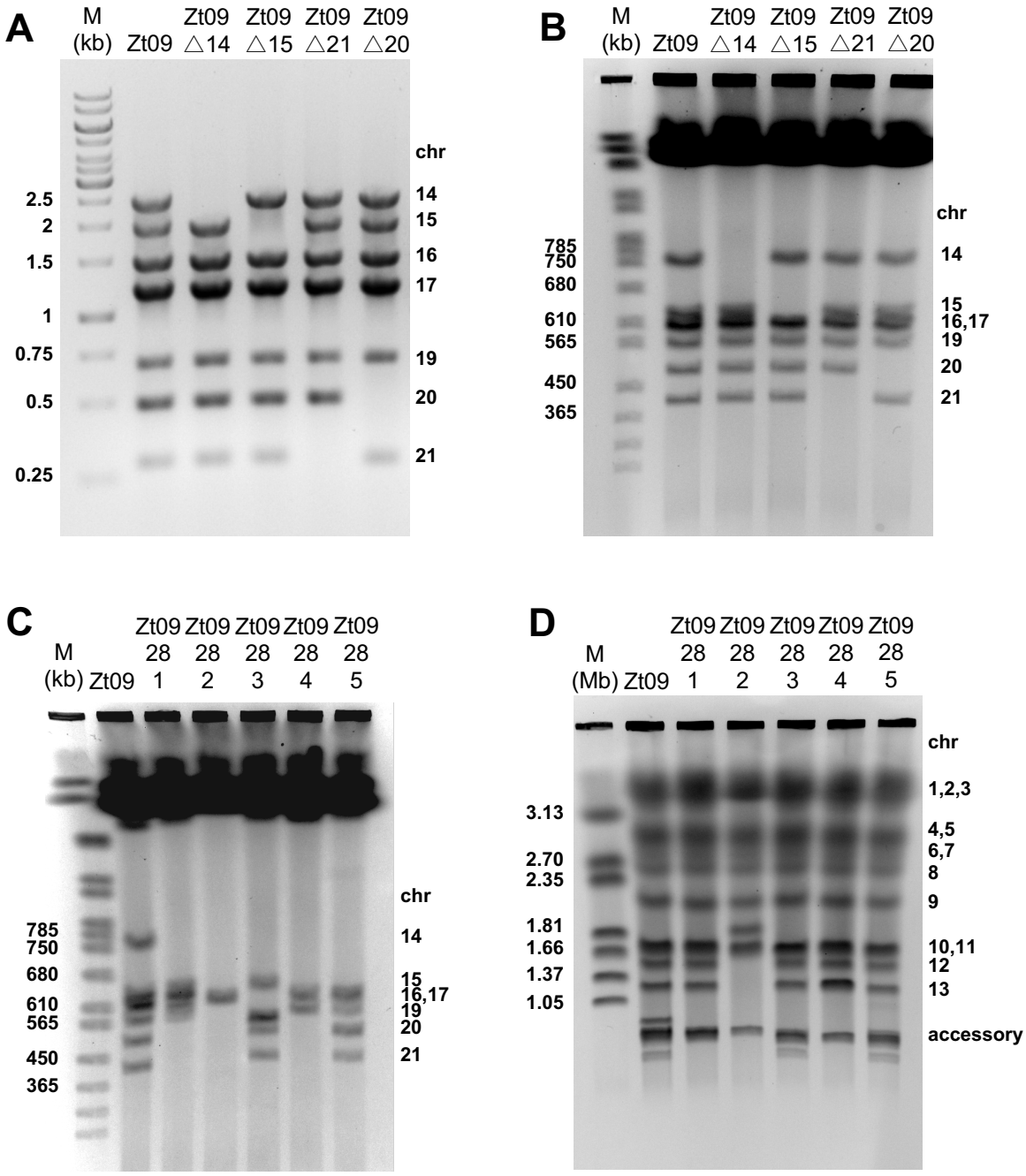

Figure 1. Screening by PCR and pulsed-field gel electrophoresis to identify accessory chromosome-loss strains in *Z. tritici*. (A) Screening by PCR of the progenitor Zt09 strain and evolved strains to assess chromosome losses using primer pairs located close to the centromeric region of the respective accessory chromosome. Multiplex PCR was used to simultaneously screen for the presence or absence of all accessory chromosomes in one strain. Absence of a PCR product indicates the absence of the chromosome; chromosome 18 is not present in Zt09. **(B)** Pulsed-field gel electrophoresis (PFGE) was conducted to validate the absence of accessory chromosomes in chromosome

loss candidates identified by the initial PCR. Here, the separation of small accessory chromosomes of the progenitor strain Zt09 and four chromosome-loss strains is shown. The corresponding chromosome to each band is indicated on the right. The absence of chromosomal bands confirms the loss of the respective chromosome; chromosome 18 is similar in length to 16 and 17 but is absent in Zt09. PFGE of the accessory **(C)** and mid-size **(D)** chromosomes of strains originating from the *in vitro* temperature stress experiment confirms multiple accessory chromosome losses, size alterations and chromosome fusions (see also Figures 3 and S1 and Table S3). The bands for chromosomes 3, 12, 13 and 21 are absent in strain 28-2, however, genome sequencing confirms that the chromosomes are still present in the genome (Figure 2C). The absence of bands on the PFGE can be explained by chromosome size changes whereby chromosomes 3 and 13 and 12 and 21 have experienced chromosome fusions (Figure 3 and S1). Note a new chromosome band with a size of ~1.8 Mb resulting from the fusion of chromosomes 12 and 21. In the strain 28-3, the accessory chromosomes 17 and 19 are shorter than the reference chromosomes due to chromosome breakage (Figure 2C and Table S3). Strain 28-4 has an additional band of ~1.2 Mb, representing the fusion of a duplicated chromosome 17 (Figure S1). All images of stained gels are color-inverted to make differences more obvious.

Table 1. Summary of chromosome losses in *Z. tritici* during evolution experiments *in vitro* and *in planta*. Listed are the number of cells that lost an accessory chromosome and which accessory chromosomes were lost. Sizes of the accessory chromosomes are listed next to the chromosome number. Strains with more than one chromosome lost are listed in brackets.

Chromosome (kb)	**Zt09 *in vitro* culture**	**Zt09 *in vitro* plate**	**IPO323 *in planta***	**Zt09 *in vitro* temperature stress**
14 (773)	18	0	1	108 (33)
15 (639)	8	0	6	2 (8)
16 (607)	9	4	1	0 (9)
17 (584)	0	0	0	0
18 (574)	N/A	N/A	7	N/A
19 (550)	0	0	2	2 (2)
20 (472)	2	0	0	1 (17)
21 (409)	1	1	0	1 (7)
Total chr loss strains	**38**	**5**	**17**	**114 (34)**
Total strains tested	**576**	**40**	**986**	**188**

We considered the possibility that natural selection acted on a large population of cells in the liquid *Z. tritici* cultures and thereby contributed to the observed non-random chromosome losses. To test this, we designed a second evolution experiment to propagate individual cell lineages in the absence of selection. For this experiment, 40 strains originating from one common progenitor (Zt09) were cultivated on plates. Every week, randomly selected colonies derived from single cells were transferred to a fresh plate. These repeated strong bottlenecks allowed us to propagate single lineages of *Z. tritici* without an effect of natural selection (Barrick & Lenski, 2013). After four weeks of growth (including four transfers to new plates), the 40 evolved strains were tested for the presence of accessory chromosomes as described above. Five out of 40 (~13 %) strains, twice as many as in the previous experiment, lacked an accessory chromosome suggesting that selection in a larger population of cells indeed had removed some of the spontaneously occurring chromosome losses. Interestingly, in this experiment we observe the loss of only two different chromosomes: Chromosome 16 was lost in four strains, and chromosome 21 in one strain. Our two *in vitro* experiments suggest that chromosome loss is not entirely random, and that specific chromosomes are lost at a higher rate (Table 1), depending on the *in vitro* growth conditions. The frequency of chromosome losses during asexual growth *in vitro* is extremely high in *Z. tritici* and exceeds previously reported spontaneous chromosome losses in *F. oxysporum* f. sp. *lycopersici* by far (Vlaardingerbroek *et al.*, 2016).

Accessory chromosomes are unstable *in planta*

The growth of *Z. tritici* in rich medium *in vitro* is highly distinct from growth of the fungus in its natural environment. *Zymoseptoria tritici* is a hemi-biotrophic pathogen infecting the mesophyll of wheat leaves (Ponomarenko *et al.*, 2011; Goodwin *et al.*, 2011), where it forms asexual fruiting bodies, pycnidia, containing presumably clonal conidiospores (pycnidiospores). Pycnidia develop in the sub-stomatal cavities, where the environment and nutrient availability differ from our tested *in vitro* conditions (Rudd *et al.*, 2015; Haueisen *et al.*, 2017). To test whether chromosome loss occurs only *in vitro* or also during the natural lifecycle of *Z. tritici*, we assessed the loss of accessory chromosomes *in planta*. We collected pycnidia from wheat leaves infected with the *Z. tritici* strain IPO323 and tested single pycnidiospores for the presence of accessory chromosomes. A total number of 968 pycnidiospores originating from 42 separate pycnidia were screened by PCR. In total, 17 strains missing an accessory chromosome were identified (~1.7%).

Chromosomes 15 and 18 were the most frequently lost chromosomes, while chromosomes 17, 20 and 21 were not lost in any of the strains (Table 1 and Table S2). As for the *in vitro* experiments, no strains lacking more than one chromosome were found. Interestingly, chromosome 18, which was found to be lost at high rates in our plant experiments, was shown to be frequently absent in field isolates *of Z. tritici* (Croll *et al.*, 2013; McDonald *et al.*, 2016). In summary, our findings show that chromosome loss in *Z. tritici* not only results from the non-disjunction of homologous chromosomes during meiosis II, as proposed previously (Wittenberg *et al.*, 2009), but also from frequent chromosome losses during asexual growth and mitotic spore formation *in planta*. The observed frequency of chromosome losses *in planta* is not as high as during *in vitro* growth, however, the number of mitotic divisions to develop pycnidia is presumably lower than during four weeks of *in vitro* growth. Therefore, we propose that the reduced number of chromosome losses *in planta* rather reflects the reduced number of cell divisions than possible fitness effects of chromosome losses.

Chromosome instability is greatly increased during exposure to heat stress

In their natural environments, pathogens are exposed to various kinds of biotic and abiotic stresses. For example, the local environment on the leaf surface can fluctuate severely in temperature and humidity conditions (Zhan & McDonald, 2011). We assessed the impact of an increase in temperature on chromosome stability of *Z. tritici*. To this end, we cultivated Zt09 *in vitro* at elevated temperatures, namely an increase of ten degrees Celsius from 18° to 28°C during four weeks of incubation. Subsequent screening by PCR for accessory chromosomes revealed severe chromosome losses in the tested strains. Out of 188 evolved and tested strains, 148 (~80 %) were missing at least one accessory chromosome. Chromosome 14 was the most frequently lost chromosome and 34 evolved strains were lacking more than one chromosome. The maximum number of missing chromosomes was six in one strain (Table 1 and Table S2). PFGE revealed that karyotype alterations were not restricted to simple chromosome loss as observed in the *in vitro* experiments at 18°C and the *in planta* experiments. In contrast, we observed frequent size variation of both core and accessory chromosomes as a consequence of chromosome breakage, fusions and duplications (see below) (Figure 1C and 1D, Figure S1, Table S3).

Genome sequencing of chromosome-loss strains reveals chromosome breakage and fusion, but a low number of SNPs

In total, we sequenced 19 genomes originating from the different *in vitro* and the *in planta* experiment and the respective progenitor strains; all sequencing results have been deposited in the Sequence Read Archive (SRA) under BioProject ID PRJNA428438. Overall, we confirmed the absence of complete accessory chromosomes (Figure 2A), and we found very few additional changes. After filtering to exclude reads of poor quality and coverage (see Materials and Methods, Supplementary Text) we identified a total number of nine SNPs in eight sequenced strains originating from the *in vitro* experiment in liquid culture at 18°C and the *in planta* experiment. Of these, three SNPs were located in coding regions (Table S4). Besides the complete loss of accessory chromosomes and the identified SNPs, we found no other mutations when comparing the progenitor and evolved strains. However, we identified SNPs distinguishing Zt09 from our IPO323 reference strain, and the published genome sequence; most of these SNPs were in non-coding sequences (Table S4). As we show chromosome losses in different strains, we conclude that the few point mutations do not have measurable impact on chromosome loss.

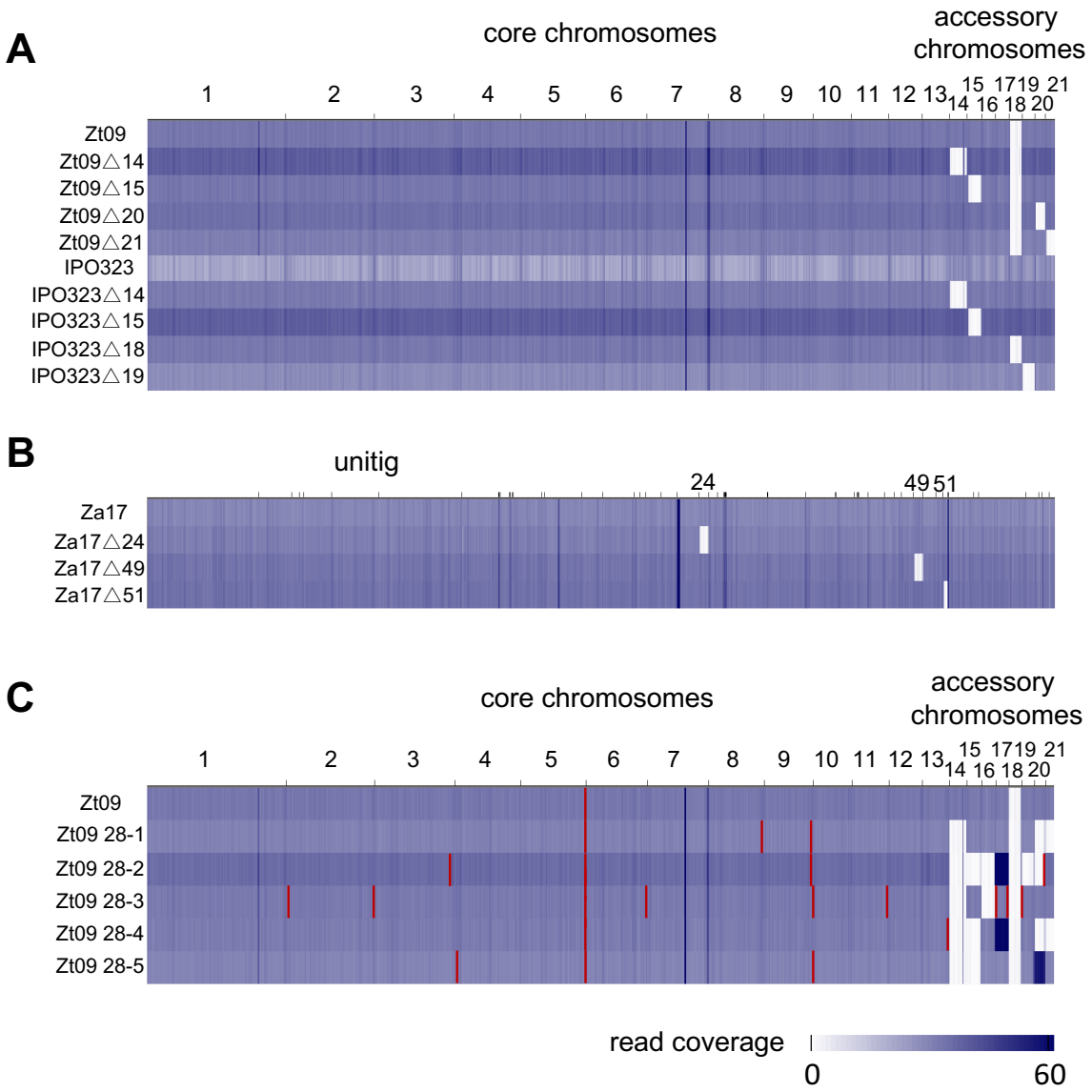

Figure 2. Whole genome sequencing confirms loss of accessory chromosomes in *Z. tritici* and *Z. ardabiliae*. The genomes of chromosome-loss strains derived from **(A)** the *Z. tritici in vitro* evolution experiment and the *in planta* pycnidiospore isolations, and **(B)** the *Z. ardabiliae in vitro* evolution experiment and the respective progenitor strains were sequenced by paired-end Illumina sequencing and mapped to the respective reference isolates, IPO323 (*Z. tritici*) or Za17 (*Z. ardabiliae*). The losses of entire chromosomes (white boxes) were verified for each strain, but few mutations in form of SNPs, INDELs or copy number variation were detected (Table S4). The *Z. tritici* reference genome consists of whole chromosomes, while the *Z. ardabiliae* reference genome is composed of unitigs obtained from the SMRT sequencing assembly (ordered by name of the unitig). **(C)** Genome sequencing of strains derived from the temperature stress experiment revealed, besides verification of accessory chromosome losses, chromosome breaks at the ends of core and accessory chromosomes (red lines) and accessory chromosome duplications. Darker blue shading indicates higher coverage. Most repetitive sequences have a higher coverage than single copy regions resulting in different shades of blue in the coverage graph. The intense dark blue lines indicate high coverage regions on rDNA clusters or repetitive DNA due to underestimation of repeats in the reference assembly (for example,

the thin black line in chromosome 7 indicates the location of several rDNA cluster repeats, the only such repeats in the annotated genome sequence, but the expected true number of rDNA repeats is ~50).

Whole genome sequencing of five strains evolved at 28°C verified the losses of several accessory chromosomes. Furthermore, comparison of the re-sequenced genomes of the progenitor and the evolved strains revealed substantial size variation resulting from chromosome breakage of core and accessory chromosomes, and duplications of accessory chromosomes (Figure 2C). Chromosome breaks located close to the ends of chromosomes resulted in shortened chromosomes caused by subtelomeric deletions of ~0.2-60 kb (Table S3). Detailed analyses of the distribution of discordant paired-end reads mapping to different chromosomes revealed a high number of reads at the chromosome breakpoints with the respective read mates mapping to telomeric repeats (Figure 3). This suggested that most chromosome breaks resulted in shorter chromosomes to which telomeres were added *de novo*. Besides *de novo* telomere formation, we found evidence for fusion of core chromosomes in strain Zt09 28-2, where discordant read mapping indicated fusion of the right arms of chromosomes 3 and 13 (Table S3 and Figure 3). PFGE and Southern blots further showed fusion of chromosomes 12 and 21 in Zt09 28-2 (Figure S1). In a previous study, we reported evidence for the likely fusion of an ancestral accessory chromosome and core chromosome 7 in the reference isolate IPO323 and Zt09 (Kellner *et al.*, 2014; Schotanus *et al.*, 2015). Here, we deduced a fusion of the duplicated chromosome 17 in strain Zt09 28-4 (Figure 1C and D, Figure S1). Similar fusions of the same accessory chromosome 17 following meiosis had been suggested previously, and "breakage-fusion bridge" cycles (McClintock, 1938, 1941) were invoked as a mechanism to form a new accessory chromosome (Croll *et al.*, 2013). In total, in the five analyzed genomes derived from strains grown at 28°C, we identified spontaneous changes: (1) fifteen chromosome breakages (twelve with *de novo* telomere formation and three without evidence for new telomeres), (2) three chromosome fusions, (3) three chromosome duplications, and (4) 16 chromosome losses (Table S3). A key observation from our genome data analyses is the frequent involvement of *de novo* telomere formation and chromosomal fusion as a mechanism to heal broken chromosome ends. While this has been reported for cancer cells (Murnane, 2012), it is generally considered a rare event in normal, non-transformed cells. Here we show that *de novo* telomere formation and chromosome fusion readily occur in a filamentous fungus during growth at temperature stress.

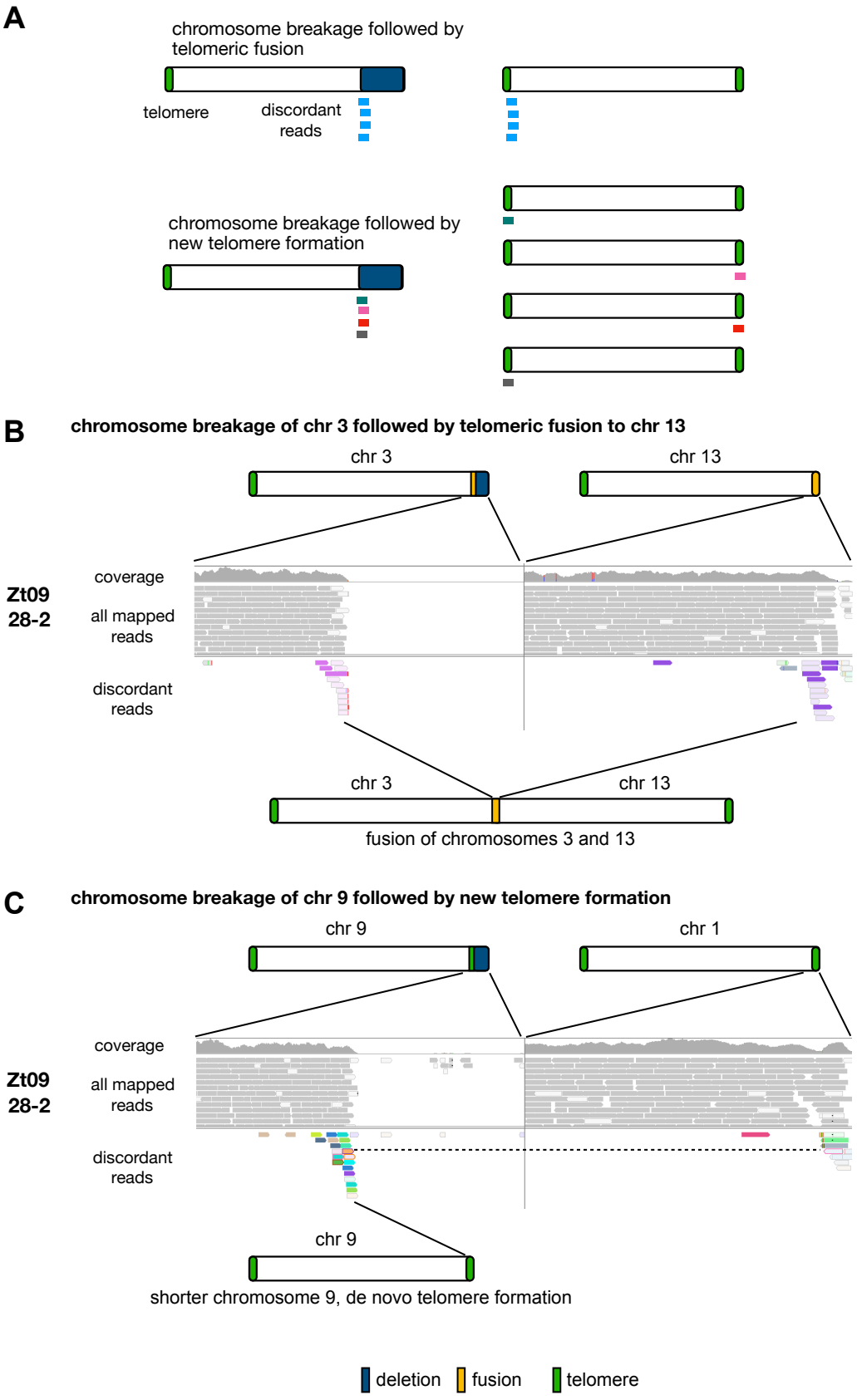

Figure 3. Discordant read analysis reveals chromosome fusion and chromosome breakage. (A) Schematic illustration of discordant read mapping in the case of chromosome breakage and fusion. If chromosome breakage is followed by fusion to a

different chromosome, the discordantly mapping reads at the breakpoint will have their respective read mate on the chromosome that is fused to the breakpoint. If breakage is followed by *de novo* telomere formation, the discordant reads have their respective read mates on telomeric repeats on random chromosomes. **(B)** and **(C)** Read mapping to the genome of the reference isolate IPO323. **(B)** In the experimentally evolved strains of *Z. tritici* at 28°C, the fusion of chromosomes 3 and 13 in the strain Zt09 28-2 is indicated by the increased occurrence of discordant reads at the chromosome breakpoint of the right arm of chromosome 3 and the right arm of chromosome 13. The color of the reads represents the chromosome their respective mate is mapping to. Color intensity of the reads indicates the mapping quality. **(C)** New telomere formation at the breakpoint, here, as example, shown for chromosome 9 in the strain Zt09 28-2. Telomere formation is indicated by a high number of discordant reads, where the read mates are mapping to the telomeric repeats of different chromosomes. As an example, the right telomere of chromosome 1 is shown, where one mate of the discordant reads at the breakpoint of chromosome 9 is located (dashed line). A total of twelve breakage events that were followed by *de novo* telomere formation were detected in the five analyzed strains derived from the experiment at elevated temperature.

Accessory chromosome instability also occurs in *Zymoseptoria* sister species

To assess whether the high frequency of mitotic chromosome loss is specific to *Z. tritici*, we conducted a short-term *in vitro* evolution experiment on the fungus *Z. ardabiliae,* a closely related sister species of *Z. tritici* that infects wild grasses. We used the previously characterized isolate STIR04 1.1.1 (Stukenbrock *et al.*, 2011), here called Za17, in our experiments.

We first generated a high-quality reference genome based on long-read SMRT sequencing (Supplementary Text). To identify sequences of accessory chromosomes we first combined analyses of a population genomic dataset and PFGE (Stukenbrock et al. 2011; Stukenbrock & Dutheil 2018). Our analyses reveal at least four accessory chromosomes varying in their frequency among 17 *Z. ardabiliae* isolates. Based on these, we designed primers to amplify six loci located on putative accessory chromosomes of Za17 (Table S1). Next, we conducted an *in vitro* evolution experiment at 18°C for four weeks in liquid culture with Za17 as the progenitor strain. Screening of 288 single clones by PCR identified five strains lacking one of the accessory chromosomes (~1.7%). We further verified the absence of accessory chromosomes by PFGE and whole genome sequencing for three of the five *Z. ardabiliae* strains (Figure 2B). These findings resemble the rapid loss of chromosomes in *Z. tritici* and suggest a common phenomenon, most likely related to mitotic cell division in the two *Zymoseptoria* species.

Accessory chromosome losses affect *in planta* phenotypes

We next addressed the impact of spontaneous chromosome loss by comparing the fitness of the progenitor and evolved *Z. tritici* strains under different *in vitro* growth conditions, and during infection of a susceptible wheat variety by comparing growth and pycnidia formation. *In vitro*, the growth rate of strains lacking an additional accessory chromosome (Zt09Δ14 and Zt09Δ21) was comparable to the growth rate of the progenitor, Zt09, but with a slight tendency to slower growth of the derived chromosome-loss strains (Figure S2). For a more detailed phenotypic characterization, we used the five chromosome-loss strains isolated from pycnidia from the *in planta* experiment (Table S2). Several stress conditions including osmotic, oxidative, temperature, and cell wall stresses were tested *in vitro.* We compared the fungal phenotypes of the chromosome-loss strains and the progenitor strain IPO323 and observed no difference in growth rate or colony morphology between any chromosome-loss strain and IPO323 (Figure S3). *In planta*, however, we observed phenotypic differences between the evolved chromosome-loss strains and their progenitor. We measured fitness by counting the number of asexual fruiting bodies formed in stomata on infected wheat leaves and found a slightly higher fitness of the chromosome-loss strains compared to the progenitor strain (Figure 4). The difference was most pronounced for the strains lacking chromosome 14 and chromosome 19 where the density of pycnidia was found to be significantly higher (p values of 0.0003 and 0.015, Wilcoxon-Rank-Sum test and Holm's correction for multiple testing) compared to the IPO323 progenitor (Figure 4).

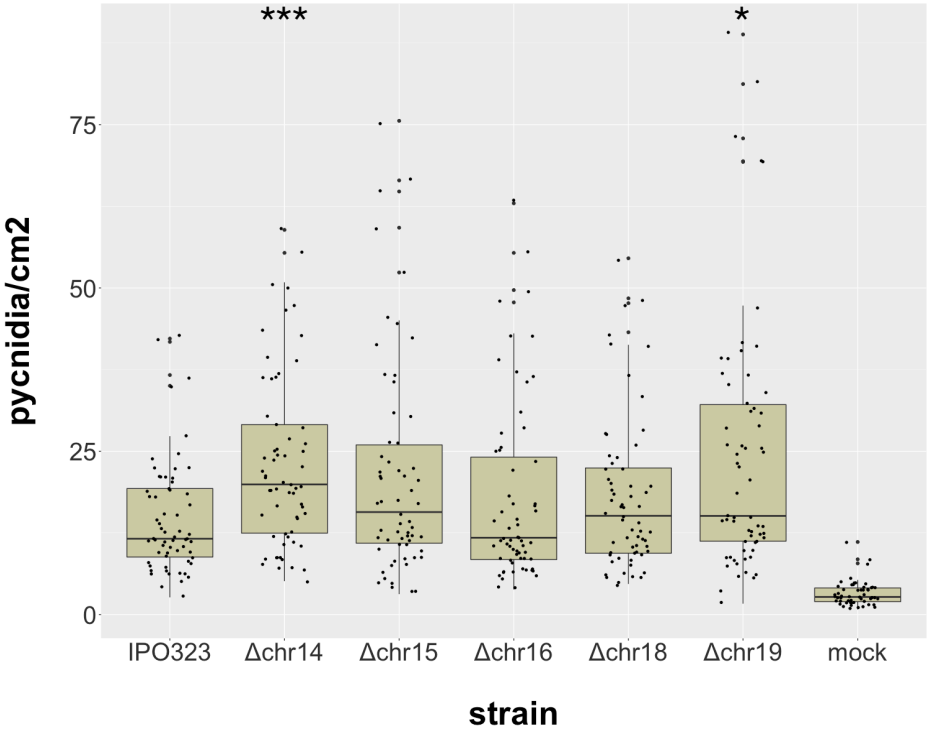

Figure 4. *In planta* infection assays reveal a negative effect of accessory chromosomes on fitness. To investigate the effect of accessory chromosome losses on *Z. tritici* infection of wheat, three independent experiments with the reference strain IPO323 and five chromosome-loss strains were conducted. The fitness of each strain was measured by counting the number of pycnidia per cm^2 on the leaf surface. Statistical analysis (Wilcoxon-rank-sum test and Holms correction, *P*-values 0.0003 and 0.015) identified two chromosome-loss strains (Chr. 14 and 19) that show a significantly higher number of pycnidia compared to the reference strain IPO323 under the conditions used in this experiment.

Discussion

Consequences for evolution of accessory chromosomes

Accessory chromosomes were proposed to serve as an 'evolutionary cradle' for creating novel virulence genes without risking the disruption of essential genes on the core chromosomes (Croll & McDonald, 2012). Indeed, signatures for accelerated evolution were shown by overall higher dN/dS ratios of genes on the accessory chromosomes compared to the core chromosomes (Stukenbrock *et al.*, 2010). However, natural selection acts at the level of individuals and cannot maintain "a playground" for future beneficial effects. Rather, we hypothesize that the dynamic of accessory chromosome loss reflects a dynamic in the selective environment of *Z. tritici*, where under certain conditions these small chromosomes confer a fitness advantage, while under different conditions they cause decrease in fitness. A fitness advantage of chromosome-loss strains *in planta* may indicate the presence of avirulence factors on at least some accessory chromosomes. Avirulence factors can be recognized by the host to induce a resistance response resulting in reduction in virulence or even abortion of infection (Petit-Houdenot & Fudal, 2017; Zhong *et al.*, 2017). Our previous findings support this notion, as we found small but significant negative effects of accessory chromosomes during host infection (Habig *et al.*, 2017). In other pathogenic fungi, however, the opposite effect has been demonstrated in several cases. A strong positive impact on virulence of accessory chromosomes have been observed in *Fusarium oxysporum* f. spp. and *Nectria haematococca* (Coleman *et al.*, 2009; Ma *et al.*, 2010; van Dam *et al.*, 2018). In these pathogens chromosome losses resulted in complete loss of pathogenicity. While these cases are currently considered the norm, our observations show that responses to accessory chromosome loss can be more varied. Even though this fungus is an important pathogen in all wheat-growing countries, the biology of *Z. tritici* is still not completely understood. Mating and overwintering in the soil or litter layer remain largely unknown lifecycle stages, and we postulate that they impose different selection pressures on the fungus. During these stages, accessory chromosomes may confer significant fitness advantages that have not been demonstrated yet. Besides spontaneous chromosome loss during meiosis (Wittenberg *et al.*, 2009), accessory chromosomes have been shown to follow non-Mendelian segregation and are transmitted at a significantly higher rate than expected, if one of the two mating partners lacks an accessory chromosome (Habig et al, submitted). While there is no comprehensive mechanistic explanation yet, chromosome conservation by re-replication during meiosis may counteract the chromosome loss

during vegetative growth and therefore maintain accessory chromosomes in pathogen populations. In *Alternaria alternata*, the spontaneous loss of a conditionally dispensable chromosome during sub-culturing has been described for one isolate (Johnson *et al.*, 2001). Furthermore, loss of a conditionally dispensable chromosome after meiosis has been observed in *Nectria haematococca* (aka *Fusarium solani* MPVI) (Miao *et al.*, 1991b). A recent study of the plant pathogenic fungus *Fusarium oxysporum* forma specialis *lycopersici* describes the spontaneous loss of dispensable chromosomes *in vitro* in one cell out of 35,000 (Vlaardingerbroek *et al.*, 2016). This rate is much lower than the chromosome loss rate that we observe in *Z. tritici* and *Z. ardabiliae*, where, depending on the growth conditions, more than one cell out of two to one cell out of 50, lacks an accessory chromosome. In combination, these results indicate that chromosome instability is a common phenomenon in fungi, but the stability of chromosomes can vary substantially between different species. Studies in *Saccharomyces* and *Candida* species have shown that chromosome loss resulting in aneuploidy is a relatively frequent phenomenon in diploid cells and is advantageous under certain conditions (Selmecki *et al.*, 2010; Kumaran *et al.*, 2013; Bennett *et al.*, 2014; Zhu *et al.*, 2014). The loss of chromosomes in haploid organisms, such as *Z. tritici*, is expected to have more severe consequences, as genetic information is lost from the cell. We considered, however, that the effect of rapid chromosome loss or instability may be advantageous if these traits are selected for in pathogens like *Zymoseptoria*.

The temperature stress experiment *in vitro* showed that genome instability in *Z. tritici,* at this temperature, is not restricted to the accessory chromosomes, but also involves the core genome. New chromosome formation induced by telomere to telomere fusion followed by breakage of the dicentric chromosome was reported in *Cryptococcus neoformans* (Fraser *et al.*, 2005) but likely occurred during meiosis rather than mitosis. In the asexual *Candida glabrata*, clinical isolates frequently inhabit chromosomal rearrangements indicating that structural variation acts as a virulence mechanism (Poláková *et al.*, 2009) and might be a response to stresses such as antifungal treatment or elevated temperature as observed here. The instable regions close to the chromosome ends on the core chromosomes, however, show structural characteristics similar to the accessory chromosomes, such as higher repeat content, lower gene density and specific histone modification patterns (Dhillon *et al.*, 2014; Grandaubert *et al.*, 2015; Schotanus *et al.*, 2015).

The accessory chromosomes of *Z. tritici* do not differ in terms of centromere or telomere organization from the core chromosomes, but the chromatin is largely transcriptionally inactive and potentially more condensed due to an enrichment with the histone H3 that is trimethylated at lysine 27 (H3K27me3), which covers almost all of the accessory chromosomes (Schotanus *et al.*, 2015). H3K27me3 is also enriched in subtelomeric regions of core chromosomes, that we show here as prone to instability. High-resolution microscopic analyses indicate an unusual localization of centromeres in the *Z. tritici* nuclei, suggesting a distinct spatial organization of different chromosomes (Schotanus *et al.*, 2015). Heterochromatin has been found close to the nuclear periphery, and H3K27me3 has been shown to be involved in facilitating lamina-proximal positioning (Harr *et al.*, 2015). We hypothesize that the heterochromatic structure reflects a distinct physical organization of core and accessory chromosomes and likely the subtelomeric regions in the nucleus of *Z. tritici*, and that this is correlated to the instability of heterochromatic regions and chromosomes. A Hi-C study on *Neurospora crassa* showed that absence of H3K27me3 resulted in movement of subtelomeric regions and centromeres from the nuclear periphery into the nuclear matrix (Klocko *et al.*, 2016). Further experiments focusing on localization of specific *Zymoseptoria* chromosomes in the nucleus by cytology or Hi-C (Galazka *et al.*, 2016) should be conducted to address this hypothesis.

In conclusion, using experimental evolution, electrophoretic karyotyping and genome sequencing we showed that the accessory chromosomes of *Z. tritici* are highly unstable during asexual growth across numerous mitotic cell divisions ("mitotic growth") *in vitro* as well as *in planta.* Surprisingly, increasing the temperature from 18 to 28°C dramatically increased overall genome instability in *Z. tritici*. Besides chromosome losses we observed structural variation in form of chromosome breakage, duplication, and fusion involving both core and accessory chromosomes, and all events were increased near telomeric sequences. In *Z. tritici,* all of these chromosome abnormalities have thus far been associated with meiosis (Wittenberg *et al.*, 2009; Croll *et al.*, 2013), however, our study highlights an important role of mitotic growth in generating genetic diversity. The variability in chromosome number and structure obtained over a relatively short period of time (during one infection event, or four weeks of vegetative growth) correlates with the genomic diversity observed in field populations of this important plant pathogen (McDonald & Martinez, 1991; Linde *et al.*, 2002; Zhan *et al.*, 2003; Mehrabi *et al.*, 2007). Our findings demonstrate that even sexual fungal pathogens can accelerate the generation

of new genetic diversity by mitosis-associated structural variation. The mitotic events responsible for these rearrangements are still to be characterized.

Lastly, chromosome instability has been observed in various organisms and is a frequent phenomenon in cancer cells (McGranahan *et al.*, 2012). Epigenetic factors and heterochromatin in particular have been shown to impact chromosome stability in human cancer cells (Slee *et al.*, 2012). The accessory chromosome dynamics correlating with distinct chromatin patterns suggest that *Z. tritici* may provide a new model for mechanistic studies of chromosome instability in cancer cells.

Materials and Methods

Short term *in vitro* growth experiment in liquid culture

Zymoseptoria strains were diluted from glycerol stocks (-80°C), plated on YMS agar (4 g yeast extract, 4 g malt extract, 4 g sucrose, and 20 g agar per 1 liter) plates and grown for seven days at 18°C to obtain single colonies. One single colony was picked and suspended in 100 µL of YMS. Three replicate cultures were inoculated with 20 µL of cells from the single colony (~50,000 cells). Cells were grown in 25 mL YMS medium at 18°C or 28°C shaking at 200 rpm and 900 µL of the cultures were transferred to fresh medium after 3-4 days of growth. In total eight transfers were conducted, for a total time course of four weeks.

Short term *in vitro* growth experiment on agar plates

A single colony derived directly from a plated dilution of frozen stock for Zt09 (IPO323Δ18) was resuspended in 1000 µL YMS including 25% glycerol by 2 min vortexing on a VXR basic Vibrax at 2,000 rpm, and 10-50 µL were replated onto a YMS agar plate. Forty replicates were produced. Cells were grown for seven days at 18°C whereby a random colony (based on vicinity to a prefixed position on the plate) derived from a single cell was picked and transferred to a new plate as described above. The transfer was conducted for a total of four times before a randomly chosen colony of each replicate was PCR screened and their complement on accessory chromosomes characterized as described below.

Screening by PCR

Cells from transfer eight of liquid cultures were diluted and plated on YMS-agar plates to obtain single colonies. To extract DNA, single colonies were suspended in 50 µL of 25 mM NaOH and boiled at 98°C for 10 min; 50 µL of 40 mM Tris-HCl, pH 5.5, were added and 4 µL were used as template for the PCR. Primers for the right and left subtelomeric regions and close to the centromere were used for the chromosome loss screening in our *Z. tritici* isolates, for *Z. ardabiliae* primers in the center of candidate accessory chromosome unitigs were used. Primers and expected fragment lengths are listed in Table S1. Primers were designed with Clonemanager (Sci-Ed Software, Denver, USA) and MacVector and ordered from eurofins Genomics (Ebersberg, Germany).

Plant experiments and pycnidia isolation

Growth conditions for plants were 16 h at light intensity of ~200 µmol/$m^{-2}s^{-1}$ and 8 h darkness in growth chambers at 20°C with 90% humidity. Seeds of the *Z. tritici* susceptible wheat cultivar Obelisk (Wiersum Plantbreeding BV, Winschoten, The Netherlands) were germinated on wet sterile Whatmann paper for four days at growth conditions before potting. Following potting, plants were further grown for seven days before infection.

For the phenotypic analyses, three independent experiments were conducted and 21 plants were used per strain per experiment. An ~5 cm long section on the second leaf of each plant was infected by brushing a cell suspension with 10^7 cell/ml in H_2O + 0.1% Tween 20 on the abaxial and adaxial side of the second leaf. Plants were placed into sealed bags containing ~1 L of water for 48 h to facilitate infection at maximum air humidity. Infected leaf areas were harvested 21 days post infection for further phenotypic analysis or prepared for pycnidia isolation by surface sterilization with 1.2% NaClO for 2 min followed by 70% ethanol for a few seconds and washed twice with H_2O. Leaves were placed into a sterile environment with maximum air humidity and incubated for 7-14 days at plant growth conditions. Spores that had been pressed out from pycnidia were isolated using a sterile syringe needle and resuspended into 50 µL YMS medium with 50% glycerol. Cells were suspended by 30 min vortexing on a VXR basic Vibrax (IKA, Staufen, Germany) at 2,000 rpm, plated on YMS agar, and incubated for seven days at 18°C. Colonies arising from single cells were PCR screened and their complement on accessory chromosomes characterized as described below.

Phenotypic characterization of infected leaves

Harvested leaves were taped to a sheet of paper and scanned using a flatbed scanner at a resolution of 2,400 dpi. The scanned leaves were analyzed using ImageJ (Schneider *et al.*, 2012) and a plug-in described previously (Stewart *et al.*, 2016). The measurement of pycnidia/cm^2 was used for further statistical analyses in R (Ihaka & Gentleman, 1996). The Wilcoxon-Rank-Sum test and the Holm's correction for multiple testing were applied to assess statistical differences between the samples.

***In vitro* phenotype assay**

A spore solution containing 10^7 cells/mL and tenfold dilution series to 1,000 cells/mL was prepared. To test for responses to different stress conditions *in vitro*, YMS plates containing NaCl (0.5 M and 1 M), sorbitol (1 M and 1.5 M), Congo Red (300 µg/mL and

500 µg/ml), H_2O_2 (1.5 mM and 2 mM), MMS (methyl methanesulfonate, 0.01 %), a H_2O-agar plate and two plates containing only YMS were prepared. Three µL of the spore suspension dilutions were pipetted on the plates and incubated at 18°C for seven days. One of the YMS plates was incubated at 28°C to test for thermal stress responses.

In vitro growth assay

YMS liquid cultures containing 10^5 cells/mL of either Zt09 or the chromosome-loss strains Zt09Δ14 and Zt09Δ21 were prepared. Three replicates per strain were used in each experiment. The spores were grown for four days at 18°C at 200 rpm in 25 mL YMS and the OD_{600} was measured at different time points throughout the experiment. The data was fitted using the R package growthcurver (Sprouffske & Wagner, 2016) and the r values of each replicate used for statistical comparison. Wilcoxon-rank-sum test was used to compare the r values of the different strains.

Pulsed field gel electrophoresis (PFGE) and Southern blotting

Fungal strains were grown in YMS medium for five days. Cells were harvested by centrifugation for 10 min at 3,500 rpm. 5 x 10^8 cells were used for plug preparation. The cells were resuspended in 1 mL H_2O and mixed with 1 mL of 2.2 % low range ultra agarose (Bio-Rad, Munich, Germany). The mixture was pipetted into plug casting molds and cooled for 1 h at 4°C. The plugs were transferred to 50 mL screw cap Falcon tubes containing 5 mL of lysis buffer (1 % SDS; 0.45 M EDTA; 1.5 mg/ml proteinase K, Roth, Karlsruhe, Germany), and incubated in lysis buffer for 48 h at 55°C, replacing the buffer once after 24 h. Chromosomal plugs were washed three times for 20 min with 1 x TE buffer before storage in 5 mL of 0.5 M EDTA at 4°C. PFGE was performed with a CHEF-DR III pulsed field electrophoresis system (BioRad, Munich, Germany). To separate the small accessory chromosomes, the following settings were applied: switching time 50 s – 150 s, 5 V/cm, 120° angle, 1 % pulsed field agarose (BioRad, Munich, Germany) in 0.5 x TBE (TRIS/borate/EDTA) for 48 h. Separation of mid-size chromosomes was conducted with the settings: switching time 250 s – 1000 s, 3 V/cm, 106° angle, 1 % pulsed field agarose in 0.5 x TBE for 72 h. *Saccharomyces cerevisiae* chromosomal DNA (BioRad, Munich, Germany) was used as size marker for the accessory chromosomes, and *Hansenula wingei* chromosomal DNA (BioRad, Munich, Germany) for mid-size chromosomes. Gels were stained in ethidium bromide staining solution (1 µg/ml ethidium bromide in H_2O) for 30 min. Detection of chromosomal bands was performed with the GelDocTM XR+ system

(Bio-Rad, Munich, Germany).

Southern blotting was performed as described previously (Southern, 1975) using DIG-labeled probes generated with the PCR DIG labeling Mix (Roche, Mannheim, Germany) following the manufacturer's instructions.

Sequencing and genome comparison

DNA for whole genome sequencing was prepared as described in (Allen *et al.*, 2006). Library preparation with a reduced number of PCR cycles (four cycles) and sequencing were performed by the Max Planck Genome Center, Cologne, Germany (http://mpgc.mpipz.mpg.de/home/) using an Illumina HiSeq3000 machine, obtaining ~30x coverage with 150-nt paired-end reads. Raw reads were quality filtered using Trimmomatic and mapped to the reference genome of *Z. tritici* or *Z. ardabiliae* using bowtie2. SNP calling was conducted with samtools and bcftools and further quality filtered. The filtered SNPs were validated by manual inspection. The data was visualized in IGV (Integrative Genomics Viewer, http://software.broadinstitute.org/software/igv/) (Thorvaldsdóttir *et al.*, 2013). Detailed commands for each step of the data processing pipeline can be found in the Supplementary Text.

Accession numbers: The sequencing data generated for this project were deposited in the Sequence Read Archive under BioProject ID PRJNA428438.

Acknowledgements

Marcello Zala, Daniel Croll and Christoph J. Eschenbrenner are acknowledged for the preparation and assembly of the SMRT sequencing. Kathrin Happ for assistance during plant experiments. We thank all current and past members of the Environmental Genomics Group for fruitful discussions and overall support. Research in the group of EHS is supported by the Max-Planck Society, the state of Schleswig-Holstein and the DFG priority program SPP1819.

Competing interests

The authors declare no competing interests.

References

Allen GC, Flores-Vergara M a, Krasynanski S, Kumar S, Thompson WF. **2006**. A modified protocol for rapid DNA isolation from plant tissues using cetyltrimethylammonium bromide. *Nature protocols* **1**: 2320–2325.

Barrick JE, Lenski RE. **2013**. Genome dynamics during experimental evolution. *Nature reviews. Genetics* **14**: 827–39.

Bennett RJ, Forche A, Berman J. **2014**. Rapid mechanisms for generating genome diversity: Whole ploidy shifts, aneuploidy, and loss of heterozygosity. *Cold Spring Harbor Perspectives in Medicine* **4**.

Chuma I, Isobe C, Hotta Y, Ibaragi K, Futamata N, Kusaba M, Yoshida K, Terauchi R, Fujita Y, Nakayashiki H, *et al.* 2011. Multiple Translocation of the *AVR-Pita* Effector Gene among Chromosomes of the Rice Blast Fungus *Magnaporthe oryzae* and Related Species. *PLoS Pathog* **7**: e1002147.

Coleman JJ, Rounsley SD, Rodriguez-Carres M, Kuo A, Wasmann CC, Grimwood J, Schmutz J, Taga M, White GJ, Zhou S, *et al.* 2009. The genome of Nectria haematococca: Contribution of supernumerary chromosomes to gene expansion. *PLoS Genetics* **5**.

Croll D, Lendenmann MH, Stewart E, McDonald BA. **2015**. The impact of recombination hotspots on genome evolution of a fungal plant pathogen. *Genetics* **201**: 1213–1228.

Croll D, McDonald BA. **2012**. The accessory genome as a cradle for adaptive evolution in pathogens. *PLoS Pathogens* **8**: 8–10.

Croll D, Zala M, McDonald B a. **2013**. Breakage-fusion-bridge cycles and large insertions contribute to the rapid evolution of accessory chromosomes in a fungal pathogen. *PLoS genetics* **9**: e1003567.

van Dam P, de Sain M, ter Horst A, van der Gragt M, Rep M. **2018**. Use of Comparative Genomics-Based Markers for Discrimination of Host Specificity in Fusarium oxysporum. *Applied and Environmental Microbiology* **84**.

Dhillon B, Gill N, Hamelin RC, Goodwin SB. **2014**. The landscape of transposable elements in the finished genome of the fungal wheat pathogen Mycosphaerella graminicola. *BMC genomics* **15**: 1132.

Faino L, Seidl MF, Shi-Kunne X, Pauper M, van den Berg GCM, Wittenberg AHJ, Thomma BPHJ. **2016**. Transposons passively and actively contribute to evolution of the two-speed genome of a fungal pathogen. *Genome Research*: gr.204974.116.

Fones H, Gurr S. **2015**. The impact of Septoria tritici Blotch disease on wheat: An EU perspective. *Fungal Genetics and Biology* **79**: 3–7.

Fouche S, Plissonneau C, McDonald BA, Croll D. **2017**. Meiosis leads to pervasive segregation distortion and copy-number variation in accessory chromosomes of the wheat pathogen *Zymoseptoria tritici*. *bioRxiv*. doi: https://doi.org/10.1101/214882

Fraser JA, Huang JC, Pukkila-worley R, Alspaugh A, Mitchell TG, Heitman J, Alspaugh JA. **2005**. Chromosomal Translocation and Segmental Duplication in Cryptococcus neoformans Chromosomal Translocation and Segmental Duplication in Cryptococcus neoformans †. **4**: 401–406.

Galazka JM, Klocko AD, Uesaka M, Honda S, Selker EU, Freitag M. **2016**. *Neurospora* chromosomes are organized by blocs of importin alpha- dependent heterochromatin that are largely independent of H3K9me3. *Genome Research*: 1069–1080.

Goodwin SB, M'barek S Ben, Dhillon B, Wittenberg AHJ, Crane CF, Hane JK, Foster AJ, Van der Lee T a J, Grimwood J, Aerts A, *et al.* 2011b. Finished genome of the fungal wheat pathogen Mycosphaerella graminicola reveals dispensome structure, chromosome plasticity, and stealth pathogenesis. *PLoS genetics* **7**: e1002070.

Grandaubert J, Bhattacharyya A, Stukenbrock EH. **2015**. RNA-seq Based Gene Annotation and Comparative Genomics of Four Fungal Grass Pathogens in the Genus Zymoseptoria Identify Novel Orphan Genes and Species-Specific Invasions of Transposable Elements. *G3 (Bethesda, Md.)* **5**: g3.115.017731-.

Habig M, Quade J, Stukenbrock EH. **2017**. Forward genetics approach reveals host-genotype dependent importance of accessory chromosomes in the fungal wheat pathogen Zymoseptoria tritici. *mBio* **8**: Forthcoming.

Harr JC, Luperchio TR, Wong X, Cohen E, Wheelan SJ, Reddy KL. **2015**. Directed targeting of chromatin to the nuclear lamina is mediated by chromatin state and A-type lamins. *Journal of Cell Biology* **208**: 33–52.

Haueisen J, Moeller M, Eschenbrenner CJ, Grandaubert J, Seybold H, Adamiak H, Stukenbrock EH. **2017**. Extremely flexible infection programs in a fungal plant pathogen. *bioRxiv* **doi:** https://doi.org/10.1101/229997

Ihaka R, Gentleman R. **1996**. R: A Language for Data Analysis and Graphics. *Journal of Computational and Graphical Statistics* **5**: 299–314.

Johnson LJ, Johnson RD, Akamatsu H, Salamiah A, Otani H, Kohmoto K, Kodama M. **2001**. Spontaneous loss of a conditionally dispensable chromosome from the Alternaria alternata apple pathotype leads to loss of toxin production and pathogenicity. *Current Genetics* **40**: 65–72.

De Jonge R, Bolton MD, Kombrink A, Van Den Berg GCM, Yadeta KA, Thomma BPHJ. **2013**. Extensive chromosomal reshuffling drives evolution of virulence in an asexual pathogen. *Genome Research* **23**: 1271–1282.

Kellner R, Bhattacharyya A, Poppe S, Hsu TY, Brem RB, Stukenbrock EH. **2014**. Expression Profiling of the Wheat Pathogen Zymoseptoria tritici Reveals Genomic Patterns of Transcription and Host-Specific Regulatory Programs. *Genome biology and evolution* **6**: 1353–65.

Klocko AD, Ormsby T, Galazka JM, Leggett NA, Uesaka M, Honda S, Freitag M, Selker EU. **2016**. Normal chromosome conformation depends on subtelomeric facultative heterochromatin in *Neurospora crassa*. *Proceedings of the National Academy of Sciences* **113**: 15048–15053.

Kumaran R, Yang S-Y, Leu J-Y. **2013**. Characterization of Chromosome Stability in Diploid, Polyploid and Hybrid Yeast Cells. *PLOS ONE* **8**: e68094.

Linde CC, Zhan J, McDonald BA. **2002**. Population Structure of Mycosphaerella graminicola: From Lesions to Continents. *Phytopathology* **92**: 946–955.

Ma L-J, van der Does HC, Borkovich K a, Coleman JJ, Daboussi M-J, Di Pietro A, Dufresne M, Freitag M, Grabherr M, Henrissat B, *et al.* 2010. Comparative genomics reveals mobile pathogenicity chromosomes in Fusarium. *Nature* **464**: 367–373.

McClintock B. **1938**. The Production of Homozygous Deficient Tissues with Mutant Characteristics by Means of the Aberrant Mitotic Behavior of Ring-Shaped Chromosomes. *Genetics* **23**: 315–376.

McClintock B. **1941**. The Stability of Broken Ends of Chromosomes in Zea Mays. *Genetics* **26**: 234–282.

McDonald B a., Martinez JP. **1991**. Chromosome length polymorphisms in a Septoria tritici population. *Current Genetics* **19**: 265–271.

McDonald MC, McGinness L, Hane JK, Williams AH, Milgate A, Solomon PS. **2016**. Utilizing Gene Tree Variation to Identify Candidate Effector Genes in Zymoseptoria tritici. *G3 (Bethesda, Md.)* **6**: 779–91.

McGranahan N, Burrell RA, Endesfelder D, Novelli MR, Swanton C. **2012**. Cancer chromosomal instability: therapeutic and diagnostic challenges. *EMBO Rep* **13**: 528–538.

Mehrabi R, Taga M, Kema GHJ. **2007**. Electrophoretic and cytological karyotyping of the foliar wheat pathogen Mycosphaerella graminicola reveals many chromosomes with a large size range. *Mycologia* **99**: 868–76.
Miao V, Covert S, VanEtten H. **1991a**. A fungal gene for antibiotic resistance on a dispensable ("B") chromosome. *Science* **254**: 1773–1776.
Miao VP, Covert SF, VanEtten HD. **1991b**. A fungal gene for antibiotic resistance on a dispensable (" B") chromosome. *Science* **254**: 1773.
Murnane JP. **2012**. Telomere dysfunction and chromosome instability. *Mutation Research/Fundamental and Molecular Mechanisms of Mutagenesis* **730**: 28–36.
Persoons A, Morin E, Delaruelle C, Payen T, Halkett F, Frey P, De Mita S, Duplessis S. **2014**. Patterns of genomic variation in the poplar rust fungus Melampsora larici-populina identify pathogenesis-related factors. *Frontiers in Plant Science* **5**: 450.
Petit-Houdenot Y, Fudal I. **2017**. Complex Interactions between Fungal Avirulence Genes and Their Corresponding Plant Resistance Genes and Consequences for Disease Resistance Management. *Frontiers in Plant Science* **8**.
Plissonneau C, Stürchler A. **2016**. The Evolution of Orphan Regions in Genomes of a Fungal Pathogen of Wheat. **7**.
Poláková S, Blume C, Zárate JA, Mentel M, Jørck-Ramberg D, Stenderup J, Piskur J. **2009**. Formation of new chromosomes as a virulence mechanism in yeast Candida glabrata. *Proceedings of the National Academy of Sciences of the United States of America* **106**: 2688–2693.
Ponomarenko A, Goodwin SB, Kema GHJ. **2011**. Septoria tritici blotch (STB) of wheat Septoria tritici blotch (STB) of wheat. *Plant Health Instructor*: 1–7.
Rudd JJ, Kanyuka K, Hassani-Pak K, Derbyshire M, Andongabo A, Devonshire J, Lysenko A, Saqi M, Desai NM, Powers SJ, *et al.* 2015. Transcriptome and metabolite profiling of the infection cycle of Zymoseptoria tritici on wheat reveals a biphasic interaction with plant immunity involving differential pathogen chromosomal contributions and a variation on the hemibiotrophic lifestyle def. *Plant physiology* **167**: 1158–85.
Schneider C a, Rasband WS, Eliceiri KW. **2012**. NIH Image to ImageJ: 25 years of image analysis. *Nature Methods* **9**: 671–675.
Schotanus K, Soyer JL, Connolly LR, Grandaubert J, Happel P, Smith KM, Freitag M, Stukenbrock EH. **2015**. Histone modifications rather than the novel regional centromeres of Zymoseptoria tritici distinguish core and accessory chromosomes. *Epigenetics & chromatin* **8**: 41.
Selmecki A, Forche A, Berman J. **2010**. Genomic plasticity of the human fungal pathogen Candida albicans. *Eukaryotic Cell* **9**: 991–1008.
Slee RB, Steiner CM, Herbert B-S, Vance GH, Hickey RJ, Schwarz T, Christan S, Radovich M, Schneider BP, Schindelhauer D, *et al.* 2012. Cancer-associated alteration of pericentromeric heterochromatin may contribute to chromosome instability. *Oncogene* **31**: 3244–53.
Southern EM. **1975**. Detection of specific sequences among DNA fragments separated by gel electrophoresis. *Journal of Molecular Biology* **98**: 503–517.
Sprouffske K, Wagner A. **2016**. Growthcurver: an R package for obtaining interpretable metrics from microbial growth curves. *BMC Bioinformatics* **17**: 172.
Stewart EL, Hagerty CH, Mikaberidze A, Mundt C, Zhong Z, McDonald BA. **2016**. An improved method for measuring quantitative resistance to the wheat pathogen Zymoseptoria tritici using high throughput automated image analysis. *Phytopathology*.

Stukenbrock EH, Bataillon T, Dutheil JY, Hansen TT, Li R, Zala M, McDonald BA, Wang J, Schierup MH. **2011**. The making of a new pathogen: insights from comparative population genomics of the domesticated wheat pathogen Mycosphaerella graminicola and its wild sister species. *Genome research* **21**: 2157–66.

Stukenbrock EH, Dutheil JY. **2018**. Fine-scale recombination maps of fungal plant pathogens reveal dynamic recombination landscapes and intragenic hotspots. *Genetics* **208**: 1209–1229.

Stukenbrock EH, Jørgensen FG, Zala M, Hansen TT, McDonald B a, Schierup MH. **2010**. Whole-genome and chromosome evolution associated with host adaptation and speciation of the wheat pathogen Mycosphaerella graminicola. *PLoS genetics* **6**: e1001189.

Thorvaldsdóttir H, Robinson JT, Mesirov JP. **2013**. Integrative Genomics Viewer (IGV): High-performance genomics data visualization and exploration. *Briefings in Bioinformatics* **14**: 178–192.

Torriani SFF, Melichar JPE, Mills C, Pain N, Sierotzki H, Courbot M. **2015**. Zymoseptoria tritici: A major threat to wheat production, integrated approaches to control. *Fungal Genetics and Biology* **79**: 8–12.

Tsuge T, Harimoto Y, Hanada K, Akagi Y, Kodama M, Akimitsu K, Yamamoto M. **2016**. Evolution of pathogenicity controlled by small, dispensable chromosomes in Alternaria alternata pathogens. *Physiological and Molecular Plant Pathology* **95**: 27–31.

Vlaardingerbroek I, Beerens B, Schmidt SM, Cornelissen BJC, Rep M. **2016**. Dispensable chromosomes in Fusarium oxysporum f . sp lycopersici . *Molecular Plant Pathology*: 1–12.

Wang B, Brubaker CL, Tate W, Woods MJ, Matheson BA, Burdon JJ. **2006**. Genetic variation and population structure of Fusarium oxysporum f.sp. vasinfectum in Australia. *Plant Pathology* **55**: 746–755.

Wittenberg AHJ, van der Lee T a J, Ben M'barek S, Ware SB, Goodwin SB, Kilian A, Visser RGF, Kema GHJ, Schouten HJ. **2009**. Meiosis drives extraordinary genome plasticity in the haploid fungal plant pathogen Mycosphaerella graminicola. *PloS one* **4**: e5863.

Zhan J, McDonald BA. **2011**. Thermal adaptation in the fungal pathogen Mycosphaerella graminicola. *Molecular Ecology* **20**: 1689–1701.

Zhan J, Pettway RE, McDonald BA. **2003**. The global genetic structure of the wheat pathogen Mycosphaerella graminicola is characterized by high nuclear diversity, low mitochondrial diversity, regular recombination, and gene flow. *Fungal Genetics and Biology* **38**: 286–297.

Zhong Z, Marcel TC, Hartmann FE, Ma X, Plissonneau C, Zala M, Ducasse A, Confais J, Compain J, Lapalu N, *et al.* 2017. A small secreted protein in Zymoseptoria tritici is responsible for avirulence on wheat cultivars carrying the Stb6 resistance gene. *New Phytologist* **214**: 619–631.

Zhu YO, Siegal ML, Hall DW, Petrov DA. **2014**. Precise estimates of mutation rate and spectrum in yeast. *Proceedings of the National Academy of Sciences* **111**: E2310–E2318.

Supplement

All supplementary tables and texts are deposited on the supplementary USB key.

Table S1. List of primers used for screening for accessory chromosomes in *Z. tritici* and *Z. ardabiliae*.

Table S2. List of chromosome-loss strains identified in the *in vitro* and *in planta* experiments.

Table S3. Chromosome variation of sequenced Zt09-derived strains grown at 28°C.

Table S4. Location and annotation of SNPs and INDELs found in the sequenced chromosome-loss strains.

Supplementary text. Programs and commands used for quality filtering, mapping, visualization, and SNP calling for genome sequencing data and assembly of long-read SMRT sequencing reads of the *Zymoseptoria ardabiliae* reference strain Za17.

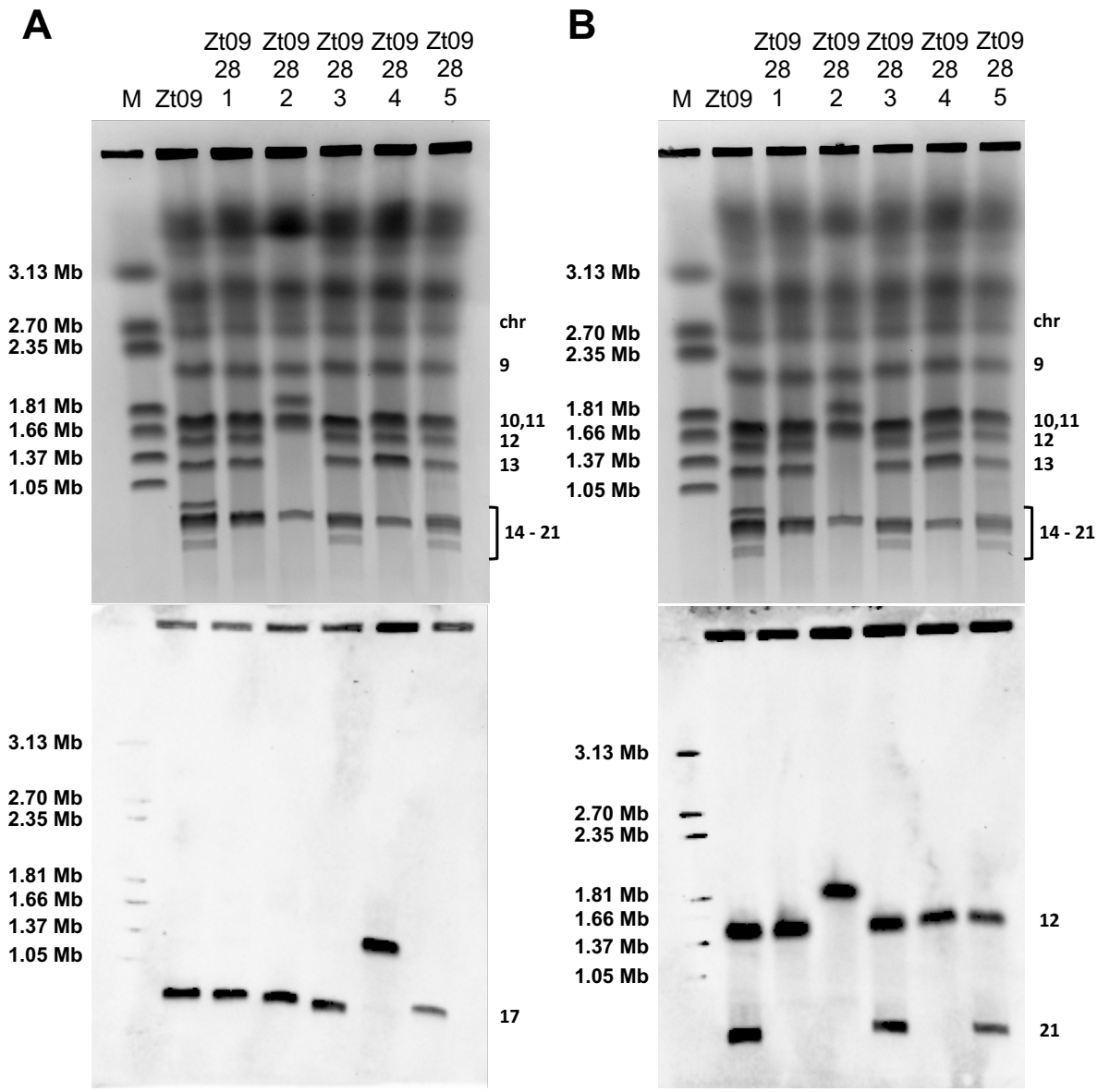

Figure S1. Southern blotting of pulsed-field gels using chromosome-specific probes confirms chromosome fusions. To prove and visualize chromosome fusions in the strains derived from the temperature stress experiment, we conducted PFGE followed by Southern blots with probes specific to the chromosomes, which based on genome data and karyotype analyses, were found to have fused. Panel (A) shows a color-inverted image of the pulsed-field gel (top) and Southern blot (bottom) using a probe specific for chromosome 17. The genomes of all tested strains have chromosome 17, and the genomes of strains Zt09 28-2 and Zt09 28-4 contain a duplicated chromosome 17 (Figure 2C). While in Zt09 28-2 the duplication resulted in two separate copies of the chromosome, the two chromosomes 17 in Zt09 28-4 fused and formed a new ~ 1.2 Mb chromosome. (B) For the second Southern blot, we used probes for chromosomes 12 and 21. Chromosome 21 is absent in the strains Zt09 28-1 and Zt09 28-3 (PFGE, top and Southern analyses, bottom). Genome sequencing shows that chromosome 21 is present in Zt09 28-2 (Figure 2C), however the respective band on the pulsed-field gel is missing. Similarly,

chromosomes 12 and 13 are not present in this strain (PFGE, top), while the chromosome sequences are present in the whole genome sequence data. Apparent loss of chromosome 13 can be explained by the fusion of chromosomes 3 and 13, as indicated by the sequence analysis (Figure 3). The probes for chromosomes 12 and 21 both hybridize to one band in the size of ~1.8 Mb (Southern, bottom) matching the size expected if a chromosome fusion occurred and explaining the absence of their respective 'original' chromosomal bands.

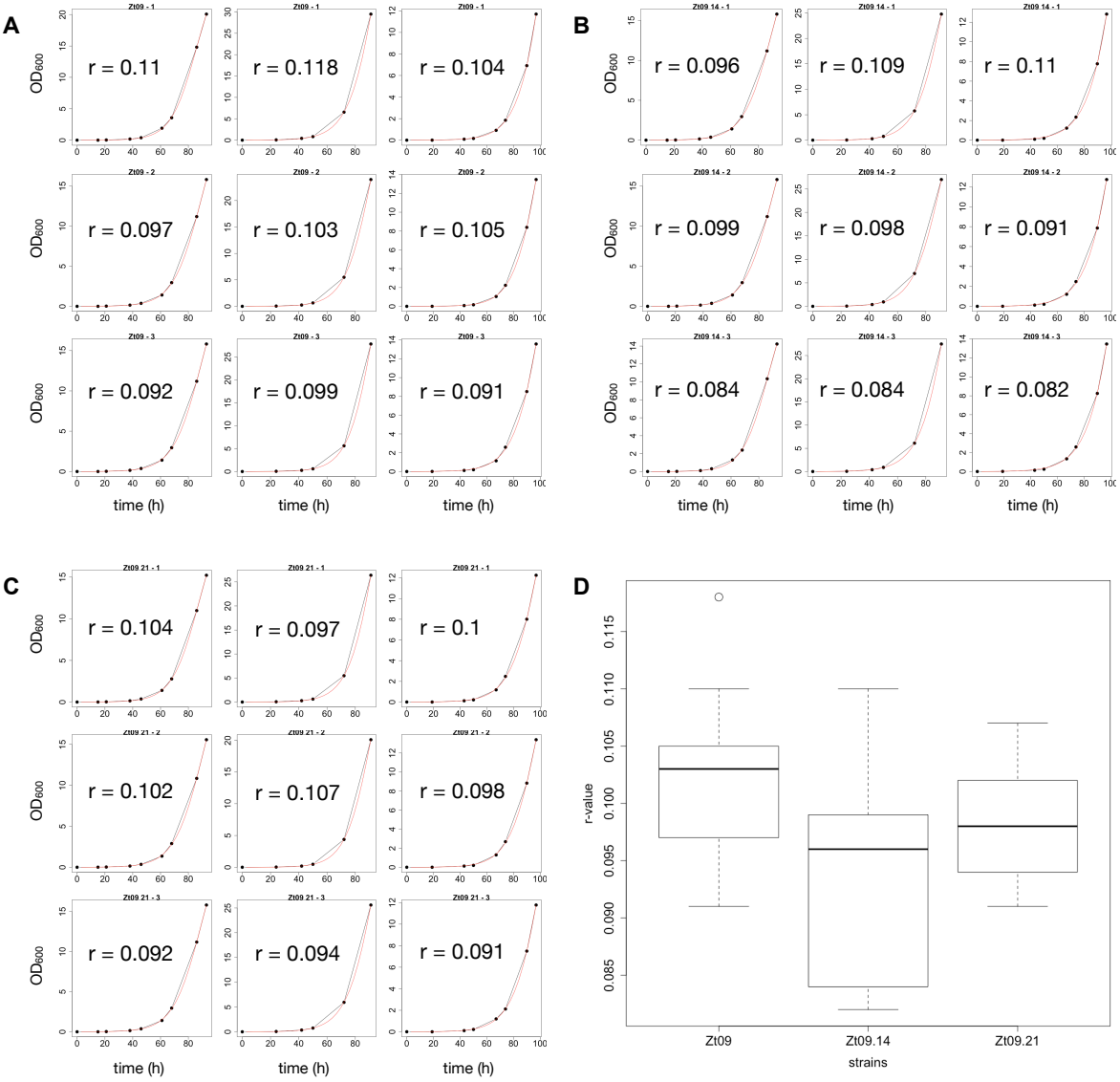

Figure S2. Growth assay of Zt09 and chromosome-loss strains Zt09Δ14 and Zt09Δ21. Three independent growth assays were conducted with the progenitor strain Zt09 **(A)** and two chromosome-loss strains Zt09Δ14 **(B)** and Zt09Δ21 **(C)**, representing the loss of the largest and smallest accessory chromosome. Plotted are the fitted growth curves of all replicates and experiments generated with the R package growthcurver. The growth curves are based on OD_{600} measurements. Panel **(D)** displays a boxplot of all r values of the different strains. There are no significant differences between the growth curves of the three tested strains (Wilcoxon-rank-sum test Zt09 – Zt09Δ14: *P*-value = 0.1443, Zt09 - Zt09Δ21: *P*-value = 0.3762).

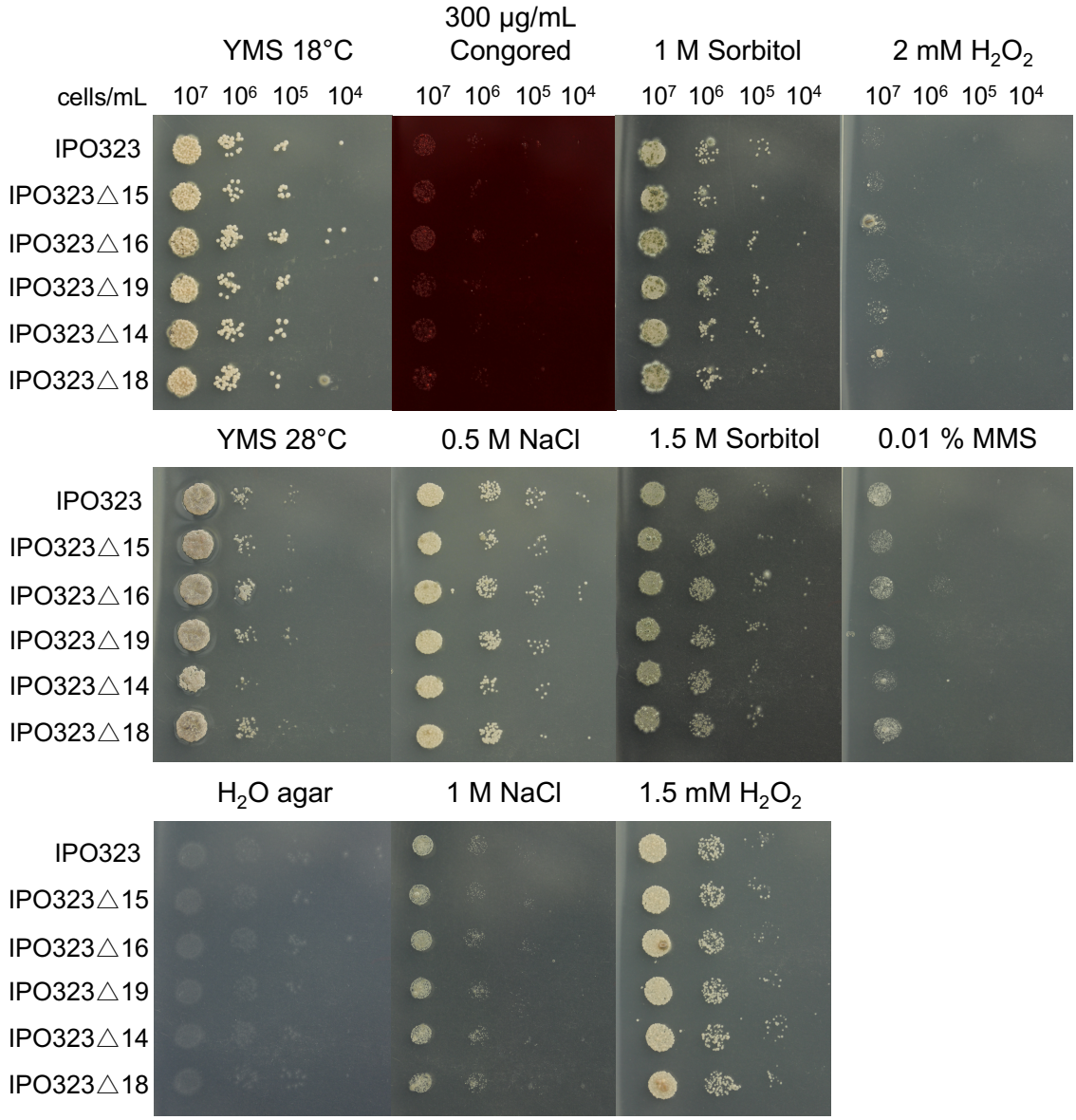

Figure S3. *In vitro* stress assays of the *Z. tritici* reference isolate IPO323 and the *in planta* chromosome-loss strains. Several *in vitro* stress conditions were tested to assess the effect of accessory chromosome losses on fitness. Five *in planta* chromosome-loss strains were tested, IPO323 was used as the reference strain. We observed no noteworthy differences in growth rate or colony morphology between reference and chromosome-loss strains.

Chapter III

The role of heterochromatin in genome and chromosome stability in a fungal plant pathogen

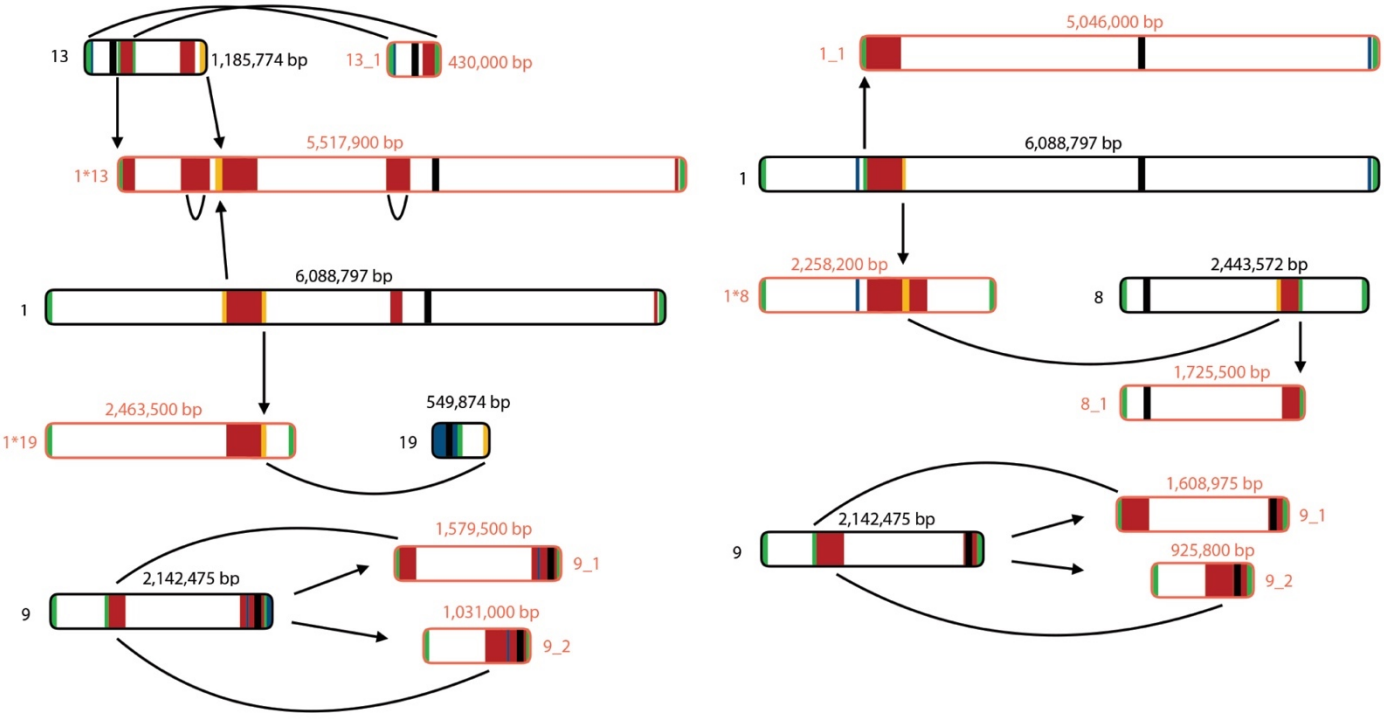

Chapter III

The role of heterochromatin in genome and chromosome stability in a fungal plant pathogen

Mareike Möller[1,2], Klaas Schotanus[3], Jessica Soyer[4], Janine Haueisen[1,2], Kathrin Happ[1], Maja Stralucke[1], Petra Happel[5], Kristina M. Smith[6], Lanelle R. Connolly[6], Michael Freitag[6], and Eva H. Stukenbrock[1,2]

[1]Environmental Genomics, Christian-Albrechts University, Am Botanischen Garten 1-9, D-24118 Kiel, Germany

[2]Max Planck Institute for Evolutionary Biology, August-Thienemann-Str. 2, D-24306 Plön, Germany

[3]Departments of Molecular Genetics and Microbiology (MGM), Pharmacology and Cancer Biology, and Medicine, Duke University Medical Center, Durham, North Carolina, United States of America

[4]UMR BIOGER, INRA, AgroParisTech, Université Paris-Saclay, 78850 Thiverval-Grignon, France

[5]Max Planck Institute for Terrestrial Microbiology, Karl-von-Frisch-Straße 10, D-35043 Marburg, Germany

[6]Department of Biochemistry and Biophysics, Oregon State University, Corvallis, OR 97331-7305, United States of America

Abstract

Chromosome and genome stability are important for normal cell function and often instability correlates with disease and dysfunction of DNA repair mechanisms. Many organisms inhabit supernumerary or accessory chromosomes that deviate from standard chromosomes. The pathogenic fungus *Zymoseptoria tritici* has as many as eight accessory chromosomes. These chromosomes are highly instable during meiosis and mitosis, transcriptionally repressed and show enrichment of repetitive elements and of the heterochromatic histone methylation marks H3K27me3 and H3K9me3. To elucidate the role of heterochromatin on genome stability in *Z. tritici,* we created deletion mutants of the methyltransferases responsible for H3K27me3 and H3K9me3, respectively. We combined experimental evolution and genomic analyses to follow the impact of these deletions on chromosome and genome stability. We used ChIP-seq, whole genome sequencing and RNA-seq to compare changes in chromatin and genome structure and differences in gene expression between mutant and wild type strains. Analyses of genome and ChIP-seq data reveal dramatic chromatin reorganizations, genome rearrangements and formation of new chromosomes in the absence of H3K9me3 together with transposable element activation. Loss of H3K27me3, however, increases the stability of accessory chromosomes under normal growth conditions *in vitro* compared to the wild type. Based on these results, we conclude a strong impact of H3K9me3 on chromatin organization and genome stability and an important role of H3K27me3 for the stability of accessory chromosomes.

Introduction

Epigenetic mechanisms play an important role in gene and genome organization ranging from structural determinants of chromosome and chromatin structure to fine scale transcriptional regulation (Kornberg & Lorch, 1992; Goldberg *et al.*, 2007; Venkatesh & Workman, 2015). A well-studied hallmark of epigenetic regulation is the modification of histone tails altering chromatin structure (Bannister & Kouzarides, 2011). The chromatin structure determines accessibility of the underlying DNA to regulatory elements (Harr *et al.*, 2016). Tightly packed DNA, known as heterochromatin, is less accessible for DNA binding proteins and shows little transcriptional activity. Heterochromatic regions often cluster together and are spatially separated from more active and accessible, euchromatic regions (Zimmer & Fabre, 2011). Specific histone modifications are associated with either heterochromatic or euchromatic regions. Some of the most studied histone modifications

are H3K9me2/3 and H3K27me2/3 as heterochromatin marks and H3K4me2/me3 as euchromatin markers. Threefold methylation of histone 3 lysine 9 is catalyzed by the histone methyltransferase KMT1 (Su(Var)3-9) (Rea *et al.*, 2000; Allis *et al.*, 2007) and previous studies demonstrated a clear link between this constitutive heterochromatin mark and repeat-rich genome regions and the control of transposable elements (Mikkelsen *et al.*, 2007; Zeller *et al.*, 2016).

The distribution and role of the facultative heterochromatin-associated H3K27me3 (threefold methylation of histone 3 lysine 27), mediated by KMT6 (E(Z)) as part of the PRC2 complex (Müller *et al.*, 2002), is more variable and seems to differ in different species. In plants and animals, H3K27 methylation is required for development and cell differentiation (Goodrich *et al.*, 1997; O'Carroll *et al.*, 2001; Lee *et al.*, 2006; Holec & Berger, 2012), and aberration of normal H3K7me3 distribution is often associated with developmental defects and is prevalent in cancer cells (Wei *et al.*, 2008; Holm *et al.*, 2012; Ngollo *et al.*, 2017). In fungi, H3K27me3 correlates with subtelomeric gene silencing (Jamieson *et al.*, 2013; Basenko *et al.*, 2015), and has been shown to play a role in transcriptional regulation of secondary metabolite gene clusters in some species (Connolly *et al.*, 2013; Chujo & Scott, 2014; Studt *et al.*, 2016). Furthermore, H3K27me3 appears to be a hallmark of so-called accessory chromosomes that are found in several plant pathogen species. These accessory chromosomes show presence/absence variation among individuals and are often characterized by extensive structural rearrangements and length variation (Covert, 1998; Möller & Stukenbrock, 2017). The functional role of accessory chromosomes in fungal pathogens could be related to increased virulence in some species such as *Fusarium oxysporum*, *Nectria haematococca* and *Leptosphaeria maculans* (Miao *et al.*, 1991; Ma *et al.*, 2010). However, in another fungal plant pathogen, *Zymoseptoria tritici*, some accessory chromosomes have been demonstrated to confer a fitness cost and decrease in virulence (Habig *et al.*, 2017). Interestingly, accessory chromosomes often structurally differ from core chromosomes. In *Z. tritici*, accessory chromosomes exhibit a higher repeat and lower gene density compared to core chromosomes and show only very little transcriptional activity (Goodwin *et al.*, 2011; Kellner *et al.*, 2014; Rudd *et al.*, 2015).

Consistently, their chromatin structure is predominantly heterochromatic with H3K27me3 covering the entire accessory chromosomes and H3K9me3 covering repetitive sequences (Schotanus *et al.*, 2015). This unusual, wide-ranging distribution of H3K27me3 has also been reported for accessory chromosomes of fungal species in the

genus *Fusarium* (Galazka & Freitag, 2014; Studt *et al.*, 2016) suggesting a special role of facultative heterochromatin for these chromosomes in fungi. Though accessory chromosomes are a frequent phenomenon in fungi, little is known about their origin and maintenance. Studies on chromosome stability revealed that accessory chromosomes are highly unstable, both during mitosis (Miao *et al.*, 1991; Vlaardingerbroek *et al.*, 2016; Moeller *et al.*, 2018) and meiosis (Wittenberg *et al.*, 2009). Centromeres and telomeres are important structural components of chromosomes. In plants, centromeres of B chromosomes, equivalents to fungal accessory chromosomes, differ compared to A chromosomes (Jin *et al.*, 2005). However, in a previous study we addressed the composition of centromeres and telomeres in *Z. tritici* and could not detect differences between core and accessory chromosomes (Schotanus *et al.*, 2015). An intriguing question is therefore, to what extent the particular histone methylation pattern on the accessory chromosomes contributes to the structural differences, transcriptional repression and instability?

In this study, we elucidated the roles of H3K9me3 and H3K27me3 on genome stability in the wheat pathogen *Z. tritici*. The presence of eight accessory chromosomes in the reference isolate IPO323 makes *Z. tritici* an excellent model to study accessory chromosome characteristics and dynamics. By combining experimental evolution with genome, transcriptome and ChIP sequencing, we could show that both heterochromatin-associated histone methylation marks contribute significantly, but in distinct ways, to chromosome stability and integrity. While the presence of H3K27me3 enhances chromosome loss and instability, loss of H3K9me3 promotes chromosome breakage, segmental duplications as well as the formation of new chromosomes – possibly resembling the emergence of accessory chromosomes. Surprisingly, loss of H3K27me3 did not result in an overall increased transcriptional activation, but rather decreases the number of expressed genes. However, the mutant strain lacking H3K9me3 and a double deletion mutant lacking both, H3K9me3 and H3K27me3, showed a higher number of expressed genes, as well as transposable element activation. Taken together, our findings demonstrate the importance of constitutive heterochromatin for maintaining genome stability and gene silencing as well as an unexpected destabilizing influence of facultative heterochromatin on mitotic accessory chromosome transmission.

Results

Deletion of histone methyltransferase encoding genes *kmt1* and *kmt6* in *Zymoseptoria tritici*

To investigate the impact of heterochromatin on fitness, transcription and genome stability in *Z. tritici*, we generated mutants of the two histone methyltransferases KMT1 (Dim-5) and KMT6 (Set-7). KMT1 is the histone methyltransferase responsible for threefold methylation of H3K9 (Rea *et al.*, 2000; Allis *et al.*, 2007), whereas KMT6 has been shown to add methyl groups to H3K27 (Müller *et al.*, 2002). In *Z. tritici* we identified the genes predicted to encode the homologs of KMT1, *Zt_chr_1_01919* and KMT6, *Zt_chr_4_00551*, hereafter referred to as *kmt1* and *kmt6,* respectively (Grandaubert *et al.*, 2015).

We used an *Agrobacterium tumefaciens*-mediated transformation protocol (Bowler *et al.*, 2010) to delete the two genes encoding for KMT1 and KMT6 in the *Z. tritici* isolate Zt09, a derivate of the reference isolate IPO323 that has lost chromosome 18 during *in vitro* growth (Goodwin et al. 2011; Kellner et al. 2014). Correct integrations of the hygromycin resistance cassette and resulting gene deletions were verified by PCR and Southern blot (Figure S1). We furthermore generated a double deletion mutant by deleting the *kmt1* gene in a *kmt6* deletion mutant background using nourseothricin resistance as an additional selection marker. In total, we identified eight *Δkmt1*, six *Δkmt6* and ten independent *Δkmt1/kmt6* transformants, hereafter called *Δk1/k6*. *Δkmt1* and *Δkmt6* single mutants were complemented by integrating the respective deleted gene and a *neo*$^{+}$ resistance marker (conferring G418 resistance) at the native gene loci (Table S1).

To confirm absence of histone modifications and to assess changes in histone modification patterns in the methyltransferase mutants, we performed ChIP-seq on Zt09, *Δkmt1*, *Δkmt6* and the double deletion mutant *Δk1/k6.* Analysis of ChIP-seq data verified the absence of H3K9me3 in *Δkmt1* and *Δk1/k6* as well as the absence of H3K27me3 in *Δkmt6* and *Δk1/k6* mutants (Figure S2).

Deletion of *kmt1*, but not *kmt6*, severely impacts *in vitro* and *in planta* growth

To assess if deletion of *kmt1* and *kmt6* has an impact on *in vitro* growth or pathogenicity on wheat, we performed comparative growth and virulence assays including the mutants and the wild type isolate Zt09. To compare growth rates, deletion and complementation strains were grown in liquid YMS cultures and the OD_{600} was measured until the cells

reached the stationary phase. Overall, the Δ*kmt1* strains and Δ*k1/k6* double deletion mutants showed significantly reduced growth in *in vitro* cultures (Figure S3). The Δ*kmt6* mutants and both *kmt1*$^{+}$ and *kmt6*$^{+}$ complementation strains showed no significant differences in growth compared to Zt09 (Wilcoxon-rank-sum test, *P*-values: Δ*kmt1* 0.025; Δ*kmt6* 0.42; Δ*k1/*6 0.005; *kmt1*$^{+}$ 0.28; *kmt6*$^{+}$ 0.63).

We furthermore assessed the tolerance of the Δ*kmt1*, Δ*kmt6* and Δ*k1/k6* mutants towards different abiotic stressors *in vitro* testing temperature, cell wall, oxidative and genotoxic stresses. As observed in the growth assay, the Δ*kmt1* and Δ*k1/k6* double deletion mutants showed reduced overall growth under all tested conditions (Figure S4). Especially, when exposed to osmotic stress in form of high sorbitol concentrations and the cell wall-interfering agent Congored, growth of Δ*kmt1* and Δ*k1/k6* deletion mutants was strongly impaired. The Δ*kmt6* mutants showed little differences compared to Zt09, however, elevated temperatures led to increased melanization in the Δ*kmt6* mutants suggesting involvement of H3K27me3 in temperature stress response. This phenotype was reversed in the complementation strain (Figure S5).

To study the effect of the histone methyltransferase deletions on the ability to infect the natural *Z. tritici* host plant wheat, we inoculated leaves of the susceptible wheat cultivar Obelisk with single cells of Δ*kmt1*, Δ*kmt6,* the Δ*k1/k6* double deletion mutant and wild type strains. We conducted three independent experiments, including 40 leaves per treatment and using at least two biological replicates per strain. Infection symptoms were evaluated and compared as the percentage of leaf area covered with pycnidia (asexual fruiting bodies) and necrotic lesions within the inoculated leaf areas by manual inspection as well as by automated image analysis of scanned leaves (Stewart *et al.*, 2016). The infection assays demonstrated little impact of the H3K27me3 histone modification on virulence. The reference strain Zt09 as well as the Δ*kmt6* mutants were able to infect and produce pycnidia, however, the number of pycnidia was lower and necrotic leaf areas smaller in the Δ*kmt6* mutants (Figure S6). Consistent with the observed *in vitro* phenotype and overall reduced fitness of the Δ*kmt1* and Δ*k1/k6* mutants, wheat infection by the two mutants resulted in the formation of almost no infection symptoms. If any symptoms developed, these appeared considerably later than symptoms caused by the wild type Zt09 and the Δ*kmt6* mutants (Figure S6).

Loss of H3K9me3 impacts H3K27me3 localization

We next addressed how the deletion of *kmt1* and *kmt6* impacts the distribution of the other tested histone modifications. To this end, we generated ChIP-seq datasets to identify patterns of H3K4me2, H3K9me3 and H3K27me3 histone methylation in Zt09 and the methyltransferase mutant strains. A previous study in *Z. tritici* found that H3K4me2 is associated with gene-rich, transcriptionally active regions on core chromosomes, while it is rarely present on accessory chromosomes. Constitutive heterochromatin associated with H3K9me3 locates almost exclusively on repetitive elements. The facultative heterochromatin mark H3K27me3 covers nearly the entire length of all accessory chromosomes and is enriched predominantly in the subtelomeric regions of core chromosomes (Schotanus *et al.*, 2015). Other studies in different *Fusarium* species confirmed the facultative heterochromatic pattern on accessory chromosomes (Galazka & Freitag, 2014) suggesting that H3K27me3 represents a hallmark of accessory chromosomes in fungi.

Analyses of ChIP-seq data confirmed the loss of H3K9me3 in the *Δkmt1* mutant, loss of H3K27me3 in the *Δkmt6* mutant and the absence of both marks in the *Δk1/k6* mutants (Figure S2).

We computed the sequence coverage of each histone modification per chromosome to estimate the global effects on chromatin structure. Interestingly, the absence of a histone methylation mark had different effects on the distribution of other methylation marks on core and accessory chromosomes (Figure 1, Table S2). On core chromosomes, the amount of neither H3K4me2 nor H3K9me3 (Figure 1A and B) changes in any of the mutants, while an increased number of sequences were associated with H3K27me3 in the *Δkmt1* mutant (Figure 1C). On the accessory chromosomes we observe changes in coverage of H3K4me2 and H3K27me3. We find higher amounts of H3K4me2 in the *Δkmt1* and *Δk1/k6* mutants and a slight increase in *Δkmt6* mutants (Table S2).

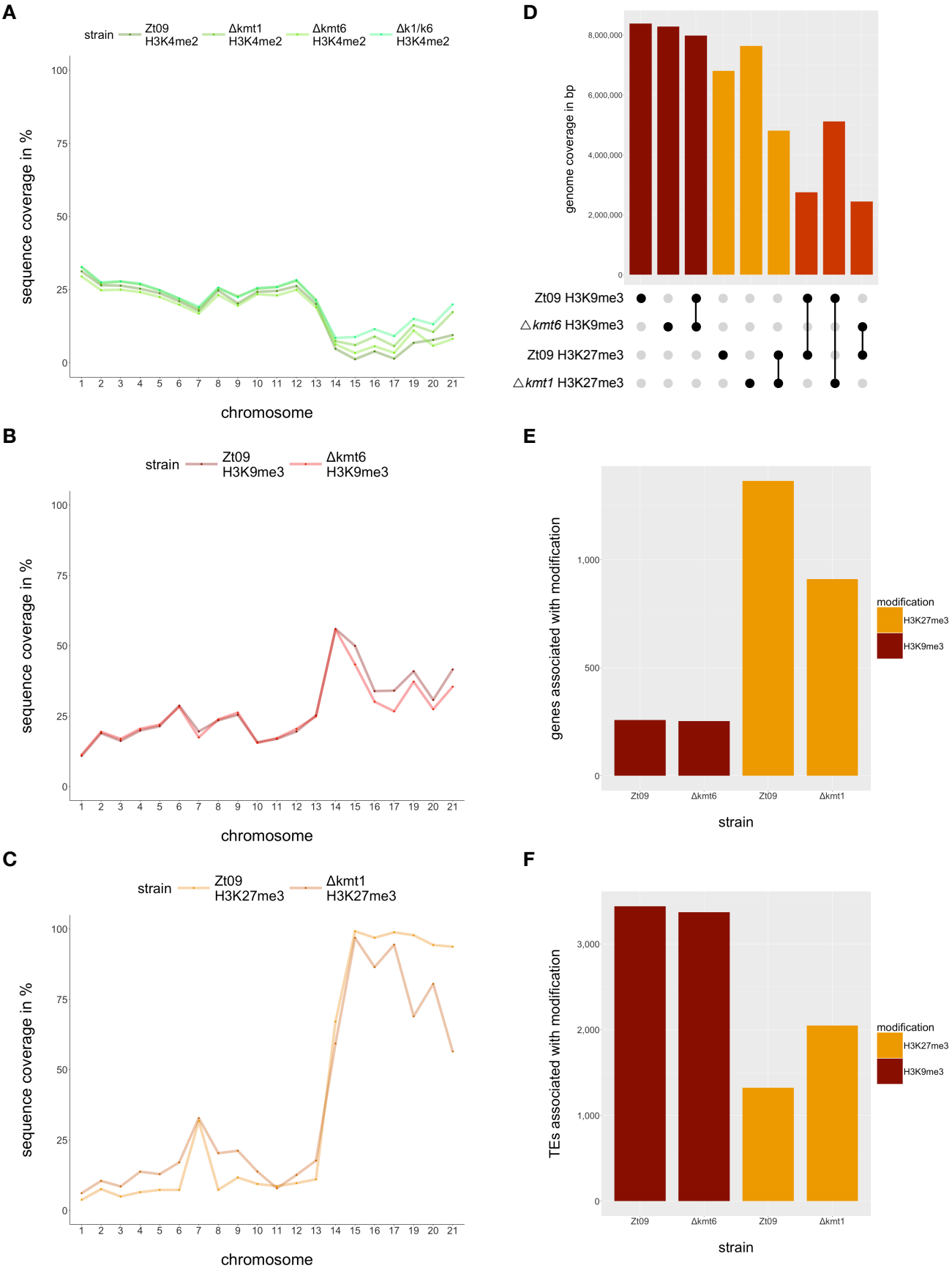
A
strain
Zt09 H3K4me2
Δkmt1 H3K4me2
Δkmt6 H3K4me2
Δk1/k6 H3K4me2
sequence coverage in %
chromosome
B
strain
Zt09 H3K9me3
Δkmt6 H3K9me3
sequence coverage in %
chromosome
C
strain
Zt09 H3K27me3
Δkmt1 H3K27me3
sequence coverage in %
chromosome
D
genome coverage in bp
Zt09 H3K9me3
△kmt6 H3K9me3
Zt09 H3K27me3
△kmt1 H3K27me3
E
genes associated with modification
modification
H3K27me3
H3K9me3
strain
F
TEs associated with modification
modification
H3K27me3
H3K9me3
strain

Figure 1. Histone methylation enrichment per chromosome and dynamics of H3K9me3 and H3K27me3. (A), **(B)** and **(C)** display the percentage of sequence coverage of core and accessory chromosomes with H3K4me2, H3K9me3 and H3K27me3 relative to the chromosome length. H3K4me2 coverage on accessory chromosomes increases in all mutant strains **(A)**, while there are little differences in the overall coverage with H3K9me3 between Zt09 and *Δkmt6* **(B)**. H3K27me3 enrichment increases on core chromosomes and decreases on accessory chromosomes in the *Δkmt1* mutant **(C)**. **(D)** Genome coverage in bp of H3K9me3 (red), H3K27me3 (orange) or regions that are covered by both marks (dark orange). Depicted is the number of bp enriched with the respective methylation in one strain (e.g. Zt09, *Δkmt1*, *Δkmt6*) and the overlap of the detected enriched regions between strains. The amount of H3K9me3 enriched sequences is very similar in Zt09 and *Δkmt6* mutants, as is the location of these regions, shown by the high amount of overlap. Total H3K27me3 coverage increases in *Δkmt1* and the locations differ based on the smaller amount of regions overlapping with H3K27me3 in Zt09. This can be explained by movement of H3K27me3 to former H3K9me3 sites in *Δkmt1*. While overlap of H3K9me3 and H3K27me3 is similar in Zt09 and *Δkmt6* mutants, the overlap notably increases in the *Δkmt1* strain. H3K27me3 thereby relocates from genes **(E)** to transposable elements **(F)**. A similar movement of H3K9me3 in the *Δkmt6* mutant was not observed.

In the *Δkmt1* mutants, the amount of sequences covered by H3K27me3 decreases on the accessory chromosomes compared to Zt09, representing the opposite trend to the observations made on the core chromosomes. However, this effect varies on different accessory chromosomes. Upon deletion of *kmt1*, chromosomes 19, 20 and 21 lose between 14 and 40 % of H3K27me3 coverage, while chromosomes 14, 15, 16 and 17 only lose between 2 and 10 % of coverage (Figure 1 and Table S2). The difference in H3K27me3 distribution can be explained by movement of H3K27me3 to former H3K9me3-associated sequences in the *Δkmt1* mutant (Figure 1D). While enrichment on genes decreases (Figure 1E), more transposable elements (TEs) show H3K27me3 enrichment in the *Δkmt1* mutant (Figure 1F). These observations reveal that loss of H3K9me3 promotes H3K27me3 movement to transposable elements and simultaneous loss of H3K27me3 at its original positions. The subtelomeric H3K27me3 enrichment is not affected by the relocation. This might explain why we observe opposite effects on core and accessory chromosomes, as core chromosomes predominantly show H3K27me3 enrichment in subtelomeric regions while accessory chromosomes contain an overall enrichment.

In conclusion, loss of H3K9me3 has a great impact on H3K27me3 distribution, while loss of H3K27me3 has little influence on H3K9me3. Absence of both, H3K9me3 and H3K27me3, enables new enrichment of H3K4me2, on which, however, H3K9me3 has a larger impact than H3K27me3 shown by higher increase of H3K4me2 enriched sequences in those mutants. In addition, deletion of *kmt1* promotes large scale rearrangements of other histone modifications, indicating more dramatic effects on genome organization and expression than deletion of *kmt6.*

H3K27me3 has little effects on transcriptional activation, loss of H3K9me3 enhances expression of transposable elements

In other species, H3K27me3 plays a crucial role in gene regulation, while H3K9me3 is involved in silencing of transposable elements (Connolly *et al.*, 2013; Studt *et al.*, 2016; Zeller *et al.*, 2016). Based on our observations in the ChIP-seq data, we hypothesized that the two histone methylation marks have the same effects in *Z. tritici*. To test this hypothesis, we sequenced the *in vitro* transcriptomes of two replicates of the reference isolate Zt09 as well as of the Δ*kmt1*, Δ*kmt6* and the *Δk1/k6* double deletion mutants.

First, we compared the total number of expressed genes. In total, 11,839 genes are annotated in the reference isolate (Grandaubert *et al.*, 2015). Out of these, 8,906 are expressed (RPKM > 2) in our reference strain Zt09. The number of expressed genes is considerably higher in both, the *Δkmt1* (9,259) and the *Δk1/k6* (9,459) mutants, but surprisingly lower in the *Δkmt6* (8,717) mutants. This is in contrast to previous studies, where deletion of *kmt6* entails an activation of otherwise silenced gene clusters and an overall transcriptional activation (Connolly *et al.*, 2013; Studt *et al.*, 2016). While 80 % of genes on core chromosomes are expressed in Zt09, only ~ 25 % of genes located on accessory chromosomes display transcriptional activity. This number is higher in all mutant strains: ~ 40 – 50 % (Figure 2A, Table S3). Consistent with the higher total number of expressed genes, we found the majority of differentially expressed (DE) genes (DESeq2, $P_{adj} < 0.001$, $|\log2 \text{ fold-change}| > 2$) to be significantly upregulated (↑) in the *Δkmt1* mutant (↑ 365 of 477) and in the *Δk1/k6* mutant (↑ 368 of 477), whereas the majority of DE genes was downregulated (↓) in the *Δkmt6* mutant (↓ 188 of 310) (Table S3).

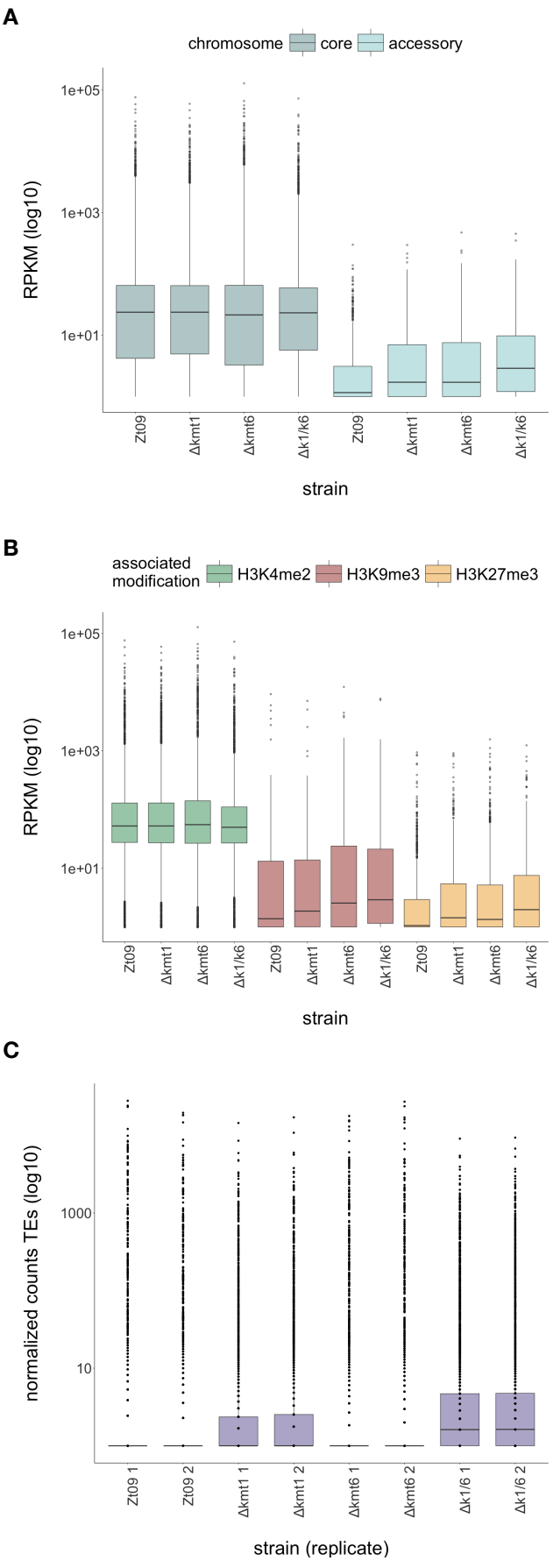

Figure 2. Transcriptome analysis reveals activation of transcription on accessory chromosomes and of transposable elements. Boxplots showing the distribution of expression values (RPKM) for genes located on core and accessory chromosomes **(A)** and associated to the tested histone modifications **(B)** as well as normalized read counts of transposable elements **(C)** during *in vitro* growth. Expression on core chromosomes is in general higher than on accessory chromosomes. However, transcription on accessory chromosomes is increased in all histone methyltransferase mutant strains. Genes associated to H3K4me2 display the highest expression, while genes associated to H3K9me3 and H3K27me3 show in general less transcriptional activity. Transcription of H3K27me3-associated genes is to some extent increased in all mutants but does not correlate to an overall activation of associated genes. Transcription of annotated transposable elements is in general very low but increases in the absence of H3K9me3 (*Δkmt1*) and is further elevated when both H3K9me3 and H3K27me3 are absent (*Δk1/6*).

Genome wide, 1,365 genes are associated with H3K27me3 and 259 genes with H3K9me3. Interestingly, only a small fraction of genes associated with these histone marks were activated or differentially expressed (Figure 2B). Surprisingly, the expression of H3K9me3-associated genes was on average higher than of H3K27me3-associated genes (Figure 2B) indicating a stronger effect on transcriptional repression by H3K27me3. However, although transcription of H3K9me3 or H3K27me3-associated genes slightly increases in the respective methyltransferase deletion mutants, loss of any of these methylation marks is not sufficient for transcriptional activation suggesting additional mechanisms involved in the transcriptional regulation of these genes.

In other fungal species, removal of H3K9me3 and especially H3K27me3 was linked to the activation of certain gene classes, in particular secondary metabolite gene clusters (Connolly *et al.*, 2013; Chujo & Scott, 2014; Studt *et al.*, 2016). To assess if genes with a specific function are enriched amongst the activated genes, we performed a Gene Onthology (GO) enrichment analysis (topGO, Fisher's exact test, *P*-value < 0.01). We found two GO categories enriched amongst upregulated genes in *Δkmt1* and *Δk1/k6* mutants: DNA integration (GO:0015074) and RNA-dependent DNA replication (GO:0006278). Predicted functions assessed by BLAST analyses of the proteins encoded by the upregulated genes in these categories include reverse transcriptases, integrases, recombinases and genes containing transposon- or virus-related domains (Table S4). Consistent with these findings, we detected an increased number of transcripts originating from annotated transposable elements in the *Δkmt1* and *Δk1/k6* mutants, but not in *Δkmt6* mutant (Figure 2C). Annotated TEs are strongly associated with H3K9me3 (Schotanus *et al.*, 2015). Transposons in subtelomeric regions and on accessory chromosomes show additional H3K27me3 enrichment. Removal of H3K9me3, but not of H3K27me3, appears to be responsible for transposon activation. Certainly, their transcription is further enhanced, when H3K27me3 is removed in addition to H3K9me3 in the *Δk1/k6* mutant. Amongst the genes upregulated in the *Δkmt6* mutant no GO categories were enriched but based on the previous finding of secondary metabolite activation, we further investigated possible roles of H3K9me3 and H3K27me3 in secondary metabolite gene regulation. Therefore, we identified putative secondary metabolite cluster in the *Z. tritici* reference genome using antiSMASH (antibiotics & Secondary Metabolite Analysis SHell) (Weber *et al.*, 2015). We found a total of 27

secondary metabolite clusters, all located on core chromosomes, and merged the identified genes with the existing gene annotation (Table S5). Except for the activation of one putative cluster on chromosome 7 in the *Δk1/k6* mutant, we did not identify any differential expression of genes belonging to secondary metabolite clusters. Based on these findings, we conclude that, unlike in other fungi, H3K9me3 and H3K27me3 are not involved in transcriptional regulation of secondary metabolites in *Z. tritici*. Taken together, the effects of losing H3K9me3 and H3K27me3 on gene expression under the tested conditions are limited. Removal of these histone modifications has little consequences for the expression of the vast majority of associated genes and seems to rather indirectly impact the expression of non-associated genes. Loss of H3K9me3 rather affects transposable element expression while absence of H3K27me3 overall has very little impact on transcriptional activation.

Loss of heterochromatin dramatically affects chromosome and genome stability

Core and accessory chromosomes share the same basic components required for chromosome transmission: centromeres and telomeres (Schotanus *et al.*, 2015). Accessory chromosomes are enriched with transposable elements, but share the same TE families as core chromosomes (Grandaubert *et al.*, 2015). However, accessory chromosomes of *Z. tritici* have been shown to be highly instable, both during meiosis and vegetative growth (Wittenberg *et al.*, 2009; Moeller *et al.*, 2018). The most striking feature that sets these chromosomes apart is the particular enrichment of facultative heterochromatin in form of H3K27me3 and, as a consequence of the higher TE content, an enrichment with H3K9me3.

To test whether loss of these modifications affects genome and chromosome stability in *Z. tritici*, we conducted two different evolution experiments to study genome stability and to detect dynamics of accessory chromosome losses in different strains. The first experiment addresses genome stability over a long period of mitotic growth (Figure 3A), while the second experiment examines stability under reduced selection to detect spontaneous accessory chromosomes losses during a short time of asexual propagation (Figure 3B).

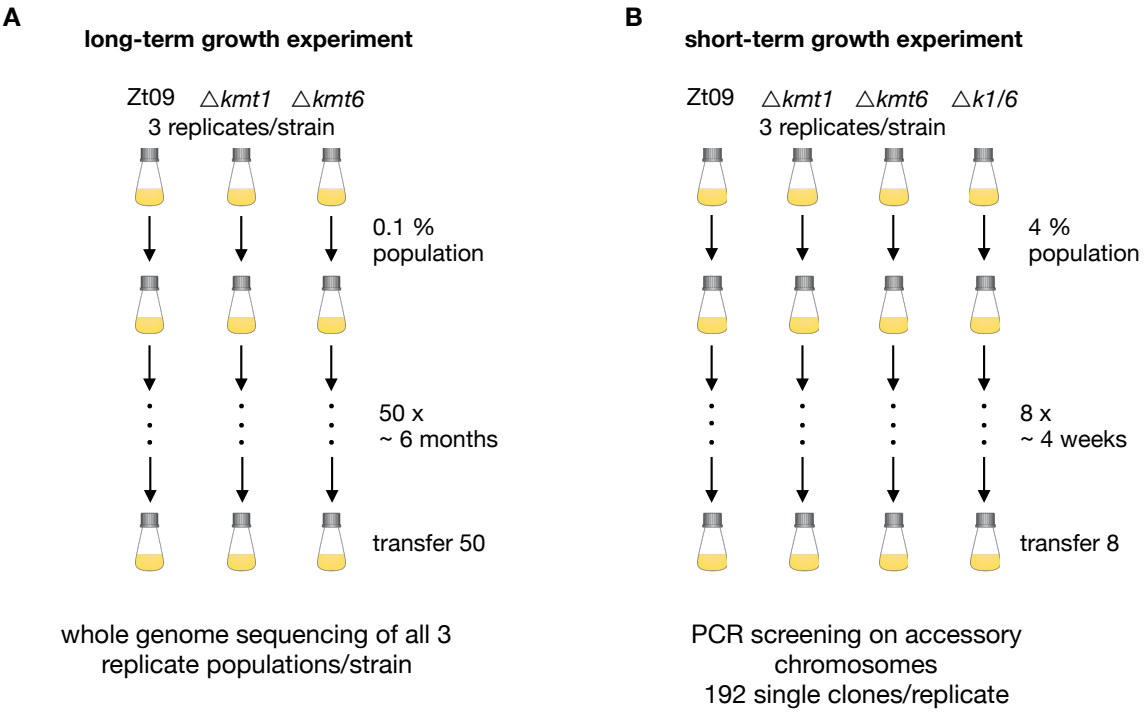

Figure 3. Evolution experiments to monitor genome and chromosome stability during mitotic growth. (A) A long-term growth experiment over six months was conducted to monitor genome stability in *Z. tritici* populations. Three replicate populations per strain (Zt09, *Δkmt1*, *Δkmt6*) were grown in parallel exposed to the same growth conditions. 0.1 % of the populations were transferred to fresh medium every three to four days. The genomes of the progenitor strains and all populations after six months of growth were sequenced to detect structural variation. **(B)** The short-term growth experiment over four weeks assessed stability of accessory chromosomes by screening individual clones in the populations for presence/absence of accessory chromosomes. Strains (Zt09, *Δkmt1*, *Δkmt6*, *Δk1/6*) were grown in triplicates for four weeks and 4 % of the population were transferred to fresh medium every three to four days. After four weeks, single clones were isolated and screened for the presence/absence of accessory chromosomes by PCR.

Loss of H3K9me3 promotes large-scale structural rearrangements mediated by the activation of transposable elements

For the first experiment, the single mutants (*Δkmt1* and *Δkmt6*) and Zt09 were grown in triplicates for ~ 6 months. We sequenced full genomes of progenitors and the evolved populations after 50 transfers to identify possible structural variations that arose during the experiment. All strains were sequenced with ~ 100 X coverage and paired-end reads were mapped to the reference genome of IPO323 (Goodwin *et al.*, 2011).

We focused our analysis on large scale chromosomal rearrangements such as duplications, deletions and chromosome breakage. Structural variation was first detected

computationally and confirmed manually, and additional rearrangements were identified. A summary of all detected rearrangements is listed in Table S6. Except for the already known absence of chromosome 18 (Kellner *et al.*, 2014) and the previously described variation in Zt09 to the reference genome (Moeller *et al.*, 2018), we found lower sequence coverage (~ 0.6 X) on chromosome 17 in the *Δkmt6* progenitor strain (Figure 4A). This difference can only be explained by a lower copy number of chromosome 17 in the sequenced DNA pool. We interpret this observation as the loss of chromosome 17 in ca. 40 % of the sequenced *Δkmt6* cells that likely occurred at the beginning of the experiment. Unexpectedly, the *Δkmt1* progenitor displays a large high-coverage (~ 1.6 X) region on chromosome 1, breakage of chromosome 6 and loss of chromosome 20 (Figure 4A and B, Table S6). Analysis of discordant read mappings at both ends of the ~ 1 MB high-coverage region on chromosome 1 revealed formation of new telomeres. Pulsed-field gel electrophoresis and Southern blotting confirmed the formation of two new chromosomes both containing the high-coverage region and either the right or left arm of chromosome 1 (Figure 4B). The breakpoint on the left side coincides with a large TE-rich region that is associated with H3K9me3 in the wild type. The right end is very close (~ 15 kb) to the centromere and the breakpoint localizes within a gene-rich region enriched with H3K4me2 (Figure 4C). Chromosome breakage on chromosome 6 comprised approximately 11 kb on the left arm of chromosome 6. In this case we also detected *de novo* telomeres at the breakpoint indicating that the chromosome breakage led to a shortening of chromosome 6.

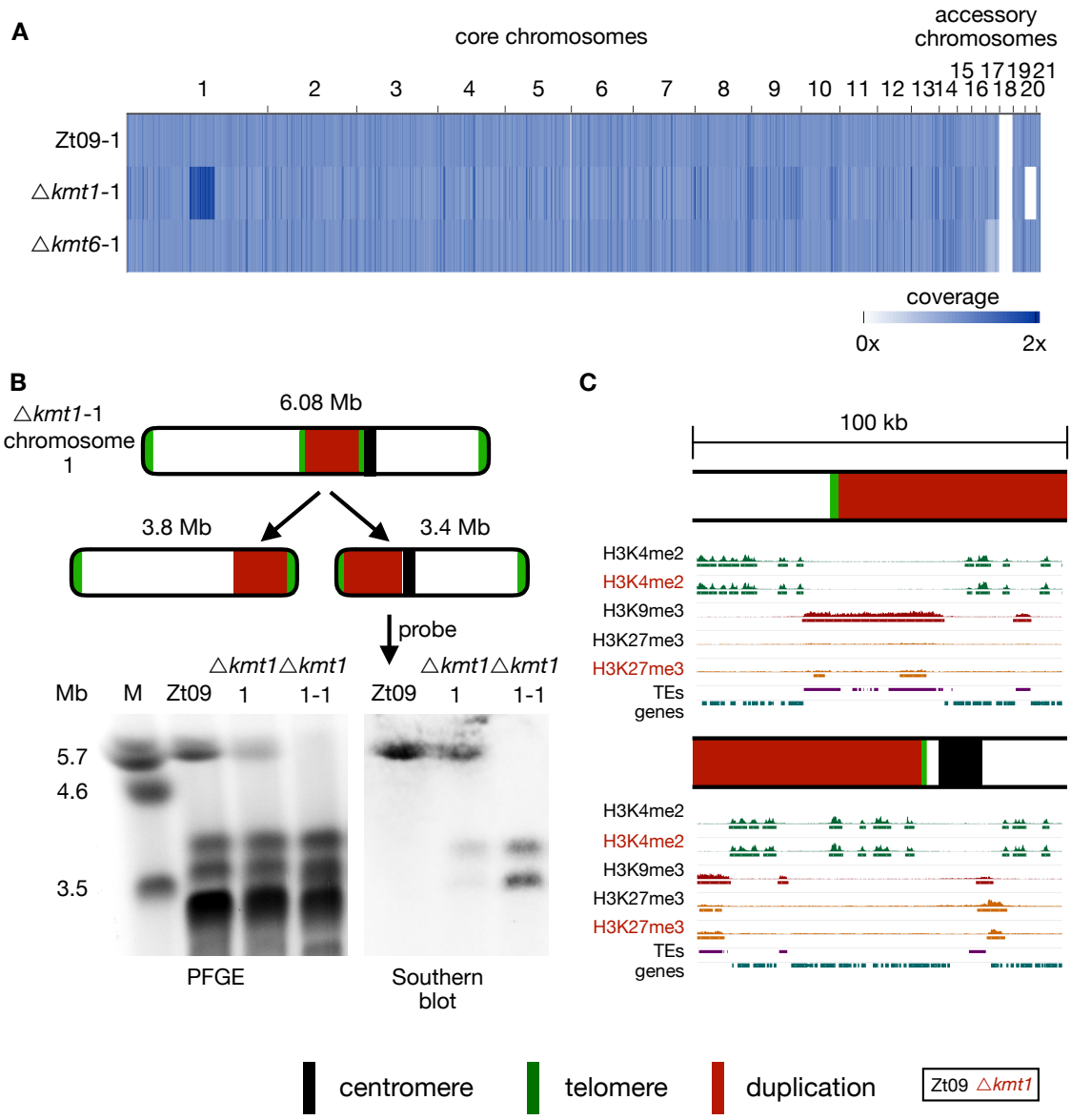

Figure 4. Genome sequencing of progenitor strains for the long-term growth experiment and analysis of structural variation in the *Δkmt1* mutant. (A) The genomes of all progenitor strains were sequenced and reads were mapped to the reference genome. Genome coverage was normalized to 1 X coverage to allow identification and comparison of differences within and between strains. All strains are missing chromosome 18, as expected. *Δkmt6* has lower coverage (0.4 X) of chromosome 17. *Δkmt1* lost chromosome 20 and, most notably, shows a large (~ 1Mb) high-coverage (1.6 X) region on chromosome 1. **(B)** Further analysis of this high-coverage region revealed *de novo* telomere formation at the breakpoints indicating a chromosome breakage at both ends of the high-coverage region. To validate chromosome breakage and possible new chromosome formation, we conducted PFGE and separated the large chromosomes of Zt09, of the *Δkmt1* progenitor strain (*Δkmt1*-1) and of a single clone originating from the *Δkmt1* progenitor strain stock (*Δkmt1*-1-1). Chromosome 1 (~ 6 Mb) is present in Zt09 and *Δkmt1*-1 (faint band), but not in the *Δkmt1*-1-1 single clone. We

conducted Southern analysis on the PFGE blot using a sequence of the high-coverage region as a probe. It hybridized to the original chromosome 1 band in Zt09 and *Δkmt1*-1, but additionally to a ~ 3.4 Mb and ~ 3.8 Mb band in *Δkmt1*-1 and only to these bands in *Δkmt1*-1-1. This confirms the formation of new chromosomes, both containing the high-coverage region and ending at the respective breakpoints. **(C)** Examination of the high-coverage region breakpoints on chromosome 1. The first breakpoint locates within a TE-rich region that is enriched with H3K9me3 in Zt09 and shows little new enrichment with H3K27me3 in *Δkmt1*. The second breakpoint is within a gene-rich region that is not enriched for neither H3K9me3 nor H3K27me3 but is located very close to the centromere (~ 15 kb).

After six months of vegetative growth, we sequenced the pooled genomes of all nine 'evolved' populations. In none of the evolved Zt09 or *Δkmt6* populations, we found evidence for large-scale genomic rearrangements (Figure 5A). Apart from very few, small deletions or duplications (Table S6), the largest structural variation found in one of the evolved *Δkmt6* populations (*Δkmt6*-50-2) was a chromosome breakage of ~ 18 kb at the right end of chromosome 15. However, we found variation in the coverage of accessory chromosomes in all sequenced genomes indicating whole chromosome losses in individual cells of the population. The distinct dynamics of individual accessory chromosome losses were revealed by the second, short-term evolution experiment.

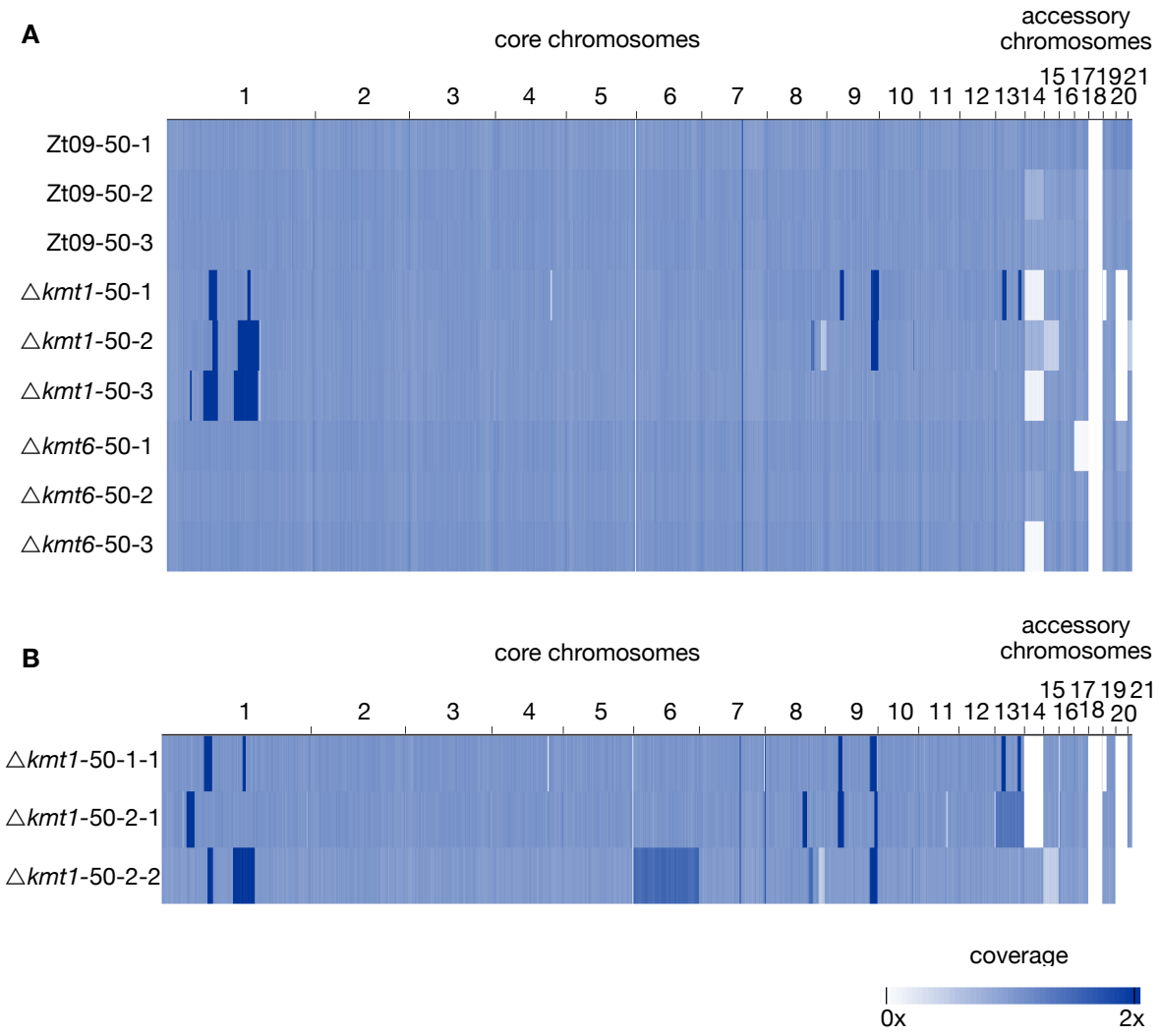

Figure 5. Genome sequencing of evolved populations and single clones originating from the long-term growth experiment. (A) The genomes of each replicate population after 50 transfers were sequenced and mapped to the reference. Coverage is normalized to 1 X. Except for coverage differences on the accessory chromosomes, there are hardly any structural variations detectable for the evolved Zt09 and *Δkmt6* populations. In contrast, *Δkmt1* populations contain multiple high-coverage regions on core chromosomes as well as large deletions indicated by 0 X coverage. **(B)** To further characterize structural variation in the evolved *Δkmt1* strains, three single clones originating from populations *Δkmt1*-50-1 (*Δkmt1*-50-1-1) and *Δkmt1*-50-2 (*Δkmt1*-50-2-1 and *Δkmt1*-50-2-2) were sequenced. Clones *Δkmt1*-50-1-1 and *Δkmt1*-50-2-2 show a very similar pattern as their respective populations, while *Δkmt1*-50-2-1 resembles a genotype that appears to be rare in population *Δkmt1*-50-2. High coverage on entire core chromosomes 13 (*Δkmt1*-50-2-1) and 6 (*Δkmt1*-50-2-2) indicates whole core chromosome duplications.

In contrast to the few detected variations in the Zt09 and *Δkmt6* populations, we found numerous large-scale high-coverage regions on different core chromosomes, chromosome breakages followed by *de novo* telomere formation, chromosomal fusions, as well as several smaller deletions and duplications in the evolved *Δkmt1* populations (Figure 5A, Table S6). All evolved *Δkmt1* populations have large duplicated regions on chromosome 1 (Figure 6), but their locations as well as the resulting structural variations differ from the one identified in the progenitor strain (Figure 6A). This can be explained by independent events, as not all *Δkmt1* progenitor cells underwent the rearrangement of chromosome 1 (Figure 4B), or by continuous structural rearrangement events as a consequence of the presence of large duplicated regions in the genome. Analyses of the affected regions and breakpoints indicate a connection between the structural variations of progenitor (compared to the reference) and evolved strains. In all evolved *Δkmt1* populations, duplicated regions fully or partially overlap with the high-coverage region of the progenitor strain (Figure 6A-D). In population *Δkmt1*-50-2, the region close to the centromere, where one of the breakpoints of the progenitor strain is located, is deleted (Figure 6C). Similarly, population *Δkmt1*-50-3 contains a deletion of the breakpoint region close to the centromere in the progenitor strain, which furthermore includes the complete centromeric sequence (Figure 6D).

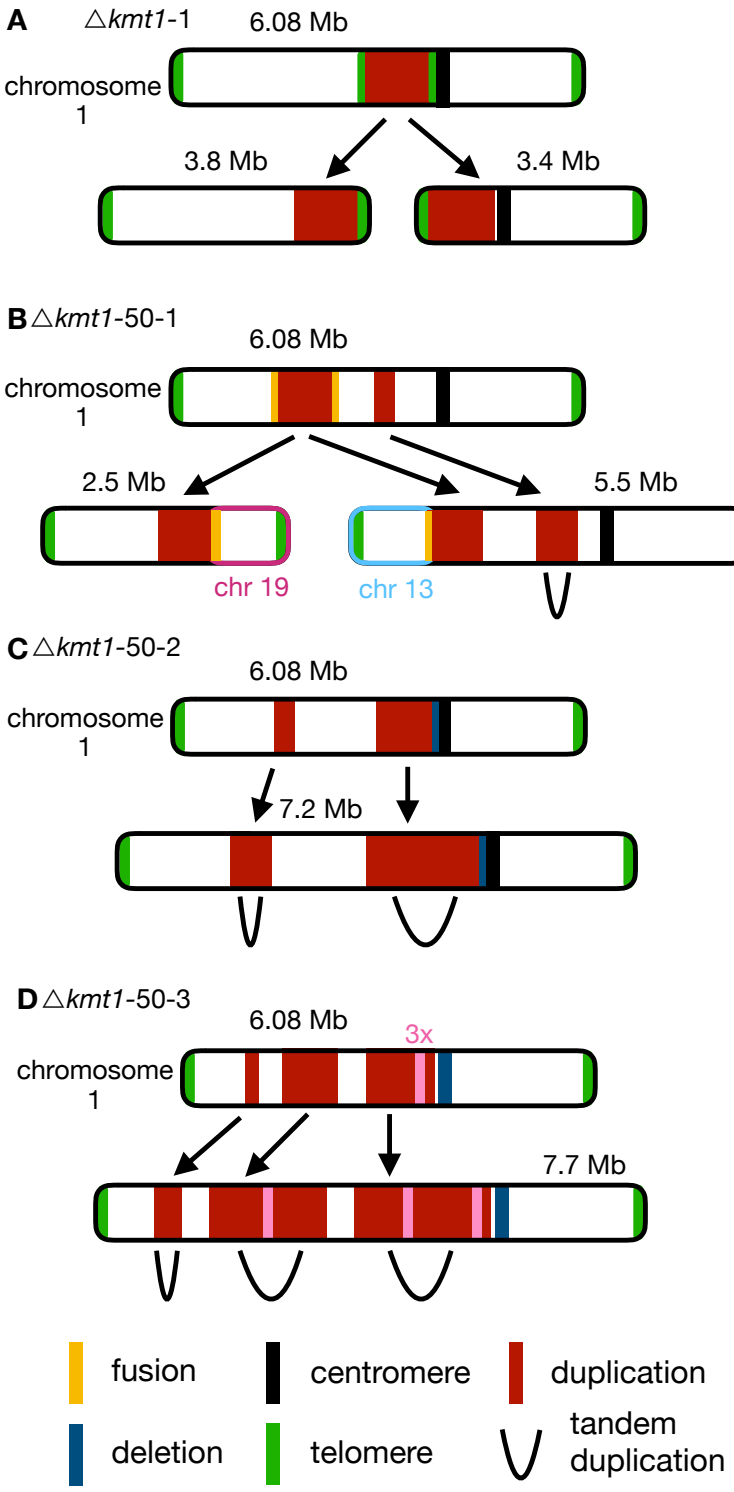

Figure 6. Different forms of structural variation of chromosome 1 in the *Δkmt1* progenitor strain (A) and the three evolved *Δkmt1* populations. (B-D) Upper panels display the mappings to the reference genome including indicated fusion and *de novo* telomere events, while the respective lower panels show the consequential structural rearrangements. **(A)** In the progenitor strain, a duplicated region was involved in the formation of two new chromosomes. At both breakpoints of the duplicated sequence, the chromosome broke and telomeres were added *de novo* to these breakpoints. Thus, two new chromosomes were formed, both containing the duplicated sequence. **(B)** In the

evolved population *Δkmt1*-50-1, two duplicated sequences were detected. The borders of the first region mark chromosome breakages that are fused to telomeres of other chromosomes. The first breakpoint is attached to the telomere of chromosome 13 forming a new 5.5 Mb chromosome while the second breakpoint is fused to the telomere of chromosome 19 (new 2.5 Mb chromosome). The second duplicated region represents a tandem duplication located on the new 5.5 Mb chromosome that falls within the duplicated region of the progenitor strain. **(C)** Population *Δkmt1*-50-2 contains two duplicated regions, that both resemble tandem duplications. The second duplication is very similar to the one found in the progenitor strain but includes half of the centromere and has a deletion, where the breakpoint close to the centromere in the progenitor strain is located. **(D)** Population *Δkmt1*-50-3 displays three duplicated sequences that all form tandem duplications resulting in the formation of a 7.7 Mb version of chromosome 1. The third duplicated region is, as in population *Δkmt1*-50-2, very similar to the one in the progenitor strain. However, in this case the complete centromere-associated sequence is deleted. Furthermore, a ~ 50 kb region inside the third duplicated region exhibits 3 X sequencing coverage and is found in between the tandem duplication of the second duplicated region.

Since populations reflect a mixture of distinct genotypes, we additionally sequenced three single *Δkmt1* clones of the populations from transfer 50 to characterize the structural variation in more detail (Figure 5B). The single clones were selected based on different karyotypes in pulsed-field gel electrophoresis (Figure S7) and originate from population *Δkmt1*-50-1 (*Δkmt1*-50-1-1) and *Δkmt1*-50-2 (*Δkmt1*-50-2-1 and *Δkmt1*-50-2-2). As two of these single clones (*Δkmt1*-50-1-1 and *Δkmt1*-50-2-2) largely resemble the genotypes found in their respective populations, we conclude the presence of predominant genotypes in the evolved replicate populations. However, *Δkmt1*-50-2-1 clearly differs from this genotype and therefore indicates the existence of additional, rare genotypes in the cell populations. Relatively small deletions and duplications (up to 30 kb) as well as chromosome breakage followed by *de novo* telomere formation were found on almost all chromosomes and occurred mainly associated to annotated transposable elements (Table S7). However, major rearrangements, including chromosomal fusions, were always linked to large duplicated sequences. The consequences of these major rearrangements on chromosome structure are described in Figure 7. Read coverage and PCR analyses indicate that *Δkmt1*-50-2-2, as well as the majority of the *Δkmt1*-50-2 population, possibly underwent a whole genome duplication. As structural variation could not be predicted as

precisely as for the other two single clones, we did not include *Δkmt1*-50-2-2 in this prediction.

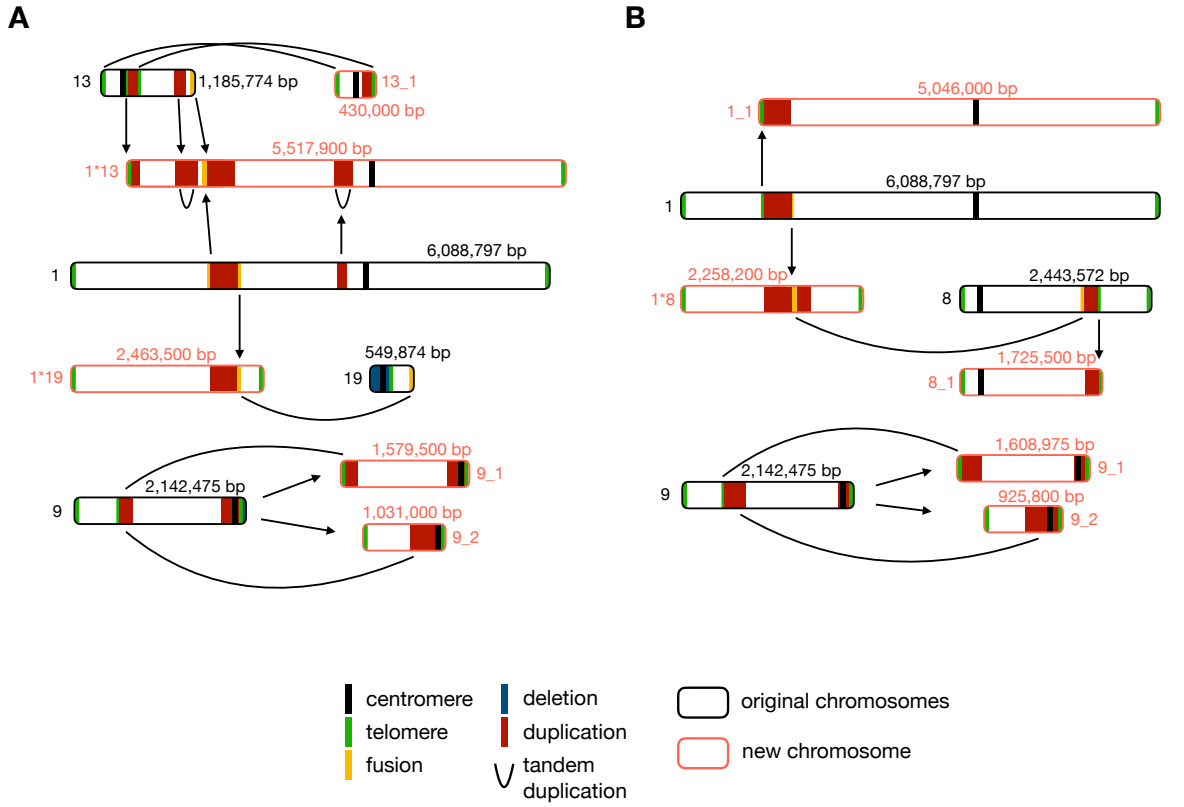

Figure 7. Consequences of detected structural variation for chromosome structure in the evolved *Δkmt1* clones *Δkmt1*-50-1-1 and *Δkmt1*-50-2-1. (A) A total of six duplicated regions was found in *Δkmt1*-50-1-1, two each on chromosomes 1, 9 and 13. The breakpoints of the first duplicated sequence on chromosome 1 fused to the right telomeres of chromosome 13 (1*13) and 19 (1*19), the second duplication is a tandem duplication. While the right telomere of chromosome 19 fused to chromosome 1, the left arm including the centromere is deleted and *de novo* telomere formation occurred at the breakpoint. Chromosome 13 has two duplicated regions, one is a tandem duplication and one shows *de novo* telomere formation on both ends indicating a breakage of chromosome 13. The right telomere is fused to chromosome 1, the first breakpoint of the first duplicated region provides the new left telomere of the 1*13 chromosome. This breakpoint is located very close to the centromere. The left arm including the centromere forms a new, smaller chromosome 13_1, ending at the right breakpoint of the first duplicated region with *de novo* telomeres. Chromosome 9 did not fuse with another chromosome, but the structural variation rather led to the formation of two smaller chromosomes, both containing the duplicated sequences. The larger chromosome 9 (9_1), ends at the first breakpoint of the first duplicated region with *de novo* telomeres and ends at the breakpoint of the second duplicated region with *de novo* telomeres. The second

duplicated region ends at the end of the chromosome where *de novo* telomere formation occurred as a result of chromosome breakage (~ 12 kb). In the smaller chromosome 9 (9_2), the two duplicated regions fused, deleting the entire sequence between the duplicated regions. **(B)** In the clone *Δkmt1*-50-2-1, we detected four duplicated regions. While two are located on chromosome 9 and result in a very similar structural variation as described in **(A)**, the other two are found on chromosome 1 and 8. One breakpoint of each duplicated region marks a fusion of the respective chromosomes, while the other one displays *de novo* telomere formation. As a result, three new chromosomes form. A new chromosome that represents a fusion of chromosomes 1 and 8 (1*8) and two chromosomes that are shorter version of chromosomes 1 (1_1) and 8 (8_1). The new, shorter versions both contain the centromeric sequence, while the fused chromosome does not contain any sequences of the original centromeres.

To investigate if the underlying sequence is involved in the formation of rearrangements, we analyzed the breakpoints of each duplicated region. The location of breakpoints does not show a clear TE-associated pattern as observed for the smaller deletions or chromosome breakages. Out of 28 analyzed breakpoints, only seven are directly located in annotated transposable elements, while thirteen fall into genes, seven are intergenic and one is located in the centromere (Table 1). Based on these observations, we hypothesize TE associated instability as the initial event followed by continuous rearrangements resulting in breakpoints that are not directly associated to the initial event. In summary, deletion of *kmt1* has a great impact on genome and chromosome stability resulting in large scale rearrangements, while *Δkmt6* and Zt09 genomes only show very few, small changes during the course of the experiment.

Table 1. Annotation of breakpoints of segmental duplications in the single clones originating from evolved populations *Δkmt1*-50-1 and *Δkmt1*-50-2.

strain	chromosome	breakpoint location	type of structural variation associated to breakpoint	sequence annotation
Δ*kmt1*-50-1-1				
	1	1753118	fusion to chromosome 13	intergenic
	1	2089657	fusion to chromosome 19	in gene
	1	3339041	tandem duplication	in gene
	1	3459235	tandem duplication	in gene
	9	563000	*de novo* telomere formation	in TE
	9	725793	deletion	in gene
	9	1837211	deletion	in TE
	9	2129950	*de novo* telomere formation	in TE
	13	922381	tandem duplication	intergenic
	13	1065311	tandem duplication	intergenic
	13	266400	*de novo* telomere formation	intergenic
	13	430000	*de novo* telomere formation	intergenic
Δ*kmt1*-50-2-1				
	1	1043000	*de novo* telomere formation	in gene
	1	1386377	fusion to chromosome 8	in gene
	8	1553337	fusion to chromosome 1	in gene
	8	1725500	*de novo* telomere formation	in gene
	9	533352	*de novo* telomere formation	intergenic
	9	800760	deletion	intergenic
	9	2017411	deletion	in gene
Δ*kmt1*-50-2-2				
	1	1908864	tandem duplication	in gene
	1	2127270	tandem duplication	in gene
	1	2936604	tandem duplication	in gene
	1	3844993	tandem duplication	centromere
	8	1813873	tandem duplication	in TE
	8	1961605	tandem duplication	in gene
	9	1839250	*de novo* telomere formation	in TE
	9	1957300	deletion	in TE
	9	1963300	deletion	in TE

Loss of H3K27me3 drastically reduces the loss of accessory chromosomes

Accessory chromosomes of *Z. tritici* are highly instable, both during meiosis and mitosis (Wittenberg *et al.*, 2009; Moeller *et al.*, 2018). To assess if the specific histone methylation pattern on accessory chromosomes contributes to the observed instability, we performed a short-term *in vitro* growth experiment over four weeks. As in the first experiment, each strain was grown in three replicate cultures, this time transferring ~ 4 % of the cell population to fresh medium every three to four days (Figure 3B). Also, a different *Δkmt1* transformant that still contains chromosome 20 was used as progenitor and in addition the *Δk1/k6* double deletion mutant. In this evolution experiment, our goal was to reduce the effect of selection and to improve our ability to detect spontaneous losses by conducting a short-time experiment and by increasing the number of transferred cells compared to the first experiment. After four weeks of growth, we plated dilutions of each culture to obtain single colonies that were subsequently screened by a PCR assay for the presence of accessory chromosomes. For each replicate, we screened 192 single colonies whereby in total 576 colonies were tested per strain (Table 2).

Table 2. Chromosome loss rates and frequency of individual accessory chromosome losses in the Zt09 reference strain and mutants during short-term evolution experiment.

chromosome	Zt09	Δ*kmt1*	Δ*kmt6*	Δ*k1/6*
14	18	26	2	12
15	8	0	0	0
16	9	2	0	2
17	0	0	5	0
18	-	-	-	-
19	0	0	0	3
20	2	52	2	17
21	1	6	1	6
total loss	38	86	10	40
total tested	576	576	576	576
loss rate	6.6%	14.9%	1.7%	6.8%

In a previous study, we showed that the accessory chromosomes are lost at a rate of ~ 7 % and we documented that particular accessory chromosomes (14, 15 and 16) are more frequently lost than others (Moeller *et al.*, 2018). In comparison to wild type, the *Δkmt1* mutant showed a significantly increased chromosome loss rate (one sided Fisher's exact

test for count data, *P*-value = 2.722e-06). Interestingly, this was not due to an overall increase of accessory chromosome losses, but rather by the dramatically increased (*P*-value = 3.692e-09) loss frequency of chromosome 20 (Table 2). The chromosome loss frequency of the other accessory chromosomes was either comparable to wild type (14, 17, 19, 21) or even significantly lower (15 and 16, *P*-values = 0.001181 and 2.504e-05).

In contrast to the *Δkmt1* strains, we detected significantly less chromosome losses (*P*-value = 0.0001189) in the *Δkmt6* mutants. Out of 576 tested cells, only ten had lost an accessory chromosome. This represents a four times lower chromosome loss rate compared to wild type. Hence, absence of H3K27me3 seems to promote stability of accessory chromosomes. Notably, chromosome 17 that was lost with the highest frequency in this mutant- five out of ten chromosome losses - was not lost in any of the other mutant strains nor in the wild type. This suggests a special role of H3K27me3 or *Δkmt6* for the maintenance of chromosome 17.

The double deletion mutant displayed a similar chromosome loss rate as wild type but showed a chromosome loss distribution comparable to the *Δkmt1* deletion strain with chromosome 20 being lost significantly more (*P*-value = 0.0001258) and chromosomes 15 and 16 lost less frequently (*P*-values = 0.00195 and 0.008987, respectively).

With the short-term growth experiment, we could show that the chromosome loss rate of accessory chromosomes significantly differed between the *Z. tritici* heterochromatin mutants and wild type. While loss of H3K9me3 increased the loss rate, in particular of chromosome 20, the absence of H3K27me3 decreased the chromosome loss rate. When both histone marks are absent, the loss frequency is comparable to wild type, but the occurrence of individual chromosome losses resembles the pattern observed in the *Δkmt1* mutant.

Discussion

Effects of chromatin reorganization on phenotypes and transcription

In this study, we elucidated the roles of the heterochromatin-associated histone marks H3K9me3 and H3K27me3 in the pathogenic fungus *Z. tritici* by deletion of the respective histone methyltransferases KMT1 and KMT6. We found that both histone marks have important but distinct functions. Loss of H3K9me3 and combinational loss of H3K9me3 and H3K27me3 in the double deletion mutant had severe effects on growth and reproduction *in vitro* and *in planta*, while loss of H3K27me3 alone only resulted in slight differences to wild type growth.

The phenotypic consequences *in vitro* by the absence of H3K9me3 are consistent with previous observations in filamentous fungi (Palmer *et al.*, 2008; Basenko *et al.*, 2015; Zhang *et al.*, 2016). In *Neurospora crassa*, the loss of H3K9me3 causes a redistribution of H3K27me3 to former H3K9me3 positions and the resulting growth defects can be rescued by additional elimination of H3K27me3 (Basenko *et al.*, 2015). While we see a similar relocation of H3K27me3 in the *Z. tritici Δkmt1* mutant, the growth defects cannot be restored in the *Δk1/6* double deletion mutant but are even more severe. This suggests that redistribution of H3K27me3 is not responsible for poor growth in the *Z. tritici Δkmt1* strains.

The observed strongly reduced virulence of *Δkmt1* and *Δk1/6* strains is likely a result of the overall impaired growth as found *in vitro*. However, H3K9me3 has been shown to be involved in effector gene regulation in the oilseed rape pathogen *Leptosphaeria maculans* (Soyer *et al.*, 2014). Based on this finding in another Dothideomycete plant pathogen, we speculate that the reduced virulence in the *Δkmt1 Z. tritici* mutant may also result from impaired regulation of pathogenicity-related genes.

Loss of H3K27me3 in the *Δk*mt6 mutants has little impact on *in vitro* and *in planta* growth, consistent with observations in *N. crassa* (Basenko *et al.*, 2015), but contrasts with studies in different *Fusarium* species, where absence of H3K27me3 either leads to severe developmental defects or is even essential for growth and devolpment (Connolly *et al.*, 2013; Studt *et al.*, 2016). Furthermore, limited transcriptional activation in the *Δkmt6* mutants is consistent with similar observations in *N. crassa* (Jamieson *et al.*, 2013; Basenko *et al.*, 2015) as opposed to other studies in fungi, plants and animals, where loss of H3K27me3 results in global de-repression of genes (Reddington *et al.*, 2013; Connolly *et al.*, 2013; Studt *et al.*, 2016). Our analysis revealed that loss of H3K9me3 has a more

dramatic effect on transcriptional activation than loss of H3K27me3. In particular transposable elements and genes that are associated with transposable elements display higher expression or are activated in the *Δkmt1* and *Δk1/6* mutants. This is consistent with previous findings (Ding *et al.*, 2007; Penke *et al.*, 2016; Zeller *et al.*, 2016) and reflects the strong correlation of H3K9me3 to transposable elements (Schotanus *et al.*, 2015). Activation of transposable elements can have severe consequences for genome stability and integrity (Zeller *et al.*, 2016) and may contribute to the extreme amount of genome rearrangements that we detected in the *Δkmt1* mutants (Table S6 and S7).

H3K9me3 loss and consequences for genome stability

The replication of heterochromatin-associated DNA is challenging for the cell. Repeated sequences can form secondary structures that aggravate the replication machinery (Voineagu *et al.*, 2008). Instability of repeated sequences has consequently been linked to errors during DNA replication (Khurana & Oberdoerffer, 2015; Allshire & Madhani, 2017). Replication fork stability is an important factor to preserve repeat stability and normally, the replication machinery and heterochromatin-associated proteins work together to ensure faithful replication and genome integrity (Li *et al.*, 2013). In *Caenorhabditis elegans*, loss of H3K9me promotes transposable element transcription and formation of R-loops (RNA:DNA hybrids) at repeated sequences during replication resulting in copy-number variations (Zeller *et al.*, 2016). These R-loops may induce replication fork stalling and subsequent DNA double-strand breaks. This phenomenon could be an explanation for the accumulation of the small deletions and duplications, chromosome breakage or the formation of large segmental duplications that we observed in the *Δkmt1* mutants (Table S6 and S7). Double-strand breaks can be repaired by non-homologous end joining causing deletions or translocations (Chiruvella *et al.*, 2013). Alternatively, they are healed by *de novo* telomere formation (Pennaneach *et al.*, 2006). The structural rearrangements detected in the *Δkmt1* mutants indicate that repair of double-strand breaks involves both non-homologous end joining and *de novo* telomere formation.

H3K9me3 has further been shown to be involved in large-scale genome and chromosome rearrangements in *Drosophila melanogaster* (Peng & Karpen, 2009). Based on the structural variation, predominantly associated to transposable elements in the *Δkmt1* mutants, we propose that the main factor for genome instability is replication-associated

instability of repeated sequences promoting the formation of large-scale rearrangements (Figure 8).

The new chromosome variants that are formed in the *Δkmt1* mutants do not always contain the original centromere-associated sequences. We hypothesize that neocentromeres are readily established on these chromosomes. Previously, we have shown that the structure of *Z. tritici* centromeres is unusual, as they do not display typical pericentric heterochromatin regions but contain actively transcribed genes (Schotanus *et al.*, 2015). These characteristics are similar to neocentromeres found in *Candida albicans* (Ketel *et al.*, 2009; Thakur & Sanyal, 2013) suggesting that centromere formation in *Z. tritici* is highly dynamic.

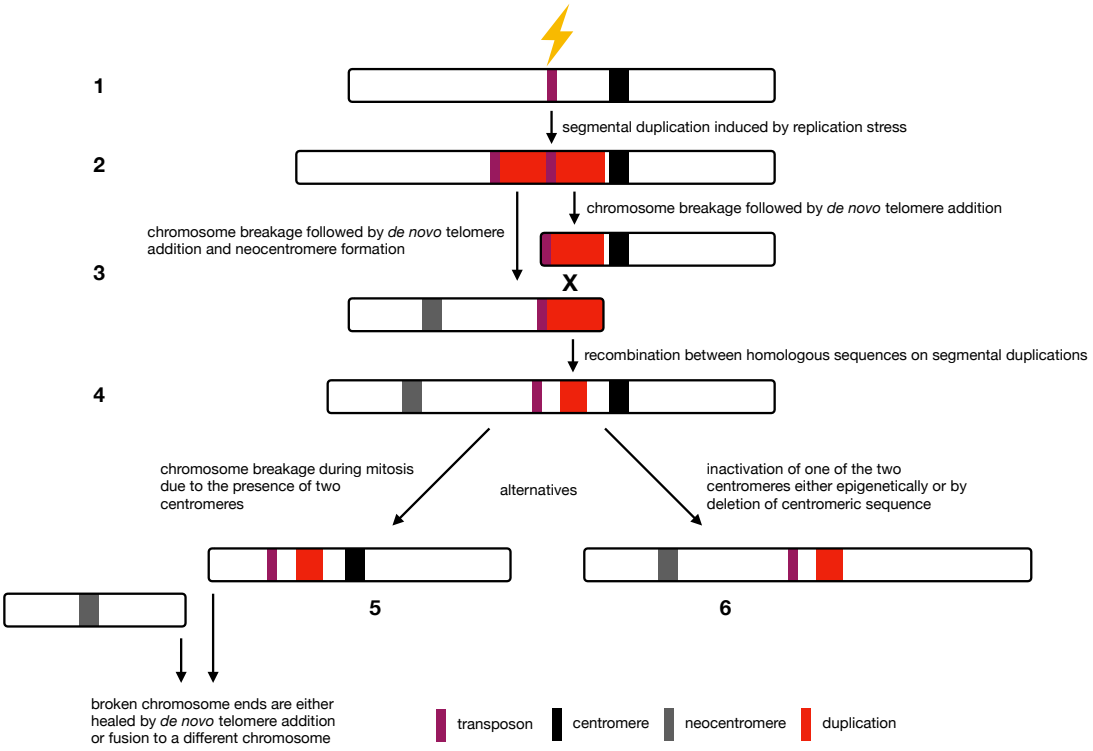

Figure 8. Model for the formation of large structural rearrangements in the *Δkmt1* mutants. 1) Initially, replication stress at repeated sequences promotes structural variation in form of deletion or duplications. 2) Large segmental duplications arise during that process and are either followed by chromosome breakage or represent a consequence of double-strand breakage and unfaithful repair. 3) New chromosomes are formed by adding *de novo* telomeres at the chromosomal breakpoints. While one of the chromosomes contains the original centromere, the other chromosome forms a neocentromere. 4) The duplicated sequences are target of mitotic recombination resulting in a fusion of the chromosomes. 5) The now dicentric chromosome becomes unstable during mitosis and breaks between the centromeres. The broken chromosome

ends are repaired either by *de novo* telomere formation or fusion to a different chromosome giving rise to new breakage-fusion bridge cycles. 6) Alternatively, one of the two centromeres is inactivated, either epigenetically or by deletion of the underlying sequence and the chromosome remains stable during mitosis.

We found that duplicated sequences in the experimentally evolved *Δkmt1* mutants fully or partially overlap with the duplicated regions of the *Δkmt1* progenitor strain. This strongly indicates that structural variations are highly dynamic implying continuous rearrangements. This led us to the hypothesis that the presence of large segmental duplications promotes mitotic recombination. In yeast, artificially duplicated sequences as well as naturally occurring repeats serve as substrates for ectopic, mitotic recombination (Liefshitz *et al.*, 1995). Furthermore, breakage-fusion bridge cycles mediated by mitotic recombination and translocations can lead to chromosomal rearrangements (McClintock, 1938, 1941). Repair of double-strand breaks by translocation to different chromosomes or mitotic recombination can result in the formation of dicentric chromosomes that are instable during mitosis giving rise to new chromosome rearrangements (Figure 8). In a previous study, it was shown that the formation of a new accessory chromosome was conferred by breakage-fusion bridge cycles during meiosis in *Z. tritici* (Croll *et al.*, 2013). In our study, we find evidence for the occurrence of breakage-fusion bridge cycles by the observed fusion events between chromosomes 1 and 19 and between 1 and 13 (Figure 7A). For these chromosomes we observe that the breakpoints of a large duplicated sequence on chromosome 1 are fused to telomeres of chromosomes 13 and 19. Both chromosomes broke close to their centromeres resulting in loss of the centromeric sequence. A mechanism to avoid breakage-fusion bridge cycles is the inactivation of centromeres. This can either be accomplished by epigenetic inactivation or by deletion of the underlying sequence (Stimpson *et al.*, 2012). We detected deletions and partial duplications of centromeres (Figure 6) but further analyses have to be conducted to investigate neocentromere formation and centromere inactivation.

The formation of new chromosomes described in this study may resemble the emergence of accessory chromosomes in *Z. tritici*. The newly arranged chromosomes contain a high proportion of duplicated sequences, but functional centromeres and telomeres could be readily maintained. However, accessory chromosomes in *Z. tritici* do not contain a high number of paralogs of core chromosome genes (Kellner *et al.*, 2014). Duplicated sequences might not be stable over longer evolutionary timescales and those

chromosomes may shrink over time, resulting in an accessory chromosome mainly composed of unique sequences of ancestral core chromosomes (Galazka & Freitag, 2014). In summary, *Δkmt1* mutants show a high rate of structural variation that is possibly mediated by replication stress at repetitive sequences that are normally enriched with H3K9me3. Our data suggests that once structural variation arises, it serves to promote further instability. The presence of KMT1 and of H3K9me3 respectively, is therefore essential to maintain genome integrity in this fungus. Transposable element-mediated rearrangements may be involved in the genetic variability detected in *Z. tritici* isolates (McDonald & Martinez, 1991; Linde *et al.*, 2002; Mehrabi *et al.*, 2007) and have been suggested as drivers of genome evolution in various species (Hedges & Batzer, 2005; Feschotte & Pritham, 2007; Barrón *et al.*, 2014). Our findings concerning the role of H3K9me3 for genome stability provide a basis for future studies focusing on the influence of heterochromatin on structural rearrangements using *Z. tritici* as a model organism.

H3K27me3 and the stability of accessory chromosomes

Although ~20 % of the genome of *Z. tritici* is enriched with H3K27me3 the role of KMT6 in transcriptional regulation is not as pronounced as in other fungal systems. Hence, we hypothesize that H3K27me3 has other important functions apart from gene silencing. In contrast to the destabilizing effect of KMT1 deletion and the resulting H3K9me3 loss on genome integrity, we demonstrate that the absence of H3K27me3 leads to a reduction of accessory chromosome losses during mitotic growth (Table 2). This implies that the enrichment of H3K27me3 on accessory chromosomes in wild type cells is a main driver of their mitotic instability.

We propose different scenarios how chromosomes could get lost during mitosis and how H3K27me3 may be linked to these processes: Accessory chromosomes may not be accurately replicated whereby only one sister chromatid is transmitted. Or non-disjunction of sister chromatids during mitosis produces one cell with two copies and one cell lacking the respective chromosome. Previous microscopic studies of *Z. tritici* centromeres indicated that chromosomes might be physically separated in the nucleus (Schotanus *et al.*, 2015). Interestingly, it was shown that H3K27me3 localizes close to the nuclear periphery and loss of H3K27me3 enables movement of the previously associated regions to the inner nucleus in mammals and fungi (Harr *et al.*, 2015; Klocko *et al.*, 2016). Proximity to the nuclear membrane and heterochromatic structure can furthermore result in different, often late replication timing (Heun *et al.*, 2001; Jørgensen *et al.*, 2007).

Loss of H3K27me3 and possible movement to the inner nucleus might therefore alter replication dynamics of accessory chromosomes resulting in higher rates of faithfully replicated chromosomes and lower rates of mitotic losses.
Repressed chromatin regions, especially associated to H3K27me3, tend to cluster together and form distinct foci in the nucleus of *D. melanogaster* visualized by microscopic analyses (Messmer *et al.*, 1992; Buchenau *et al.*, 1998). Loss of H3K27me3 consequently reduces interaction between these regions (Denholtz *et al.*, 2013). We hypothesize that enrichment of H3K27me3 on the entire accessory chromosomes fuels physical interactions that persist throughout mitosis. This may decrease the efficiency to separate sister chromatids resulting in loss of the chromosome in one cell and a duplication in the other cell. So far, we focused our screenings on chromosome losses but determining the exact rates of accessory chromosome duplications is necessary to test this hypothesis. Genome sequencing of *Z. tritici* chromosome-loss strains revealed that duplications of accessory chromosomes can occur (Moeller *et al.*, 2018). Similar, B chromosomes in plants are preferentially inherited during meiosis by non-disjunction of sister chromatids during the first pollen mitosis (Banaei-Moghaddam *et al.*, 2012) indicating that deviation from normal chromosome segregation is a common mechanism. Accessory chromosomes are commonly found in natural isolates, despite the high loss rates we demonstrated during mitotic growth (Moeller *et al.*, 2018). This observation implies the presence of other mechanisms that counteract the frequent losses of accessory chromosomes. Recent analyses of meiotic transmissions show that unpaired accessory chromosomes are transmitted at higher rates in a uniparental way (Habig et al., submitted). We speculate that H3K27me3 might be involved in accessory chromosome transmission both during mitosis and meiosis.

In summary, we demonstrate that the histone methyltransferases KMT1 and KMT6 play important but distinct roles in genome stability in the fungus *Z. tritici*. H3K9me3 is essential for transcriptional regulation and replication of repeats while loss of KMT1 results in repeat-associated, large-scale genome rearrangements. H3K27me3 has a crucial function in accessory chromosome transmission, whereby presence of H3K27me3 results in elevated chromosome loss rates in individual cells. Although detailed mechanisms still have to be elucidated, we present the first evidence of the importance of histone methylation in genome dynamics in fungal plant pathogens.

Materials and Methods

Culturing conditions of fungal and bacterial strains

Zymoseptoria tritici strains were cultivated on solid (2 % [w/v] bacto agar) or in liquid YMS medium (0.4 % [w/v] yeast extract, 0.4 % [w/v] malt extract, 0.4 % [w/v] sucrose). Liquid cultures were inoculated from plate or directly from glycerol stocks and grown for 3 – 4 days at 18°C in a shaking incubator at 200 rpm. Plates were inoculated from glycerol stocks and grown for 5 – 6 days at 18°C. *Escherichia coli* TOP10 cells were grown overnight in dYT (1.6 % [w/v] trypton, 1 % [w/v] yeast extract, 0.5 % [w/v] NaCl and 2 % bacto agar for solid medium)) supplemented with antibiotics for plasmid selection (40 µg/mL kanamycin) at 37°C and at 200 rpm for liquid cultures . *Agrobacterium tumefaciens* strain AGL1 was grown in dYT containing rifampicin (50 µg/mL) and carbenicillin (100 µg/mL) supplemented with antibiotics for plasmid selection (40 µg/mL kanamycin) at 28°C at 200 rpm in liquid culture for 18 h and on plate at 28°C for two days.

Transformation of *Z. tritici*

Z. tritici deletion and complementation strains were engineered using *Agrobacterium tumefaciens*-mediated transformations as described before (Bowler *et al.*, 2010; Poppe *et al.*, 2015). Flanking regions of the respective genes were used to facilitate homologous recombination for integration at the correct genomic location. The plasmid pES61 (a derivate of the binary vector pNOV-ABCD (Bowler *et al.*, 2010)) was used for targeted gene deletion and complementation. Plasmids were assembled using a restriction enzyme-based approach or Gibson assembly (Gibson *et al.*, 2009). Plasmids were amplified in *E. coli* TOP10 cells and transformed in the *A. tumefaciens* strain AGL1 as described previously (Zwiers & De Waard, 2001). Gene deletions of *kmt1* (*Zt09_chr_1_01919*) and *kmt6* (*Zt09_chr_4_00551*) were facilitated by replacement of the respective ORF with a hygromycin resistance cassette. The *kmt1/kmt6* double deletion mutant was constructed by integrating a nourseothricin resistance cassette replacing *kmt1* in a *kmt6* deletion mutant background. Complementation constructs containing the respective gene and a G418 resistance cassette were integrated at the native loci in the deletion strains. All plasmids and strains constructed in this study are listed in Table S1. Transformed strains were screened by PCR for correct integrations of the construct followed by Southern blot (Southern, 1975) using DIG-labeled probes generated with the DIG labeling kit (Roche, Mannheim, Germany) following manufacturer's instructions.

DNA isolation for PCR screenings and Southern blotting

For rapid PCR screenings (candidates for transformation and chromosome loss), a single *Z. tritici* colony was resuspended in 50 µL 25 mM NaOH, incubated at 98°C for 10 min and afterwards 50 µL 40 mM Tris-HCl pH 5.5 were added. 4 µl mix subsequently were used as template for PCRs. For Southern blotting, we used a standard phenol-chloroform extraction protocol (Sambrock & W. Russel, 2001) for DNA isolation.

Phenotypic characterization *in vitro*

For the *in vitro* growth assays, liquid YMS cultures were inoculated with 100 cells/µL (OD_{600} = 0.01); cells were grown in 25 mL YMS at 18°C and 200 rpm. For each mutant and complementation strain, two transformants (biological replicates), and three replicate cultures per transformant (technical replicates) were used. For the reference strain Zt09, two separate pre-cultures were grown as biological replicates and each pre-culture was used to inoculate three replicate cultures. OD_{600} was measured at different time points throughout the experiment until the stationary phase was reached. The R package growthcurver (Sprouffske & Wagner, 2016) was used to fit the growth curve data enabling to compare *in vitro* growth of the different strains.

To test the tolerance of mutant and reference strains towards different stressors, we performed an *in vitro* stress assay on YMS plates. Each plate contained additives constituting different stress conditions. Cell suspensions containing 10^7 cells/mL and a tenfold dilution series down to 100 cells/mL were prepared; 3 µL of each dilution were pipetted on solid YMS containing the following additives: 0.5 M NaCl, 1 M NaCl, 1 M sorbitol, 1.5 M sorbitol, 1.5 mM H_2O_2, 2 mM H_2O_2, 300 µg/mL Congo red, 0.01 % MMS (methyl methane sulfonate), 0.025 % MMS, 1 µg/mL actinomycin D and 1.5 µg/mL actinomycin D. Furthermore, we included a H_2O-agar (2 % bacto agar) plate. All plates were incubated at 18°C for six days, except for one YMS plate that was exposed to 28°C to test for thermal stress responses.

Phenotypic characterization *in planta*

Seedlings of the susceptible wheat cultivar Obelisk (Wiersum Plantbreeding BV, Winschoten, The Netherlands) were potted (three plants per pot) after four days of pre-germination and grown for seven more days. Single cell suspensions of mutant and reference strain were prepared (10^8 cells / mL in H_2O with 0.1 % Tween 20) and brush inoculated on a marked area on the second leaf. Following inoculation, the plants were

incubated in sealed plastic bags containing ~ 1 L of H_2O for 48 h providing high humidity to promote infections. Growth conditions for the plants throughout the complete growth phase and infection were 16 h light (200 µmol/$m^{-2}s^{-1}$) and 8 h dark at 20°C and 90 % humidity. . First appearances of symptoms, necrosis or pycnidia, were assessed by manual inspection of every treated leaf. 21 days post infection, inoculated leaves were finally screened for infection symptoms. Manual visual inspection of each leaf was performed to evaluate the percentage of leaf area covered by necrosis and pycnidia. Six different categories were differentiated based on the observed coverage (0: 0 %, 1: 1 – 20 %, 2: 21 – 40 %, 3: 41 – 60 %, 4: 61 -80 %, 5: 81 – 100 %). Automated symptom evaluation was performed by analysis of scanned images of infected leaf areas as described previously (Stewart *et al.*, 2016).

Long-term evolution experiment

For the long-term evolution experiment (~6 months), cells were inoculated directly from the glycerol stocks into 20 mL liquid YMS cultures. We used Zt09, *Δkmt6* and *Δkmt1*, each strain grown in triplicates. Every three to four days, cells were transferred to new YMS medium. Cells were grown at 18°C and 200 rpm. For every transfer, cell density of the cultures was measured by OD_{600} and the new cultures were inoculated with a cell density of ~ 100 cells / µL (correlating to a transfer of 0.1 % of the population). After 50 transfers, the genomes of the evolved populations and each progenitor strain were sequenced. Additionally, three genomes of single clones derived from the *Δkmt1* populations after 50 transfers were sequenced to characterize genome rearrangements in more detail.

Short-term evolution experiment

For the short-term evolution experiment over a time period of four weeks, cultures were inoculated from single colonies grown on solid YMS. Zt09, *Δkmt6*, *Δkmt1*, and the *Δkmt6*/*Δkmt1* double mutant were grown in triplicate YMS cultures. For this experiment we used a different *Δkmt1* mutant clone, as we discovered that the strain used in the previous long-term evolution experiment was missing chromosome 20. Every three to four days, 900 µL culture were transferred to 25 mL fresh YMS (correlating to a transfer of ~ 4 % of the population). After four weeks of growth (including eight transfers to new medium) at 18°C and 200 rpm, cultures were diluted and plated on YMS agar to obtain

single colonies. These single colonies were PCR screened for presence of accessory chromosomes as described in (Moeller *et al.*, 2018).

Pulsed-field gel electrophoresis (PFGE)

Cells were grown in YMS medium for five days and harvested by centrifugation for 10 min at 3,500 rpm. We used 5 x 10^8 cells for plug preparation that were washed twice with Tris-HCl, pH 7.5, resuspended in 1 mL TE buffer (pH 8) and mixed with 1 mL of 2.2 % low range ultra agarose (Bio-Rad, Munich, Germany). The mixture was pipetted into plug casting molds and cooled for 1 h at 4°C. Plugs were placed to 50 mL screw cap Falcon tubes containing 5 mL of lysis buffer (1 % SDS; 0.45 M EDTA; 1.5 mg/mL proteinase K[Roth, Karlsruhe, Germany]) and incubated for 48 h at 55°C while the buffer was replaced once after 24 h. Chromosomal plugs were washed three times for 20 min with 1 X TE buffer before storage in 0.5 M EDTA at 4°C. PFGE was performed with a CHEF-DR III pulsed-field electrophoresis system (BioRad, Munich, Germany). Separation of mid-size chromosomes was conducted with the settings: switching time 250 s – 1000 s, 3 V/cm, 106° angle, 1 % pulsed-field agarose in 0.5 X TBE for 72 h. Large chromosomes were separated with the following settings: switching time 1000 s – 2000 s, 2 V/cm, 106° angle, 0.8 % pulsed-field agarose in 1 X TAE for 96 h. *Saccharomyces cerevisiae* chromosomal DNA (BioRad, Munich, Germany) was used as size marker for the for mid-size chromosomes, *Schizosaccharomyces pombe* chromosomal DNA (BioRad, Munich, Germany) for the large chromosomes. Gels were stained in ethidium bromide staining solution (1 µg/mL ethidium bromide in H_2O) for 30 min. Detection of chromosomal bands was performed with the GelDocTM XR+ system (Bio-Rad, Munich, Germany). Southern blotting was performed as described previously (Southern 1975) using DIG-labeled probes generated with the PCR DIG labeling Mix (Roche, Mannheim, Germany) following the manufacturer's instructions.

ChIP-sequencing

Cells were grown in liquid YMS medium at 18°C for 2 days until an OD_{600} of ~ 1 was reached. Chromatin immunoprecipitation was performed as previously described (Soyer *et al.*, 2015) with minor modifications. We used antibodies against H3K4me2 (#07-030, Merck Millipore), H3K9me3 (#39161, Active Motif) and H3K27me3 (#39155, Active Motif). ChIP DNA was purified using SureBeads™ Protein G Magnetic Beads (Bio-Rad, Munich, Germany) and, replacing phenol/chloroform extractions, we used the ChIP DNA

Clean & Concentrator Kit (Zymo Research, Freiburg, Germany). We sequenced two biological and one additional technical replicate for Zt09, *Δkmt1*, *Δkmt6*, and the *Δk1/k6* strains. Sequencing was performed at the OSU Center for Genome Research and Biocomputing on an Illumina HiSeq2000 obtaining 50-nt reads and at the Max Planck-Genome-centre Cologne, Germany (https://mpgc.mpipz.mpg.de/home/) on an Illumina Hiseq3000 platform obtaining 150-nt reads (Table S8).

RNA-sequencing

For RNA extraction, cells were grown in liquid YMS at 18°C and 200 rpm for two days until an OD_{600} of ~ 1 was reached. Cells were harvested by centrifugation and ground in liquid nitrogen. Total RNA was extracted using TRIzol (Invitrogen, Karlsruhe, Germany) according to manufacturer's instructions. The extracted RNA was further DNAse-treated and cleaned up using the RNA Clean & Concentrator-25 Kit (Zymo Research, Freiburg, Germany). RNA samples of two biological replicates of Zt09, *Δkmt1*, *Δkmt6*, and the *Δkmt1/Δkmt6* double mutant were sequenced. Poly(A)-captured, stranded library preparation and sequencing were performed by the Max Planck-Genome-centre Cologne, Germany (https://mpgc.mpipz.mpg.de/home/) on an Illumina Hiseq3000 platform obtaining ~ 20 million 150-nt reads per sample (Table S8).

Genome sequencing

Genomic DNA for sequencing was prepared as described previously (Allen *et al.*, 2006). Library preparation and genome sequencing of the progenitor strains used for the evolution experiments were performed at Aros, Skejby, Denmark using an Illumina Hiseq2500 platform obtaining 100-nt paired-end reads. Library preparation (PCR-free) and sequencing of the evolved populations and the three evolved single *Δkmt1* mutants were performed by the Max Planck-Genome-centre Cologne, Germany (https://mpgc.mpipz.mpg.de/home/) on an Illumina Hiseq3000 platform resulting in 150-nt paired-end reads (Table S8).

Short read mapping and data analysis

A detailed list of all programs and commands used for mapping and sequencing data analyses can be found in the supplementary text S1. All sequencing data was quality filtered using the FastX toolkit (http://hannonlab.cshl.edu/fastx_toolkit/) and

Trimmomatic (Bolger *et al.*, 2014). RNA-seq reads were mapped using hisat2 (Kim *et al.*, 2015), mapping of ChIP and genome data was performed with Bowtie2 (Langmead & Salzberg, 2012). Conversion of sam to bam format, sorting and indexing of read alignments was done with samtools (Li, 2011).

To detect enriched regions in the ChIP mappings, we used HOMER (Heinz *et al.*, 2010). Peaks were called individually for replicates and merged with bedtools (Quinlan & Hall, 2010). Only enriched regions found in all replicates were considered for further analyses. Genome coverage of enriched regions and overlap to genes and transposable elements was calculated using bedtools (Quinlan & Hall, 2010).

We used cuffdiff (Trapnell *et al.*, 2010) to calculate RPKM values and to estimate expression in the different strains. Raw reads mapping on genes and transposable elements were counted by HTSeq (Anders *et al.*, 2015), differential expression analysis was performed in R (Ihaka & Gentleman, 1996) with DESeq2 (Love *et al.*, 2014). Cutoff for significantly differentially expressed genes was padj < 0.001 and |log2 fold-change| > 2. The R package topGO (Alexa *et al.*, 2006) was used to perform gene ontology enrichment analyses. Fisher's exact test (*P*-value < 0.01) was applied to detect significantly enriched terms in the category 'biological process'.

To detect structural variation in the sequenced genomes, we used SpeedSeq (Chiang *et al.*, 2015) and LUMPY (Layer *et al.*, 2014). All detected variation was further verified by manual visual inspection. Visualization was performed with the integrative genome browser (IGV) (Thorvaldsdóttir *et al.*, 2013).

References

Alexa A, Rahnenführer J, Lengauer T. 2006. Improved scoring of functional groups from gene expression data by decorrelating GO graph structure. *Bioinformatics* **22**: 1600–1607.

Allen GC, Flores-Vergara M a, Krasynanski S, Kumar S, Thompson WF. 2006. A modified protocol for rapid DNA isolation from plant tissues using cetyltrimethylammonium bromide. *Nature protocols* **1**: 2320–2325.

Allis CD, Berger SL, Cote J, Dent S, Jenuwien T, Kouzarides T, Pillus L, Reinberg D, Shi Y, Shiekhattar R, *et al.* 2007. New Nomenclature for Chromatin-Modifying Enzymes. *Cell* **131**: 633–636.

Allshire RC, Madhani HD. 2017. Ten principles of heterochromatin formation and function. *Nature Reviews Molecular Cell Biology* **19**: 229–244.

Anders S, Pyl PT, Huber W. 2015. HTSeq-A Python framework to work with high-throughput sequencing data. *Bioinformatics* **31**: 166–169.

Banaei-Moghaddam AM, Schubert V, Kumke K, Weiß O, Klemme S, Nagaki K, Macas J, González-Sánchez M, Heredia V, Gómez-Revilla D, *et al.* 2012. Nondisjunction in Favor of a Chromosome: The Mechanism of Rye B Chromosome Drive during Pollen Mitosis. *The Plant Cell* **24**: 4124–4134.

Bannister AJ, Kouzarides T. 2011. Regulation of chromatin by histone modifications. *Cell Research* **21**: 381–395.

Barrón MG, Fiston-Lavier A-S, Petrov DA, González J. 2014. Population Genomics of Transposable Elements in *Drosophila*. *Annual Review of Genetics* **48**: 561–581.

Basenko EY, Sasaki T, Ji L, Prybol CJ, Burckhardt RM, Schmitz RJ, Lewis Z a. 2015. Genome-wide redistribution of H3K27me3 is linked to genotoxic stress and defective growth. *Proceedings of the National Academy of Sciences*: 201511377.

Bolger AM, Lohse M, Usadel B. 2014. Trimmomatic: A flexible trimmer for Illumina sequence data. *Bioinformatics* **30**: 2114–2120.

Bowler J, Scott E, Tailor R, Scalliet G, Ray J, Csukai M. 2010. New capabilities for Mycosphaerella graminicola research. *Molecular Plant Pathology* **11**: 691–704.

Buchenau P, Hodgson J, Strutt H, Arndt-jovin DJ. 1998. The Distribution of Polycomb-Group Proteins During Cell Division and Development in. *Cell* **141**: 469–481.

Chiang C, Layer RM, Faust GG, Lindberg MR, Rose DB, Garrison EP, Marth GT, Quinlan AR, Hall IM. 2015. SpeedSeq: Ultra-fast personal genome analysis and interpretation. *Nature Methods* **12**: 966–968.

Chiruvella KK, Liang Z, Wilson TE. 2013. Repair of double-strand breaks by end joining. *Cold Spring Harbor perspectives in biology* **5**: a012757.

Chujo T, Scott B. 2014. Histone H3K9 and H3K27 methylation regulates fungal alkaloid biosynthesis in a fungal endophyte-plant symbiosis. *Molecular Microbiology* **92**: 413–434.

Connolly LR, Smith KM, Freitag M. 2013. The Fusarium graminearum histone H3 K27 methyltransferase KMT6 regulates development and expression of secondary metabolite gene clusters. *PLoS genetics* **9**: e1003916.

Covert SF. 1998. Supernumerary chromosomes in filamentous fungi. *Current Genetics* **33**: 311–319.

Croll D, Zala M, McDonald B a. 2013. Breakage-fusion-bridge cycles and large insertions contribute to the rapid evolution of accessory chromosomes in a fungal pathogen. *PLoS genetics* **9**: e1003567.

Denholtz M, Bonora G, Chronis C, Splinter E, de Laat W, Ernst J, Pellegrini M, Plath K. 2013. Long-Range Chromatin Contacts in Embryonic Stem Cells Reveal a Role for Pluripotency Factors and Polycomb Proteins in Genome Organization. *Cell Stem Cell* **13**: 602–616.

Ding Y, Wang X, Su L, Zhai J, Cao S, Zhang D, Liu C, Bi Y, Qian Q, Cheng Z, *et al.* 2007. SDG714, a Histone H3K9 Methyltransferase, Is Involved in Tos17 DNA Methylation and Transposition in Rice. *the Plant Cell Online* **19**: 9–22.
Feschotte C, Pritham EJ. 2007. DNA Transposons and the Evolution of Eukaryotic Genomes. *Annual Review of Genetics* **41**: 331–368.
Galazka JM, Freitag M. 2014. Variability of chromosome structure in pathogenic fungi-of "ends and odds." *Current Opinion in Microbiology* **20**: 19–26.
Gibson DG, Young L, Chuang RY, Venter JC, Hutchison CA, Smith HO. 2009. Enzymatic assembly of DNA molecules up to several hundred kilobases. *Nature Methods* **6**: 343–345.
Goldberg AD, Allis CD, Bernstein E. 2007. Epigenetics: A Landscape Takes Shape. *Cell* **128**: 635–638.
Goodrich J, Puangsomlee P, Martin M, Long D, Meyerowitz EM, Coupland G. 1997. A Polycomb-group gene regulates homeotic gene expression in Arabidopsis. *Nature* **386**: 44–51.
Goodwin SB, M'barek S Ben, Dhillon B, Wittenberg AHJ, Crane CF, Hane JK, Foster AJ, Van der Lee T a J, Grimwood J, Aerts A, *et al.* 2011. Finished genome of the fungal wheat pathogen Mycosphaerella graminicola reveals dispensome structure, chromosome plasticity, and stealth pathogenesis. *PLoS genetics* **7**: e1002070.
Grandaubert J, Bhattacharyya A, Stukenbrock EH. 2015. RNA-seq Based Gene Annotation and Comparative Genomics of Four Fungal Grass Pathogens in the Genus Zymoseptoria Identify Novel Orphan Genes and Species-Specific Invasions of Transposable Elements. *G3 (Bethesda, Md.)* **5**: g3.115.017731-.
Habig M, Quade J, Stukenbrock EH. 2017. Forward genetics approach reveals host-genotype dependent importance of accessory chromosomes in the fungal wheat pathogen Zymoseptoria tritici. *mBio* **8**: Forthcoming.
Harr JC, Gonzalez-Sandoval A, Gasser SM. 2016. Histones and histone modifications in perinuclear chromatin anchoring: from yeast to man. *EMBO reports* **17**: e201541809.
Harr JC, Luperchio TR, Wong X, Cohen E, Wheelan SJ, Reddy KL. 2015. Directed targeting of chromatin to the nuclear lamina is mediated by chromatin state and A-type lamins. *Journal of Cell Biology* **208**: 33–52.
Hedges DJ, Batzer MA. 2005. From the margins of the genome: Mobile elements shape primate evolution. *BioEssays* **27**: 785–794.
Heinz S, Benner C, Spann N, Bertolino E, Lin YC, Laslo P, Cheng JX, Murre C, Singh H, Glass CK. 2010. Simple Combinations of Lineage-Determining Transcription Factors Prime cis-Regulatory Elements Required for Macrophage and B Cell Identities. *Molecular Cell* **38**: 576–589.
Heun P, Laroche T, Raghuraman MK, Gasser SM. 2001. The positioning and dynamics of origins of replication in the budding yeast nucleus. *Journal of Cell Biology* **152**: 385–400.
Holec S, Berger F. 2012. Polycomb Group Complexes Mediate Developmental Transitions in Plants. *Plant Physiology* **158**: 35–43.
Holm K, Grabau D, Lövgren K, Aradottir S, Gruvberger-Saal S, Howlin J, Saal LH, Ethier SP, Bendahl PO, Stål O, *et al.* 2012. Global H3K27 trimethylation and EZH2 abundance in breast tumor subtypes. *Molecular Oncology* **6**: 494–506.
Ihaka R, Gentleman R. 1996. R: A Language for Data Analysis and Graphics. *Journal of Computational and Graphical Statistics* **5**: 299–314.
Jamieson K, Rountree MR, Lewis Z a, Stajich JE, Selker EU. 2013. Regional control of histone H3 lysine 27 methylation in Neurospora. *Proceedings of the National Academy of Sciences of the United States of America* **110**: 6027–32.

Jin W, Lamb JC, Vega JM, Dawe RK, Birchler JA, Jiang J. **2005**. Molecular and Functional Dissection of the Maize B Chromosome Centromere. *The Plant Cell* **17**: 1412 LP-1423.
Jørgensen HF, Azuara V, Amoils S, Spivakov M, Terry A, Nesterova T, Cobb BS, Ramsahoye B, Merkenschlager M, Fisher AG. **2007**. The impact of chromatin modifiers on the timing of locus replication in mouse embryonic stem cells. *Genome Biology* **8**: 1–13.
Kellner R, Bhattacharyya A, Poppe S, Hsu TY, Brem RB, Stukenbrock EH. **2014**. Expression Profiling of the Wheat Pathogen Zymoseptoria tritici Reveals Genomic Patterns of Transcription and Host-Specific Regulatory Programs. *Genome biology and evolution* **6**: 1353–65.
Ketel C, Wang HSW, McClellan M, Bouchonville K, Selmecki A, Lahav T, Gerami-Nejad M, Berman J. **2009**. Neocentromeres form efficiently at multiple possible loci in candida albicans. *PLoS Genetics* **5**.
Khurana S, Oberdoerffer P. **2015**. Replication stress: A lifetime of epigenetic change. *Genes* **6**: 858–877.
Kim D, Langmead B, Salzberg SL. **2015**. HISAT: a fast spliced aligner with low memory requirements. *Nature methods* **12**: 357–60.
Klocko AD, Ormsby T, Galazka JM, Leggett NA, Uesaka M, Honda S, Freitag M, Selker EU. **2016**. Normal chromosome conformation depends on subtelomeric facultative heterochromatin in *Neurospora crassa*. *Proceedings of the National Academy of Sciences* **113**: 15048–15053.
Kornberg RD, Lorch Y. **1992**. Chromatin structure and transcription. *Annual review of cell biology* **8**: 563–587.
Langmead B, Salzberg SL. **2012**. Fast gapped-read alignment with Bowtie 2. *Nat Methods* **9**: 357–359.
Layer RM, Chiang C, Quinlan AR, Hall IM. **2014**. LUMPY: A probabilistic framework for structural variant discovery. *Genome Biology* **15**: 1–19.
Lee TI, Jenner RG, Boyer LA, Guenther MG, Levine SS, Kumar RM, Chevalier B, Johnstone SE, Cole MF, Isono K ichi, *et al.* 2006. Control of Developmental Regulators by Polycomb in Human Embryonic Stem Cells. *Cell* **125**: 301–313.
Li H. **2011**. A statistical framework for SNP calling, mutation discovery, association mapping and population genetical parameter estimation from sequencing data. *Bioinformatics* **27**: 2987–2993.
Li PC, Petreaca RC, Jensen A, Yuan JP, Green MD, Forsburg SL. **2013**. Replication Fork Stability Is Essential for the Maintenance of Centromere Integrity in the Absence of Heterochromatin. *Cell Reports* **3**: 638–645.
Liefshitz B, Parket A, Maya R, Kupiec M. **1995**. The role of DNA repair genes in recombination between repeated sequences in yeast. *Genetics* **140**: 1199–1211.
Linde CC, Zhan J, McDonald BA. **2002**. Population Structure of Mycosphaerella graminicola: From Lesions to Continents. *Phytopathology* **92**: 946–955.
Love MI, Huber W, Anders S. **2014**. Moderated estimation of fold change and dispersion for RNA-seq data with DESeq2. *Genome Biology* **15**: 1–21.
Ma L-J, van der Does HC, Borkovich K a, Coleman JJ, Daboussi M-J, Di Pietro A, Dufresne M, Freitag M, Grabherr M, Henrissat B, *et al.* 2010. Comparative genomics reveals mobile pathogenicity chromosomes in Fusarium. *Nature* **464**: 367–373.
McClintock B. **1938**. The Production of Homozygous Deficient Tissues with Mutant Characteristics by Means of the Aberrant Mitotic Behavior of Ring-Shaped Chromosomes. *Genetics* **23**: 315–376.
McClintock B. **1941**. The Stability of Broken Ends of Chromosomes in Zea Mays. *Genetics* **26**: 234–282.

McDonald B a., Martinez JP. **1991**. Chromosome length polymorphisms in a Septoria tritici population. *Current Genetics* **19**: 265–271.
Mehrabi R, Taga M, Kema GHJ. **2007**. Electrophoretic and cytological karyotyping of the foliar wheat pathogen Mycosphaerella graminicola reveals many chromosomes with a large size range. *Mycologia* **99**: 868–76.
Messmer S, Franke A, Paro R. **1992**. Analysis of the functional role of the Polycomb chrom domain in Drosophila melanogaster. *Genes and Development* **6**: 1241–1254.
Miao V, Covert S, VanEtten H. **1991**. A fungal gene for antibiotic resistance on a dispensable ("B") chromosome. *Science* **254**: 1773–1776.
Mikkelsen TS, Ku M, Jaffe DB, Issac B, Lieberman E, Giannoukos G, Alvarez P, Brockman W, Kim TK, Koche RP, *et al.* 2007. Genome-wide maps of chromatin state in pluripotent and lineage-committed cells. *Nature* **448**: 553–560.
Moeller M, Habig M, Freitag M, Holtgrewe Stukenbrock E. **2018**. Extraordinary genome instability and widespread chromosome rearrangements during vegetative growth. *bioRxiv*. doi: https://doi.org/10.1101/304915
Möller M, Stukenbrock EH. **2017**. Evolution and genome architecture in fungal plant pathogens. *Nature Reviews Microbiology* **15**: 756–771.
Müller J, Hart CM, Francis NJ, Vargas ML, Sengupta A, Wild B, Miller EL, O'Connor MB, Kingston RE, Simon J a. **2002**. Histone methyltransferase activity of a Drosophila Polycomb group repressor complex. *Cell* **111**: 197–208.
Ngollo M, Lebert A, Daures M, Judes G, Rifai K, Dubois L, Kemeny JL, Penault-Llorca F, Bignon YJ, Guy L, *et al.* 2017. Global analysis of H3K27me3 as an epigenetic marker in prostate cancer progression. *BMC Cancer* **17**: 1–8.
O'Carroll D, Erhardt S, Pagani M, Barton SC. **2001**. The Polycomb -Group Gene Ezh2 Is Required for Early Mouse Development. *Molecular and cellular biology* **21**: 4330–4336.
Palmer JM, Perrin RM, Dagenais TRT, Keller NP. **2008**. H3K9 methylation regulates growth and development in Aspergillus fumigatus. *Eukaryotic cell* **7**: 2052–60.
Peng JC, Karpen GH. **2009**. Heterochromatic genome stability requires regulators of histone H3 K9 methylation. *PLoS Genetics* **5**.
Penke TJR, McKay DJ, Strahl BD, Gregory Matera A, Duronio RJ. **2016**. Direct interrogation of the role of H3K9 in metazoan heterochromatin function. *Genes and Development* **30**: 1866–1880.
Pennaneach V, Putnam CD, Kolodner RD. **2006**. Chromosome healing by de novo telomere addition in Saccharomyces cerevisiae. *Molecular Microbiology* **59**: 1357–1368.
Poppe S, Dorsheimer L, Happel P, Stukenbrock EH. **2015**. Rapidly Evolving Genes Are Key Players in Host Specialization and Virulence of the Fungal Wheat Pathogen Zymoseptoria tritici (Mycosphaerella graminicola). *PLoS Pathogens* **11**: 1–21.
Quinlan AR, Hall IM. **2010**. BEDTools: a flexible suite of utilities for comparing genomic features. *Bioinformatics* **26**: 841–842.
Ramírez F, Ryan DP, Grüning B, Bhardwaj V, Kilpert F, Richter AS, Heyne S, Dündar F, Manke T. **2016**. deepTools2: a next generation web server for deep-sequencing data analysis. *Nucleic acids research* **44**: W160–W165.
Rea S, Eisenhaber F, O'Carroll D, Strahl BD, Sun ZW, Schmid M, Opravil S, Mechtier K, Ponting CP, Allis CD, *et al.* 2000. Regulation of chromatin structure by site-specific histone H3 methyltransferases. *Nature* **406**: 593–599.
Reddington JP, Perricone SM, Nestor CE, Reichmann J, Youngson NA, Suzuki M, Reinhardt D, Dunican DS, Prendergast JG, Mjoseng H, *et al.* 2013. Redistribution of H3K27me3 upon DNA hypomethylation results in de-repression of Polycomb target genes. *Genome Biology* **14**: R25.

Rudd JJ, Kanyuka K, Hassani-Pak K, Derbyshire M, Andongabo A, Devonshire J, Lysenko A, Saqi M, Desai NM, Powers SJ, *et al.* 2015. Transcriptome and metabolite profiling of the infection cycle of Zymoseptoria tritici on wheat reveals a biphasic interaction with plant immunity involving differential pathogen chromosomal contributions and a variation on the hemibiotrophic lifestyle def. *Plant physiology* **167**: 1158–85.

Sambrock J, W. Russel D. **2001**. Molecular Cloning: A Laboratory Manual(3rd edition).

Schotanus K, Soyer JL, Connolly LR, Grandaubert J, Happel P, Smith KM, Freitag M, Stukenbrock EH. **2015**. Histone modifications rather than the novel regional centromeres of Zymoseptoria tritici distinguish core and accessory chromosomes. *Epigenetics & chromatin* **8**: 41.

Southern EM. **1975**. Detection of specific sequences among DNA fragments separated by gel electrophoresis. *Journal of Molecular Biology* **98**: 503–517.

Soyer JL, El Ghalid M, Glaser N, Ollivier B, Linglin J, Grandaubert J, Balesdent M-H, Connolly LR, Freitag M, Rouxel T, *et al.* 2014. Epigenetic control of effector gene expression in the plant pathogenic fungus Leptosphaeria maculans. *PLoS genetics* **10**: e1004227.

Soyer JL, Möller M, Schotanus K, Connolly LR, Galazka JM, Freitag M, Stukenbrock EH. **2015**. Chromatin analyses of Zymoseptoria tritici: Methods for chromatin immunoprecipitation followed by high-throughput sequencing (ChIP-seq). *Fungal Genetics and Biology* **79**: 63–70.

Sprouffske K, Wagner A. **2016**. Growthcurver: an R package for obtaining interpretable metrics from microbial growth curves. *BMC Bioinformatics* **17**: 172.

Stewart EL, Hagerty CH, Mikaberidze A, Mundt C, Zhong Z, McDonald BA. **2016**. An improved method for measuring quantitative resistance to the wheat pathogen Zymoseptoria tritici using high throughput automated image analysis. *Phytopathology*.

Stimpson KM, Matheny JE, Sullivan BA. **2012**. Dicentric chromosomes: Unique models to study centromere function and inactivation. *Chromosome Research* **20**: 595–605.

Studt L, Rösler SM, Burkhardt I, Arndt B, Freitag M, Humpf H-U, Dickschat JS, Tudzynski B. **2016**. Knock-down of the methyltransferase Kmt6 relieves H3K27me3 and results in induction of cryptic and otherwise silent secondary metabolite gene clusters in Fusarium fujikuroi. *Environmental microbiology*

Thakur J, Sanyal K. **2013**. Efficient neocentromere formation is suppressed by gene conversion to maintain centromere function a.pdf. : 638–652.

Thorvaldsdóttir H, Robinson JT, Mesirov JP. **2013**. Integrative Genomics Viewer (IGV): High-performance genomics data visualization and exploration. *Briefings in Bioinformatics* **14**: 178–192.

Trapnell C, Williams BA, Pertea G, Mortazavi A, Kwan G, van Baren MJ, Salzberg SL, Wold BJ, Pachter L. **2010**. Transcript assembly and quantification by RNA-Seq reveals unannotated transcripts and isoform switching during cell differentiation. *Nature Biotechnology* **28**: 511–515.

Venkatesh S, Workman JL. **2015**. Histone exchange, chromatin structure and the regulation of transcription. *Nature Reviews Molecular Cell Biology* **16**: 178–189.

Vlaardingerbroek I, Beerens B, Schmidt SM, Cornelissen BJC, Rep M. **2016**. Dispensable chromosomes in Fusarium oxysporum f . sp lycopersici . *Molecular Plant Pathology*: 1–12.

Voineagu I, Narayanan V, Lobachev KS, Mirkin SM. **2008**. Replication stalling at unstable inverted repeats: Interplay between DNA hairpins and fork stabilizing proteins. *Proceedings of the National Academy of Sciences* **105**: 9936–9941.

Weber T, Blin K, Duddela S, Krug D, Kim HU, Bruccoleri R, Lee SY, Fischbach MA, Müller R, Wohlleben W, *et al.* 2015. AntiSMASH 3.0-A comprehensive resource for the genome mining of biosynthetic gene clusters. *Nucleic Acids Research* **43**: W237–W243.
Wei Y, Xia W, Zhang Z, Liu J, Wang H, Adsay N V, Albarracin C, Yu D, Abbruzzese JL, Mills GB, *et al.* 2008. Loss of trimethylation at lysine 27 of histone H3 is a predictor of poor outcome in breast, ovarian, and pancreatic cancers. *Molecular Carcinogenesis* **47**: 701–706.
Wittenberg AHJ, van der Lee T a J, Ben M'barek S, Ware SB, Goodwin SB, Kilian A, Visser RGF, Kema GHJ, Schouten HJ. **2009**. Meiosis drives extraordinary genome plasticity in the haploid fungal plant pathogen Mycosphaerella graminicola. *PloS one* **4**: e5863.
Zeller P, Padeken J, Van Schendel R, Kalck V, Tijsterman M, Gasser SM. **2016**. Histone H3K9 methylation is dispensable for Caenorhabditis elegans development but suppresses RNA:DNA hybrid-associated repeat instability. *Nature Genetics* **48**: 1385–1395.
Zhang X, Liu X, Zhao Y, Cheng J, Xie J, Fu Y, Jiang D, Chen T. **2016**. Histone H3 Lysine 9 Methyltransferase DIM5 Is Required for the Development and Virulence of Botrytis cinerea. *Frontiers in Microbiology* **7**.
Zimmer C, Fabre E. **2011**. Principles of chromosomal organization: Lessons from yeast. *Journal of Cell Biology* **192**: 723–733.
Zwiers LH, De Waard MA. **2001**. Efficient Agrobacterium tumefaciens-mediated gene disruption in the phytopathogen Mycosphaerella graminicola. *Current Genetics* **39**: 388–393.

Supplementary Tables and Text

All supplementary tables and texts are deposited on the supplementary USB key.

Table S1. Plasmids, strains and primer designed for this study. Listed are all primers used to create plasmids and probes for Southern blots.

Table S2. Sequence coverage of histone modifications per chromosome in Zt09 and mutant strains.

Table S3. Expressed genes (RPKM > 2) and differentially expressed genes (P_{adj} < 0.001, |log2 fold-change| > 2) per chromosome.

Table S4. Enriched GO terms and upregulated genes in the categories DNA replication and RNA-dependent DNA replication.

Table S5. Predicted secondary metabolite gene clusters merged with the *Z. tritici* annotation (Grandaubert *et al.*, 2015).

Table S6. Structural variation detected in sequenced progenitor and evolved strains. Listed are location, size and type of structural variation. Only events that have not been described before for Zt09 are listed here.

Table S7. Detailed description and annotation of structural variation detected in the single *Δkmt1* clones.

Table S8. Statistics and overview of sequencing data generated in this study.

Supplementary text S1. Data analysis – programs and commands used for analysis of ChIP-seq, RNA-seq and genome sequencing data

Supplementary Figures

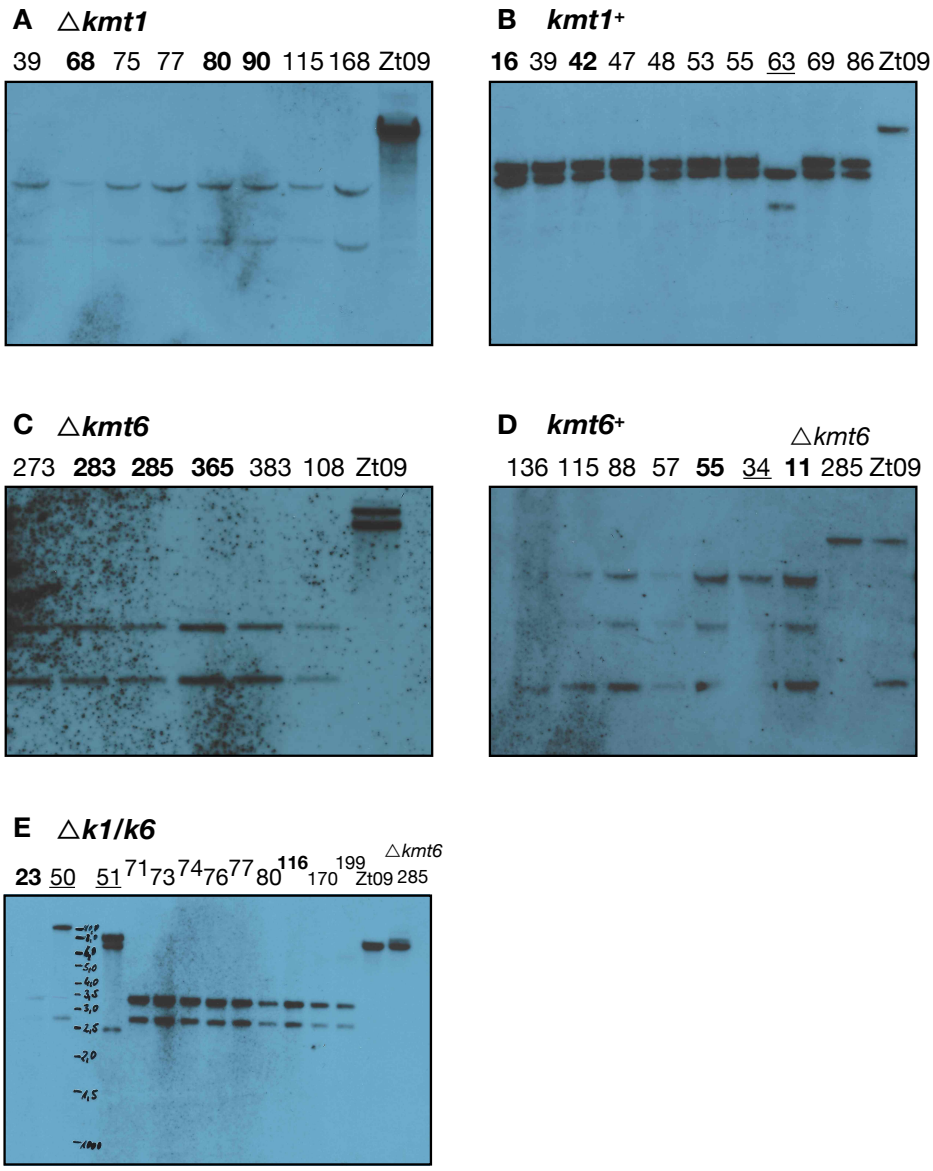

Figure S1. Southern blots to confirm correct integration of deletion and complementation constructs: for deletion of *kmt1* **(A)**, complementation of *kmt1* **(B)**, deletion of *kmt6* **(C)**, complementation of *kmt6* **(D)** and deletion of *kmt1* in a *kmt6* deletion background resulting in the generation of a double deletion mutant **(E)**. All tested strains, except for the underlined, were verified as correct mutants. The strains used for experiments in this study are highlighted in **bold**.

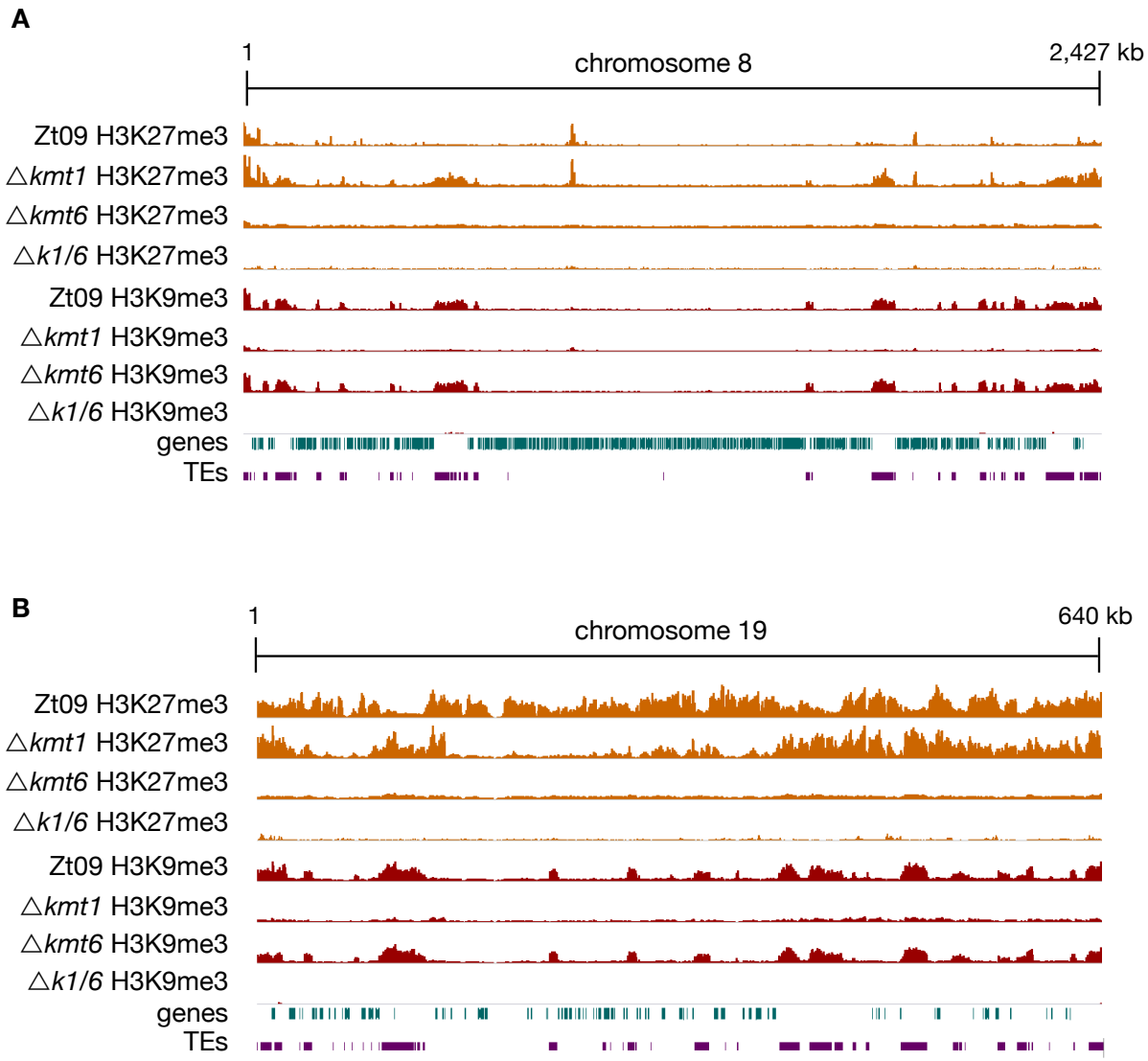

Figure S2. Verification of absence of H3K9me3 and H3K27me3 in the respective histone methyltransferase mutant strains. Shown are the ChIP-seq coverage tracks (normalized to RPKM using deeptools (Ramírez *et al.*, 2016)) of one replicate per strain. As an example, the coverage of a core chromosome (8) and an accessory chromosome (19) is displayed. Based on the missing coverage, we confirm absence of H3K9me3 in the *Δkmt1* and the *Δk1/6* strains and loss of H3K27me3 in the *Δkmt6* and *Δk1/6* strains.

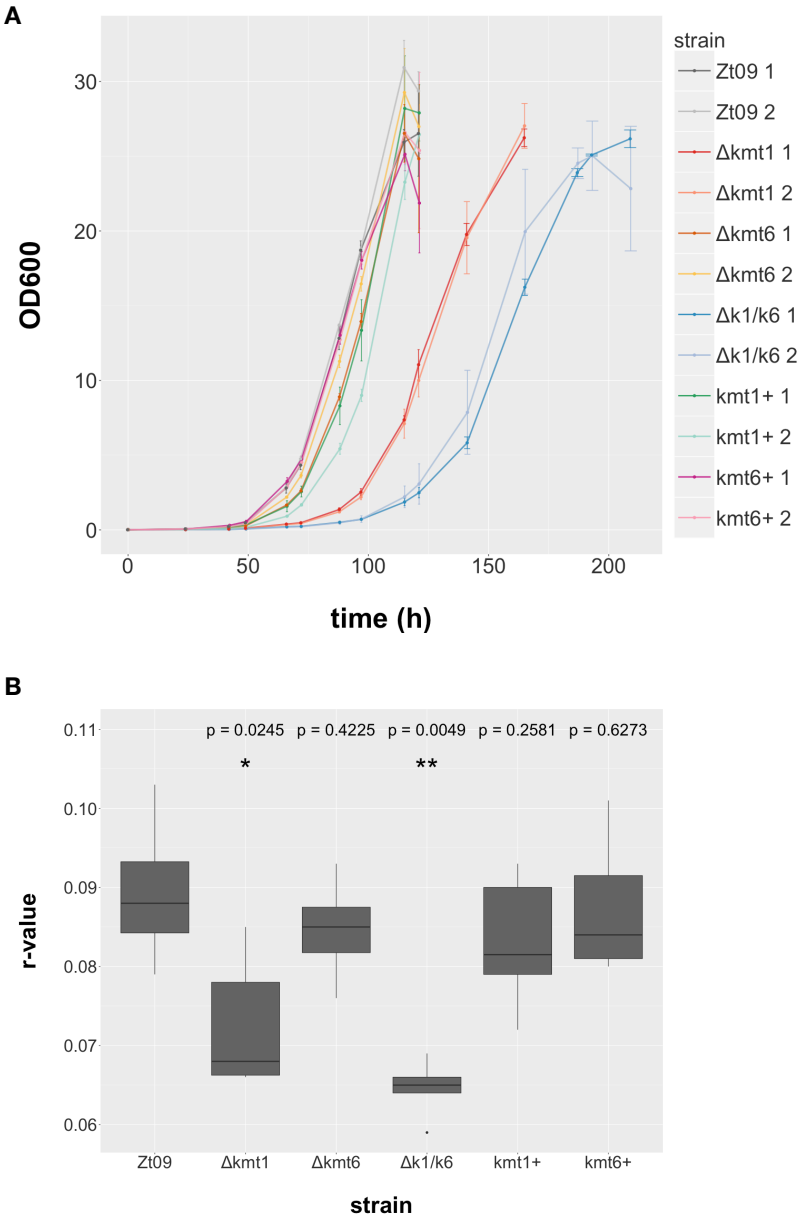

Figure S3. Growth assay to compare *in vitro* fitness of mutant strains to Zt09. All strains were grown in liquid YMS medium at 18°C and the OD_{600} was measured until the stationary phase was reached **(A)**. For each strain, two biological replicates were grown in technical triplicates each. The growth of *Δkmt1* and *Δk1/6* mutants was impaired compared to Zt09 and *Δkmt6* but could be restored in the respective complementation strains. **(B)** We used the R package growthcurver (Sprouffske & Wagner, 2016) to calculate r-values for each growth curve. The values for *Δkmt1* and *Δk1/6* were significantly lower compared to Zt09, but not in the complementation strains and *Δkmt6*.

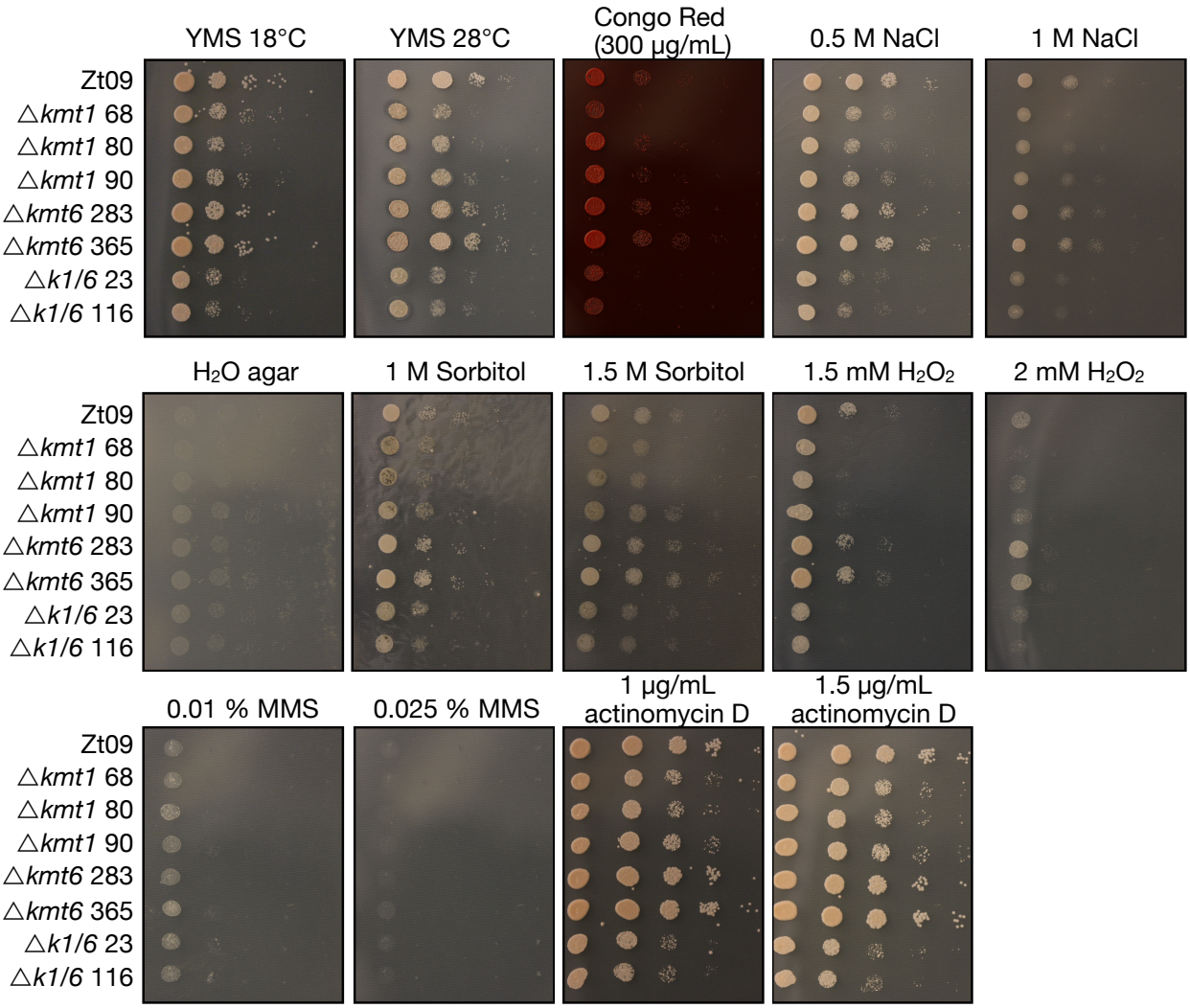

Figure S4. Assay to compare tolerance of Zt09 and mutants to different stress conditions including osmotic stress (NaCl and Sorbitol), oxidative stress (H_2O_2), genotoxic stress (MMS, actinomycin D), temperature stress (28°C), cell wall stress (Congo Red), and nutrient starvation (H_2O agar). We observed almost no differences between Zt09 and *Δkmt6* strains, whereas *Δkmt1* and *Δk1/6* mutants displayed decreased growth, as observed in the growth rate comparison.

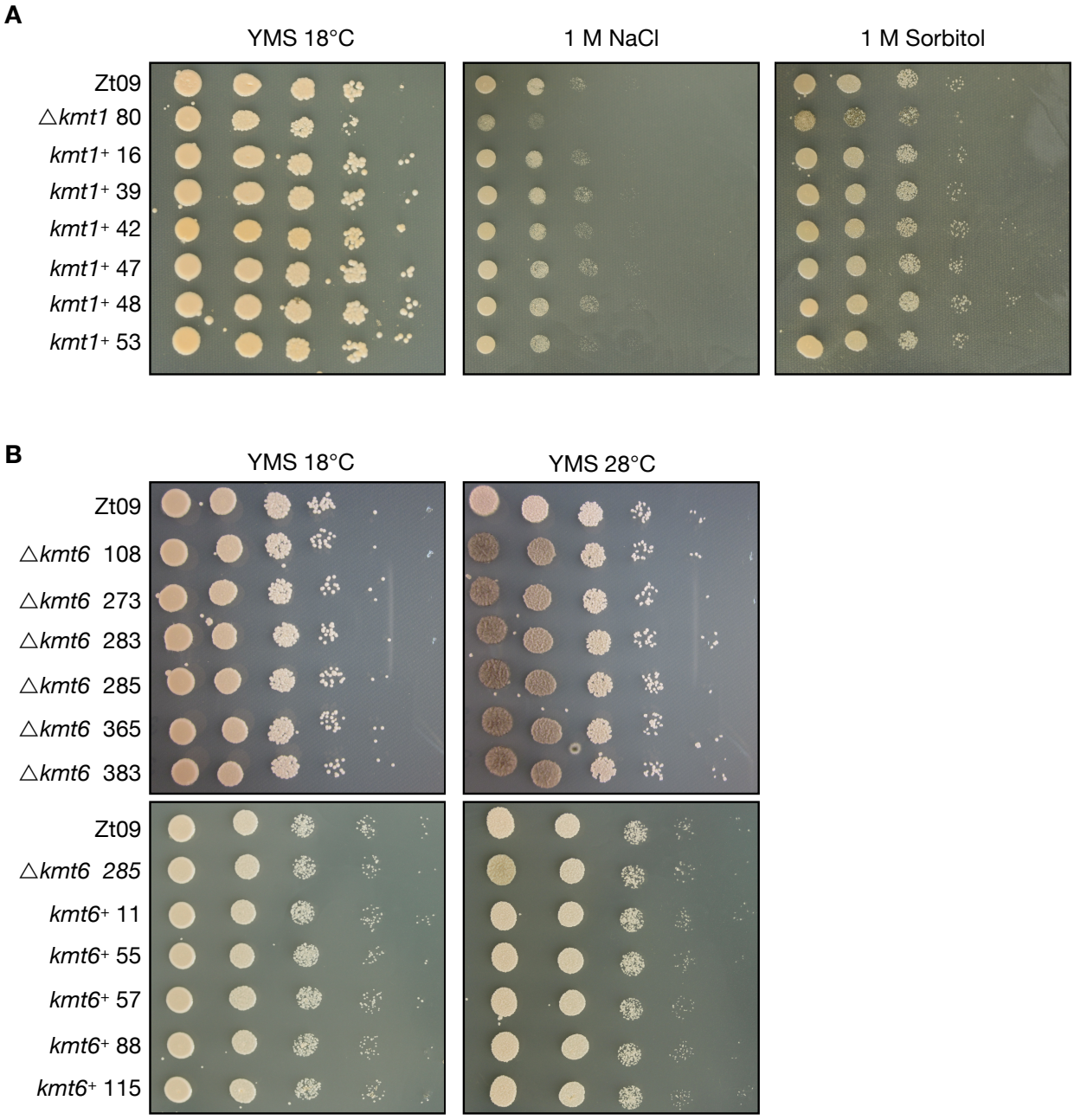

Figure S5. Stress assay to compare growth of deletion and respective complementation strains. (A) The *Δkmt1* mutants showed overall decreased growth and were particularly sensitive to osmotic stress. These phenotypes could be restored in the complementation strains. **(B)** Increased melanization at high temperatures, observed in the *Δkmt6* mutants, was also reversed in the respective complementation strains.

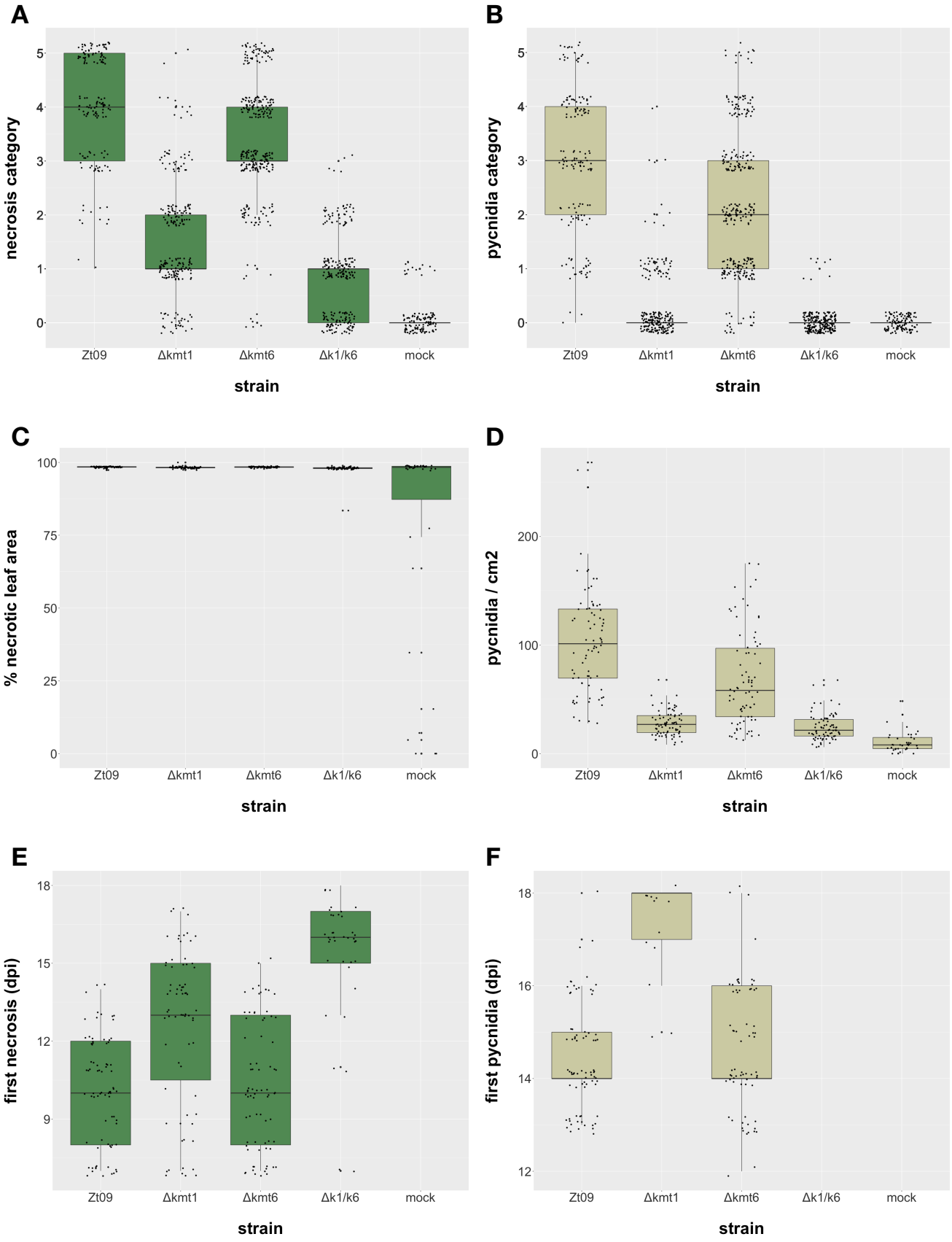
A
necrosis category
0
1
2
3
4
5
Zt09
Δkmt1
Δkmt6
Δk1/k6
mock
strain
B
pycnidia category
0
1
2
3
4
5
Zt09
Δkmt1
Δkmt6
Δk1/k6
mock
strain
C
% necrotic leaf area
0
25
50
75
100
Zt09
Δkmt1
Δkmt6
Δk1/k6
mock
strain
D
pycnidia / cm2
0
100
200
Zt09
Δkmt1
Δkmt6
Δk1/k6
mock
strain
E
first necrosis (dpi)
9
12
15
18
Zt09
Δkmt1
Δkmt6
Δk1/k6
mock
strain
F
first pycnidia (dpi)
12
14
16
18
Zt09
Δkmt1
Δkmt6
Δk1/k6
mock
strain

Figure S6. Plant infection phenotypes of Zt09 and mutant strains. Symptoms in form of necrotic lesions and pycnidia were quantified after 21 days of infection either manually **(A)** and **(B)** or by automated image analysis of infected leaves **(C)** and **(D)**. Furthermore, first appearance of symptoms was documented by daily screening of inoculated leaves **(E)** and **(F)**. Virulence of both, *Δkmt1* and *Δk1/6* strains was highly impaired. Symptoms of *Δkmt6* strains were slightly reduced compared to Zt09.

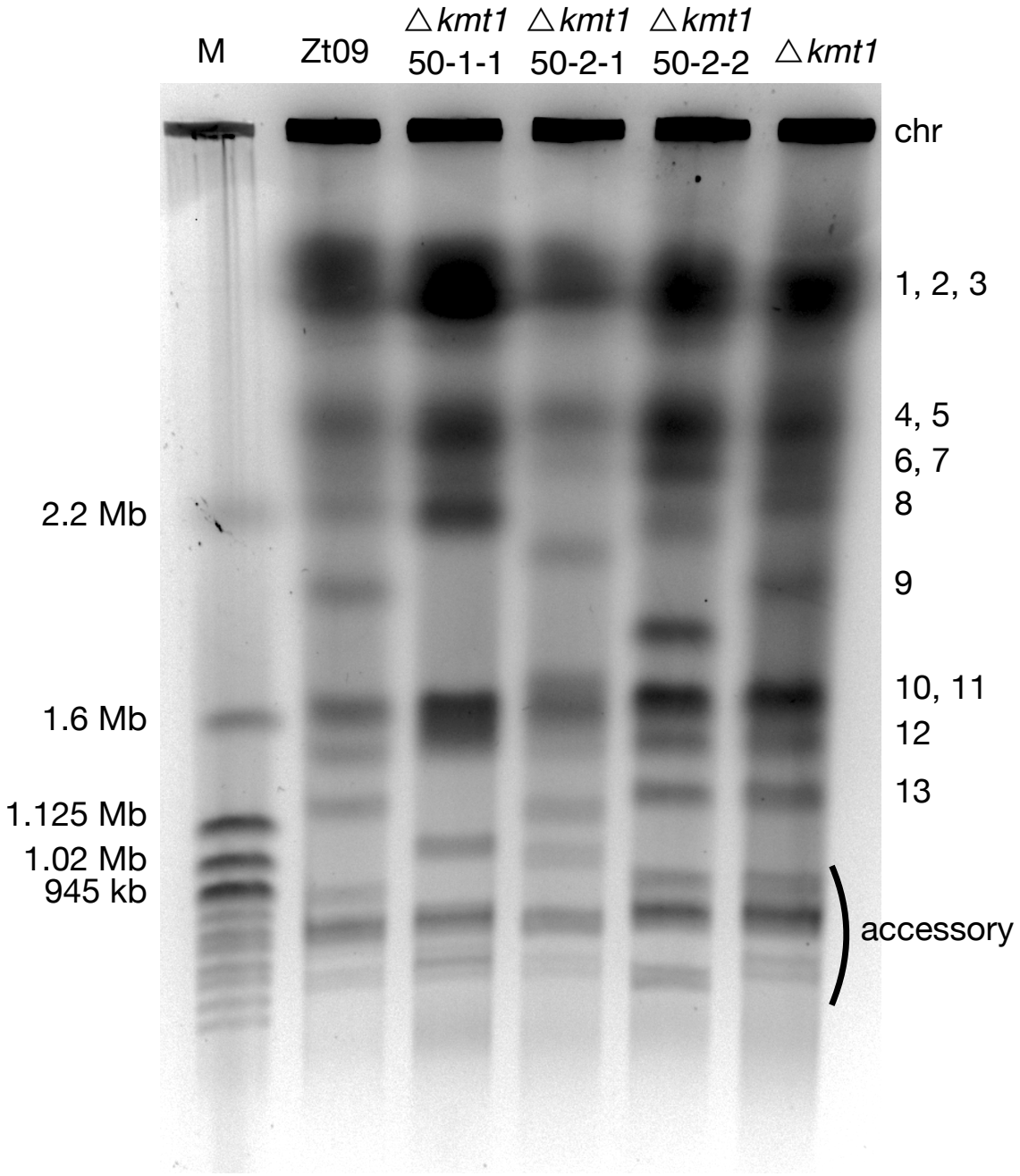

Figure S7. Pulsed-field gel electrophoresis of mid-size chromosomes of Zt09 and *Δkmt1* progenitor strains and the three single *Δkmt1* clones originating from the evolved populations after 50 transfers. While there are no visible differences between the progenitor strains, all three single *Δkmt1* clones exhibit different karyotypes. Chromosome size marker (M): *Saccharomyces cerevisiae*.

Chapter IV

DNA methylation varies in *Zymoseptoria* species

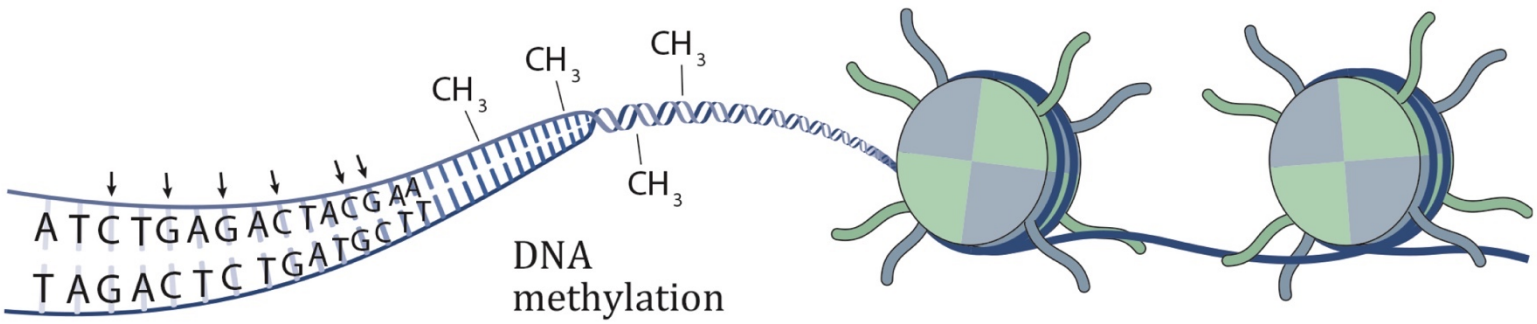

Repeat-**I**nduced
Point mutations

Title picture is modified from
Möller & Stukenbrock 2017,
“Evolution and genome architecture in fungal plant pathogens”
Nature Reviews Microbiology

Chapter IV

DNA methylation varies in *Zymoseptoria* species

Mareike Möller[1,2], Kathrin Happ[1,2], Maja Stralucke[1,2], Michael Freitag[3], and Eva H. Stukenbrock[1,2]

[1]Environmental Genomics, Christian-Albrechts University, Am Botanischen Garten 1-9, D-24118 Kiel, Germany

[2]Max Planck Institute for Evolutionary Biology, August-Thienemann-Str. 2, D-24306 Plön, Germany

[3]Department of Biochemistry and Biophysics, Oregon State University, Corvallis, OR 97331-7305, United States of America

Abstract

Methylation of DNA is an important component of epigenetic regulation and found throughout all forms of life ranging from prokaryotes to mammals. However, the extent and function of DNA methylation differ between taxa. DNA methylation in fungi has mainly been characterized in the model species *Neurospora crassa* where it is associated to sequences targeted by the genome defense mechanism repeat-induced point mutation (RIP). Previous studies in the plant pathogenic fungus *Zymoseptoria tritici* report absence of DNA methylation in the reference strain IPO323 due to inactivation of the DNA methyltransferase gene *Ztdim2* by RIP. In this study, we demonstrate that *Ztdim2* however is functional in other strains of *Z. tritici*. The presence of a functional of *Ztdim2* in these strains correlates with widespread DNA methylation. Furthermore, we discovered a second DNA methyltransferase, *ZtdmtA*, in all *Z. tritici* strains that is putatively involved in the maintenance of DNA methylation, but also shows high sequence diversity within the *Zymoseptoria* species complex. We present evidence for the presence of small amounts of DNA methylation, even in the strains containing an inactive *Ztdim2* gene suggesting that DNA methylation could be maintained in conserved regions by the alternative DNA methyltransferase, *ZtdmtA,* over time. Integration of a functional *Ztdim2* variant in IPO323 restores DNA methylation in previously non-methylated regions indicating *de novo* methylation activity. Deletion of the functional *Ztdim2* in another *Z.*

tritici isolate does not result in loss of DNA methylation in those regions. Taken together, our results indicate that the loss of a putative *de novo* methyltransferase, *Ztdim2*, resulted in highly reduced overall DNA methylation, but not complete elimination of DNA methylation likely due to the presence of a maintenance DNA methyltransferase protein that is highly diverse in different *Z. tritici* strains and closely related sister species.

Introduction

DNA methylation is an important factor of epigenetic regulation and related functions range from dynamic control of gene expression to transposon silencing and the maintenance of genome integrity (Slotkin & Martienssen, 2007; Jones, 2012). DNA methylation has been detected on cytosines and adenines in eukaryotes, while cytosine methylation has been the focus of most studies so far. In mammals, cytosine methylation is mainly found in CpG (cytosine followed by guanine) contexts. In plants and fungi also non-CpG methylation is commonly detected (Martienssen, 2001). Different DNA methyltransferases (DNMTs) are involved in the establishment and maintenance of DNA methylation but the presence and number of enzymes involved is highly variable in different species (Lyko, 2018). In mammals, enzymes in the group of DNMT1 are classified as maintenance methyltransferases that detect hemi-methylated DNA sequences, for example after replication, when only one of the two DNA strands is methylated, and methylate the respective cytosine of the newly synthesized strand. *De novo* methyltransferases can act on sequences that were not methylated before presumably by recognition of specific motifs or patterns. Although DNMTs are classified in maintenance or *de novo* transferases their function is not necessarily limited to one or the other but can be rather dynamic (Jeltsch & Jurkowska, 2014).

In fungi, several DNMTs have been identified that do not directly fall within the categories found in mammals. In *Neurospora crassa,* DNA methylation is mediated by a single enzyme, DIM2 (Kouzminova & Selker, 2001). This enzyme shows sequence homology to other DNMT1 maintenance methyltransferases, however it is likely a fungal specific DNMT (Goll & Bestor, 2005). A second putative DNA methyltransferase, RID, was detected in *N. crassa* (Freitag *et al.*, 2002) with homology to enzymes in other fungi such as *Aspergillus nidulans* (DmtA) (Lee *et al.*, 2008) and *Ascobolus immersus* (Masc1) (Malagnac *et al.*, 1997). Interestingly, despite the presence of a putative DNA methyltransferase, no clear evidence for the presence of DNA methylation was found in *A. nidulans*. RID in *N. crassa* and Masc1 in *A. immersus* are part of the genome defense mechanisms RIP (repeat-

induced point mutation) and MIP (methylation-induced premeiotically) acting against the integration of repeated DNA (Selker & Stevens, 1985).

In a previous study, a transposon-associated amplification of the DNA methyltransferase gene *Ztdim2*, a homolog of *N. crassa dim2*, and subsequent inactivation by RIP was reported in the *Zymoseptoria tritici* reference isolate IPO323 (Dhillon *et al.*, 2010; Goodwin *et al.*, 2011). This resulted in a total of 23 copies of *Ztdim2* carrying signatures of RIP. As a consequence, no cytosine methylation could be detected in the *Z. tritici* reference isolate and amplification of *Ztdim2* was found in 15 additional studied isolates. However, a single intact *dim2* gene, as well as cytosine methylation, is present in the sister species *Zymoseptoria ardabiliae* and *Zymoseptoria pseudotritici* (Dhillon *et al.*, 2010). The loss of cytosine methylation therefore must have occurred only recently after speciation (~ 11000 years ago) as the closely related sister species of *Z. tritici* contain an intact *dim2* gene.

Goal of this study is to address the evolution and function of the *Ztdim2* gene in the *Zymoseptoria* species complex. We report the presence of an intact and functional *Ztdim2* in other *Z. tritici* isolates despite transposon-associated amplification and RIP-mediated mutation of additional copies in all analyzed isolates. We furthermore find evidence that DNA methylation is not absent in *Z. tritici*, even if ZtDim2 is not functional. This is likely due to the presence of a second, highly variable, DNA methyltransferase that shows homology to the previously identified putative DNMTs RID, MascI and DmtA (Malagnac *et al.*, 1997; Freitag *et al.*, 2002; Lee *et al.*, 2008). We propose that ZtDim2 is a *de novo* transferase, as integration of a non-mutated, intact *Ztdim2* in a *Ztdim2*-RIPed background promotes methylation of previously non-methylated regions. Further, ZtDmta might function as a maintenance DNMT that preserves DNA methylation in *Ztdim2* RIP mutated strains.

Results

The DNA methyltransferase gene *Ztdim2* is not inactivated in several *Z. tritici* isolates

We addressed evolution of the *Ztdim2* locus and conducted a detailed comparison of the genomic region encoding the gene in *Zymoseptoria tritici* strains and the genomes of the sister species *Z. ardabiliae* and *Zymoseptoria brevis*. We used a BLAST approach to search for the sequence of *Ztdim2* in 35 genomes of *Z. tritici*, 17 genomes of *Z. ardabiliae* and 9 genomes of *Z. brevis* (Table S1). We detected a single *Ztdim2* homolog in each *Z. ardabiliae* and *Z. brevis* strain, while we found multiple copies of RIPed *Ztdim2* genes in 32 out of 35 *Z. tritici* genomes. However, three strains contained an intact non-mutated copy of *Ztdim2*. Two of the three strains that were isolated in Iran (Zt10) and in Australia (WA329) (Stukenbrock *et al.*, 2011; McDonald *et al.*, 2016) carry multiple additional RIPed *Ztdim2* copies. The genome assembly of another Iranian isolate Zt11 only contained the intact *Ztdim2.* Presumably, further copies are also present in Zt11, but due to the repetitive structure of the RIPed genes not detectable in the Illumina short read-based genome assembly (Stukenbrock *et al.*, 2012a). The presumably intact copy of the strain WA329 was not completely assembled but split on two very small contigs. We therefore focused on the two Iranian strains for our further analyses.

In the previous study by Dhillon and colleagues, a non-telomeric sequence of *Ztdim2* on chromosome 6 was identified as the original gene locus, while all additional copies were located in repetitive subtelomeric regions (Dhillon *et al.*, 2010). We aligned the intact Zt*dim2* genes of the two Iranian strains and the inactivated, non-telomeric copy of the reference strain IPO323 including their respective flanking regions to evaluate if the genes are located at the same genomic position (Figure 1). While the regions flanking the gene are conserved between all three strains, the *Ztdim2* open reading frame (ORF) is heavily mutated due to numerous G/C to A/T transitions in IPO323 reflected by an elevated AT content in this region. This indicates that the original *Ztdim2* is indeed present and not mutated in the Iranian isolates Zt10 and Zt11.

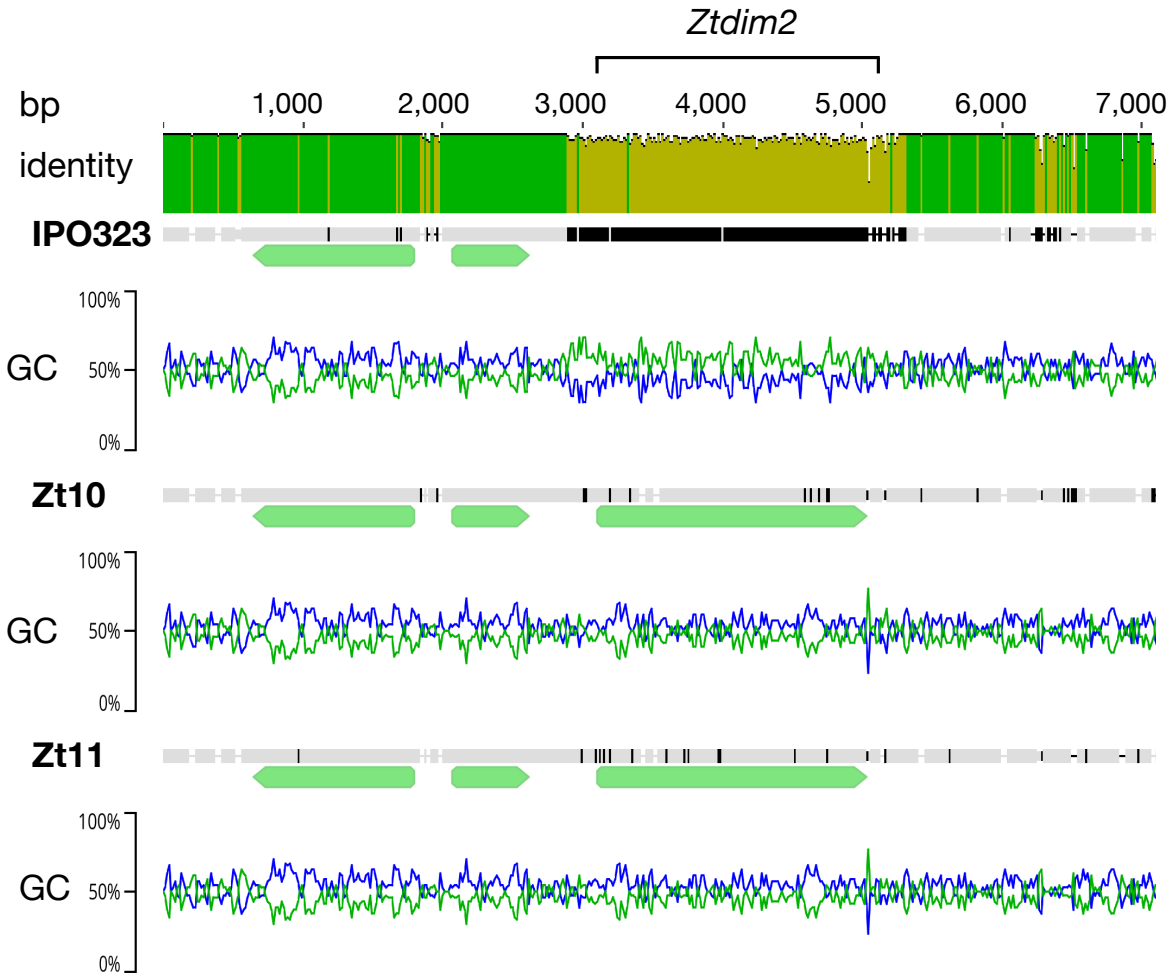

Figure 1. Alignment of the non-telomeric *Ztdim2* in IPO323 and the two intact *Ztdim2* sequences of the Iranian strains Zt10 and Zt11. The gene-flanking regions are highly conserved, however there is no open reading frame detectable anymore in IPO323 because of numerous G/C -> A/T mutations. The average GC content is therefore lower in IPO323 compared to Zt10 and Zt11 in this region. Percentage of AT is shown as green lines, percentage of GC as blue lines. 100 % identity between the sequences is shown as green bars, greeny-brown bars indicate 30 – less than 100 % identity.

DNA methylation is detectable if *Ztdim2* is intact

The presence of a non-RIPed *Ztdim2* gene does not necessarily result in the presence of DNA methylation. To test if DNA methylation is present in the Iranian isolates carrying the intact *Ztdim2*, we performed DNA restriction analyses using DNA methylation sensitive restriction enzymes. Genomic DNA of Zt10 and Zt11 was restricted either with an cytosine methylation sensitive (*BfuCI*, inhibited by cytosine methylation) or insensitive enzyme (*DpnII*, not inhibited by cytosine methylation). Both enzymes cut at the same sequence and hence, observation of different restriction patterns of the two enzymes

indicates the presence of DNA methylation. In addition to the two cytosine methylation sensitive or insensitive enzymes, we used *DpnI* to test for the presence of adenine methylation that was recently discovered in other eukaryotes (Greer *et al.*, 2015; Zhang *et al.*, 2015; Chen *et al.*, 2017). However, we did not find indications for the presence of 6mA methylation in *Z. tritici*. We used two different probes that are likely to be methylated if DNA methylation is present: a highly abundant transposable element (retrotransposon RIL2, Figure 2B) and the rDNA spacer region (Figure 2A). For all experiments we used the *Z. tritici* isolate Zt09, a derivative of the reference isolate IPO323 that has lost chromosome 18 during *in vitro* growth (Goodwin *et al.*, 2011; Kellner *et al.*, 2014) as *Ztdim2*-RIPed strain.

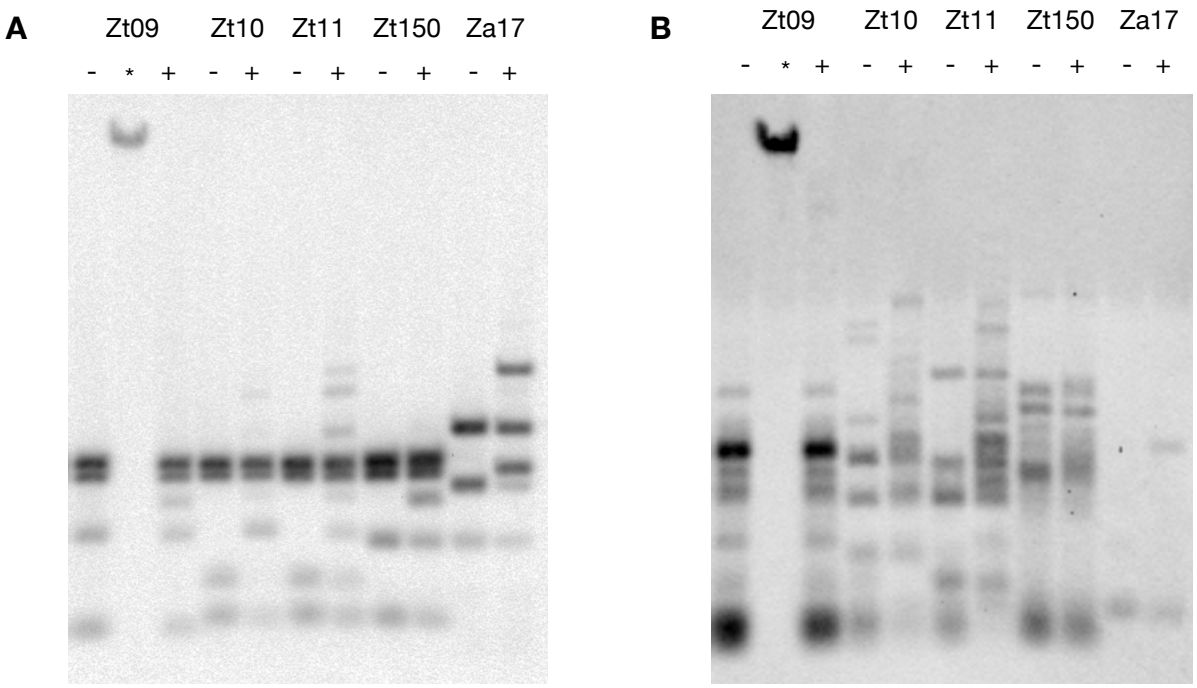

Figure 2. Restriction enzyme analysis followed by Southern blots using the rDNA spacer (A) or a retrotransposon RIL2 (B) as probes. In addition to the cytosine methylation sensitive (*BfuCI*, **+**) or insensitive (*DpnII*, **-**) enzymes, we used *DpnI* (*****) to test for the presence of adenine methylation. Zt09 and Zt150 contain the inactivated *Ztdim2* gene, whereas the Iranian strains Zt10, Zt11 and the *Z. ardabiliae* strain Za17 have an intact copy. In all strains, where *Ztdim2* is not mutated, we see a clear difference between the restrictions with *BfuCI* and *DpnII*, indicating the presence of DNA methylation. In Zt09 and Zt150 this difference is not detectable except for one band that is not restricted in both strains in the rDNA blot. The genomic DNA of Zt09 treated with *DpnI* is not restricted at all suggesting absence of 6mA methylation.

Based on the restriction analyses, DNA methylation is present in both Iranian strains Zt10 and Zt11 as well as in the sister species *Z. ardabiliae*. Zt09 and Zt150 (strain collected in Germany that contains only RIPed *Ztdim2* copies, Table S1) do not show different restriction patterns similar to those seen in Zt10 or Zt11. However, there is an observable difference in the restriction pattern of both isolates in the rDNA restriction blot (Figure 2A) suggesting the presence of putatively rare DNA methylation.

DNA methylation is present, even if *Ztdim2* is not functional

The restriction pattern of the rDNA spacer region suggested the presence of some DNA methylation even in those strains where *Ztdim2* is not functional anymore. To further validate if DNA methylation is indeed present in these strains, we conducted bisulfite sequencing of the rDNA spacer regions of Zt09 and Zt10. Analysis of the ~ 600 bp region revealed the presence of cytosine methylation in both strains (Figure 3). DNA methylation was exclusively found in an CpG context in Zt09, whereas cytosine methylation in Zt10 was not restricted to CpG dinucleotides. Although further genome-wide analyses of DNA methylation will be necessary to confirm patterns of DNA methylation in these two strains, the sequencing results combined with the restriction analyses strongly indicate that DNA methylation is still present in Zt09 and likely in other *Z. tritici* strains, where *Ztdim2* was inactivated by RIP. However, the amount of DNA methylation seems to be reduced compared to the strains that contain a functional *Ztdim2*.

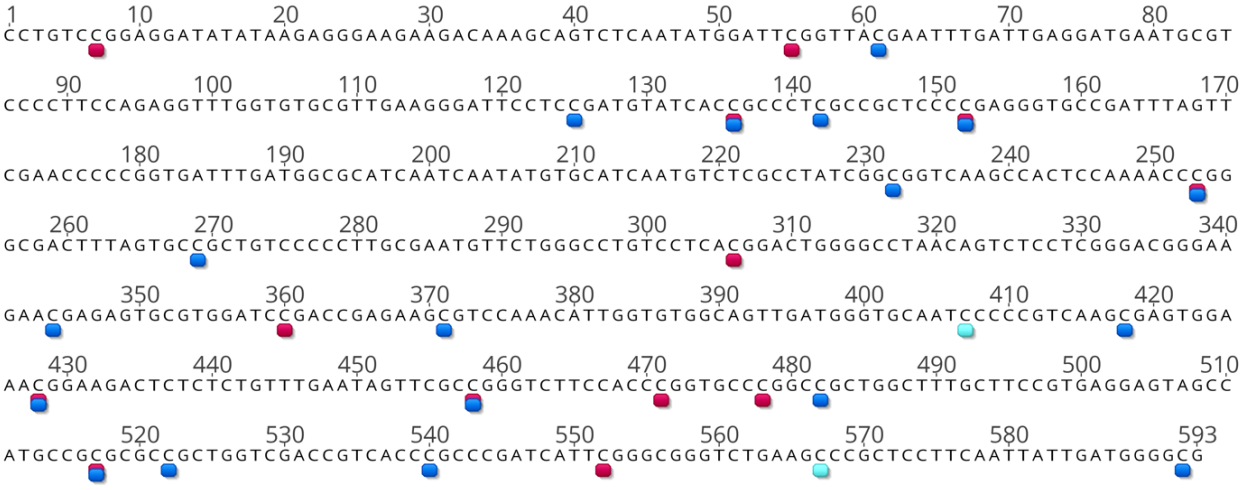

Figure 3. 600 bp sequence of the rDNA spacer of Zt09 and Zt10 and methylated cytosines detected by bisulfite sequencing. Highlighted are the detected methylated cytosines in Zt09 (red) and Zt10 (blue). While all methylated cytosines in Zt09 are positioned next to a guanine, we also found non-CpG methylated cytosines in Zt10 (light blue).

DNA methylation can be restored in *Z. tritici* isolates by reintegration of an intact *Ztdim2* ORF

Our restriction analysis and the bisulfite sequencing indicate that DNA methylation is not completely absent in *Z. tritici,* however, in the rDNA spacer sequence and RIL2 transposon sequences we show that it is more frequent in those strains that contain the functional DNA methyltransferase encoding gene *Ztdim2*. To assess the role of *Ztdim2* for DNA methylation in *Z. tritici* we generated mutants in which we either deleted or restored *Ztdim2*. We integrated the functional *Ztdim2* gene of Zt10, together with a hygromycin resistance cassette, into the genome of Zt09 (Zt09::*Ztdim2*). The integration was at the native locus of *Ztdim2* on chromosome 6. In Zt10, we replaced the functional *Ztdim2* gene with a hygromycin resistance cassette resulting in the deletion of *Ztdim2* (Zt10Δ*Ztdim2*). Integration and deletion strains were verified by Southern blots (Figure S1). To validate changes in DNA methylation between reference and respective mutant strains, we repeated the restriction analyses as described above (Figure 3). In this experiment we used the sequence of the transposable element RIL2 as a probe in the Southern blot as there appeared to be no DNA methylation in Zt09 in this region. This time, we observed an obvious difference in the restriction patterns generated by methylation sensitive and insensitive enzymes in the Zt09::*Ztdim2* strains that is not present in the Zt09 reference without a functional *Ztdim2*. This suggests that the integration of the functional *Ztdim2* gene restored DNA methylation to a similar extent as previously observed in Zt10. However, the deletion of *Ztdim2* in Zt10 did not lead to an altered restriction pattern. Based on these and the above-mentioned findings, we hypothesize that *Ztdim2* is not the only DNA methyltransferase that is present and functional in the genome of *Z. tritici*.

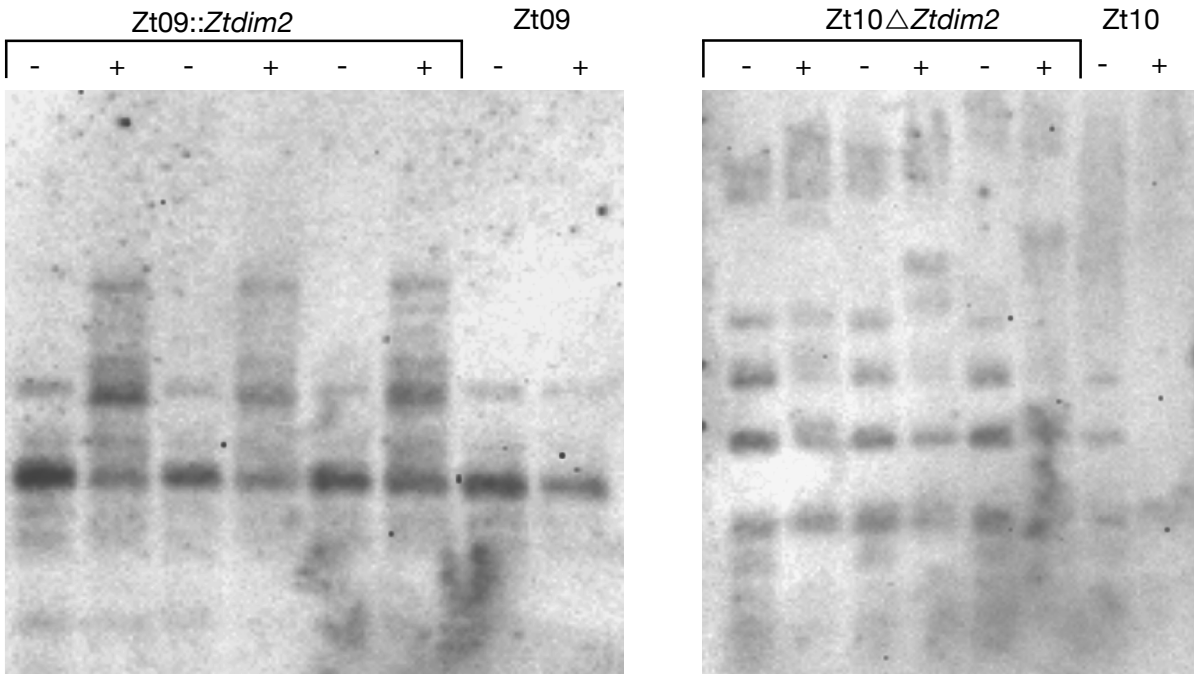

Figure 4. DNA restriction analyses to evaluate presence/absence of DNA methylation in the strains, where the functional *Ztdim2* was integrated (Zt09::*Ztdim2*) and where *Ztdim2* was deleted (Zt10Δ*Ztdim2*). In clones of the *Ztdim2* integration strain, there are differences between restrictions by *BfuCI* (**+**) and *DpnII* (**-**), whereas this difference is not visible in the reference Zt09. The Zt10Δ*Ztdim2* mutants show variable patterns between the restrictions, therefore the absence of DNA methylation cannot be confirmed in these strains. The signal of the Zt10 wild type reference strain is very weak and can therefore not be compared to the mutant strains.

A second highly diverse DNA methyltransferase gene is present in all *Zymoseptoria* genomes

The occurrence of DNA methylation in Zt10 despite the deletion of *Ztdim2* as well as the occurrence of some DNA methylation in Zt09 suggests the presence of an additional DNA methyltransferase in *Z. tritici*. We therefore searched for putative DNA methyltransferases in the genomes of *Z. tritici*, *Z. ardabiliae* and *Z. brevis* using the DNA methyltransferase domain of the ZtDim2 protein as query for a protein BLAST search. In all genomes, we found a second predicted DNA methyltransferase. However, we excluded five *Z. ardabiliae* strains where the gene was not completely assembled and split on different contigs. The protein shows homology to the previously described putative DNA methyltransferases RID, Masc1 and DmtA (Malagnac *et al.*, 1997; Freitag *et al.*, 2002; Lee *et al.*, 2008) and we therefore named it ZtDmtA. The gene is located on chromosome 5 of the *Z. tritici* reference isolate. In the current annotation (Grandaubert *et al.*, 2015), *ZtdmtA*

is part of a predicted open reading frame (*Zt_chr_5_00047*) that however very likely contains two separate genes. The annotated gene consists of two separate open reading frames connected via a predicted intron. However, one of the ORFs displays very high expression, while the putative *ZtdmtA* gene shows very little expression *in vitro* (Möller *et al.*, 2018) (Figure S2). While the identified homologs in the different strains are all predicted C-5 cytosine methyltransferases, their sequences are highly diverse. We found three distinct alleles: A, B and C, whereas allele C is only present in one strain, Zt04. This strain was sampled in Denmark together with strains Zt02, Zt05 and Zt07 that all contain another allele: A. Interestingly, these different alleles are not just present within *Z. tritici*, but also in *Z. ardabiliae* (Za) and *Z. brevis* (Zb) (Figure 5A). The gene length varies between ~ 2100 to 2300 bp in the different strains and the number of SNPs found between the different alleles is as high as ~ 900 to 1000 resulting in almost 50 % variable sites. This results in highly different amino acid sequences of the translated protein (Figure 5B) but based on functional analysis using InterPro (Finn *et al.*, 2017) the predicted function remains identical (Figure S2). However, the genomic location of these alleles seems to be conserved.

We next aligned the *ZtdmtA* sequences and flanking regions of *Z. tritici* strains with the three different allele groups to determine if the genomic location is conserved. We found the flanking regions to be conserved whereas, as expected, the *ZtdmtA* gene body was highly variable. Variability of *ZtdmtA* does not correlate with the presence of an intact *Ztdim2* in *Z. tritici* as strains with nonfunctional and functional *Ztdim2* genes share the same alleles (Table S1). Our previous results showing that DNA methylation is still present in the Zt10Δ*Ztdim2* strains as well as in Zt09 indicates that *ZtdmtA* is functional and contributes to DNA methylation, either by *de novo* DNA methylation or by maintenance of DNA methylation. Since DNA methylation is likely very limited in those strains that do not have a functional *Ztdim2* and seems to increase when a functional *Ztdim2* is integrated, we hypothesize that ZtDmtA might function as a maintenance DNA methyltransferase whereas ZtDim2 generates *de novo* DNA methylation. However, cytosine methylation activity of any of the known homologs in *Neurospora*, *Ascobolus* or *Aspergillus* has not been shown, and has to be further validated experimentally in *Z. tritici*.

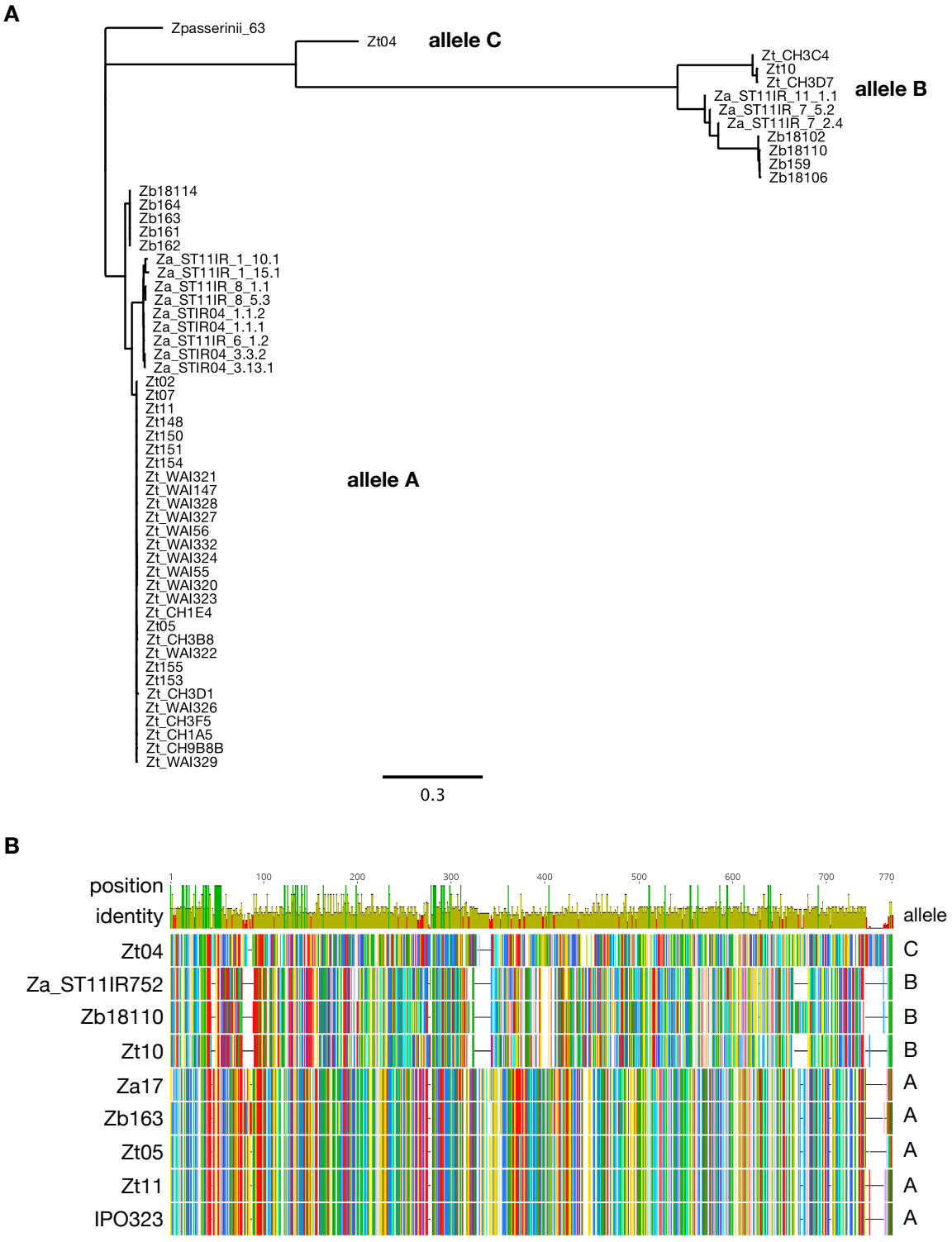

Figure 5. High variability of DmtA proteins in different *Zymoseptoria* species. (A) Tree generated based on alignments of all identified *dmtA* sequence translations. *Zymoseptoria passerinii* (SP63) was used as an outgroup. The most abundant allele A was found in 31 out of 35 *Z. tritici* strains, nine out of twelve *Z. ardabiliae* strains and in five out of nine *Z. brevis* strains. Allele B was detected in three *Z. tritici* and *Z. ardabiliae* isolates and four *Z. brevis* isolates. Allele C was only found in one strain, Zt04. **(B)** Protein alignments of representatives of the different alleles. Although length, function and

location are conserved, the amino acid sequence between the different alleles is highly diverse. The variability within alleles, even in different species, is rather low (100 % identity between the sequences is shown as green bars, greeny-brown indicates 30 – less than 100 % identity, red indicates less than 30 % identity).

Ztdim2 has little impact on disease development *in planta*

The contribution of DNA methylation to normal development and virulence has been studied in various fungi including *Magnaporthe oryzae* (Ikeda *et al.*, 2013; Jeon *et al.*, 2015) and *Aspergillus flavus* (Yang *et al.*, 2016). We here aimed to elucidate the role DNA methylation in the life cycle of *Z. tritici*. To this end we assessed the fitness of the *Z. tritici* methyltransferase mutants in comparison to wild type during plant infection and asexual sporulation. *Z. tritici* is a hemibiotroph pathogen infecting the mesophyll tissue of wheat leaves resulting in necrotic lesions and the formation of asexual (pycnidia) and sexual (pseudothecia) fruiting bodies (Ponomarenko *et al.*, 2011). We infected 30 leaves of the susceptible wheat cultivar Obelisk per strain using two biological replicates for each mutant. After 23 days, the leaves were harvested, and the infection symptoms were scored manually to evaluate the extent of necrosis and pycnidia density on the infected leaves.

Infection symptoms of Zt10 were in general reduced compared to Zt09 but deletion of *Ztdim2* did not have a significant impact on necrosis or pycnidia formation (Figure 6). Integration of *Ztdim2* in Zt09 significantly reduced the necrotic area (Wilcoxon-rank-sum test, *P*-value = 2.4×10^{-5}) but did not have significant effects on pycnidia formation. We therefore conclude that under the tested conditions, DNA methylation has little impact on the ability of *Z. tritici* to infect its host. Nevertheless, further tests, including deletion mutants for the second DNA methyltransferase gene *ZtdmtA*, have to be carried out to determine possible functions of DNA methylation in *Z. tritici*.

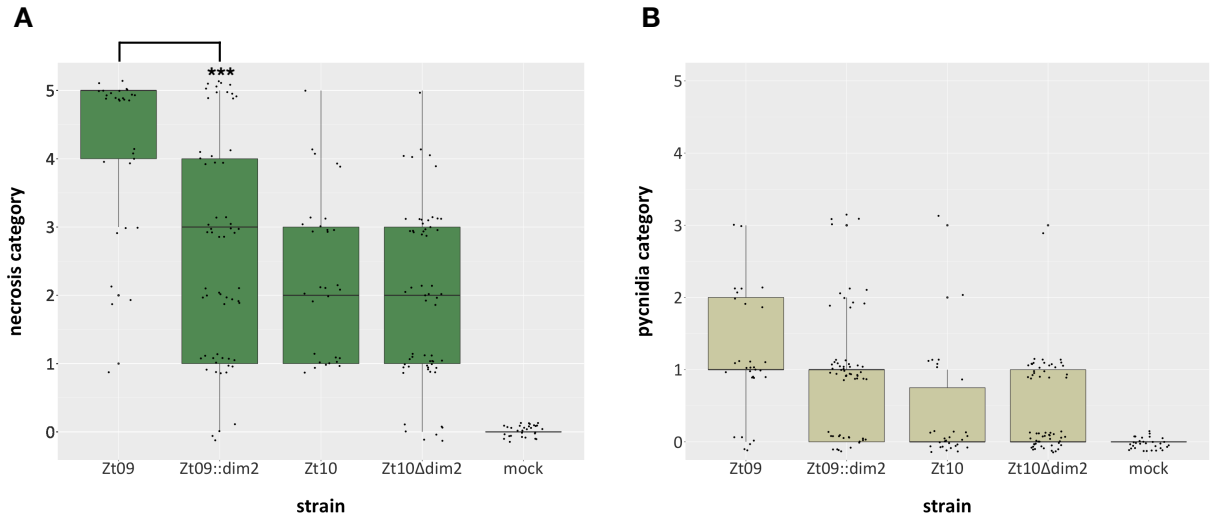

Figure 6. Results of wheat infection experiments with *Z. tritici* Zt09, Zt10 and the mutant strains with integrated *Ztdim2* (Zt09::*Ztdim2*) and deleted *Ztdim2* (Zt10Δ*Ztdim2*) on wheat. *Zt09::Ztdim2* strains show significantly less necrotic lesions compared to Zt09 (*** Wilcoxon-rank-sum test, *P*-value = $2.4x10^{-5}$) **(A)** while there is no difference in the quantities of necrotic lesions caused by Zt10 and Zt10Δ*Ztdim2* strains. **(B)** Coverage with pycnidia is similar between both reference and mutant strains and does not show any significant differences. Categories for necrotic lesion and pycnidia coverage: 0 = 0 %, 1 = 1-20 %, 2 = 21-40 %, 3 = 41-60%, 4 = 61-80%, 5 = 81-100%.

Discussion

Although it has been reported that cytosine methylation is absent in *Z. tritici* (Dhillon *et al.*, 2010), we found evidence that 1) DNA methylation is not completely absent in *Z. tritici*, even if the methyltransferase ZtDim2 is absent and that 2) some strains contain an intact and functional *Ztdim2* gene.

The majority of analyzed *Z. tritici* strains did not contain a functional *Ztdim2* gene whereas it was present in all analyzed *Z. brevis* and *Z. ardabiliae* strains suggesting that the inactivation of *Ztdim2* only occurred in *Z. tritici*. The two strains in which we could clearly identify non-RIPed *Ztdim2* genes were both collected in Iran. Iran lies within the Fertile Crescent, where both, domestication of wheat and speciation of *Z. tritici* took place (Stukenbrock *et al.*, 2011). The closely related sister species *Z. ardabiliae* and *Z. brevis* were all collected in Iran as well and are so far considered to be endemic to this region (Quaedvlieg *et al.*, 2011; Stukenbrock *et al.*, 2012b). We hypothesize that transposon-associated amplification and subsequent RIP-mediated inactivation of *Ztdim2* occurred

early after speciation and that either RIP was prevented in the original *Ztdim2* copy in the Iranian *Z. tritici* isolates or these isolates obtained functional copies by introgression from sister species. A recent study on mating type chromosomes of *Neurospora tetrasperma* suggests introgression as a mechanism to regenerate regions that are subject of increased degeneration (Corcoran *et al.*, 2016) and several examples of recent introgressions linked to increased fitness were reported in fungi (Gladieux *et al.*, 2014). To test if an intact *Ztdim2* allele could have been acquired by introgression in Iranian isolates of *Z. tritici*, an analysis of the distribution of functional *Ztdim2* in a widespread collection of Iranian strains has to be carried out.

Our analyses of the other methyltransferase gene *ZtdmtA* supports an importance of introgression in the evolution of *Z. tritici* and the variation in DNA methylation among natural isolates. We here show high diversity in the gene sequence and in the distribution of alleles of the second cytosine DNA methyltransferase gene, *ZtdmtA*, in *Z. tritici* as well as in other *Zymoseptoria* species. We found three highly divergent allele groups of *ZtdmtA*, for which the diversity within an allele group was comparably low, but the diversity between allele groups was extremely high. Except for allele C that was only found in one *Z. tritici* isolate (Figure 5A), the *ZtdmtA* alleles were not species specific as each allele was detected in every *Zymoseptoria* species. This further supports the hypothesis that introgression between multiple members of the *Zymoseptoria* species complex occurs frequently (Feurtey et al., in prep). Genome-wide population genetic analyses have to be performed to elucidate the extent of potential introgression in the *Zymoseptoria* species complex.

Cytosine methylation is not absent in *Z. tritici*, despite the inactivation of *Ztdim2*. The conserved rDNA spacer sequence, but not a widespread transposable element, was methylated based on restriction analyses and bisulfite sequencing in strains without an intact *Ztdim2*. We hypothesize that cytosine methylation has been maintained by the second DNA methyltransferase, ZtDmtA, after loss of function of ZtDim2. ZtDmtA hereby acts as a maintenance methyltransferase but does not add *de novo* DNA methylation. A similar scenario has been described for the fungal pathogen *Cryptococcus neoformans*, where DNA methylation was purely epigenetically inherited through a maintenance methyltransferase after ancient loss of a *de novo* methyltransferase (Catania *et al.*, 2017). The previous study on *Ztdim2* in *Z. tritici* indicated absence of cytosine methylation based on liquid chromatography coupled with electrospray ionization tandem mass spectrometry (ESI–MS/MS) (Dhillon *et al.*, 2010). Therefore, cytosine methylation levels

in strains without *Ztdim2* may be very low. In the absence of a *de novo* methyltransferase, DNA methylation is likely to decrease over time and might only be maintained in conserved regions of the genome. This is consistent with our findings that it exists in the rDNA spacer, a highly conserved sequence, but not on highly dynamic transposable elements in the *Ztdim2* deficient strain. Integration of an intact *Ztdim2* could restore methylation on the previously un-methylated transposable element, supporting the putative *de novo* methylation function of ZtDim2. Repeated regions are predominant targets of DNA methylation in fungi (Kouzminova & Selker, 2001; Nakayashiki *et al.*, 2001; Montanini *et al.*, 2014) and associated to genome defense mechanisms that act to silence transposons (Jones, 2012). A previous study on chromatin dynamics in *Z. tritici* found overlapping silencing-associated chromatin marks, H3K9me3 and H3K27me3, on annotated transposable elements (Schotanus *et al.*, 2015). This is an unusual finding in fungi but was also found in plants (Deleris *et al.*, 2012) and mammals (Saksouk *et al.*, 2014) as a consequence of the loss of DNA methylation. Transposon silencing might therefore be mediated by histone modifications rather than DNA methylation in *Z. tritici*. However, to shed light on DNA methylation dynamics and the enzymes involved in *Z. tritici*, further experiments have to be conducted including whole-genome analyses of cytosine methylation patterns in strains with and without an active ZtDim2. Importantly, the second DNA methyltransferase, ZtDmtA, has to be studied in greater detail to prove its cytosine methyltransferase activity.

Materials and Methods

Strains and growth conditions

All *Zymoseptoria* spp. strains used in this study were cultivated at 18°C in YMS (4 g yeast extract, 4 g malt, 4 g sucrose per 1 L, 20 g agar per L for plates) medium. Cultures for DNA extraction and plant infection experiments were inoculated directly from the -80°C glycerol stocks and grown in liquid YMS medium at 200 rpm for 5 days (DNA extractions) and in pre-cultures (3 days) and main cultures (2 days) for plant infections.

Sequence identification and analysis

The analyzed genomes were obtained from previous studies (Stukenbrock *et al.*, 2011, 2012a; Croll *et al.*, 2013; McDonald *et al.*, 2016; Grandaubert *et al.*, 2017; Stukenbrock & Dutheil, 2018) and are listed in Table S1. We searched for homologs of *Ztdim2* using the predicted 'deRIPed' protein sequence of *Z. tritici* IPO323 (Dhillon *et al.*, 2010) as a template. To identify additional putative DNA methyltransferases, we used the DNA methyltransferase domain of the ZtDim2 protein as query. BLAST searches, protein trees and alignments were performed using Geneious version 10.2.4 (http://www.geneious.com, (Kearse *et al.*, 2012)). The protein distance tree was generated with the following settings: alignment type: global alignment, cost matrix: identity, genetic distance: Jukes-Cantor, tree build method: neighbor joining, outgroup: *Zymoseptoria passerinii.* Protein alignments were carried out with the following settings: alignment type: global alignment, cost matrix: Blosum62, gap open penalty: 12, gap extension penalty: 3, refinement iterations: 2.

Bisulfite treatment and sequencing

For the identification of methylated cytosines, we treated genomic DNA of Zt09 and Zt10 (~ 100 ng) with bisulfite using the EZ DNA Methylation-Lightning Kit (Zymo Research, Irvine, CA) according to manufacturer's instructions. Bisulfite-converted rDNA spacer DNAs were amplified by PCR using specifically designed primers for amplification of the bisulfite-treated DNA (Table S2). PCR products were cloned using the TOPO TA kit (Thermo Fisher Scientific) and Sanger sequenced (Eurofins Genomics, Ebersberg, Germany). Analysis of bisulfite-converted DNA sequences was performed with BISMA (Rohde *et al.*, 2010) and visualized using Geneious version 10.2.4 (Kearse *et al.*, 2012).

Southern blots to detect DNA methylation

To detect presence/absence of DNA methylation, we performed Southern blots according to standard protocols (Southern, 1975). Genomic DNA was extracted using a standard phenol-chloroform extraction method (Sambrock & W. Russel, 2001). The same amount of DNA and enzymes (*BfuCI*, *DpnI*, *DpnII*, 25 units, New England Biolabs, Frankfurt, Germany) was used as input for the different restriction digestions to make restriction patterns comparable between enzymes and *Z. tritici* strains. Probes were generated with the PCR DIG labeling Mix (Roche, Mannheim, Germany) following the manufacturer's instructions and chemiluminescent signals detected using the GelDocTM XR+ system (Bio-Rad, Munich, Germany).

Generation of *Ztdim2* deletion and integration strains

We transformed the *Z. tritici* strains Zt09 and Zt10 using an *Agrobacterium tumefaciens*-mediated transformation (ATMT) protocol as previously described (Poppe *et al.*, 2015). Briefly, we created plasmids containing the integration (pES189) or deletion (pES188) constructs using Gibson assembly (Gibson *et al.*, 2009) (Table S2). Both constructs contained the hygromycin resistance cassette as selection marker. Plasmids were amplified in *E. coli* TOP10 cells and sequenced to confirm correct assembly of the constructs followed by electro-transformation of *A. tumefaciens* strain AGL2. *Z. tritici* strains were transformed with the respective *A. tumefaciens* strains by co-incubation for 3-4 days at 18°C on induction medium. Following co-incubating, the strains were grown on selection medium containing hygromycin to select for integration of the constructs and cefotaxime to eliminate *A. tumefaciens*. Single *Z. tritici* colonies were selected, streaked out twice and the correct integration of the construct was verified by PCR analyses and by Southern blot.

Phenotypic assay on wheat

Seedlings of the wheat cultivar Obelisk (Wiersum Plantbreeding BV, Winschoten, The Netherlands) were pre-germinated on wet sterile Whatman paper for four days under normal growth conditions (16 h at light intensity of ~200 µmol/$m^{-2}s^{-1}$ and 8 h darkness in growth chambers at 20°C with 90% humidity) followed by potting and further growth for additional seven days. Marked areas on the second leaves (30 leaves per strain) were inoculated with a spore suspension of 10^7 cells/mL in H_2O and 0.1 % Tween 20. Mock controls were treated with H_2O and 0.1 % Tween 20 only. 23 days post inoculation,

treated leaves were analyzed for the infection symptoms necrosis and pycnidia formation. Evaluation was performed manually by assigning categories for necrosis and pycnidia coverage to each leaf (categories: 0 = 0 %, 1 = 1-20 %, 2 = 21-40 %, 3 = 41-60%, 4 = 61-80%, 5 = 81-100%).

References

Catania S, Dumesic PA, Stoddard C, Cooke S, Burke J, Cuomo CA, Narlikar GJ, Madhani HD. **2017**. Epigenetic maintenance of DNA methylation after evolutionary loss of the de novo methyltransferase. *bioRxiv, doi: https://doi.org/10.1101/149385*.

Chen H, Shu H, Wang L, Zhang F, Li X, Ochola S, Mao F, Ma H, Ye W, Gu T, *et al.* 2017. Phytophthora methylomes modulated by expanded 6mA methyltransferases are associated with adaptive genome regions. *bioRxiv*, doi: https://doi.org/10.1101/217646

Corcoran P, Anderson JL, Jacobson DJ, Sun Y, Ni P, Lascoux M, Johannesson H. **2016**. Introgression maintains the genetic integrity of the mating-type determining chromosome of the fungus Neurospora tetrasperma. *Genome Research* **26**: 486–498.

Croll D, Zala M, McDonald B a. **2013**. Breakage-fusion-bridge cycles and large insertions contribute to the rapid evolution of accessory chromosomes in a fungal pathogen. *PLoS genetics* **9**: e1003567.

Deleris A, Stroud H, Bernatavichute Y, Johnson E, Klein G, Schubert D, Jacobsen SE. **2012**. Loss of the DNA Methyltransferase MET1 Induces H3K9 Hypermethylation at PcG Target Genes and Redistribution of H3K27 Trimethylation to Transposons in Arabidopsis thaliana. *PLoS Genetics* **8**.

Dhillon B, Cavaletto JR, Wood K V., Goodwin SB. **2010**. Accidental amplification and inactivation of a methyltransferase gene eliminates cytosine methylation in Mycosphaerella graminicola. *Genetics* **186**: 67–77.

Finn RD, Attwood TK, Babbitt PC, Bateman A, Bork P, Bridge AJ, Chang HY, Dosztanyi Z, El-Gebali S, Fraser M, *et al.* 2017. InterPro in 2017-beyond protein family and domain annotations. *Nucleic Acids Research* **45**: D190–D199.

Freitag M, Williams RL, Kothe GO, Selker EU. **2002**. A cytosine methyltransferase homologue is essential for repeat-induced point mutation in Neurospora crassa. *Proceedings of the National Academy of Sciences* **99**: 8802–8807.

Gibson DG, Young L, Chuang RY, Venter JC, Hutchison CA, Smith HO. **2009**. Enzymatic assembly of DNA molecules up to several hundred kilobases. *Nature Methods* **6**: 343–345.

Gladieux P, Ropars J, Badouin H, Branca A, Aguileta G, De Vienne DM, Rodríguez De La Vega RC, Branco S, Giraud T. **2014**. Fungal evolutionary genomics provides insight into the mechanisms of adaptive divergence in eukaryotes. *Molecular Ecology* **23**: 753–773.

Goll MG, Bestor TH. **2005**. Eukaryotic Cytosine Methyltransferases. *Annual Review of Biochemistry* **74**: 481–514.

Goodwin SB, M'barek S Ben, Dhillon B, Wittenberg AHJ, Crane CF, Hane JK, Foster AJ, Van der Lee T a J, Grimwood J, Aerts A, *et al.* 2011. Finished genome of the fungal wheat pathogen Mycosphaerella graminicola reveals dispensome structure, chromosome plasticity, and stealth pathogenesis. *PLoS genetics* **7**: e1002070.

Grandaubert J, Bhattacharyya A, Stukenbrock EH. **2015**. RNA-seq Based Gene Annotation and Comparative Genomics of Four Fungal Grass Pathogens in the Genus Zymoseptoria Identify Novel Orphan Genes and Species-Specific Invasions of Transposable Elements. *G3 (Bethesda, Md.)* **5**: g3.115.017731-.

Grandaubert J, Dutheil JY, Stukenbrock EH. **2017**. The genomic determinants of adaptive evolution in a fungal pathogen. *bioRxiv*.

Greer EL, Blanco MA, Gu L, Sendinc E, Liu J, Aristizábal-Corrales D, Hsu CH, Aravind L, He C, Shi Y. **2015**. DNA methylation on N6-adenine in C. elegans. *Cell* **161**: 868–878.

Ikeda KI, Van Vu B, Kadotani N, Tanaka M, Murata T, Shiina K, Chuma I, Tosa Y, Nakayashiki H. **2013**. Is the fungus Magnaporthe losing DNA methylation? *Genetics* **195**: 845–855.

Jeltsch A, Jurkowska RZ. 2014. New concepts in DNA methylation. *Trends in Biochemical Sciences* **39**: 310–318.
Jeon J, Choi J, Lee G-W, Park S-Y, Huh A, Dean R a, Lee Y-H. 2015. Genome-wide profiling of DNA methylation provides insights into epigenetic regulation of fungal development in a plant pathogenic fungus, Magnaporthe oryzae. *Scientific reports* **5**: 8567.
Jones PA. 2012. Functions of DNA methylation: Islands, start sites, gene bodies and beyond. *Nature Reviews Genetics* **13**: 484–492.
Kearse M, Moir R, Wilson A, Stones-Havas S, Cheung M, Sturrock S, Buxton S, Cooper A, Markowitz S, Duran C, *et al.* 2012. Geneious Basic: An integrated and extendable desktop software platform for the organization and analysis of sequence data. *Bioinformatics* **28**: 1647–1649.
Kellner R, Bhattacharyya A, Poppe S, Hsu TY, Brem RB, Stukenbrock EH. 2014. Expression Profiling of the Wheat Pathogen Zymoseptoria tritici Reveals Genomic Patterns of Transcription and Host-Specific Regulatory Programs. *Genome biology and evolution* **6**: 1353–65.
Kouzminova E, Selker EU. 2001. Dim-2 encodes a DNA methyltransferase responsible for all known cytosine methylation in Neurospora. *EMBO Journal* **20**: 4309–4323.
Lee DW, Freitag M, Selker EU, Aramayo R. 2008. A cytosine methyltransferase homologue is essential for sexual development in Aspergillus nidulans. *PLoS ONE* **3**: 1–10.
Lyko F. 2018. The DNA methyltransferase family: A versatile toolkit for epigenetic regulation. *Nature Reviews Genetics* **19**: 81–92.
Malagnac F, Wendel B, Goyon C, Faugeron G, Zickler D, Rossignol JL, Noyer-Weidner M, Vollmayr P, Trautner TA, Walter J. 1997. A gene essential for de novo methylation and development in ascobolus reveals a novel type of eukaryotic DNA methyltransferase structure. *Cell* **91**: 281–290.
Martienssen R a. 2001. DNA Methylation and Epigenetic Inheritance in Plants and Filamentous Fungi. *Science* **293**: 1070–1074.
McDonald MC, McGinness L, Hane JK, Williams AH, Milgate A, Solomon PS. 2016. Utilizing Gene Tree Variation to Identify Candidate Effector Genes in Zymoseptoria tritici. *G3 (Bethesda, Md.)* **6**: 779–91.
Möller M, Schotanus K, Soyer J, Haueisen J, Happ K, Stralucke M, Happel P, Smith KM, Connolly LR, Freitag M, *et al.* 2018. The role of heterochromatin in genome and chromosome stability in a fungal plant pathogen. In: PhD Thesis Mareike Möller. Chapter III.
Montanini B, Chen P-Y, Morselli M, Jaroszewicz A, Lopez D, Martin F, Ottonello S, Pellegrini M. 2014. Non-exhaustive DNA methylation-mediated transposon silencing in the black truffle genome, a complex fungal genome with massive repeat element content. *Genome Biology* **15**: 411.
Nakayashiki H, Ikeda K, Hashimoto Y, Tosa Y, Mayama S. 2001. Methylation is not the main force repressing the retrotransposon MAGGY in Magnaporthe grisea. *Nucleic acids research* **29**: 1278–84.
Ponomarenko A, Goodwin SB, Kema GHJ. 2011. Septoria tritici blotch (STB) of wheat Septoria tritici blotch (STB) of wheat. *Plant Health Instructor*: 1–7.
Poppe S, Dorsheimer L, Happel P, Stukenbrock EH. 2015. Rapidly Evolving Genes Are Key Players in Host Specialization and Virulence of the Fungal Wheat Pathogen Zymoseptoria tritici (Mycosphaerella graminicola). *PLoS Pathogens* **11**: 1–21.
Quaedvlieg W, Kema GHJ, Groenewald JZ, Verkley GJM, Seifbarghi S, Razavi M, Mirzadi Gohari A, Mehrabi R, Crous PW. 2011. Zymoseptoria gen. nov.: A new genus to accommodate Septoria-like species occurring on graminicolous hosts. *Persoonia: Molecular Phylogeny and Evolution of Fungi* **26**: 57–69.

Rohde C, Zhang Y, Reinhardt R, Jeltsch A. **2010**. BISMA--fast and accurate bisulfite sequencing data analysis of individual clones from unique and repetitive sequences. *BMC bioinformatics* **11**: 230.
Saksouk N, Barth TK, Ziegler-Birling C, Olova N, Nowak A, Rey E, Mateos-Langerak J, Urbach S, Reik W, Torres-Padilla ME, *et al.* 2014. Redundant Mechanisms to Form Silent Chromatin at Pericentromeric Regions Rely on BEND3 and DNA Methylation. *Molecular Cell* **56**: 580–594.
Sambrock J, W. Russel D. **2001**. Molecular Cloning: A Laboratory Manual(3rd edition).
Schotanus K, Soyer JL, Connolly LR, Grandaubert J, Happel P, Smith KM, Freitag M, Stukenbrock EH. **2015**. Histone modifications rather than the novel regional centromeres of Zymoseptoria tritici distinguish core and accessory chromosomes. *Epigenetics & chromatin* **8**: 41.
Selker EU, Stevens JN. **1985**. DNA methylation at asymmetric sites is associated with numerous transition mutations. *Proceedings of the National Academy of Sciences of the United States of America* **82**: 8114–8.
Slotkin RK, Martienssen R. **2007**. Transposable elements and the epigenetic regulation of the genome. *Nature reviews. Genetics* **8**: 272–85.
Southern EM. **1975**. Detection of specific sequences among DNA fragments separated by gel electrophoresis. *Journal of Molecular Biology* **98**: 503–517.
Stukenbrock EH, Bataillon T, Dutheil JY, Hansen TT, Li R, Zala M, McDonald BA, Wang J, Schierup MH. **2011a**. The making of a new pathogen: Insights from comparative population genomics of the domesticated wheat pathogen Mycosphaerella graminicola and its wild sister species. *Genome Research* **21**: 2157–2166.
Stukenbrock EH, Bataillon T, Dutheil JY, Hansen TT, Li R, Zala M, McDonald B a, Wang J, Schierup MH. **2011b**. The making of a new pathogen: insights from comparative population genomics of the domesticated wheat pathogen Mycosphaerella graminicola and its wild sister species. *Genome research* **21**: 2157–66.
Stukenbrock EH, Christiansen FB, Hansen TT, Dutheil JY, Schierup MH. **2012a**. Fusion of two divergent fungal individuals led to the recent emergence of a unique widespread pathogen species. *Proceedings of the National Academy of Sciences* **109**: 10954–10959.
Stukenbrock EH, Dutheil JY. **2018**. Fine-scale recombination maps of fungal plant pathogens reveal dynamic recombination landscapes and intragenic hotspots. *Genetics* **208**: 1209–1229.
Stukenbrock EH, Quaedvlieg W, Javan-Nikhah M, Zala M, Crous PW, McDonald BA. **2012b**. Zymoseptoria ardabiliae and Z. pseudotritici, two progenitor species of the septoria tritici leaf blotch fungus Z. tritici (synonym: Mycosphaerella graminicola). *Mycologia* **104**: 1397–1407.
Yang K, Liang L, Ran F, Liu Y, Li Z, Lan H, Gao P, Zhuang Z, Zhang F, Nie X, *et al.* 2016. The DmtA methyltransferase contributes to Aspergillus flavus conidiation, sclerotial production, aflatoxin biosynthesis and virulence. *Scientific Reports* **6**: 1–13.
Zhang G, Huang H, Liu D, Cheng Y, Liu X, Zhang W, Yin R, Zhang D, Zhang P, Liu J, *et al.* 2015. N6-methyladenine DNA modification in Drosophila. *Cell* **161**: 893–906.

Supplementary Tables and Figures

All supplementary tables are deposited on the supplementary USB key.

Table S1. List of strains that were used for the genome analysis including sampling location and reference publication.

Table S2. List of primers used in this study to generate plasmids, probes for Southern blots and bisulfite sequencing.

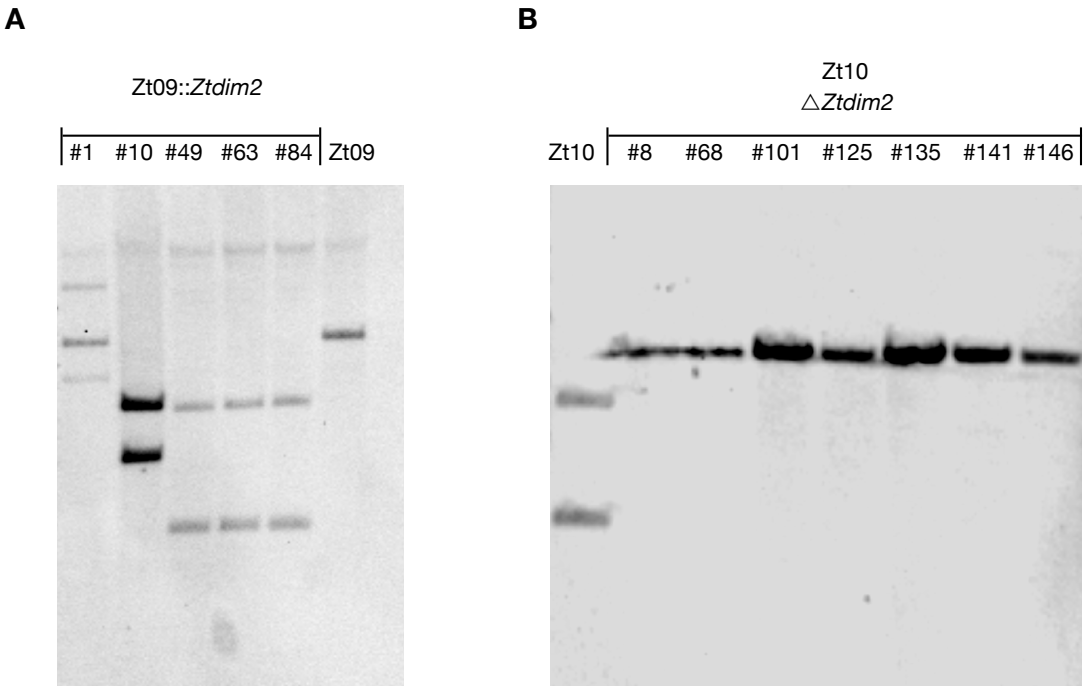

Figure S1. Southern blots were performed to verify correct integration of A) *Ztdim2* (originating from Zt10) in Zt09 (Zt09::*Ztdim2*) and B) the deletion construct for *Ztdim2* in Zt10 (Zt10Δ*Ztdim2*). Three positive transformants (#49, #63 and #84) were found amongst the Zt09::*Ztdim2* candidates, whereas all seven candidates for Zt10Δ*Ztdim2* were verified. For the plant infection experiments, we used Zt09::*Ztdim2* #49 and #63 and Zt10Δ*Ztdim2* #8 and #68.

Figure S2. (A) Genomic location of the second putative cytosine methyltransferase *ZtdmtA*. Shown are predicted genes (green) (Grandaubert *et al.*, 2015). The blue arrow indicates the position of *ZtdmtA*. It is part of the predicted gene *Zt_chr_5_00047* but RNA-seq read coverage (Möller *et al.*, 2018) indicates that the annotated gene likely consists of two separate genes. Very few reads map to the putative *ZtdmtA* open reading frame suggesting very low expression *in vitro* in Zt09. **(B)** We used InterPro (Finn et al., 2017) to predict protein families for the different alleles found for *ZtdmtA*. The strains Zt09, Zt10 and Zt04 were selected as the representatives for alleles A, B, and C, respectively. Despite the large sequence differences, all three proteins were predicted as members of the S-adenosyl-L-methionine-dependent methyltransferases superfamiliy and C-5 cytosine methyltransferase family.

General Conclusion and Perspectives

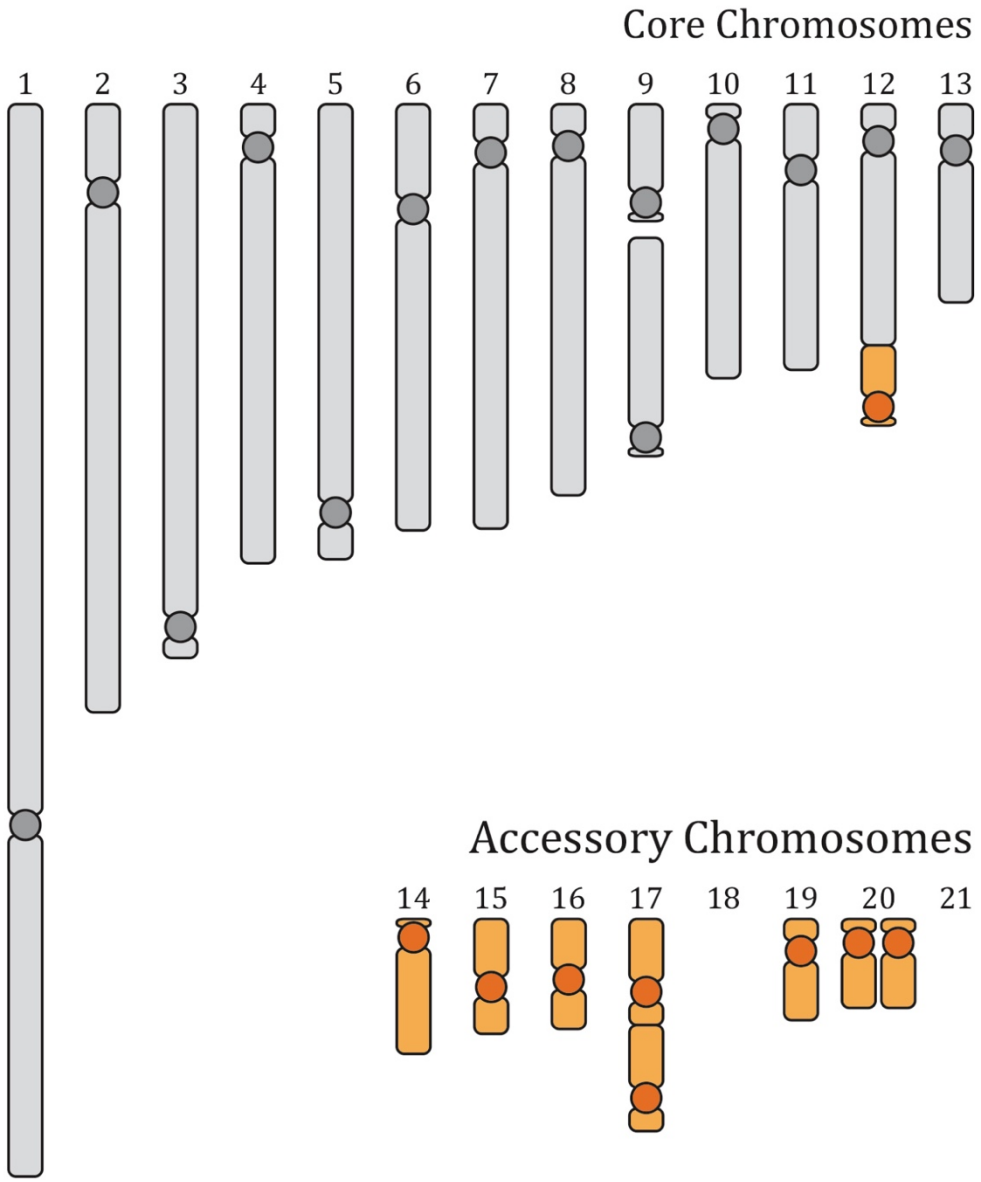

General Conclusion and Perspectives

The aim of this thesis was to explore the dynamics and epigenetic mechanisms of mitotic chromosome loss and genome stability in the plant pathogen *Zymoseptoria tritici*. As an additional component of epigenetic regulation, we also elucidated the occurrence of DNA methylation in *Zymoseptoria* species.

We show that accessory chromosomes are lost at very high rates during mitotic growth both *in vitro* and *in planta*. Similar rates were found in the closely related sister species *Zymoseptoria ardabiliae* indicating that mitotic chromosome loss is a conserved phenomenon. Indeed, chromosome losses have been observed in other fungi (Miao *et al.*, 1991; Vlaardingerbroek *et al.*, 2016) but the reported rates were considerably lower than in *Zymoseptoria* spp. Unlike in other fungal plant pathogens, accessory chromosomes do not have a virulence-determining function in *Z. tritici*. In contrast, the results presented in this thesis and a previous study (Habig *et al.*, 2017) suggest small, but significant negative effects when certain accessory chromosomes are present during wheat infection. However, these chromosomes might be relevant under environmental conditions that have not been tested so far. To date experimentally unexplored phases of the *Z. tritici* lifecycle, interactions with other microbes and abiotic stresses could be targets of future studies on accessory chromosome function. Exposed to temperature stress conditions, the accessory chromosome loss rate dramatically increased. However, instability was not restricted to accessory chromosomes but also core chromosomes underwent rearrangements suggesting abiotic stressors as triggers for genome instability. Further analyses testing different abiotic factors including osmotic and oxidative stress or even fungicides representing selection pressures in wheat fields could elucidate possible adaptive roles of genome instability.

The high variability in genome structure of fungal plant pathogens indicates that chromosome and genome rearrangements are frequent phenomena and might reflect high selection pressure and adaptation to rapidly changing environments. An intriguing question is which factors promote accessory chromosome losses. We hypothesized that enrichment of the heterochromatin histone marks H3K9me3 and H3K27me3 on accessory chromosomes (Schotanus *et al.*, 2015) contributes to the observed instability. By deleting the respective histone-methyltransferases we could demonstrate that loss of H3K27me3 significantly reduces chromosome loss rates but does not have an effect on

the overall genome structure. This indicates that H3K27me3, normally covering the entire length of accessory chromosomes, is a main driver of their mitotic instability. Detailed analyses in other fungal pathogens harboring H3K27me3-enriched accessory chromosomes have to be conducted to shed light on a potential conserved role of H3K27me3 in fungal genome stability. High-resolution microscopic analyses of accessory chromosomes in wild type and *Δkmt6* during mitotic cell divisions should be applied to elucidate the role of H3K27me3 for chromosome losses.

In contrast to the destabilizing role of H3K27me3 on accessory chromosomes, absence of H3K9me3 resulted in large-scale chromosome rearrangements including both core and accessory chromosomes as well as in transposon activation. We therefore conclude that H3K9me3 is essential to maintain overall genome stability. To our knowledge, this is the first report on the role of histone methylation in genome stability in plant pathogenic fungi. However, transposons have been correlated to highly variable regions (Fierro & Martín, 1999; Castanera *et al.*, 2016; Faino *et al.*, 2016) and our results further highlight the importance of transposable elements in creating genetic diversity. Activation under certain conditions might rapidly promote structural rearrangements that can confer fitness advantages. However, strict transposon regulation under normal conditions is essential as most rearrangements are presumably deleterious.

In many organisms, transposable elements and repetitive DNA exhibit high levels of DNA methylation associated to silencing of these sequences (Zemach & Zilberman, 2010; Zemach *et al.*, 2010). In *Z. tritici* though, DNA methylation was considered to be absent due to inactivation of the DNA methyltransferase gene *Ztdim2* (Dhillon *et al.*, 2010). We found that DNA methylation is not absent, likely due to a second DNA methyltransferase, ZtDmtA. However, levels of DNA methylation are very low in strains where *Ztdim2* is mutated and transposons do not seem to be targeted by DNA methylation. As a consequence, *Z. tritici* is lacking an important mechanism to silence transposon. In Chapter III we found that H3K9me3 and H3K27me3 frequently overlap on transposons. This observation might reflect the absence of DNA methylation at those sites and resembles findings in plants and animals (Deleris *et al.*, 2012; Saksouk *et al.*, 2014). In *Z. tritici*, H3K27me3 might function as a compensator for the loss of DNA methylation. This mechanism may not be as efficient in silencing of TEs as the presence of DNA methylation though. Comparisons of repeat content in *Z. tritici* isolates revealed substantial differences in the amount of TEs between the Iranian strains Zt10 and Zt11 that contain

a functional *Ztdim2* and strains carrying the RIPed copy (Grandaubert *et al.*, 2017). This indicates that loss of DNA methylation could entail transposon accumulation. However, extensive differences in TE content are frequently found in different fungal species (Raffaele & Kamoun, 2012; Möller & Stukenbrock, 2017) suggesting various mechanisms acting on transposon proliferation in fungal genomes. The specific effects of DNA methylation on genome stability and chromatin structure in *Z. tritici* require further studies. Integration of the functional *Ztdim2* in *Ztdim2*-RIPed strains and the *vice versa* deletion of *Ztdim2* in the Iranian strains will provide a unique experimental system to study mechanisms and evolution of fungal genome defense systems.

As a general conclusion, we demonstrated that the genome of *Z. tritici* is highly dynamic during mitotic growth. Epigenetic mechanisms, in form of histone methylation marks contribute substantially but in different ways to genome instability and chromosome rearrangements.

An important observation is that epigenetic mechanisms seem to have distinct roles in different organisms. While in some species the most important function lies in regulation of gene expression, in others these mechanisms are crucial for genome organization and chromosome stability. Some mechanisms might get lost over time, while others are selected for. This results in highly variable genome regulation pathways with severe consequences for genome evolution and the ability to rapidly adapt to changing environments. Hence, this is of special interest for pathogen management in agriculture. Resistances against applied antifungal treatments arise very fast by rapid adaptation on a genetic level. Understanding the mechanisms of genome evolution in fungal plant pathogens will improve future practices in agriculture and contribute to sustainable food production.

References General Introduction & General Conclusion

Castanera R, López-Varas L, Borgognone A, LaButti K, Lapidus A, Schmutz J, Grimwood J, Pérez G, Pisabarro AG, Grigoriev I V., *et al.* 2016. Transposable Elements versus the Fungal Genome: Impact on Whole-Genome Architecture and Transcriptional Profiles. *PLOS Genetics* **12**: e1006108.

Deleris A, Stroud H, Bernatavichute Y, Johnson E, Klein G, Schubert D, Jacobsen SE. 2012. Loss of the DNA Methyltransferase MET1 Induces H3K9 Hypermethylation at PcG Target Genes and Redistribution of H3K27 Trimethylation to Transposons in Arabidopsis thaliana. *PLoS Genetics* **8**.

Dhillon B, Cavaletto JR, Wood K V., Goodwin SB. 2010. Accidental amplification and inactivation of a methyltransferase gene eliminates cytosine methylation in Mycosphaerella graminicola. *Genetics* **186**: 67–77.

Faino L, Seidl MF, Shi-Kunne X, Pauper M, van den Berg GCM, Wittenberg AHJ, Thomma BPHJ. 2016. Transposons passively and actively contribute to evolution of the two-speed genome of a fungal pathogen. *Genome Research*: gr.204974.116.

Fierro F, Martín JF. 1999. Molecular mechanisms of chromosomal rearrangement in fungi. *Critical Reviews in Microbiology* **25**: 1–17.

Fones H, Gurr S. 2015. The impact of Septoria tritici Blotch disease on wheat: An EU perspective. *Fungal Genetics and Biology* **79**: 3–7.

Galazka JM, Freitag M. 2014. Variability of chromosome structure in pathogenic fungi-of "ends and odds." *Current Opinion in Microbiology* **20**: 19–26.

Goodwin SB, Ben M'Barek S, Dhillon B, Wittenberg AHJ, Crane CF, Hane JK, Foster AJ, Van der Lee TAJ, Grimwood J, Aerts A, *et al.* 2011. Finished Genome of the Fungal Wheat Pathogen *Mycosphaerella graminicola* Reveals Dispensome Structure, Chromosome Plasticity, and Stealth Pathogenesis. *PLoS Genet* **7**: e1002070.

Grandaubert J, Bhattacharyya A, Stukenbrock EH. 2015. RNA-seq Based Gene Annotation and Comparative Genomics of Four Fungal Grass Pathogens in the Genus Zymoseptoria Identify Novel Orphan Genes and Species-Specific Invasions of Transposable Elements. *G3 (Bethesda, Md.)* **5**: g3.115.017731-.

Grandaubert J, Dutheil JY, Stukenbrock EH. 2017. The genomic determinants of adaptive evolution in a fungal pathogen. *bioRxiv*. doi: https://doi.org/10.1101/176727

Grandaubert J, Lowe RGT, Soyer JL, Schoch CL, Van de Wouw AP, Fudal I, Robbertse B, Lapalu N, Links MG, Ollivier B, *et al.* 2014. Transposable element-assisted evolution and adaptation to host plant within the Leptosphaeria maculans-Leptosphaeria biglobosa species complex of fungal pathogens. *BMC genomics* **15**: 891.

Habig M, Quade J, Stukenbrock EH. 2017. Forward genetics approach reveals host-genotype dependent importance of accessory chromosomes in the fungal wheat pathogen Zymoseptoria tritici. *mBio* **8**: Forthcoming.

Haueisen J, Moeller M, Eschenbrenner CJ, Grandaubert J, Seybold H, Adamiak H, Stukenbrock EH. 2017. Extremely flexible infection programs in a fungal plant pathogen. *bioRxiv* **49**: 229997.

Hollister JD, Gaut BS. 2009. Epigenetic silencing of transposable elements: A trade-off between reduced transposition and deleterious effects on neighboring gene expression. *Genome Research* **19**: 1419–1428.

De Jonge R, Bolton MD, Kombrink A, Van Den Berg GCM, Yadeta KA, Thomma BPHJ. 2013. Extensive chromosomal reshuffling drives evolution of virulence in an asexual pathogen. *Genome Research* **23**: 1271–1282.

Kazazian HH. 2004. Mobile Elements: Drivers of Genome Evolution. *Science* **303**: 1626–1632.

Kellner R, Bhattacharyya A, Poppe S, Hsu TY, Brem RB, Stukenbrock EH. **2014**. Expression Profiling of the Wheat Pathogen Zymoseptoria tritici Reveals Genomic Patterns of Transcription and Host-Specific Regulatory Programs. *Genome biology and evolution* **6**: 1353–65.

Linde CC, Zhan J, McDonald BA. **2002**. Population Structure of Mycosphaerella graminicola: From Lesions to Continents. *Phytopathology* **92**: 946–955.

Ma L-J, van der Does HC, Borkovich K a, Coleman JJ, Daboussi M-J, Di Pietro A, Dufresne M, Freitag M, Grabherr M, Henrissat B, *et al.* 2010. Comparative genomics reveals mobile pathogenicity chromosomes in Fusarium. *Nature* **464**: 367–373.

McDonald B a., Martinez JP. **1991**. Chromosome length polymorphisms in a Septoria tritici population. *Current Genetics* **19**: 265–271.

McDonald BA, Stukenbrock EH. **2016**. Rapid emergence of pathogens in agro-ecosystems: global threats to agricultural sustainability and food security. *Phil. Trans. R. Soc. B* **371**: 20160026.

Miao VP, Covert SF, VanEtten HD. **1991**. A fungal gene for antibiotic resistance on a dispensable (“ B”) chromosome. *Science* **254**: 1773.

Möller M, Stukenbrock EH. **2017**. Evolution and genome architecture in fungal plant pathogens. *Nature Reviews Microbiology* **15**: 756–771.

Ponomarenko A, Goodwin SB, Kema GHJ. **2011**. Septoria tritici blotch (STB) of wheat Septoria tritici blotch (STB) of wheat. *Plant Health Instructor*: 1–7.

Raffaele S, Kamoun S. **2012**. Genome evolution in filamentous plant pathogens: why bigger can be better. *Nature Reviews Microbiology* **10**: 417–430.

Rouxel T, Grandaubert J, Hane JK, Hoede C, van de Wouw AP, Couloux A, Dominguez V, Anthouard V, Bally P, Bourras S. **2011**. Effector diversification within compartments of the Leptosphaeria maculans genome affected by Repeat-Induced Point mutations. *Nature Communications* **2**: 202.

Rudd JJ, Kanyuka K, Hassani-Pak K, Derbyshire M, Andongabo A, Devonshire J, Lysenko A, Saqi M, Desai NM, Powers SJ, *et al.* 2015. Transcriptome and metabolite profiling of the infection cycle of Zymoseptoria tritici on wheat reveals a biphasic interaction with plant immunity involving differential pathogen chromosomal contributions and a variation on the hemibiotrophic lifestyle def. *Plant physiology* **167**: 1158–85.

Saksouk N, Barth TK, Ziegler-Birling C, Olova N, Nowak A, Rey E, Mateos-Langerak J, Urbach S, Reik W, Torres-Padilla ME, *et al.* 2014. Redundant Mechanisms to Form Silent Chromatin at Pericentromeric Regions Rely on BEND3 and DNA Methylation. *Molecular Cell* **56**: 580–594.

Schotanus K, Soyer JL, Connolly LR, Grandaubert J, Happel P, Smith KM, Freitag M, Stukenbrock EH. **2015**. Histone modifications rather than the novel regional centromeres of Zymoseptoria tritici distinguish core and accessory chromosomes. *Epigenetics & chromatin* **8**: 41.

Soyer JL, El Ghalid M, Glaser N, Ollivier B, Linglin J, Grandaubert J, Balesdent M-H, Connolly LR, Freitag M, Rouxel T, *et al.* 2014. Epigenetic control of effector gene expression in the plant pathogenic fungus Leptosphaeria maculans. *PLoS genetics* **10**: e1004227.

Stukenbrock EH, Banke S, Javan-Nikkhah M, McDonald B a. **2007**. Origin and domestication of the fungal wheat pathogen Mycosphaerella graminicola via sympatric speciation. *Molecular biology and evolution* **24**: 398–411.

Stukenbrock EH, Bataillon T, Dutheil JY, Hansen TT, Li R, Zala M, McDonald BA, Wang J, Schierup MH. **2011**. The making of a new pathogen: Insights from comparative population genomics of the domesticated wheat pathogen Mycosphaerella graminicola and its wild sister species. *Genome Research* **21**: 2157–2166.

Torriani SFF, Melichar JPE, Mills C, Pain N, Sierotzki H, Courbot M. **2015**. Zymoseptoria tritici: A major threat to wheat production, integrated approaches to control. *Fungal Genetics and Biology* **79**: 8–12.

Vlaardingerbroek I, Beerens B, Schmidt SM, Cornelissen BJC, Rep M. **2016**. Dispensable chromosomes in Fusarium oxysporum f . sp lycopersici . *Molecular Plant Pathology*: 1–12.

Wittenberg AHJ, van der Lee T a J, Ben M'barek S, Ware SB, Goodwin SB, Kilian A, Visser RGF, Kema GHJ, Schouten HJ. **2009**. Meiosis drives extraordinary genome plasticity in the haploid fungal plant pathogen Mycosphaerella graminicola. *PloS one* **4**: e5863.

Wolfe D, Dudek S, Ritchie MD, Pendergrass SA. **2013**. Visualizing genomic information across chromosomes with PhenoGram. *BioData Mining* **6**: 1.

Zemach A, McDaniel IE, Silva P, Zilberman D. **2010**. Genome-wide evolutionary analysis of eukaryotic DNA methylation. *Science* **328**: 916–919.

Zemach A, Zilberman D. **2010**. Evolution of eukaryotic DNA methylation and the pursuit of safer sex. *Current Biology* **20**: R780–R785.

Acknowledgements

I am so happy to finally see the results of my PhD here. This work would not have been possible without the support and help of so many people.
First of all, I would like to thank my supervisor Eva Stukenbrock for encouraging me from the beginning of my scientific career, starting as a bachelor student in Marburg until finishing my PhD here in Kiel. I am very grateful for the support you gave me during all those years and the opportunity to work on this great project. You helped me to broaden my horizon from working in the lab to conduct bioinformatic analyses. Thank you for your advice and freedom that make me confident to pursue my further career in science.

I want to thank Michael Freitag for all the support, discussions, and contributions to this thesis. Without your help and guidance these projects would not have been possible. I am looking forward to many future discussions, maybe soon in Oregon.

Thank you to the past and present members of the Happy Office, Janine, Heike, Klaas, and Stephan. It was a pleasure to share an office with you and I always enjoyed our discussions and the good atmosphere.

I am grateful to Andrea, Alina, Christoph, Michael, Petra and all current and past members of the Environmental Genomics group in Kiel and the Fungal Biodiversity group in Marburg for the discussions and support.

I want to thank the members of my thesis advisory committee, Bernhard Haubold, Duncan Greig, Frank Kempken and Michael Freitag for helpful discussions and the interest in my research.

Furthermore, I am grateful to Martijn Rep, Frank Kempken and Matthias Leippe for agreeing to be members of my thesis committee and to evaluate my thesis.

Liebe Janine, vielen, vielen Dank für die tolle Zeit, die wir zusammen in Marburg und Kiel hatten. All die Diskussionen die wir während dieser Zeit geführt haben, die Arbeit zusammen im Labor und am Mikroskop und deine Unterstützung in allen Situationen haben maßgeblich dazu beigetragen, dass diese Arbeit jetzt in dieser Form vorliegt (die Details!). Auch für die großartige Zeit außerhalb von Büro und Labor möchte ich mich ganz herzlich bedanken, ich freue mich schon auf all die Highlights (immer ein Highlight pro Woche!), die noch kommen werden. Wer weiß was in Zukunft noch passiert, aber N1NJ4N1N3 & M03LL3R und die Kamel-DNA Garagenfirma sind auf jeden Fall eine Option. Und vielen Dank an Holger für die großartige Hilfe beim Design dieser Arbeit.

Ich möchte mich natürlich auch ganz herzlich bei meiner ganzen Familie bedanken. Mutti und Vatti, ich habe mich immer von euch unterstützt gefühlt und konnte mich immer auf euch verlassen. Ohne euch wäre ich niemals so weit gekommen. Vielen Dank dafür!
Vielen Dank auch an meine liebe Schwester Jasmin. Du warst immer für mich da und wir konnten immer über alles reden. Deine Unterstützung bedeutet mir sehr viel und ich freue mich schon auf die nächsten Besuche und Treffen rund um die Welt.

Ganz besonders möchte ich mich auch bei Christine, Marco, Manni und Nicole für die gemeinsame Zeit und Unterstützung während der Doktorarbeit, aber auch die ganze Zeit davor bedanken. Christine und Marco, ich habe mich immer sehr über eure Besuche, Karten und kleine Überraschungen gefreut. Ich freue mich auch sehr auf die nächsten gemeinsamen Urlaube und natürlich immer wieder auf gemeinsame Abende bei Claudio.

Declaration of author's contribution

The PhD thesis of **Mareike Möller** comprises four chapters in form of published and unpublished manuscripts. Specific contributions for the chapters are detailed here.

Chapter I: Evolution and genome architecture in fungal plant pathogens
Mareike Möller and Eva H. Stukenbrock

Chapter I was published in Nature Reviews Microbiology in 2017.
Mareike Möller & Eva H. Stukenbrock. **2017**. **Evolution and genome architecture in fungal plant pathogens**. *Nature Reviews Microbiology volume 15, pages 756–771 (2017)* (doi:10.1038/nrmicro.2017.76)

Conceptualization, manuscript writing and editing: MM, EHS.

Chapter II: Extraordinary genome instability and widespread chromosome rearrangements during vegetative growth
Mareike Möller, Michael Habig, Michael Freitag, and Eva H. Stukenbrock

Chapter II was published as preprint on bioRxiv (doi: 10.1101/304915) and is currently submitted to a peer-reviewed journal.

Conceptualization: MM, MH, MF, EHS. Chromosome loss *in vitro* at different temperatures: MM. Chromosome loss on plate: MH. *In planta* chromosome loss: MH. Karyotyping and Southern analyses: MM. Genome sequencing and analysis of structural variation: MM. *In vitro* stress and growth assay and wheat infection: MM. Preparation and writing of manuscript: MM, EHS. Editing of original manuscript: MM, EHS, MF, MH.

Chapter III: The role of heterochromatin in genome and chromosome stability in a fungal plant pathogen

Mareike Möller, Klaas Schotanus, Jessica Soyer, Janine Haueisen, Kathrin Happ, Maja Stralucke, Petra Happel, Kristina M. Smith, Lanelle R. Connolly, Michael Freitag, and Eva H. Stukenbrock

Conceptualization: MM, MF, EHS. Generation of mutant strains: MM, PH, JS. Wheat infection experiments and *in vitro* stress assay: MM, KH, and MS. I*n vitro* growth assay: MM, JH. RNA extraction, transcriptome sequencing data curation and analyses: MM, JH. ChIP preparation and sequencing: MM, MF, KS, LRC. ChIP data analysis and curation: MM, MF, KMS. Experimental evolution, genome sequencing and structural variation analysis: MM. Preparation and writing of manuscript: MM, EHS. Editing of original manuscript: MM, EHS.

Chapter IV: DNA methylation varies in *Zymoseptoria* species

Mareike Möller, Kathrin Happ, Maja Stralucke, Michael Freitag, and Eva H. Stukenbrock

Conceptualization: MM, MF, EHS. Generation of mutant strains: MM, KH, MS. Analysis of DNA methylation by Southern blots: MM, KH. Bisulfite sequencing and analysis: MM. Genome data analysis: MM. Preparation and writing of manuscript: MM. Editing of original manuscript: MM, EHS.

Affidavit

I hereby declare that this dissertation

- concerning content and design is the product of my own work under guidance of my supervisor Prof. Dr. Eva H. Stukenbrock. I used no other tools or sources but the cited ones. Contributions of other authors are listed in detail in the 'Declaration of author's contribution' section of this thesis.
- has been conducted and prepared following the Rules of Good Scientific Practice of the German Research Foundation.
- has not been submitted elsewhere partially or wholly as part of a doctoral degree to another examining body, and no other materials are published or submitted for publication than indicated in the thesis.

Mareike Möller
Kiel, 08.05.18